Photocopy and Use Authorization

In presenting this thesis in partial fulfillment of the requirements for an advanced degree at Idaho State University, I agree that the Library shall make it freely available for inspection. I further state that permission for extensive copying of my thesis for scholarly purposes may be granted by the Dean of the Graduate School, Dean of my academic division, or by the University Librarian. It is understood that any copying or publication of this thesis for financial gain shall not be allowed without my written permission.

Signature_____

Barbara Elaine Earles

Date_____

Seismic Performance of Columns with Grouted Couplers in Idaho Accelerated Bridge Construction Applications

by

Barbara Elaine Earles

A thesis

submitted in partial fulfillment

of the requirements for the degree of

MASTER OF SCIENCE

IN

CIVIL ENGINEERING

IDAHO STATE UNIVERSITY

December 2017

Committee Approval

To the Graduate Faculty:

The members of the committee appointed to examine the thesis of Barbara Elaine Earles find it satisfactory and recommend that it be accepted.

_____

Major Advisor:

Dr. Arya Ebrahimpour

_____

Committee Member:

Dr. Mustafa Mashal

_____

Graduate Faculty Representative:

Dr. Marco Schoen

Acknowledgments

I would like to thank my advisor, Dr. Arya Ebrahimpour, for the time and effort he put into this research and his assistance with the completion of my masters degree. I would also like to thank the Idaho Transportation Department (ITD) for funding the research assistantship that made this project possible.

I am also grateful to ITD for the plans and documents they provided for the bridges in this research. I would like to thank the engineers at ITD for all of their help and especially Leonard Ruminsky for his guidance regarding the abutment stiffness values of the bridges.

Other faculty and students of the Civil and Environmental Engineering Department helped at different stages of this research. I would like to thank Dr. Andrew Sorensen, Kyle Gagnon, Maria Tangarife, and Supreme Maskey for their assistance.

_____

Barbara Elaine Earles

Table of Contents

List of Figures

List of Tables

Abstract

Accelerated Bridge Construction (ABC) technologies are being adopted by federal and state departments of transportation because they reduce construction time and expense and mitigate other problems such as traffic stoppages. One particular ABC technology is the use of precast concrete members joined with mechanical connections. However, in some states where there is moderate to high seismic activity the use of mechanical connections in precast members has not been adopted either because it is not known how these mechanical connections will behave in a seismic event or the risk of failure is considered too great. The Idaho Transportation Department (ITD) has requested that a literature review and an analytical study be conducted on some typical Idaho bridges with mechanical connections to observe their behavior in an earthquake. Three Idaho bridges were chosen for this study. Three different analytical models were made for each bridge: a model with cracked linear-elastic columns, a model with nonlinear cast-in-place (CIP) columns, and a model with nonlinear columns with grouted couplers. The models, which were written in OpenSees, were subjected to loads that might be expected in an earthquake in Idaho in the transverse and longitudinal directions. In general, the models with the grouted couplers behaved much the same as the nonlinear CIP models in both directions. The cracked linear-elastic models, however, tended to have larger column base reactions and smaller displacements in the transverse direction. The displacement/drift demand and capacity of the bridge columns were calculated using the method outlined in the American Association of State Highway and Transportation Officials (AASHTO) Guide Specifications for LRFD Seismic Bridge Design and compared with the displacement/drift results from the analytical models of all of the bridges. These calculated values were larger and therefore more conservative than the results from the analytical models. A single column from the Parma Bridge and the Dubois

Bridge were also analyzed under large drifts to observe the behavior of the coupler and the reinforcing steel. Both the Parma and the Dubois columns were able to obtain a nonlinear drift value greater than 4 percent before the coupler failed. Based on findings in this study, guidelines were presented for the use of precast columns with grouted couplers for inclusion in ITD's Idaho Bridge Design Manual.

Chapter 1 – Introduction

1.1 Problem Statement

Accelerated Bridge Construction (ABC) is an approach to the design and construction of bridges that reduces the onsite construction time of projects. Other benefits of ABC are: work-zone safety for the traveling public, reduced environmental and traffic impacts, and an improvement of site constructability. ABC technologies include, rapid embankment construction, prefabricated elements and systems, and structural placement methods. Because these technologies can save time and money the Federal Highway Administration (FHWA) encourages their use whenever practical (FHWA 2016). Consequently many departments of transportation in the United States have adopted ABC technologies. However, in states that are more seismically active not all of these technologies can be adopted.

The use of precast structural elements in bridge substructures is one of the applications used in ABC. The precast structural elements can be joined together with mechanical connections such as grouted couplers. The behavior of precast elements with mechanical connections under seismic loads differs from that of cast-in-place elements. The connections can affect the ductility of the element in the area where they are located as well as the location of plastic hinge formation in the element. To what extent these changes affect the overall performance of bridges under seismic loads needs to be understood before appropriate design procedures can be developed.

The Idaho Transportation Department (ITD) has asked that seismic analyses of precast columns in bridges with and without grouted couplers be made in order to compare the behavior of the two types of columns. Based on these analyses, a comprehensive literature review, and a

survey of current practices of selected state departments of transportation sections of ITD's *Idaho Bridge Design Manual* can be written to outline procedures for the design of bridges that have grouted couplers connecting columns to footings and/or column caps.

1.2 Project Description

There are four main steps to this project:

- First, perform a literature review of material that covers research of mechanical connections and/or seismic analysis of concrete columns with mechanical connections,
- Create computer models of selected bridges in Idaho with both cast-in-place columns and columns with grouted couplers,
- Perform a seismic analysis of each bridge model as well as single freestanding columns,
- Finally, make recommendations to ITD for the amendment of the *Idaho Bridge Design Manual* for the design of bridges with columns that have grouted couplers between the columns and the footings and the columns and the column caps.

A brief description of each step will be presented in the following paragraphs except for the literature review which will be presented in detail in Chapter 2.

Three bridges in Idaho were chosen to be modeled using the open source software framework, OpenSees. All three bridges have different design features such as column height, column shape, deck span, and girder design. They are located near the cities of Parma and Dubois, and on the Salmon River near Clayton, see Figure 1-1.

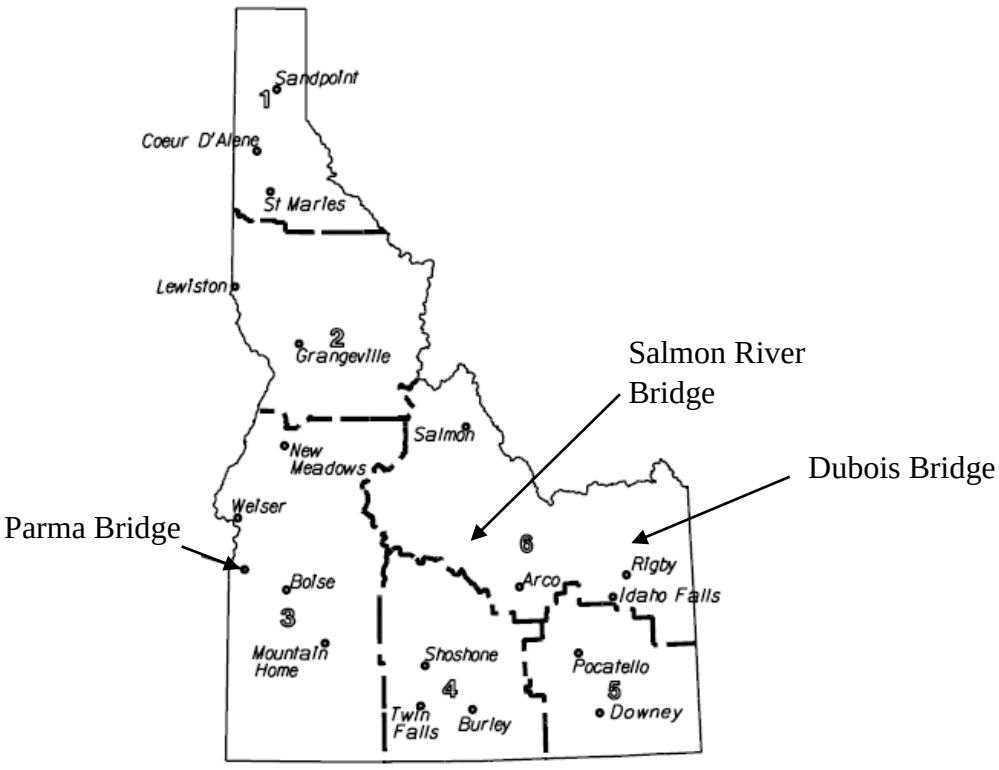

Figure 1-1. Approximate locations of the Idaho bridges selected for the project (Map taken from plans provided by ITD)

The Parma Bridge is a two span bridge with a three column bent located at the halfway point of the deck length and precast prestressed concrete girders supporting the deck. The columns are circular cast-in-place columns. The Dubois Bridge is a two span bridge with a four column bent at the halfway point of the deck length and steel girders supporting the deck. The columns are similar to Parma. The Salmon River Bridge is a three span bridge with a single oblong column in each pier. The girders supporting the deck are also precast prestressed concrete. Some changes to the design of the bridges, such as deck skew, were made in order to

simplify the modeling. It was considered appropriate to do so because the focus of the analyses was the columns and the changes made would not affect their behavior.

There are several types of mechanical connection that can be used, however the type of connection that is used in this study is a grouted coupler. Grouted couplers are cast iron sleeves which hold the ends of the connecting reinforcement in place while a cementitous grout is pumped into the sleeve from the bottom (see Figure 1-2).

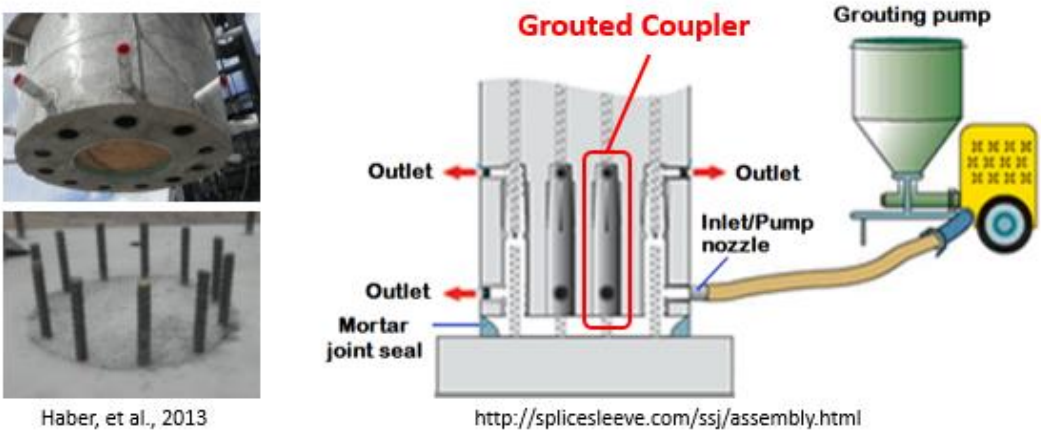

Figure 1-2. Instalation of grouted couplers (Ebrahimpour, et al. 2016)

OpenSees was used to model the bridges because it can model the nonlinear behavior of reinforced concrete with more accuracy than some other programs. In OpenSees the individual longitudinal reinforcement can be placed in exact locations within a concrete column by using a section command. Then material properties for steel and concrete can be assigned to the locations of each material. Additionally, the stress and strain at any given location within a column can be determined at any time during a test. This gives a more accurate picture of the behavior of the concrete and steel within a column.

A verification of the OpenSees code used to analyze the bridges and their columns was needed to insure the accuracy of the models. The results from tests done on half-scale concrete columns at the University of Nevada, Reno (UNR) and the FHWA *Seismic Design of Bridges Design Example No. 1* were duplicated using OpenSees. This provided some confidence in the models created for this project.

The models were developed using three types of columns; linear-elastic using a reduced second area moment of inertia which simulates a cracked section, nonlinear cast-in-place (CIP), and nonlinear columns with grouted couplers. The analyses were performed on the models with each type of column which produced three sets of results for comparison. These analyses included displacement and drift versus force in the longitudinal (along the length of the deck) and the transverse (across the deck width) directions, stress-strain curves of the most stressed reinforcement in the columns, and a comparison of the displacement and drift in the bridges against the displacement and drift capacity and demand per the AASHTO *Guide Specifications for LRFD Seismic Bridge Design*. Single columns, apart from their bridges, from the Parma and Dubois bridges were also analyzed. These analyses included determining the behavior of the reinforcement and couplers under large drifts.

Recommendations were made to ITD based on the current literature, the results from the analytical models, and the current practices of selected state departments of transportation (DOT) that use mechanical connections in precast bridge columns. The recommendations include a list of approved connections, coupler length, a drift limit, spacing and cover of longitudinal reinforcement, and a minimum for the ultimate strength of the coupler. These recommendations were derived from publications from the Utah Department of Transportation (UDOT), American

Association of State Highway and Transportation Officials (AASHTO), and the American Concrete Institute (ACI).

1.3 Thesis Overview

This thesis has seven chapters. In Chapter 1 the problem statement was presented along with a brief description of the project. Chapter 2 is a literature review. The most pertinent research concerning concrete column connections and the behavior of concrete columns in seismic areas will be presented along with a survey of current practices of selected DOT's. Chapter 3 will present the methods used in the project. The type of software and the analyses performed will be discussed in detail in this chapter. Chapter 4 is a description of the modeling and analysis of the three bridges in Idaho to be analyzed. Chapter 5 is a presentation of the analysis of a single column from the Parma Bridge and the Dubois Bridge under large drifts. Chapter 6 is the guidelines to be included in ITD's *Idaho Bridge Design Manual*. Chapter 7 is a summary of the results from Chapters 4 through 6.

Chapter 2 – Literature Review

2.1 Jansson 2008

In a report to the Michigan Department of Transportation entitled *Evaluation of Grout-filled Mechanical Splices for Precast Concrete Construction* the results of tests conducted on two different types of grout-filled mechanical connections were presented. In accordance with ASTM A1034, *Standard Test Method for Testing Mechanical Splices for Steel Reinforcing Bars* the connections underwent a combination of slip, fatigue, and ultimate load tests (ASTM 2005). Additional specimens were prepared for creep and post creep ultimate load tests. The types of connections tested were the Lenton Interlok and NMB Splice Sleeve, as shown in Figures 2-1 and 2-2.

Figure 2-1. Lenton Interlok for No. 6 steel reinforcing bar (Jansson 2008)

Figure 2-2. NMB Splice Sleeve for No. 11 reinforcing bar with longitudinal ribs (Jansson 2008)

The connections were made with No. 6 and No. 11 bar sizes. Three specimens for each bar size and connection type were fabricated for the slip, fatigue, and ultimate load test for a total of twelve specimens. The specimens were labeled using a combination of bar size, specimen designation, and connection type. The specimen designations are “A”, “B”, and “C” for the first, second, and third specimen and the connection types are “I” for Lenton Interlok and “N” for NMB Splice Sleeve, so the third specimen with a No. 6 bar of the NMB Splice Sleeve would be labeled 6CN. The specimens for the creep tests were only made with No. 6 bars and their designations were “D”, “E”, and “F”. These specimens had different combinations of epoxy coated and non-epoxy coated bars to observe the effect that had on slip.

The predominant mode of failure for the NMB Splice Sleeve connections was bar pull out, however some of the connections failed by fracture of the splice sleeve or reinforcing bar away from the connection. In the Lenton Interlok connections the reinforcing bars in the

threaded region of the bars tended to fail in shear. All the specimens tested for slip met the American Association of State Highway and Transportation Officials (AASHTO) Load and Resistance Factor Design (LRFD) requirements of less than or equal to 0.01 in. Also, all the specimens tested for fatigue at a stress range of 18 ksi (from 6 to 24 ksi) after 1,000,000 cycles passed the test. When tested to failure the specimens achieved more than 125% of the yield strength of the rebar (125% F_y) or 125% of 60,000 psi. as per the AASHTO LRFD requirements. In Figure 2-3 it can be seen that the NMB Splice Sleeve connections with a No. 6 rebar attain an ultimate strength of 102,000 psi. ($45{,}000lb/0.44in^2$) which is well above the 125% F_y. For the No. 11 bar, see Figure 2-4, with a cross-sectional area of 1.56 in.^{2} the ultimate strength is approximately 102,500 psi.

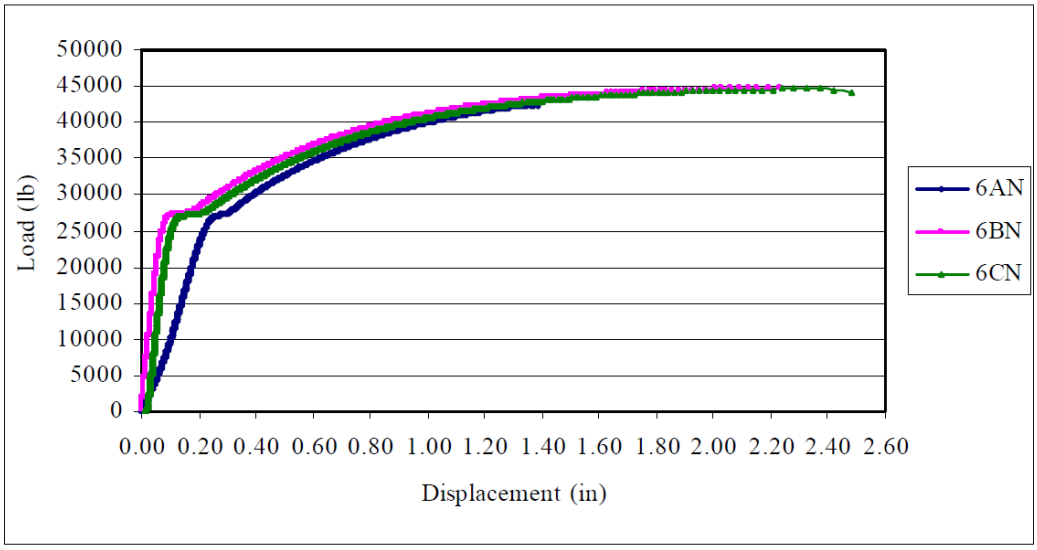

Figure 2-3. Load vs. Displacement for Specimens 6AN, 6BN, and 6CN (Jansson 2008)

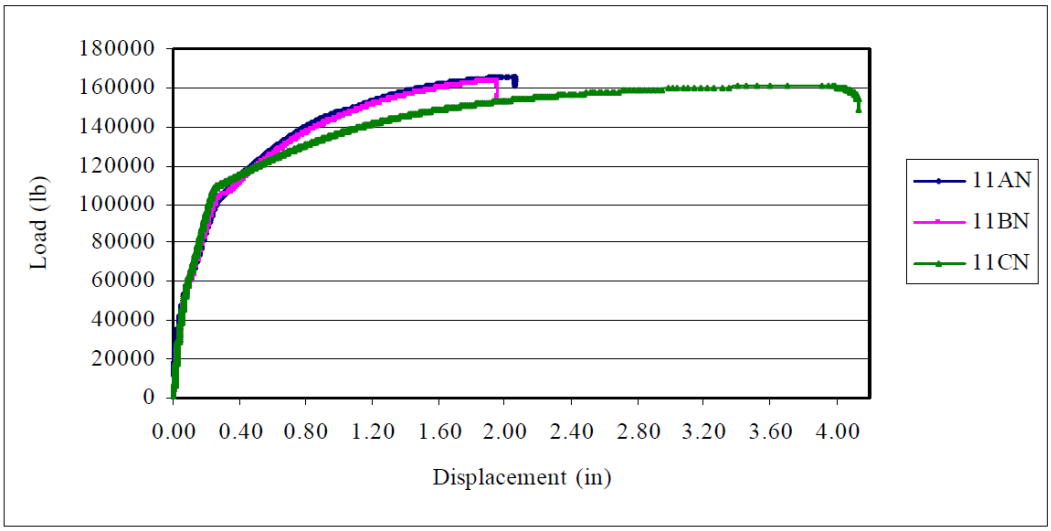

Figure 2-4. Load vs. Displacement of specimens 11AN, 11BN, and 11CN (Jansson 2008)

The epoxy coating in the creep tests did not appear to make a difference in the performance of the connections. Also all the specimens exceeded the American Concrete Association (ACI) and International Code Council (ICC) requirements in ACI 318 and ICC ACI 133 for Type 2 connections of 100% of tensile strength (F_t). (Jansson 2008)

2.2 Haber, Saiidi, and Sanders 2013

This study, conducted at the University of Nevada, Reno (UNR), entitled *Precast Column-footing Connections for Accelerated Bridge Construction in Seismic Zones,* had as its main purpose to develop, test, analyze, and evaluate precast column-to-footing connections in moderate to high seismic zones. It was comprised of three parts which were: 1) the testing of individual bar connections with static and dynamic tensile loading, elastic slip testing, and cyclic loading tests, 2) the testing of five half-scale column models under reverse slow cyclic loading, and 3) analytical studies for parametric studies and the development of design recommendations.

After reviewing the literature on various commercially available splices, two connection types were chosen to be studied, the grout-filled sleeve coupler and the up-set headed coupler (see Figure 2-5).

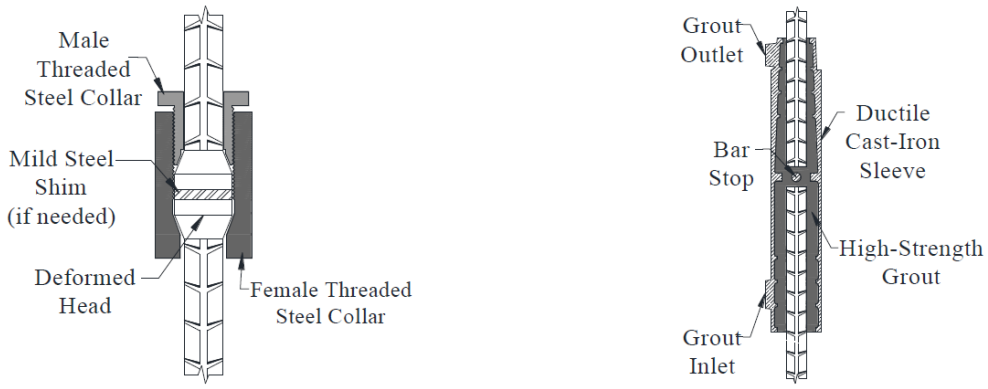

(a) Up-set headed coupler (b) Grout-filled sleeve coupler

Figure 2-5. Mechanical splices used in this investigation (Haber, et al. 2013)

There is little difference between the results of the static and dynamic tensile tests for the two couplers (see Figure 2-6). The grout-filled sleeve coupler had a similar elastic response and yield stress compared to the control bar. In most cases the splices were able to develop the full tensile capacity of the spliced bar. The up-set headed coupler also performed well under static and dynamic loading and showed little reduction in both ultimate stress and ductility.

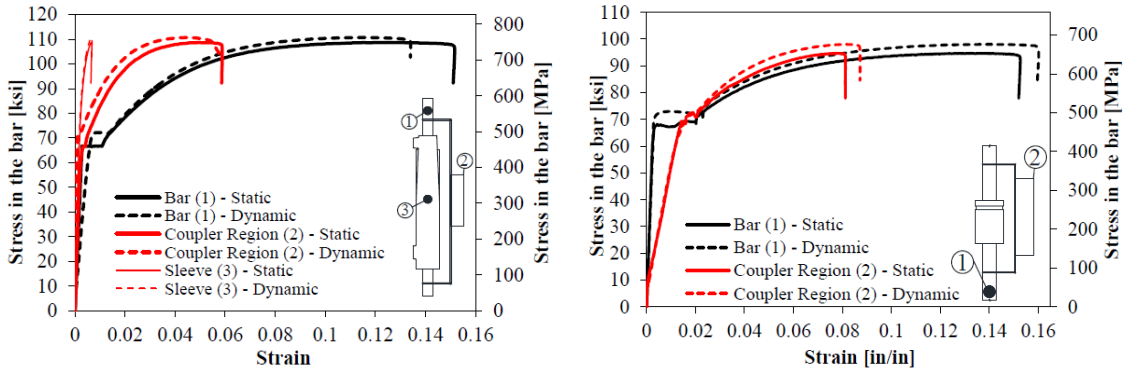

(a) Grout-filled sleeve coupler (b) Up-set headed coupler

Figure 2-6. Comparison of static and dynamic stress-strain behavior of grout-filled sleeve couplers and up-set headed couplers (Haber, et al. 2013)

The five half-scale column models consisted of one cast-in-place (CIP) model, which was used to compare to the models with mechanical connections, two columns with grout-filled sleeve couplers, and two with up-set headed couplers. The four columns with mechanical connections were designed such that two were connected directly to the footing and two were connected to a precast pedestal, which was done in order to place the connection outside the plastic hinge zone. The grout-filled sleeve couplers were given the abbreviation (GC) and the up-set headed couplers (HC). The connections with pedestals were designated by the letters (PP) and without the pedestals (NP). Therefore, the connection with grout-filled sleeve couplers and no pedestal was designated (GCNP) and with the pedestal (GCPP). The connection with the up-set headed coupler and no pedestal was designated (HCNP) and with the pedestal (HCPP). An illustration of the HCNP, GCNP, and GCPP can be seen in Figure 2-7. The design parameters for the five half-scale models can be seen in Table 2-1.

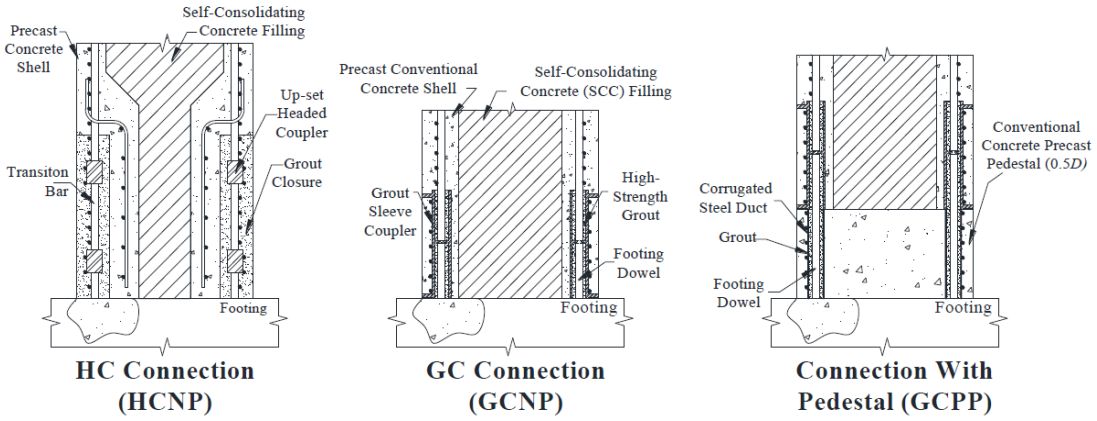

Figure 2-7. Precast connection details (Haber, et al. 2013)

Table 2-1. Half-scale column model design parameters (Haber, et al. 2013)

Design Parameter	Details
Cross-Section	Circular - 24 in [610 mm] Diameter
Cantilever Height	108 in [2743 mm]
Longitudinal Reinforcement	11 - No. 8 [D25] Bars
Longitudinal Reinforcement Ratio	1.92%
Transverse Reinforcement	No. 3 [D9.5] Spiral - 2-in [51-mm] Pitch
Transverse Reinforcement Ratio	1.05%
Aspect Ratio	4.5
Maximum Clear Cover	1.75 in [44.5 mm]
Design Axial Load	226 kip [1005 kN]

The column models were tested using a drift-based displacement-control loading protocol. They were subject to two full push and pull cycles to various drift levels up to 10% or until failure. In general the HC models performed better than the GC models. The force-displacement relationship of the HCNP and GCNP compared to the CIP can be seen in Figure 2-8. The HCNP model has a more similar response to the CIP than the GCNP model in these graphs. The GCNP does not achieve more than 6% drift at 75 kip in the pull direction before it fails. However, the HCNP achieves approximately 10% drift which is similar to the CIP.

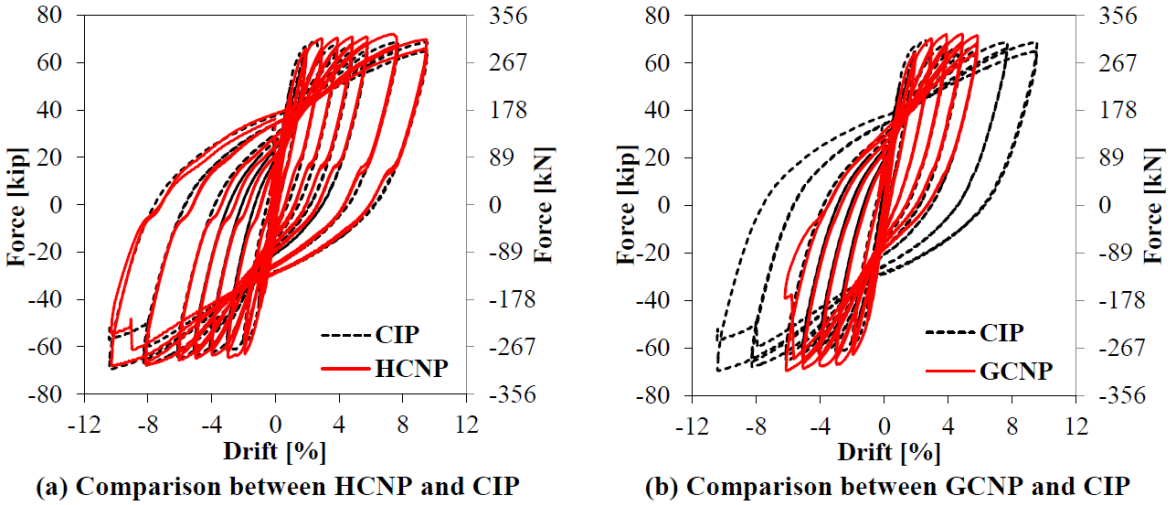

Figure 2-8. Hysteretic force-displacement behavior (Haber, et al. 2013)

The HC models also showed similar displacement ductility (a ratio of the ultimate strain to yield strain) to the CIP but the GC models were less. The progression of damage states for all the models was similar. Figure 2-9 shows the damage states for the columns using the definitions prescribed in Vosooghi and Saiidi (2010). Figure 2-10 shows the displacement ductility of all the models with the damage states.

(a) DS-1 (b) DS-2 (c) DS-3 (d) DS-4 (e) DS-5

Figure 2-9. Damage states observed in half-scale test models. (Haber, et al. 2013, Vosooghi and Saiidi 2010)

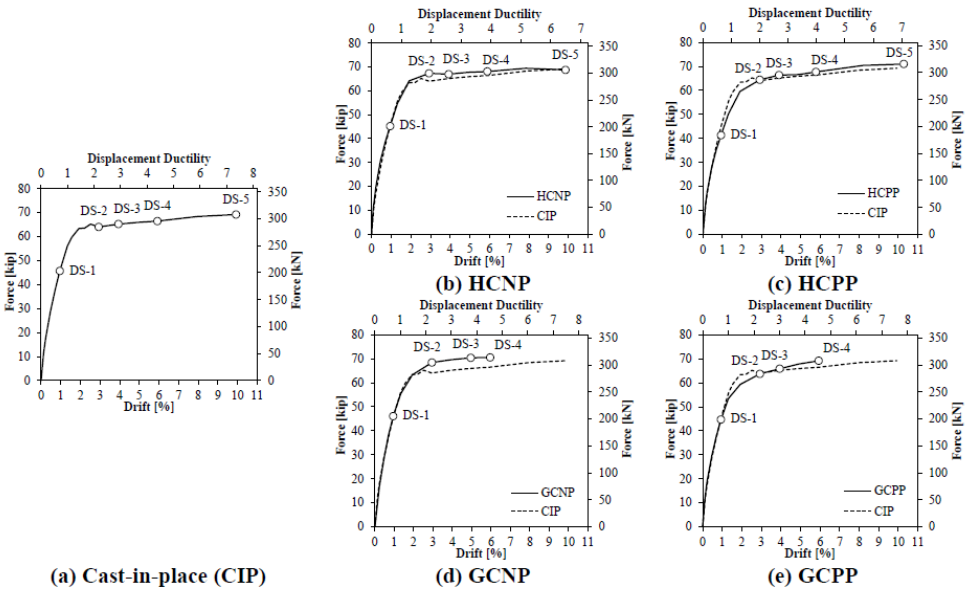

Figure 2-10. Force-displacement envelopes with damage progression indicators (Haber, et al. 2013)

OpenSees was used to model the columns and the results were compared to the experimental results. Figure 2-11 shows the details of the analytical model for the GCNP column. In general there was good correlation between the analytical and experimental results. For the force-displacement curve the average calculated load was 7% higher than the measured load. Figure 2-12 compares the calculated and measured hysteresis behavior for the GCNP.

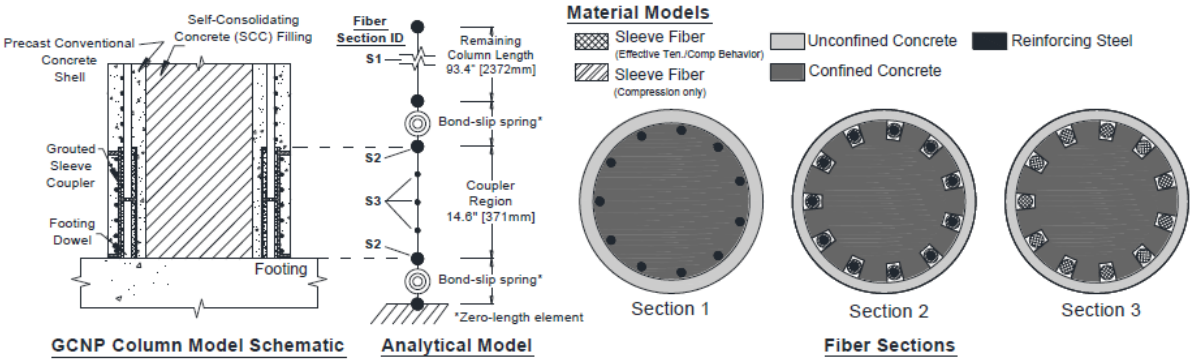

Figure 2-11. Details for the analytical model for the GCNP (Haber, et al. 2013)

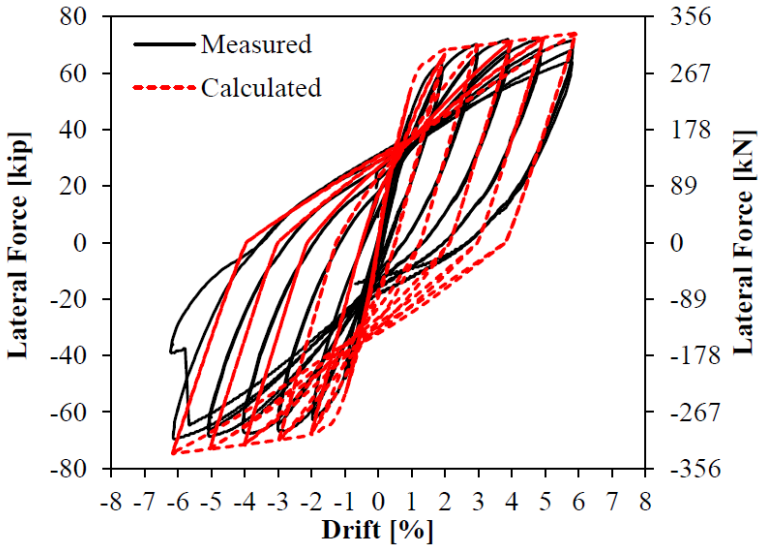

Figure 2-12. Calculated and measured hysteresis behavior of GCNP (Haber, et al. 2013)

In this study it was concluded that mechanical bar splices were a viable option for ABC substructures in seismic zones. Also, the prohibition of couplers in the plastic hinge zones in high to moderate seismic zones by California Department of Transportation (Caltrans) and AASHTO bridge seismic design documents is unnecessary. The GCNP column had a drift capacity of 6% which is adequate for high to moderate seismic zones. It is possible to create an analytical model of a column with mechanical couplers that exhibits similar behavior to the physical model. Splices that are longer than 14 bar diameters will have an effect on plastic hinge formation and behavior. (Haber, et al. 2013)

2.3 Pantelides, Ameli, Parks, and Brown 2014

In this study, entitled *Seismic Evaluation of Grouted Splice Sleeve Connections for Precast RC Bridge Piers in ABC,* eight half-scale column models were tested under cyclic quasi-static loading to evaluate the performance of two commercially available mechanical

connections. The two connection types were the Fastened-Grouted Splice Sleeve (FGSS) column-to-cap beam connection, manufactured by Lenton Interlok, and the Grouted-Grouted Splice Sleeve (GGSS) column-to-footing connection, manufactured by NMB Splice Sleeve. One cast-in-place (CIP) specimen for each connection type, column-to-footing and column-to-cap beam, were tested for comparison. The FGSS and GGSS connections are shown in Figure 2-13. The specimens were half-scale models of prototype highway bridges in Utah. The column height for all specimens was 8 ft 6 in (2.6 m) with a 21 in (530 mm) octagonal cross section. Six No. 8 (25M) longitudinal bars in a circular arrangement and a No. 4 (13M) transverse spiral with a pitch of 2 ½ in (64 mm) made up the column reinforcement. The longitudinal and volumetric transverse reinforcement ratios were 1.3% and 1.9%, respectively. Dowel bar tails were bent inward (see Figure 2-14) to achieve a better performance under lateral cyclic loads as required for seismic design category D in accordance with AASHTO LRFD *Seismic Bridge Design*.

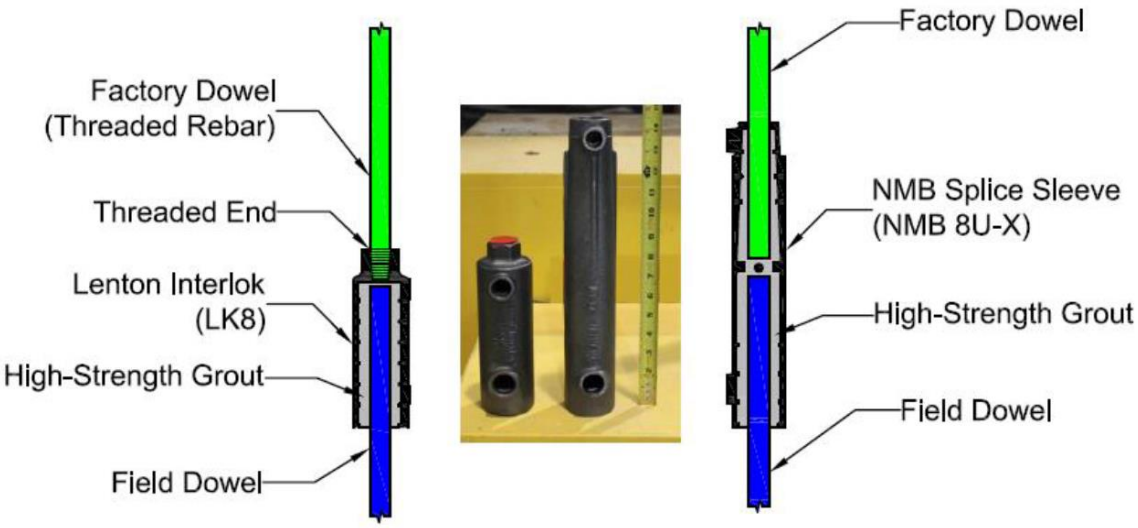

Figure 2-13. The FGSS (left) and GGSS (right) connections used in this research (Pantelides, et al. 2014)

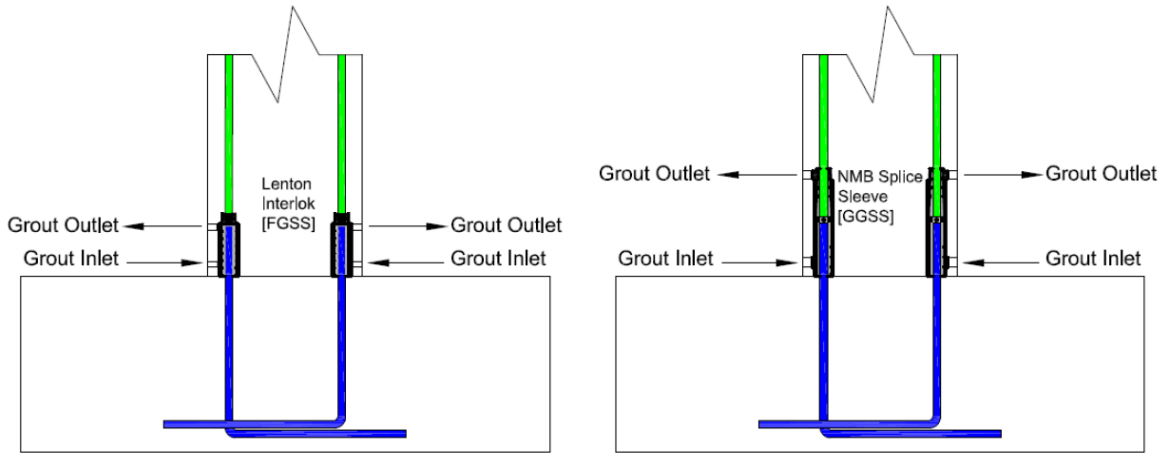

Figure 2-14. FGSS vs. GGSS connections showing dowel bars (Pantelides, et al. 2014)

As shown in Figure 2-15, the specimens with column-to-cap beam connections were tested in an inverted position. The configuration of the different specimens can be seen in Figure 2-16. The displacement history for the reversed cyclic quasi-static displacement-control protocol can be seen in Figure 2-17. Two cycles were employed for each drift ratio and a five minute pause occurred between each drift ratio.

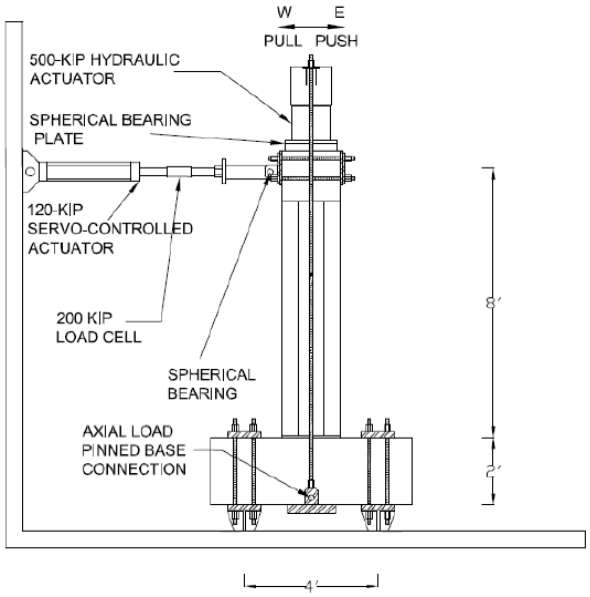

Figure 2-15. Schematic test setup for column-to-footing and column-to-cap beam connection (Pantelides, et. al, 2014)

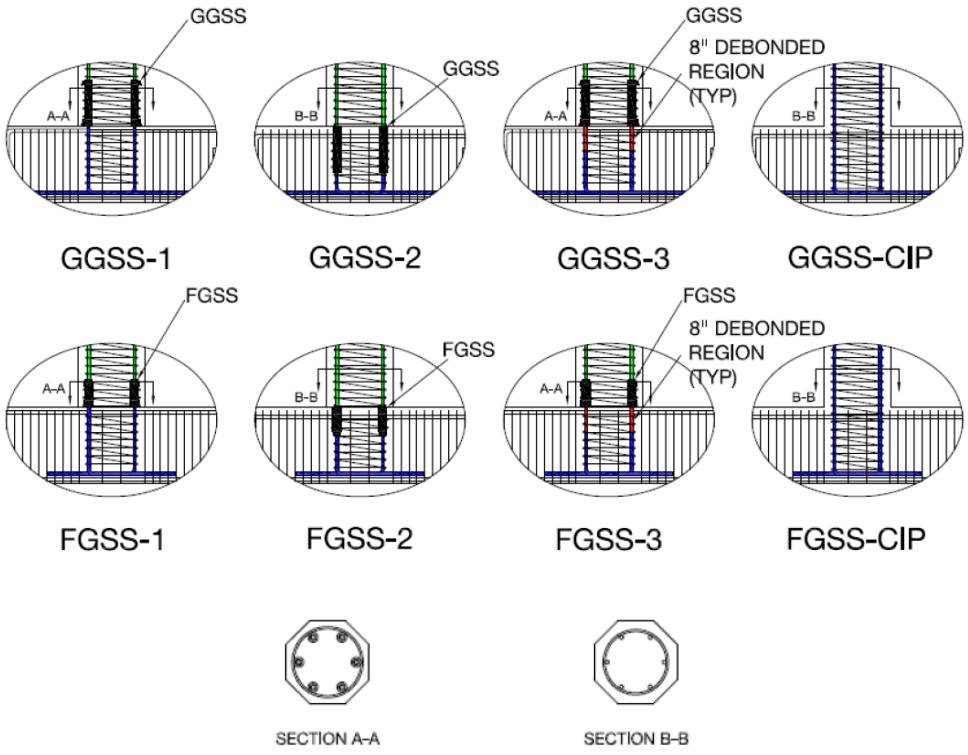

Figure 2-16. Configuration of test specimen alternatives (Pantelides, et al. 2014)

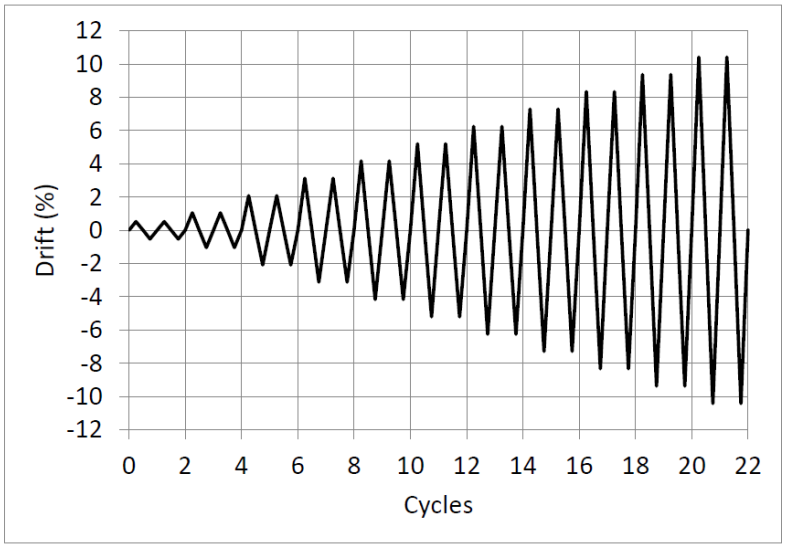

Figure 2-17. Displacement history (Pantelides, et al. 2014)

Because the research project presented in this thesis was primarily concerned with a connection similar to the GGSS-1 specimen, the results for this connection type will be emphasized. Figure 2-18 shows the lateral force-displacement of the GGSS-1 specimen with major damage states. The hysteretic response has wide and stable loops up until 7% drift ratio. The test was terminated at 9% drift ratio due to a drop larger than 20% in lateral force. Displacement ductility (the ratio of the ultimate displacement to the yield displacement) indicates the ability of a structural component to perform beyond the yield point without excessive strength deterioration. Figure 2-19 shows the average backbone curve for GGSS-1. The yield displacement is 1.45 in. and the ultimate displacement is 7.79 in. which gives a displacement ductility of 5.4. The displacement ductilities of all specimens were more than 3.0 which is the minimum required in the Caltrans (California Department of Transportation) *Seismic Design Criteria* (SDC). Figures 2-20 and 2-21 show the force-displacement response for all the specimens with the displacement ductility. The GGSS-1 specimen showed more localized damage compared to the CIP specimen that had the same detailing as the three GGSS specimens.

This involved fewer flexural cracks along the height of the column and a smaller spalled region. This specimen also had greater lateral force capacity due mostly to the GGSS being in the column which leads to the partial transition of the flexural action to the section above the GGSS. (Pantelides, et al. 2014)

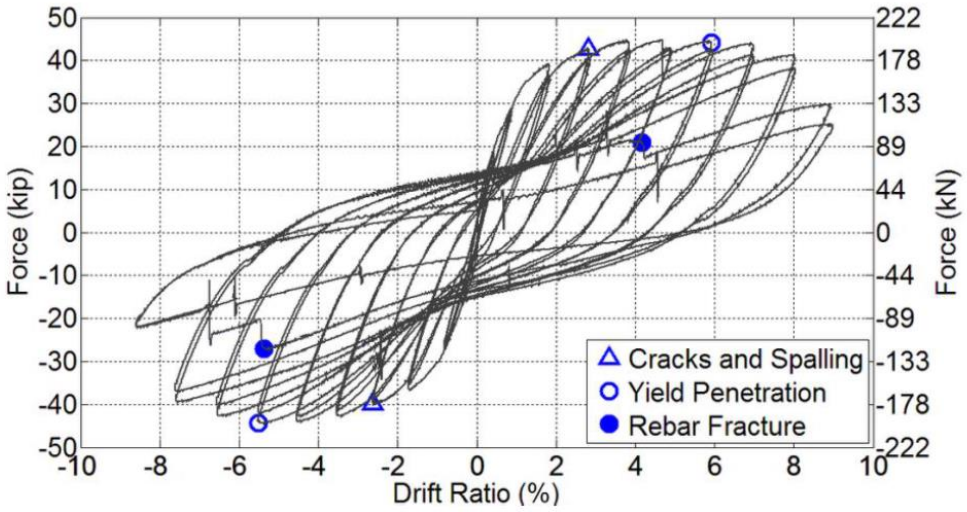

Figure 2-18. Hysteresis response of precast concrete specimen GGSS-1 (Pantelides, et. al, 2014)

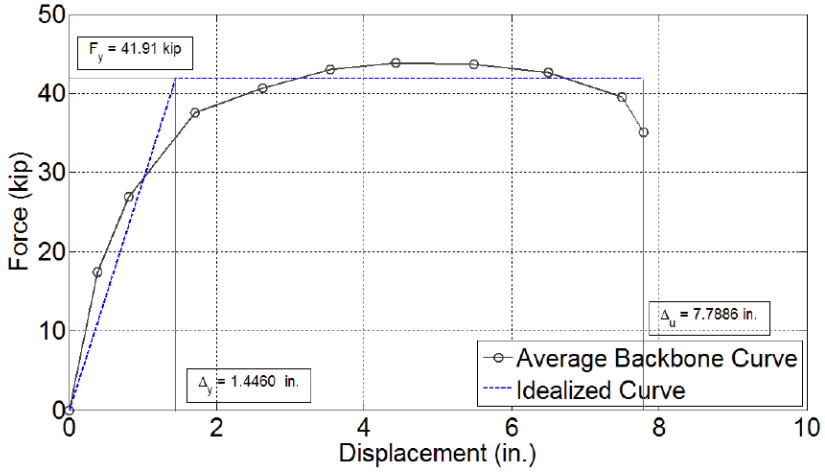

Figure 2-19. Average backbone curve for GGSS-1 (Pantelides, et. al, 2014)

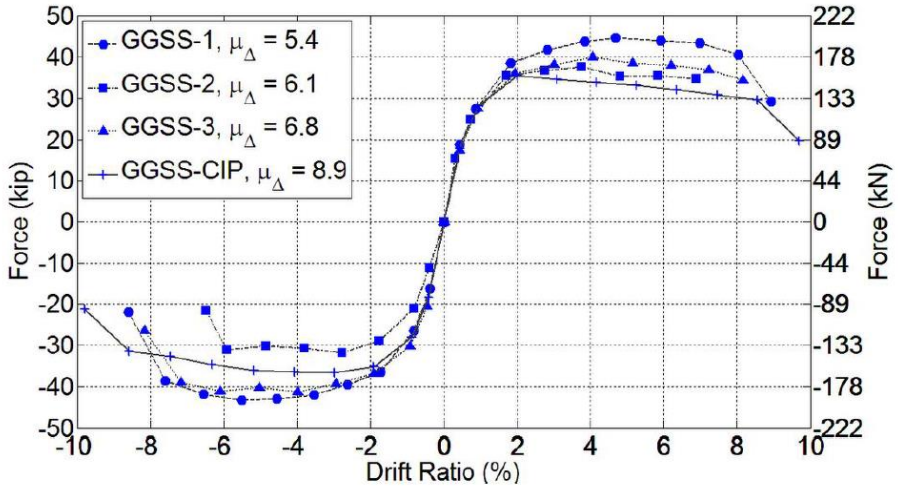

Figure 2-20. Force-displacement response for all GGSS specimens. Note μ_{Δ} = displacement ductility (Pantelides, et. al, 2014)

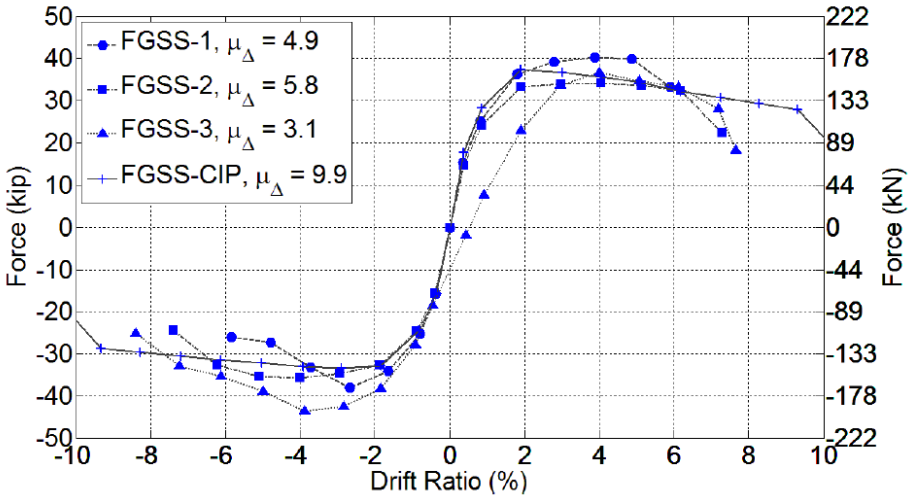

Figure 2-21. Force-displacement response for all FGSS specimens (Pantelides, et. al, 2014)

2.4 Haber, Saiidi, and Sanders 2015

In this study the deformation characteristics of two types of commercially available mechanical reinforcing bar splices were evaluated. These were the upset headed coupler (HC) and the grouted sleeve coupler (GC), see Figure 2-22. Results from the uniaxial tests were

compared to results from previous research conducted by the authors on half-scale column models in order to develop a simple method to calculate member deformation and capacity.

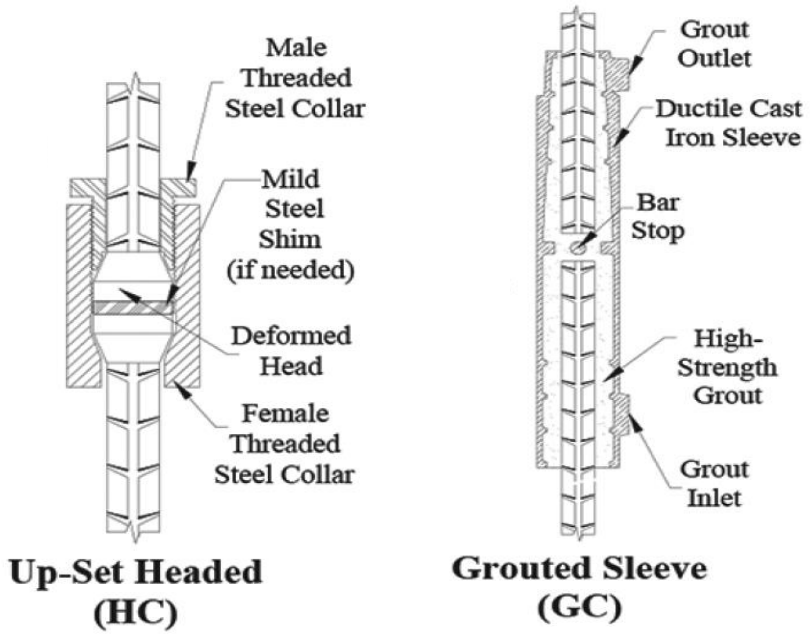

Figure 2-22. Up-set headed (HC) and grouted sleeve (GC) coupler
(Haber, et al. 2015)

Test setup and instrumentation for uniaxial load tests and slip test are shown in Figure 2-23. The coupler region length (L_{CR}) is the splice length (L_{Sp}) plus four bar diameters ($4d_b$) from both ends of the splice. Strain gages were placed on the rebar outside of the coupler region and a digital extensometer measured the strain along the length of the splice. For the GC test specimens, strain gages were placed on the coupler at its midheight. These test setups were used for the static and dynamic monotonic tests.

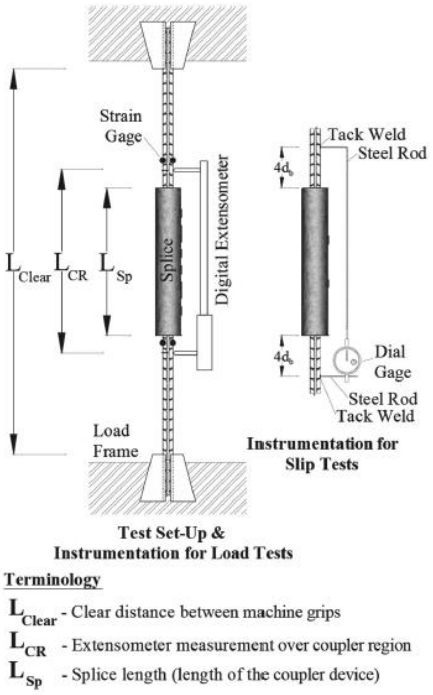

Figure 2-23. Uniaxial test setup and instrumentation plans (Haber, et. al, 2015)

Figure 2-24 shows the relationships between the strain of the rebar and that of the coupler region or the splice called the splice bar strain ratio (SR). These relationships indicate the relative stiffness of the splice to the reinforcing bar.

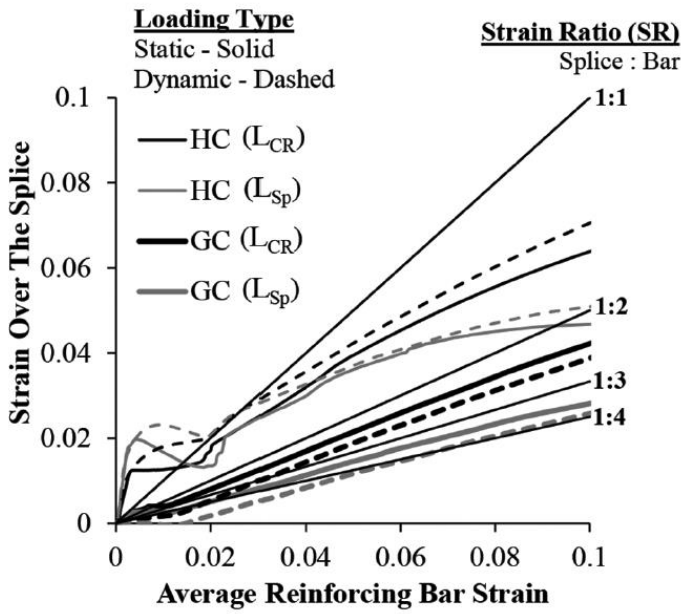

Figure 2-24. Relationships between strain in reinforcing bar and strain over splice (Haber, et al. 2015)

In the previous study an analytical model was developed using the OpenSEES program that showed good correlation to the data acquired from the tests. A new stress-strain curve, called the "Proposed Model", was created using the SR ratios from the current study in order to simplify the analytical model. Figure 2-25 shows the new stress-strain curve compared to an average stress-strain curve for mild steel. After tensile test results are known elastic SR_E and plastic SR_I strain ratios can be calculated with the equations:

$$\frac{\varepsilon_y^*}{\varepsilon_y} = \frac{E_s}{E_s^*} = SR_E \tag{2-1}$$

$$\frac{\varepsilon_u^*}{\varepsilon_u} = \frac{\varepsilon_{sh}^*}{\varepsilon_{sh}} = \frac{E_{sh}}{E_{sh}^*} = SR_I \tag{2-2}$$

Additionally, to avoid inaccurate calculations in the plastic zone if there is a yield plateau,

$$\frac{SR_I}{SR_E} \geq \frac{\varepsilon_Y}{\varepsilon_{sh}} \tag{2-3}$$

These values were used in the available OpenSees model *"ReinforcingSteel"* along with *"Concrete01"* and *"Concrete04"* for the cover concrete and confined concrete, respectively.

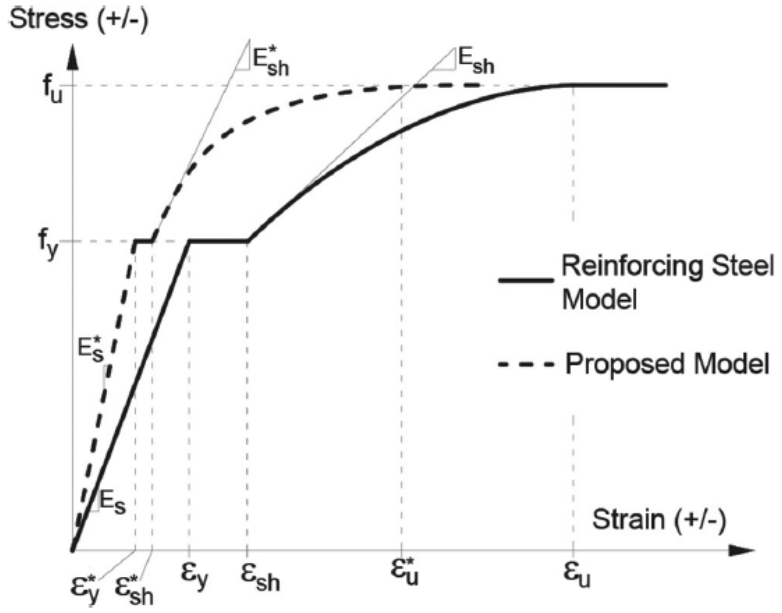

Figure 2-25. Stress-strain model for reinforcing steel and proposed splice model (Haber, et al. 2015)

In the analytical models two fiber sections were used, one for a cross-section with reinforcing bars (S_1) and one for a cross-section with the splice (S_2). The section with the splice uses the scaled values of the proposed model and the same cross-sectional area as the reinforcing steel. A space with the same cross-sectional area as the splice was removed from the concrete at

the location of the splices to keep the material properties from adding together and skewing the results. Figure 2-26 shows the proposed analytical model for the column.

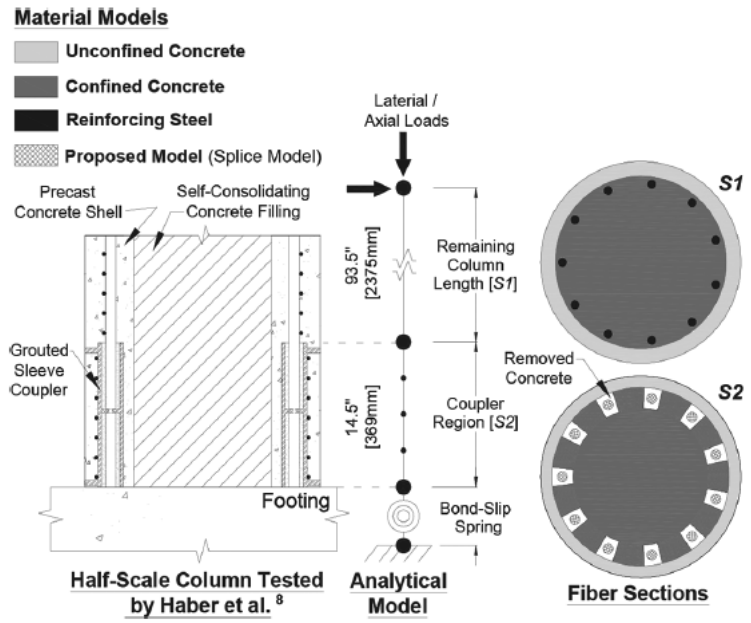

Figure 2-26. Analytical model for bridge column with grouted sleeve column-footing connection (Haber, et al. 2015)

The calculated results using the proposed model compared well with the measured results from the half-scale column model tests. The proposed model was used with and without bond-slip for a comparison. Although there was better agreement with the bond-slip the model without the bond-slip was adequate. Figure 2-27 shows the measured and calculated force-displacement response with and without bond-slip. The location of the first yield is indicated by circles on the backbone curves. (Haber, et al. 2015)

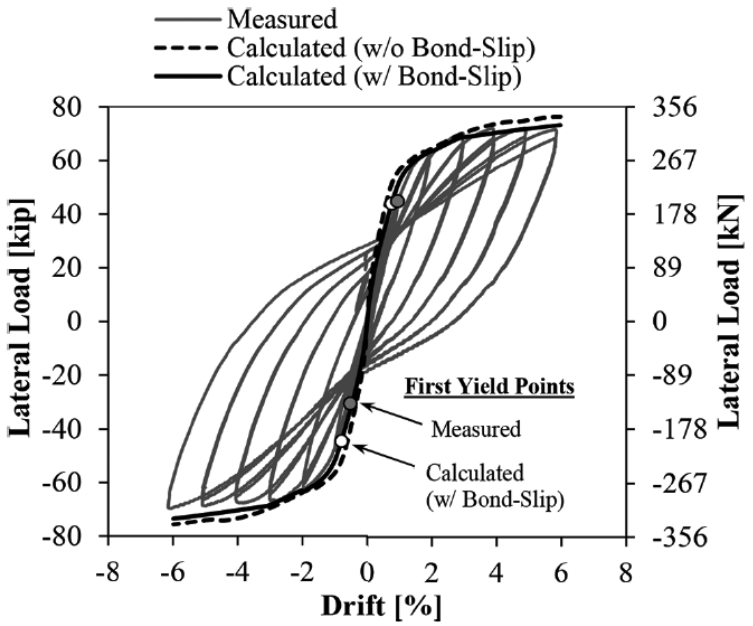

Figure 2-27. Comparison between measured and calculated force-displacement response (Haber et al. 2015)

2.5 Tazarv and Saiidi 2015

The main objectives of this study are (1) to conduct a literature search, (2) determine the characteristic seismic performance of different couplers, (3) to evaluate the constructability of different coupler types and columns with these couplers, (4) to develop a method to estimate mechanically spliced column displacement ductility capacities, and (5) to develop design guidelines for prefabricated bridge columns utilizing coupler connections.

The literature search includes a summary of U.S. Codes regarding the use of mechanical couplers in high to moderate seismic zones. These include guidelines and restrictions from AASHTO, ACI, and Caltrans.

The performance of five coupler types and columns with couplers from previous studies is presented in the literature search. The coupler types are the shear screw coupler (SSC), headed bar coupler (HC), grouted sleeve coupler (GC), threaded coupler (TC), and swaged coupler (SC) see Figure 2-28.

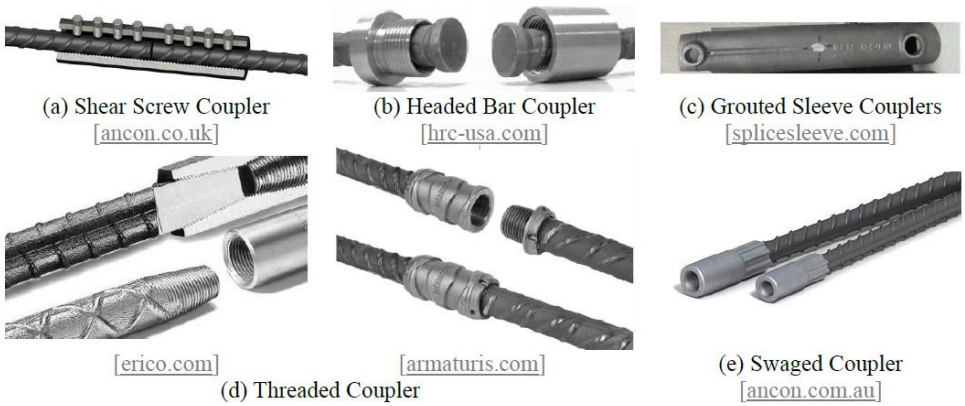

Figure 2-28. Mechanical reinforcing bar couplers (Tazarv and Saiidi, 2015)

Minimum acceptance criteria for couplers in plastic hinges were proposed based on U.S. Codes. From Caltrans and AASHTO the criteria were:

1. The total length of a mechanical bar splice (L_{sp}) shall not exceed $15d_b$ (d_b is the diameter of the smaller of the two spliced bars) to minimize adverse effects of coupler length on rotational capacity of a ductile member and

2. A spliced bar shall fracture outside coupler region regardless of loading type (e.g. monotonic, cyclic, or dynamic). The coupler region is defined as the length of a coupler plus $1.0d_b$ from each face of the coupler, see Figure 2-29. Only ASTM A706 reinforcing steel bars shall be used for seismic applications.

3. The strain capacity of a spliced bar outside the coupler region should exceed 12% for No. 10 and smaller bars. For No. 11 and larger bars the strain capacity should exceed 9%.

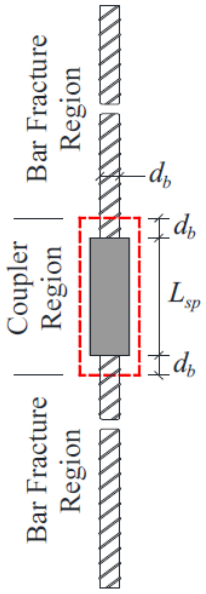

Figure 2-29. Coupler and fracture region (Tazarv and Saiidi, 2015)

The proposed acceptance criteria for columns incorporating couplers in plastic hinges are:

1. When the displacement ductility capacity of CIP is five or less, the displacement ductility capacity of columns with couplers (CWC) should be at least equal to the ductility capacity of CIP. For other cases, the displacement ductility capacity of CWC should be the greatest of 90% of CIP ductility capacity, and five.

2. The lateral load strength of CWC should not be less than 95% of the CIP strength when the displacement ductility capacity of CIP is five or less. For other cases, the lateral strength of CWC should not be less than 90% of CIP strength.

Tables 2-2 and 2-3 give a summary of the evaluations for the grouted couplers and columns with grouted couplers, respectively. Because this thesis is concerned only with the grouted couplers only those results will be shown. The performance of the grouted coupler had mixed results. One study met the minimum requirements but three others did not. For the columns only the column with the couplers half the column diameter away from the column-footing interface and debonded longitudinal reinforcing in the pedestal met the minimum requirements, see Figure 2-30.

Table 2-2. Evaluation of grouted sleeve couplers (Tazarv and Saiidi, 2015)

Study	Mode of Failure	Strain Capacity	Remark
Noureddine (1996)	Bar fractured in three tests, coupler failed in one test Length: $16d_b$	More than 11%	Not recommended
Jansson (2008)	NMB: Bar fracture (1 sample), coupler fracture (2 samples), bar pullout (3 samples) [Length: $14d_b$] Lenton Interlok: Failure of threads in all tests [Length: $8.5d_b$]	N/A	Not recommended
Rowell et al. (2009)	Bar pullout (22% of samples), bar fracture (33% of samples), coupler fracture (33% of samples) [9 samples in total] Length: $14d_b$	More than 6%	Not recommended
Haber et al. (2013)	Bar fracture, Length: $14.6d_b$	More than 13%	Recommended

Table 2-3. Evaluation of seismic performance of column test models with grouted sleeve couplers (Tazarv and Saiidi, 2015)

Reference	Coupler Length	Coupler Location	Evaluation Result
Haber et al. (2014)	$14.6d_b$: used at one level	Couplers were installed immediately above either footing surface or pedestal	Failed (both columns showed 40% lower displacement capacity compared to a reference column)
Tazarv and Saiidi (2014)	$14.6d_b$: used at one level	Couplers were installed immediately above a pedestal	Passed (column exhibited 4% lower ductility and 8% lower lateral strength compared to a reference column with ductility of 7.3)
Pantelides et al. (2014)	$14.6d_b$: standard couplers at one level	Couplers were used at one level in column-to-footing connections	Failed (columns showed 25 to 40% lower displacement ductility capacity compared to a reference column)
Pantelides et al. (2014)	$8.6d_b$: modified couplers at one level	Couplers were used in column-to-cap beam connections	Failed (columns showed 41 to 69% lower displacement ductility capacity compared to a reference column)

Note: d_b is the longitudinal bar diameter; D is either the column diameter or the column largest side dimension

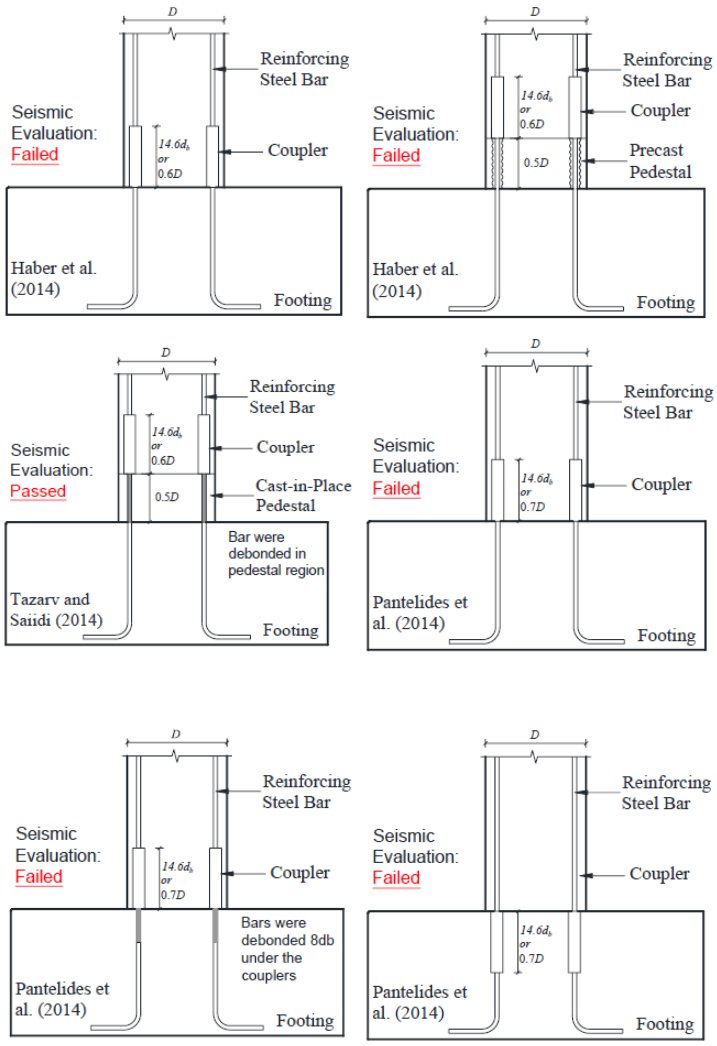

Figure 2-30. Evaluation of Columns Incorporating Grouted Couplers (Tazarv and Saiidi, 2015)

Some considerations that need to be made before a coupler type is chosen are presented in Table 2-4. Clear cover and the clear distance between couplers should be based on design codes such as AASHTO LRFD or AASHTO *Guide Specifications*. Because couplers are larger than the reinforcing bars the clear cover over the steel bars will be more than that of a cast-in-place column. Likewise, the spacing between steel bars for a column with couplers will need to be greater than that of a cast-in-place column. For grouted couplers the grout should be that provided by the manufacturer.

Table 2-4. Constructability of Mechanical Bar Couplers (Tazarv and Saiidi, 2015)

Item/Coupler	Shear Screw	Headed Bar	Grouted Sleeve	Threaded	Swaged
Bar End Preparation	Not Needed	Heading	Not Needed	Threading	Not Needed
Special Equipment	Wrench or Nut Runner	Wrench, Heading Machine	Grout Pump	Die and Tap	Press Machine
Additional Material/Piece	Screw	No Need	Grout/Sealing	No Need	No Need
Tolerance and Alignment	Loose	Tight	Loose	Tight	Loose
Field Erection Speed for precasting	Very Fast	Fast	Very Fast	Fast	Fast
Time to Complete one Splice	1 *min*	5 *min*	24 *hours*	5 *min*	5 *min*

Generally, the on-site construction time for a typical three column bent is reduced by approximately 60% for all types of mechanical bar couplers.

When the connection is in tension it is assumed that only a portion of its length contributes to its elongation. That length can be determined by the equation:

$$\varepsilon_{sp}/\varepsilon_s = \left(L_{cr} - \beta L_{sp}\right)/L_{cr} \tag{2-4}$$

β is defined as the coupler rigid length factor, L_{cr} is the length of the coupler region and $L_{sp}$is the coupler length, ε_{sp} is the strain in the coupler region, and $\varepsilon_s$is the strain of the connecting reinforcing bar.

A parametric study was done in which 12 conventional cast-in-place columns were designed using the AASHTO Guide Specification to serve as reference columns. The columns had varying displacement ductility capacities, axial load indexes, and aspect ratios. The displacement ductility is the ratio of the ultimate displacement to the effective yield displacement. The axial load index is the ratio of the axial load to the product of the specified concrete compressive strength and the column gross cross-sectional area. The aspect ratio is the ratio of the column height to the column diameter. Columns with mechanical connections were

designed with a combination of different coupler lengths, pedestal heights, rigid length factors, and spacing (S_{sp}).

A total of 560 analyses were made on the relationship of the displacement ductility capacity and the various parameters in the study. It was found that the most critical parameters were the coupler length, pedestal height, and the rigid length factor. The axial load index and the aspect ratio did not have a significant effect. Therefore a design equation was proposed to estimate the spliced column displacement ductility:

$$\mu_{sp}/\mu_{CIP} = (1 - 0.18\beta)\left(\frac{H_{sp}}{L_{sp}}\right)^{0.1\beta} \quad (2\text{-}5)$$

$\mu_{sp}$is the spliced column displacement ductility, μ_{CIP} is the non-spliced cast-in-place column displacement ductility, H_{sp} is the pedestal height, L_{sp} is the coupler length, and β is the coupler rigid length factor. A value of 0.1 in. for H_{sp} is used for columns that have the coupler placed immediately above or below the adjoining member.

Seven recommendations were made for precast bridge columns with mechanical connections along with the corresponding commentaries. The recommendations were designated R1 – R7 and the commentaries were C1 – C7. The recommendations that apply to our study are:

R2: The coupler length (L_{sp}) shall not exceed 15 times the longitudinal reinforcing bar diameter.

R3: Only couplers in which failure occurs due to bar fracture outside of coupler region shall be used in the plastic hinge zones.

R6: The displacement ductility capacity of the mechanically spliced column (μ_{sp}) shall be calculated based on the conventional cast-in-place column displacement ductility capacity (μ_{CIP}) using Eq. (2-5). (Tazarv and Saiidi 2015)

2.6 Current Practices of DOT's in Seismic Regions

In May 2015 and again in June 2016 the DOT's of several western states were contacted in regard to the use of grouted couplers in bridge column plastic hinge zones. Table 2-5 shows the results of that survey.

Table 2-5. Use of Grouted Couplers by Western DOTS in Bridge Column Plastic Hinge Zones

State	**Grouted Couplers in Column Plastic Hinge Zones**	**Comments**
Alaska	No	AKDOT prefers the use of grouted pockets or ducts when connecting precast caps to columns/piles.
California	No	The findings from UNR were presented, but it was voted not to allow grouted couplers in the plastic hinge zones columns (Haber, et al., 2013).
Hawaii	No	State of Hawaii is not currently using any ABC methodologies.
Nevada	No	Although research on ABC column connections at the University of Nevada Reno (UNR) had been considered, no ABC column connections is currently used in the State of Nevada.
Oregon	No	ODOT does not have any special specs for splices for ABC.
Utah	Yes	UDOT Structures Design and Detailing Manual has a section on grouted couplers in ABC applications. This section is based on the report by the University of Utah research reported on by Pantelides, et al. (Pantelides, et al., 2014).
Washington	No	WSDOT does not approve the use of mechanical couplers for connections of precast bridge members. The WSDOT prefers the use of grouted ducts similar to the ones used by AKDOT.

Utah's Structures Design and Detailing Manual dated Feb. 2015, Section 20.4.6.3, Commercial Grouted Splice Couplers states (UDOT, 2015):

"*… The use of grouted splice couplers is permissible in plastic hinging zones. The standard requirements for column confinement apply around the couplers. Adjust the cover to the reinforcing and spiral or ties to accommodate the larger grouted splice coupler section. Refer to the SD drawings for examples of how grouted splice couplers are used. The preferred configuration for constructability is to locate the grouted splice coupler above the joint, which reduces the chance of contamination with debris. Grouted splice couplers located below the joint must be sealed during fabrication and shipping. Also, placing the grouted splice coupler above the joint allows the reinforcing extensions at the top of the element, making shipping and handling easier. Placement of grouted couplers in the footing or in the cap improves the connection ductility capacity. Locate the coupler in the footing or in the cap when the ductility demand exceeds 4. Design the reinforcing size and grouted splice couplers to allow for crossing reinforcing patterns. Detail the spacing at approximately the maximum reinforcing spacing requirements in the LRFD Specifications. Base the spacing on the connected reinforcing. Do not use the diameter of the grouted splice couplers in the calculations. Check the clear spacing between the grouted splice couplers using the following approach.*

Use a grouted splice coupler sleeve size one reinforcing size larger than the reinforcing size used. Detail the minimum gap between the grouted splice couplers to be the greatest of the following:

- *1 in.*
- *1.33 × (maximum aggregate size of the coarse aggregate)*
- *Nominal diameter of the connected reinforcing*

Provide cover for the element based on the diameter of the grouted splice coupler. The practice requires increased cover to the reinforcing to obtain the cover over the grouted splice couplers ..."

2.7 Summary of Literature Review

In this chapter five projects involving grouted couplers were reviewed and a survey of seven western state DOT's were presented. The following paragraph presents summaries of the projects and the survey.

The Jansson 2008 project tested two kinds of grouted couplers for slip, fatigue, and ultimate strength. Additional creep tests were also conducted. The authors concluded that both

kinds of couplers fulfilled the ACI 318 and ICC ACI 133 requirements for Type 2 connections. The Haber, Saiidi, and Sanders 2013 project presented the results of half-scale columns with different coupler connections as well as cast-in-place columns. Additionally, the results from analytical models were compared to those of the physical columns. This provided a way to check the validity of the work in this current study. The Pantelides, et al. 2014 project tested two commercially available grouted couplers in half-scale columns under cyclic quasi-static loading. Because the GGSS-1 specimen was similar to the bridge columns considered in this current project the results were relevant to recommendations presented in Chapter 6. The Haber, et al. 2015 project presents a simplified method of calculating member deformation and capacity. This method was used in the current project to model the behavior of the grouted couplers used in the Idaho bridges. The Tazarv and Saiidi 2015 project evaluated different couplers with different column detailing and made recommendations based on the results. However, the performance evaluation criteria for the connections may be too stringent. The failure of a column due to a seismic event is a function of the demand on the column. If the column is restrained by other elements in the bridge the displacement ductility demand may be reduced. Therefore, requiring 95 % of the lateral load strength of CIP columns with displacement ductility capacity of five or less may be more than needed. In 2015 a survey of seven western state DOT's was made to determine what if any mechanical connections they were using in bridge design. It was found that only Utah's DOT had been using grouted couplers in bridge columns and had a section in their *Structures Design and Detailing Manual* that addressed the topic. The most relevant projects were found to be Haber, et al. 2013, Pantelides, et al. 2014, and Haber, et al. 2015.

Chapter 3 – Methods

3.1 Overview

The methods used to analyze the performance of grouted couplers in the plastic hinge zone of bridge columns under seismic conditions are presented in this chapter. The choice of the finite element software OpenSees, the modeling verification using FHWA *Bridge Design Example No. 1,* and the duplication of the single column model in the UNR study will be discussed. The computer models created from the information obtained in the two publications previously mentioned are in preparation for the models made from the three Idaho bridges that are presented in the next chapter.

In order to model the three Idaho bridges accurately results from models made using OpenSees were compared to the results from the other publications. First, models in OpenSees and STAAD were created that had similar results to that of an example published by the FHWA which uses the finite element software SAP. Also, the results from the research at UNR were compared to models for the current research for both a cast-in-place (CIP) column and a column with grouted couplers and no pedestal (GCNP).

The GCNP model will use the simplified method outlined in Haber et al. 2015. The results from uniaxial tensile tests conducted by the manufacturer of the couplers, Splice Sleeve North America (SSNA), were used to calculate the material properties for the simplified method. How the material properties calculated from the data obtained from SSNA were used are discussed in this chapter. The results from the measured and calculated hysteretic force-displacement analyses and the pushover analyses for the UNR project are compared to the analytical results of the column models created in this study.

3.2 Computer Model Verification

3.2.1 FHWA Seismic Design of Bridges – Design Example No. 1

The development of the OpenSees software framework is sponsored by the Pacific Earthquake Engineering Research (PEER) Center at the University of California, Berkeley. Its purpose, in part, is to simulate the behavior of structures subjected to seismic loads. There are a number of finite element software packages available that could be used to analyze structures, however, OpenSees can be used to model and analyze the nonlinear behavior of steel and concrete given its material properties. Since the purpose of this study is to compare the performance of columns with grouted couplers to that of cast-in-place columns OpenSees was determined to be the best fit for this study (UC Berkeley 2016).

To gain some confidence in the author's ability to model the Idaho bridges in OpenSees a computer model from the FHWA *Seismic Design of Bridges, Design Example No. 1* was duplicated using both STAAD and OpenSees and comparing the results with those presented in the example. The bridge in the example is modeled with various support conditions and loads using the finite element analysis software SAP. For simplicity, the uniform load method was used for the verification. For the support conditions the basic condition (rigid condition at the column-to-footing connection) and spring supports at the column-to-footing connection were used, making two models in both STAAD and OpenSees. An additional model in OpenSees with reinforcing steel and basic support conditions was made for a total of five models. The STAAD and OpenSees models were given the same number of nodes and elements as the SAP model except that an extra element at the top of the columns was needed to duplicate the rigid condition specified in SAP. Additionally, the OpenSees models required a geometric transformation and

for the spring supports elements called *zeroLength* elements with no physical length were used. The geometric transformation defines the relationship of the local axes of an element to the global axes with a vector in the xz plane of the local axes. The models' dimensions and a more detailed explanation of the geometric transformation along with the input command files for STAAD and OpenSees are presented in Appendix A.

The results from the STAAD model were more similar to the Example 1 model than the OpenSees model. However, all the results were within 0.22 inches of the maximum displacements of the Example 1 models except for the reinforced OpenSees model in the longitudinal direction. This result had a difference of four inches. The results of the STAAD and OpenSees models with the Example 1 results are presented in Appendix A (Mast, et al. 1996).

3.2.2 Half-scale Column Models from Haber et al. 2013

The analytical models of two of the half-scale columns found in the study conducted at UNR were recreated and the results compared with those presented in the UNR study. The CIP column and the grouted coupler with no pedestal (GCNP) column were used because they would be similar to the columns that would be modeled in the Idaho bridges. The input files for the UNR columns were not available, however, sufficient information about the columns and testing procedures were found in the UNR report so that it was possible to create an analytical model that produced similar results (Haber, et al. 2013).

The CIP model from Haber et al. 2013 has six nodes and five elements, as shown in Figure 3-1. The element designated E1 is a *zeroLength* element that acts as a spring and can be used to model bond-slip at the base of the column. The main section of the column is a *nonlinearBeamColumn* element with a fiber section also shown in Figure 3-1. The fiber section

uses the material models available in OpenSees, *Concrete01*, *Concrete04*, and *ReinforcingSteel*, for the unconfined concrete, the confined concrete, and the longitudinal steel, respectively. The remaining three elements at the top of the column, E3, E4, and E5, are *elasticBeamColumns* which have linear-elastic behavior and high stiffness values. The material properties found in the Haber study were used for the models in the verification (Haber, et al., 2013).

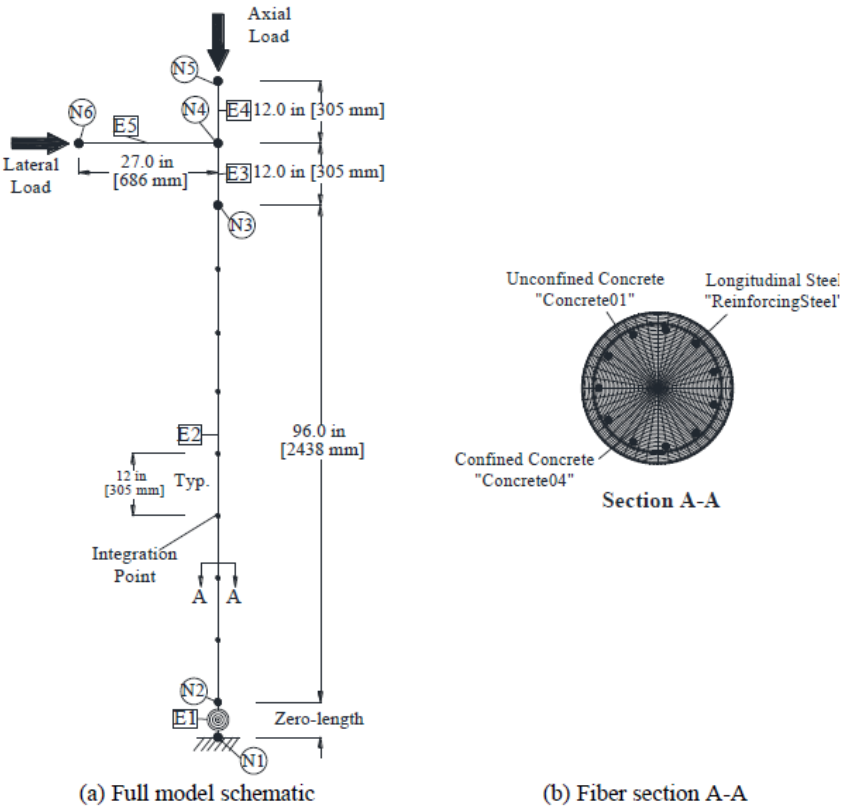

Figure 3-1. The OpenSees model of the UNR cast-in-place column (Haber et al. 2013)

At the interface of the column base and the footing, strain in the longitudinal reinforcing steel causes the column to rotate about the neutral axis, as seen in Figure 3-2. This is known as bond-slip rotation. To model bond-slip rotation in OpenSees a *zeroLength* element is used with material properties defined by a *uniaxialMaterial Hysteretic* command. The material properties

are determined by a moment-curvature analysis of the cross-section of the column. An OpenSees input file was created to record the stresses and strains at the locations of the most stressed longitudinal steel in the column when a moment is applied to the cross-section. Then the slip was calculated using the method presented in Wehbe et al. (1999). The OpenSees Tool Command Language (tcl) script for the moment-curvature analysis and a detailed discussion of bond-slip rotation calculation can be found in Appendix B (Haber, et al. 2013).

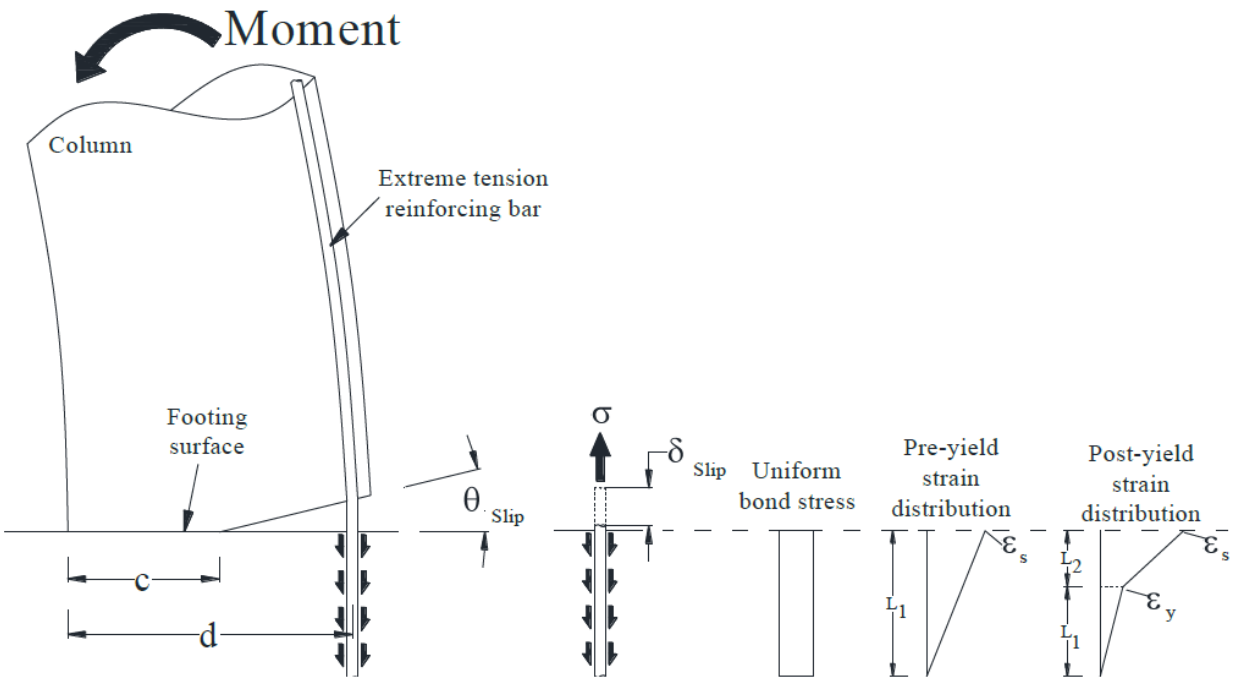

Figure 3-2. Wehbe's method of calculating bond-slip rotation (Wehbe, et al. 1999)

A graph of the moment versus rotation creates a bi-linear curve such as that shown in Figure 3-3. An idealized curve is fitted to the graph and the stress and strain at the first point of inflection $(M_{y,eff}, \theta_{y,eff})$ and the ultimate stress and strain (M_u, θ_u) are used in the *uniaxialMaterial Hysteretic* command in OpenSees to create the spring behavior at the base of the column. Because of the non-symmetrical layout for the longitudinal steel the values for the negative or "pull" direction are different from the values for the positive or "push" direction.

However, these values are within 5 percent of each other so it was decided to only use the push values calculated for this study in the column models. The values found in the Haber study and those calculated for this study, which are referred to as "ISU" values, can be seen in Table 3-1 (Haber, et al., 2013).

Table 3-1. Moment versus rotation values for the first point of inflection and the ultimate stress and strain

	UNR		ISU	
	Moment (kip-in.)	**Rotation (rad)**	**Moment (kip-in.)**	**Rotation (rad)**
Point 1	6,746	0.0028	6,580	0.0021
Point 2	7,859	0.0452	7,883	0.0422

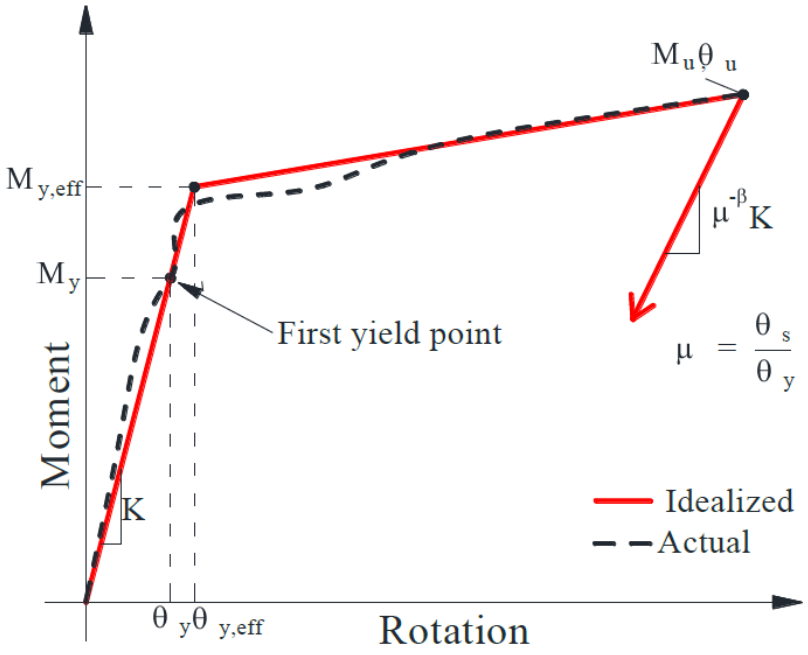

Figure 3-3. Moment rotation relationship for bond slip (Haber et al. 2013)

A constant axial load of 208 kip was applied at N5 and for the hysteretic force-displacement analysis a horizontally-applied displacement-controlled increasing cyclic load was applied at N6. For the pushover analysis, a horizontal load of 200 kips was applied at N6. The position for the axial and horizontal loads for the analytical model are shown in Figure 3-1. The loading protocol from the UNR experiments for the hysteretic force-displacement analysis can be seen in Figure 3-4. The horizontal displacement can be calculated by multiplying the drift times the height of the column, which is 9 feet (Haber, et al., 2013).

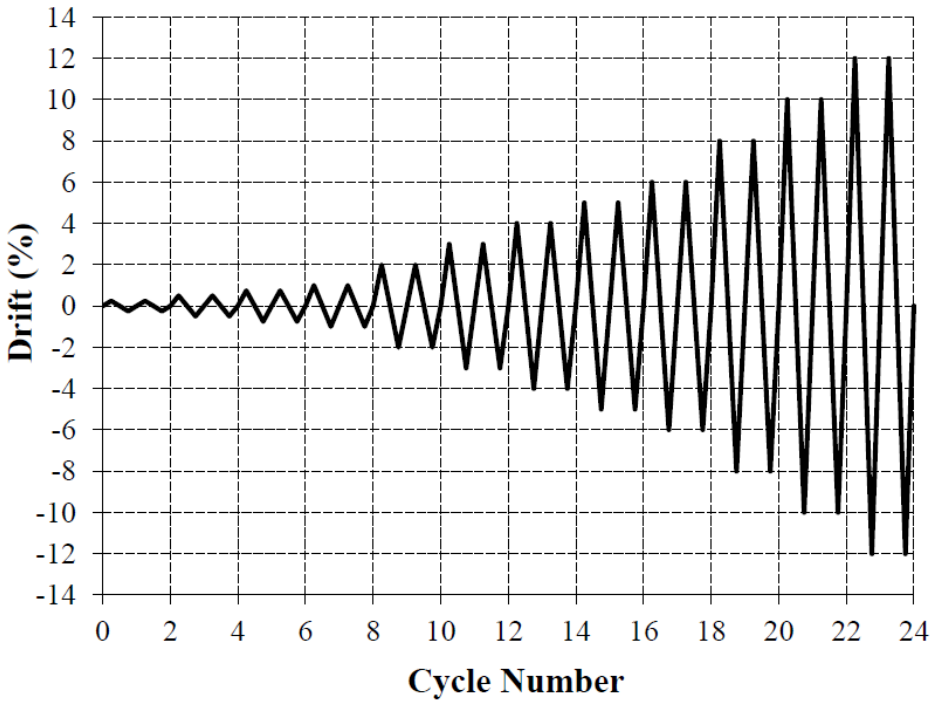

Figure 3-4. Loading protocol (Haber et al. 2013)

In Figure 3-5, UNR's experimentally measured and calculated results are compared with ISU's calculated results for the hysteretic force-displacement analysis. In Haber et al. (2013) the measured and calculated results were considered to have good correlation. Any differences were determined to be due to the reinforcement cage not being centered in the column. UNR's

measured and calculated average envelope curves can be seen in Figure 3-6 (a). The ISU pushover curve can be seen in Figure 3-6 (b). The OpenSees input files for the hysteretic force-displacement analysis and the pushover analysis are presented in Appendix B (Haber, et al., 2013).

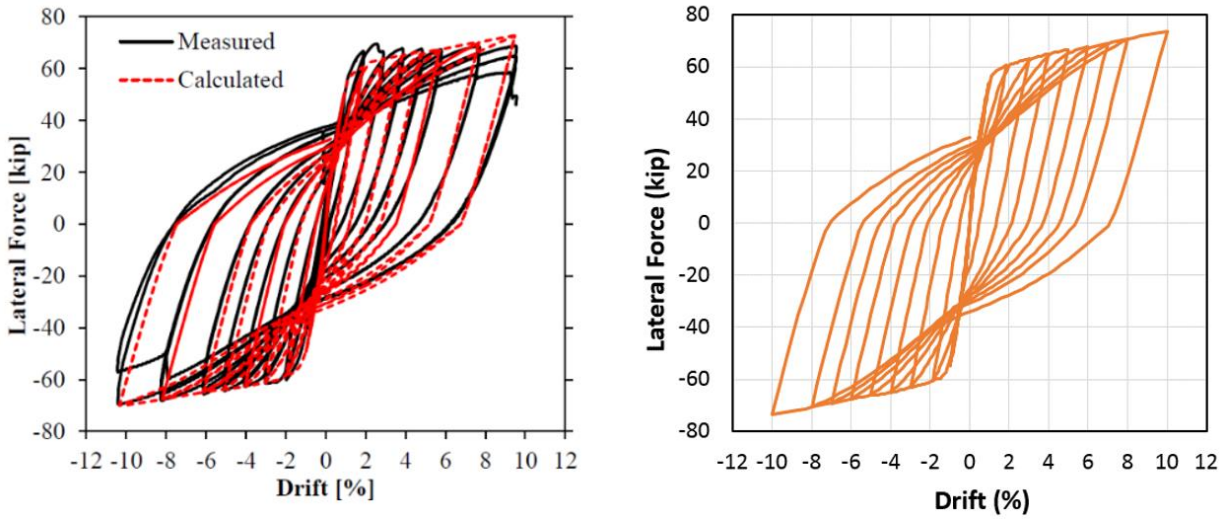

(a) (b)

Figure 3-5. (a) UNR Measured and Calculated and (b) ISU Calculated Hysteretic Force-displacement Curves of the CIP Column (Haber, et al., 2013)

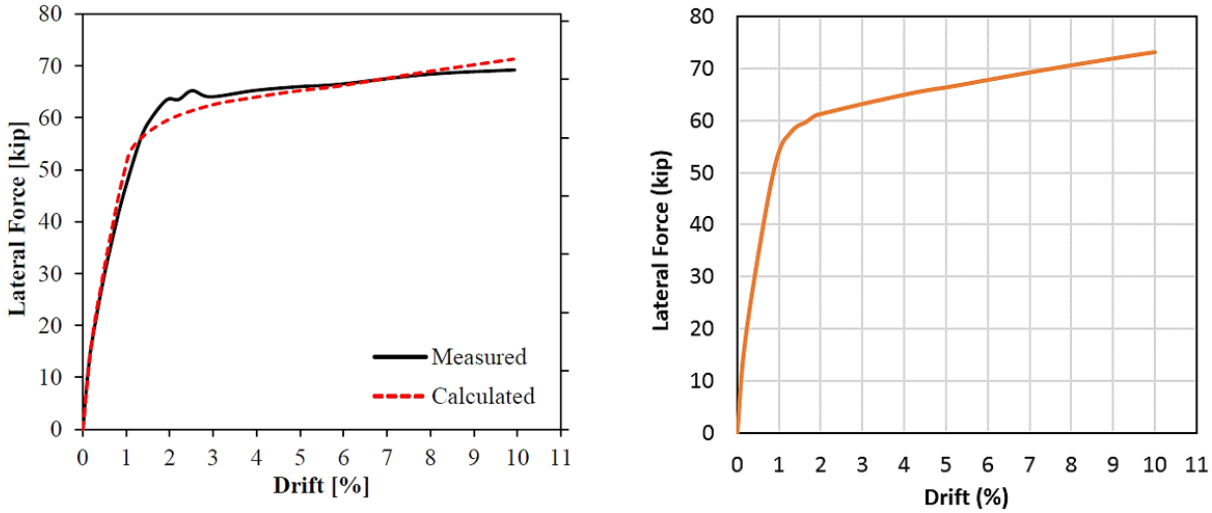

(a) (b)

Figure 3-6. (a) UNR Measured and Calculated Average Envelope Curves and (b) ISU Calculated Pushover Curve for the CIP Column (Haber, et al., 2013)

The analytical model of the GCNP column, shown in Figure 3-7, is similar to the model of the CIP column. The differences being the additional elements and nodes where the couplers are located in the column and the fiber sections in those elements. The simplified method developed in Haber et al. (2015) was used to model the grouted couplers. The OpenSees *ReinforcingSteel* command was used to model the behavior of the No. 8 grouted coupler. The data used to calculate the material properties was provided by the manufacturer, Splice Sleeve North America (SSNA). Average values of force and elongation from five tensile tests were used to calculate the average stress and strain in the coupler. The effective stress in the coupler is found by dividing the force by the area of the grouted coupler (4.94 $in.^2$ for No. 8 coupler). The average strain of the coupler is obtained by dividing the elongation of the coupler region by the length of the coupler region. As seen in Figure 2-23, the coupler region includes some of the reinforcing bar. Therefore, the elongation in the reinforcing bar in the coupler region is what is measured in the test. Figure 3-8 shows the relationship of the bar stress versus the coupler strain in the top curve and the coupler stress versus the coupler strain in the bottom curve. The coupler stress versus the coupler strain is the best fit of five experimental curves (SSNA, 2016).

The stress in the No. 8 bar versus the strain in the coupler (bottom curve in Figure 3-8) is obtained by multiplying the stress values of the coupler by the ratio of the area of the coupler over the area of the No. 8 bar ($(4.94\ in.^2)/(0.79\ in.^2) = 6.253$). The experimental data from SSNA for the coupler stresses and strains are presented in Appendix C (SSNA 2016).

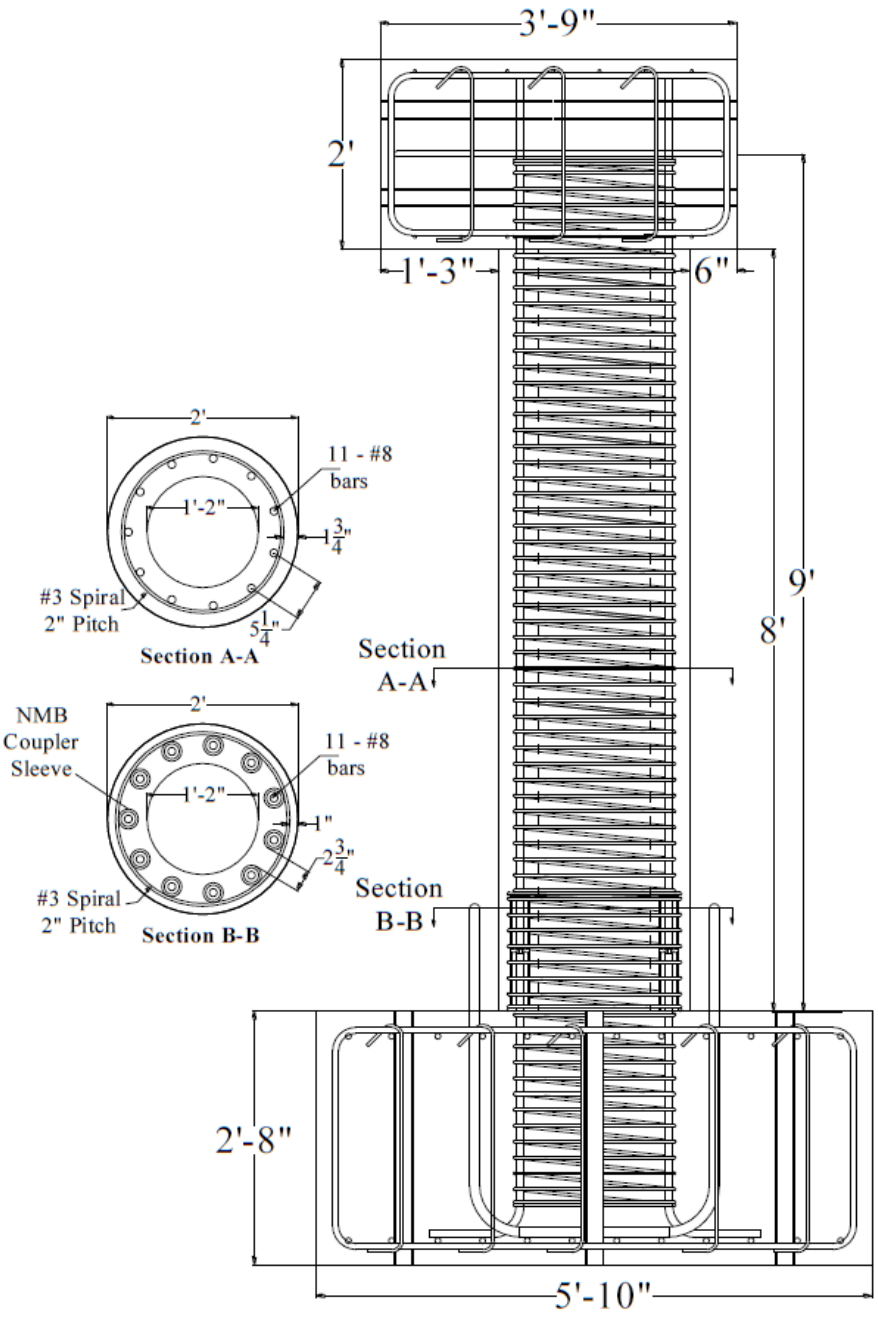

Figure 3-7. The GCNP model used in the UNR study (Haber et al. 2013)

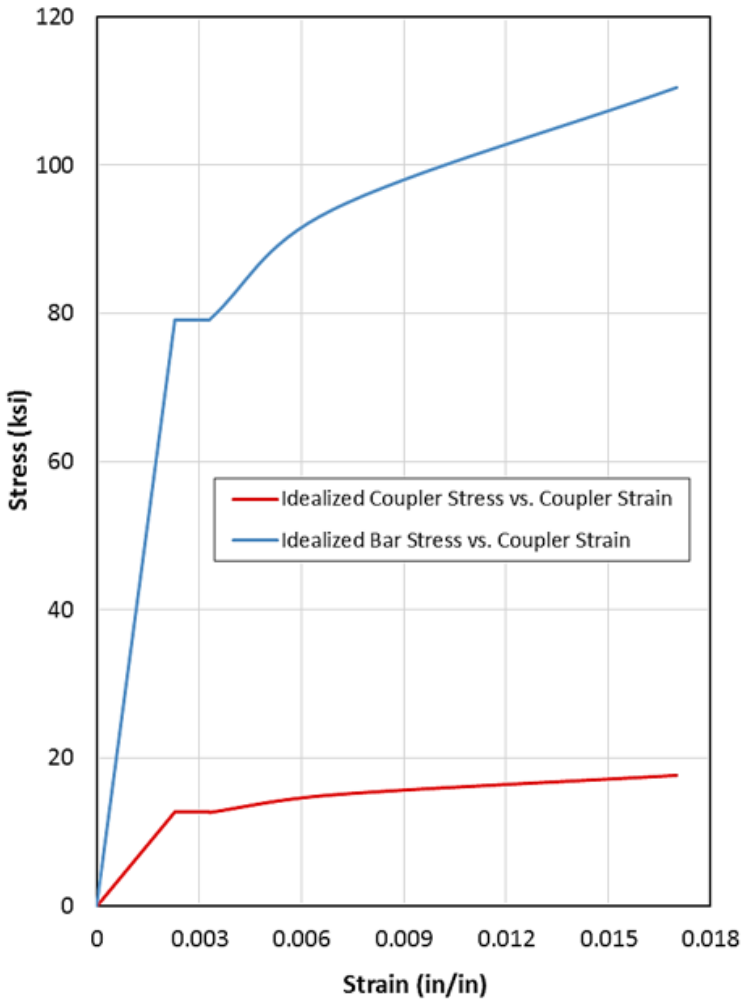

Figure 3-8. No. 8 coupler stress vs. strain (Ebrahimpour, et al. 2016)

The fiber section for the grouted coupler is modeled so that the couplers have the same cross-sectional area as the longitudinal reinforcement and the material properties of the coupler. An area equal to the cross-sectional area of the coupler is removed from the confined concrete where the reinforcement is located so that the properties of the two materials are not added together. See Figure 2-26. The material properties used for the *ReinforcingSteel* command for the steel bars and the grouted coupler can be seen in Table 3-2 (Haber, et al. 2015).

Table 3-2. Properties of Coupler and Steel Bar used in *ReinforcingSteel* nonlinear material (Ebrahimpour, et al. 2016)

	Yield Stress (ksi)	Ultimate Stress (ksi)	Modulus of Elasticity (ksi)	Strain Hardening Modulus (ksi)	Initial Strain Hardening Strain (in./in.)	Ultimate Strain (in./in.)
Coupler	79.4	110.5	35,179	4,136	0.0033	0.017
Steel Bar	66.8	111.3	29,000	1,247	0.0050	0.090

The results from the UNR project's experimentally measured and calculated as well as the ISU's calculated hysteretic force-displacement curves for the GCNP column are shown in Figure 3-9. Figure 3-10 shows UNR's measured and calculated average envelope curves and ISU's calculated curve for the GCNP column.

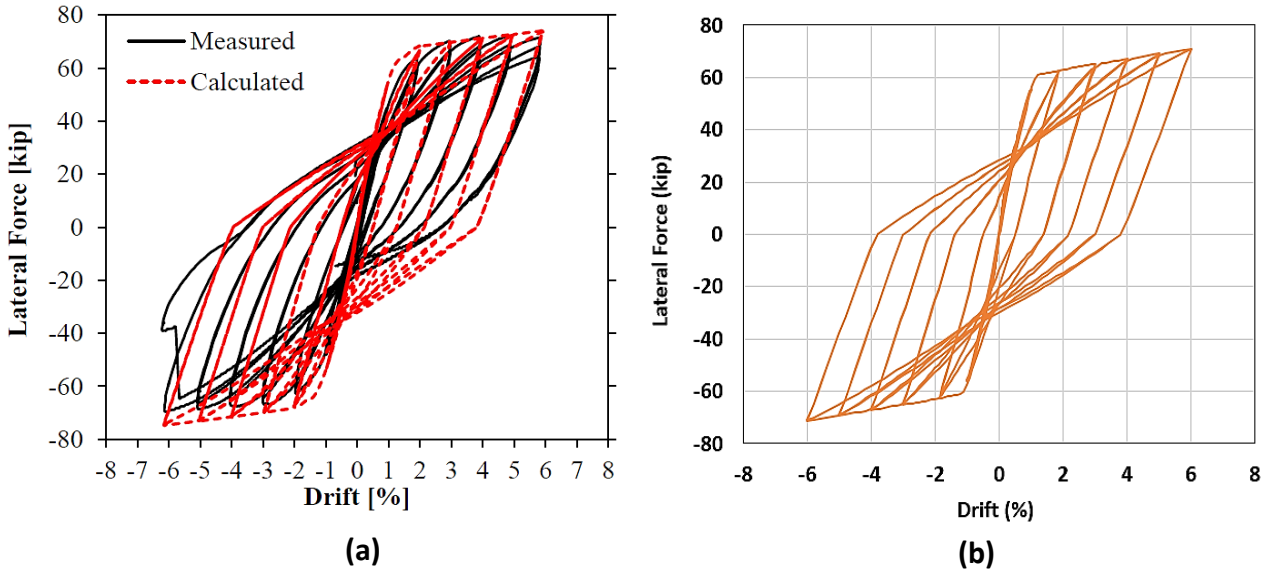

Figure 3-9. (a) UNR Measured and Calculated and (b) ISU Calculated Hysteretic Force-displacement Curves for the GCNP Column (Haber, et al., 2013)

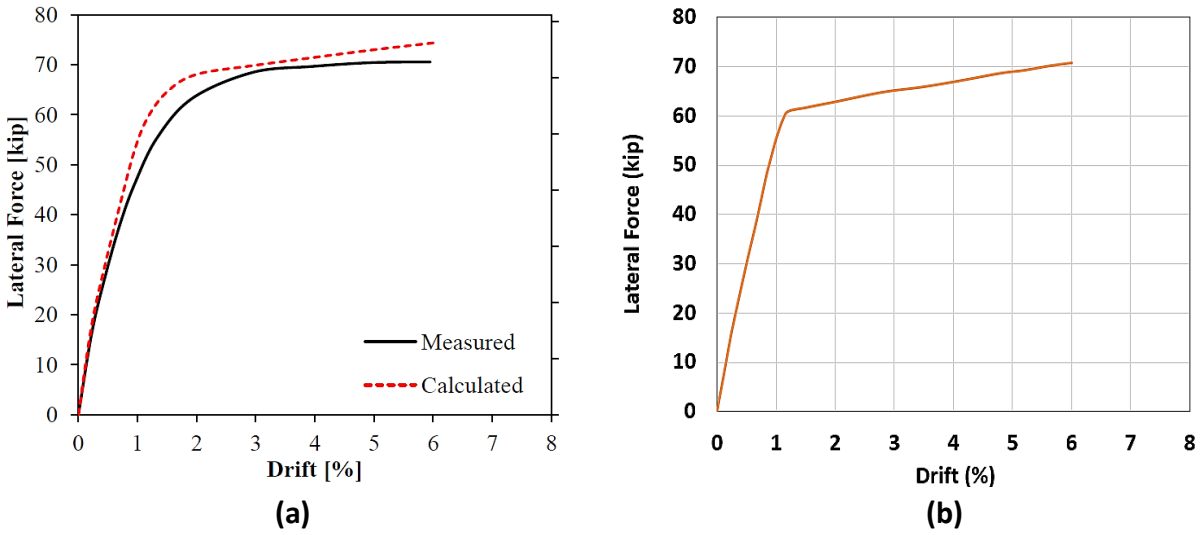

Figure 3-10. (a) UNR Measured and Calculated Average Envelope Curves and (b) ISU Calculated Curve for the GCNP Column (Haber, et al., 2013)

Chapter 4 – Modeling and Analysis of Three Idaho Bridges

4.1 Overview

The three Idaho bridges chosen for this study are located near the cities of Parma and Dubois, and on the Salmon River near Clayton, see Figure 1-1. Three analytical models of each bridge was made with different column cross-sections and material properties: the linear-elastic CIP, the non-linear CIP, and the non-linear with grouted couplers. Bond slip was modeled at the column-to-footing and column-to-cap beam interfaces of the non-linear models using a moment-curvature analysis for each bridge. The material properties for confined concrete were calculated using the method developed in Mander et al. (1988). The procedures to determine the effective section properties for the linear-elastic analysis and the soil stiffness at the abutments of the bridges will also be discussed. The geometric transformation for the Idaho bridge elements are the same as those for the models created from the FHWA *Design Guide Example No. 1* in Chapter 3.

It was determined that the bridges should be subjected to the most seismically active conditions that could be found in Idaho. Using the United States Geological Survey (USGS) website the most seismically active location in Idaho where a bridge might be built was found to be near Montpelier located in the southeast corner of the state. The parameters to create the design loads using the single-mode spectral method, presented in the FHWA *Design Guide Example No. 1*, were obtained from this website.

The results from the analytical analyses of the bridges with the couplers was compared to the results from the bridges with CIP columns to determine the relative performance of the couplers. Further analyses of single columns from the Parma and Dubois bridges under large

drifts were also performed per a request from ITD. A comparison of the displacement/drift results from the Idaho bridges with the displacement/drift capacity and demand calculated from equations found in the AASHTO *Guide Specifications for LRFD Seismic Bridge Design* was also made.

4.2 Parma Bridge

4.2.1 Bridge Description

The bridge located near Parma, ID is on US-95 and spans US-20/26 and the Union Pacific Railroad (UPRR). The drawings and specifications for the bridge were provided by ITD. The plan and elevation of the bridge can be seen in Figures 4-1 and 4-2, respectively. The bridge at Parma is a two-span bridge with a three column bent. There are integral abutments at each end of the bridge that have eight H-piles as part of the foundation. The superstructure is made up of an 8 inch thick concrete deck that rests on 5 prestressed WF66G AASHTO girders. The substructure is made up of a pier cap, three columns, and their footings all of which are cast-in-place concrete. The columns are 3.5 feet in diameter and 25.6 feet high.

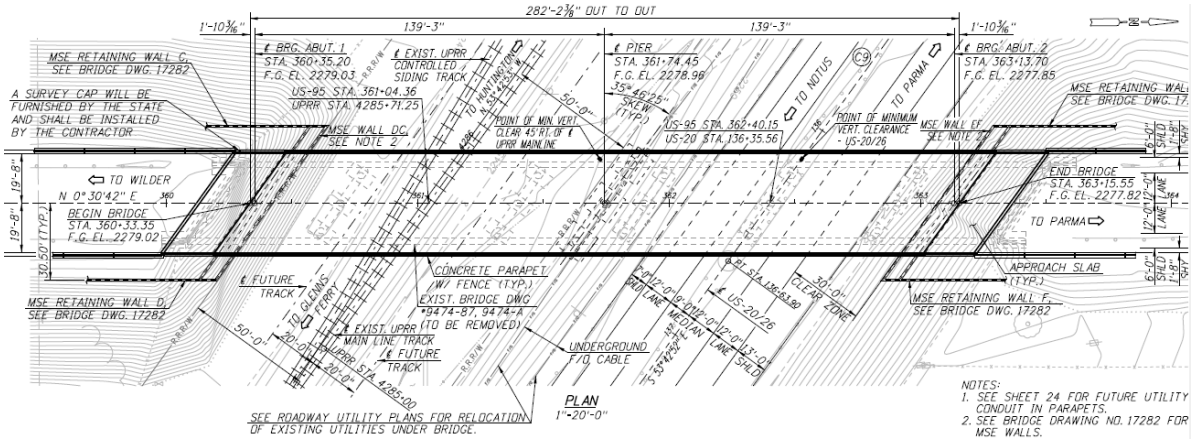

Figure 4-1. Plan View of US-95 over US-20/26 and UPRR at Parma, Not to Scale (NTS)

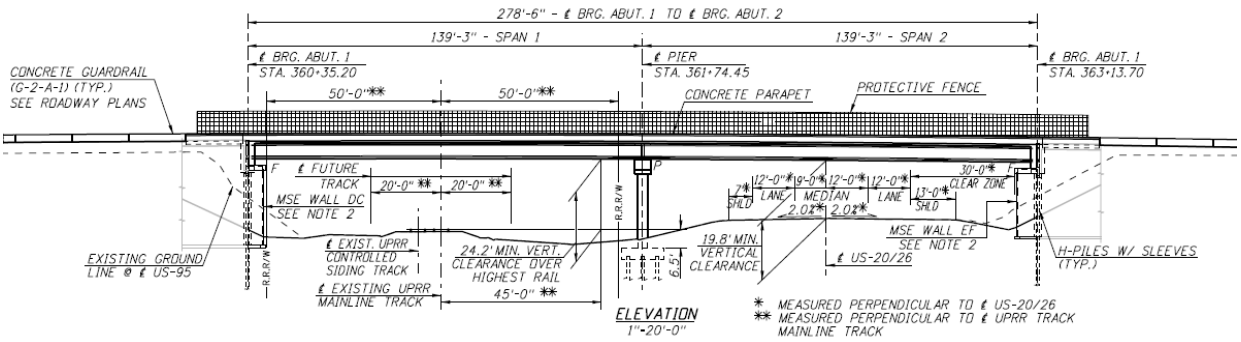

Figure 4-2. Elevation View of US-95 over US-20/26 and UPRR at Parma (NTS)

4.2.2 Linear-elastic Model of Parma Bridge

The linear-elastic model with CIP columns consists of twenty *elasticBeamColumn* elements which have linear-elastic properties. The columns have an element half the depth of the column footings at the base of the column, similar to the FHWA *Seismic Design of Bridges, Design Example No.* and the node at the base of the footing is fixed in all degrees of freedom. There are extra nodes at the abutments with a *zeroLength* element associated with each of them to model soil stiffness. The skew in the bridge was removed for ease of modeling. The overall dimensions of the bridge were maintained and the bent and abutment lengths were shortened to match the deck width. The bent elements were given a large second area moment of inertia and torsional moment of inertia to prevent any deformation. The linear-elastic columns use a reduced second area moment of inertia to account for a cracked concrete section. An illustration of the model can be seen in Figures D-5 and D-6 in Appendix D.

4.2.3 Non-linear Models of Parma Bridge

The non-linear models have the same number and type of elements in the superstructure and the bent as the linear-elastic model. The elements in the columns of the non-linear models are *nonlinearBeamColumn* elements and *zeroLength* elements are located at the base and top of

each column. The footings were removed from these models because the *zeroLength* elements which model bond-slip account for the same displacement as the footing. The longitudinal reinforcement in the columns of the Parma bridge were 16 #10 two-bar bundles as shown in Figure 4-3. This arrangement would not work with grouted couplers so16 #14 bars, which have approximately the same cross-sectional area as two #10 bars, were substituted.

The non-linear columns with grouted couplers have a *nonlinearBeamColumn* element located at the top and bottom of the column which represent the grouted couplers. An illustration of the non-linear CIP and non-linear with grouted couplers models can be seen in Figures D-9, D-10, D-13, and D-14 in Appendix D.

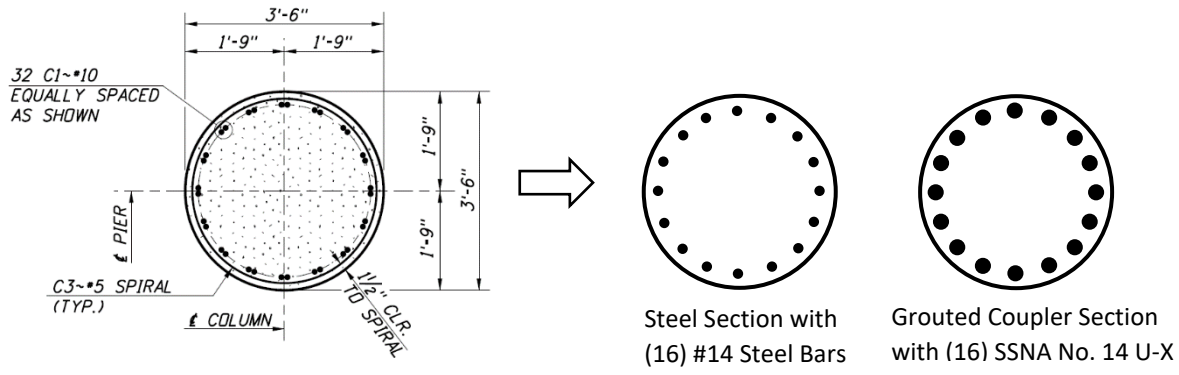

Figure 4-3. Column Steel and Grouted Coupler Sections (NTS) (Ebrahimpour, et al. 2016)

4.2.4 Estimating Integral Abutment Stiffness Values for Parma Bridge

The abutments were modeled with a spring in both the longitudinal direction (parallel to the length of the bridge) and the transverse direction (perpendicular to the length of the bridge). The iterative procedure outlined in Appendix E was used to estimate the abutment stiffness values for the transverse and longitudinal directions, which is the same as that used by ITD. The

soil properties at the abutments were provided by ITD in the Phase IV Foundation Investigation Report for each bridge.

The initial stiffness values were estimated using the spring stiffness formula $K = {}^{F}/_{d}$, where K = spring stiffness, F = force, and d = deflection. For the Parma bridge, the stiffness for one H-pile in the foundation of the abutment wall in the weak (transverse) and strong (longitudinal) directions was estimated using the graphs given in the Phase IV Foundation Investigation Report, Figures D-1 and D-2. Assuming a one inch deflection a force is determined from these graphs. The stiffness values are: for the weak direction, k_w = 690 kip/ft and for the strong direction, k_s = 1,140 kip/ft.

The initial stiffness values for the whole abutment takes into account the resistance of the abutment wall and the number of H-piles in one abutment. For the transverse direction only the product of the number of H-piles in one abutment and the stiffness in that direction are needed.

$$K_t = nk_w \tag{4-1}$$

where:

K_t = abutment stiffness in the transverse direction,

n = the number of H-piles in an abutment wall = 8,

k_w = the spring stiffness for one H-pile about the weak axis = 690 kip/ft.

For the longitudinal direction the area of the abutment wall and the deflection needed to mobilize full passive resistance are needed.

$$K_l = \frac{2nk_s + (7.7A_{aw}/d)}{2} \quad (4\text{-}2)$$

where:

K_l = the abutments spring stiffness in the longitudinal direction,

n = the number of H-piles in one abutment wall = 8,

k_s = the spring stiffness for one H-pile about the strong axis = 1,140 kip/ft,

A_{aw} = the area of the abutment wall = H_{aw} L_{aw} = 448 ft^2,

d = deflection needed to mobilize full passive resistance = 0.02H_{aw} = 0.2134 ft.

The initial abutment stiffness for the transverse direction is, K_t = 5,520 kip/ft. The initial abutment stiffness for the longitudinal direction is, K_l = 17,202 kip/ft. After completing the iterative process to determine the final abutment stiffness K_t = 3,200 kips/ft and, K_l = 17,042 kips/ft.

4.2.5 Section Properties of Linear-elastic Columns for Parma Bridge

It is assumed that the concrete in the columns will crack under a relatively small seismic load and increase the ductility of the column. The effective section properties for the cracked linear-elastic columns were calculated using a procedure outlined in Section 5.6 of the AASHTO *Guide Specifications for LRFD Seismic Bridge Design*.

The effective moment of inertia (I_{ceff}) is obtained by multiplying the gross moment of inertia (I_{cg}) by the Elastic Stiffness Ratio (I_{eff}/I_{cg}) which is determined using a graph in the AASHTO Guide Specifications and the axial load ratio (P/f'_cA_{cg}) and the ratio of the cross-

sectional area of the longitudinal steel to the cross-sectional area of the concrete (A_{st}/A_{cg}). See Figure 4-4. The calculations for the effective section properties can be seen in Appendix D. The effective torsional moment of inertia (J_{eff}) is 20 percent of the gross torsional moment of inertia (J_{gross}). (AASHTO 2015)

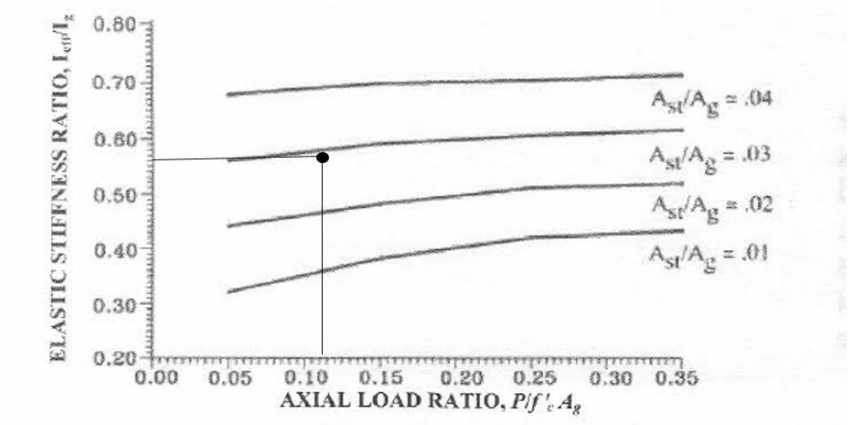

Figure 4-4. Elastic Stiffness Ratio (AASHTO 2011)

A summary of the section properties for the Parma bridge columns follow:

P/f'_cA_{cg} = 0.113

A_{st}/A_{cg} =0.25 ft^2/9.62 ft^2 = 0.029

I_{eff}/I_{cg} = 0.57

I_{ceff} = 0.57 * I_{cg} = 0.57 * 7.366 ft^4 = 4.199 ft^4

$J_{gross} = \pi D^4/32 = \pi(3.5^4)/32$ = 14.7 ft^4

$J_{eff} = 0.2J_{gross}$ = 2.95 ft^4.

4.2.6 Estimating Seismic Loads for Parma Bridge

To estimate the forces that would be seen in an earthquake on the deck of the bridge model, seismic loads were calculated using the single-mode spectral method as outlined in the

FHWA *Seismic Design of Bridges, Design Example No.1.* The method requires the displacement of the deck under a specified uniformly distributed load, the design short duration acceleration (S_{DS} = 0.907g) and the one-second design acceleration (S_{D1} = 0.486g) (USGS 2015) to calculate the factors α, β, and γ. These factors are used to calculate the seismic load ($p_e(x)$) at each node of the deck of the bridge. The distributed load on each element is the average of the two nodes at the ends of the element.

$$\alpha = \int_0^L v_s(x)\, dx \tag{4-3}$$

$$\beta = \int_0^L w(x) v_s(x) dx \tag{4-4}$$

$$\gamma = \int_0^L w(x) v_s\,(x)^2 dx \tag{4-5}$$

where:

v_s (x) = displacement due to a uniformly distributed load of 10 kip/ft.

w(x) = weight of the bridge per unit length = 12.466 kip/ft

dx = tributary length

L = total length of bridge

$$p_e(x) = \beta C_{sm} w(x) * v_s(x)/\gamma \tag{4-6}$$

where:

$$C_{sm} = S_{DS} = 0.907 \quad \text{for } T_o < T_m < T_s \text{ (longitudinal)} \tag{4-7}$$

$$C_{sm} = S_{D1}/T_m = 0.887 \quad \text{for } T_m > T_s \text{ (transverse)} \tag{4-8}$$

where:

$$T_m = 2\pi\sqrt{\gamma/P_0 g\alpha} = 0.344\text{s} \quad \text{for longitudinal loads} \tag{4-9}$$

$$T_m = 2\pi\sqrt{\gamma/P_o g\alpha} = 0.548\text{s} \quad \text{for transverse loads} \tag{4-10}$$

$$T_s = S_{D1}/S_{DS} = 0.5358 \tag{4-11}$$

$$T_o = 0.2T_s = 0.1072 \tag{4-12}$$

$g = 32.2$ ft/s^2

$P_o = 10$ kip/ft

The resulting distributed loads can be seen in Tables E-2 and E-3 in Appendix E. (Mast, et al. 1996)

4.2.7 Material Properties of Non-linear Models for Parma Bridge

The material properties of the confined and unconfined concrete as well as the reinforcing steel for the non-linear models are presented in this section. OpenSees command *uniaxialMaterial Concrete01* was used for the unconfined concrete. The required material properties for this command can be seen in Figure 4-5. (UC Berkeley 2016)

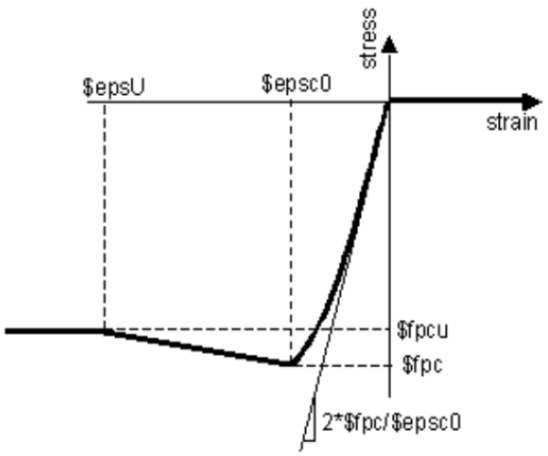

Figure 4-5. Concrete Stress-Strain Relation (UC Berkeley 2016)

These properties are defined as:

fpc maximum compressive strength,

epsc0 strain at maximum strength,

fpcu crushing strength, and

epsU strain at crushing strength.

The *fpc* for cover concrete is specified as 4.0 ksi. The *epsc0* is 0.002 and *epsU* is 0.005. The value of the crushing strength goes to zero for the cover concrete.

The OpenSees command *uniaxialMaterial ReinforcingSteel* requires six material properties Figure 4-6 shows these properties on a stress-strain curve.

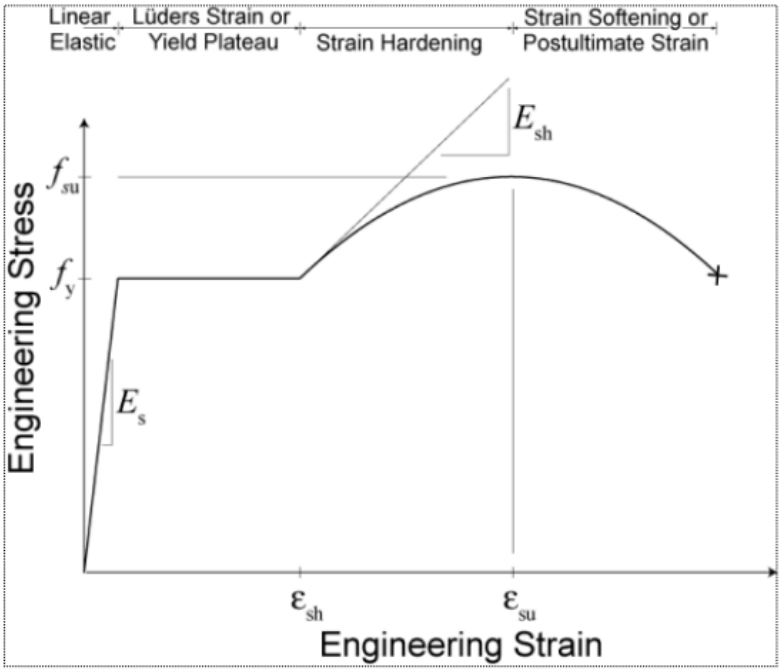

Figure 4-6. Steel stress-strain relation (UC Berkeley 2016)

These properties are defined as:

f_y yield stress,

f_{su} ultimate tensile stress,

E_s initial elastic tangent,

E_{sh} tangent at initial strain hardening,

ε_{sh} strain at initial strain hardening,

ε_{su} strain at peak stress.

The longitudinal reinforcing steel in the OpenSees model consists of 16 Number 14 bars. According to the AASHTO *Guide Specifications for LRFD Seismic Bridge Design* the values for the above properties for a Number 14 bar are:

f_y = 68 ksi = 9,792 ksf,

f_{su} = 95 ksi = 13,680 ksf,

E_s = 29,000 ksi = 4,176,000 ksf,

E_{sh} = 1247 ksi = 179,568 ksf,

ε_{sh} = 0.0075,

ε_{su} = 0.09.

Concrete confined by transverse reinforcement acquires a higher strength than the cover concrete outside of the reinforcing cage (Mander, et al. 1988). The Mander model for confined concrete was used for the concrete within the transverse reinforcement as specified in the AASHTO *Guide Specifications for LRFD Seismic Bridge Design*. Figure 4-7 shows the Mander stress-strain model for unconfined and confined concrete.

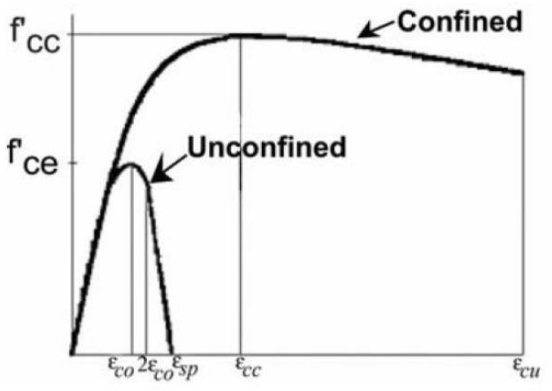

Figure 4-7. Unconfined and confined concrete stress-strain model (AASHTO 2015)

The detailed calculations for confined concrete for a circular column can be found in Appendix D.

The OpenSees command *uniaxialMaterial Concrete04* was used to model the confined concrete. Figure 4-8 shows the key properties of the *uniaxialMaterial Concrete04* model.

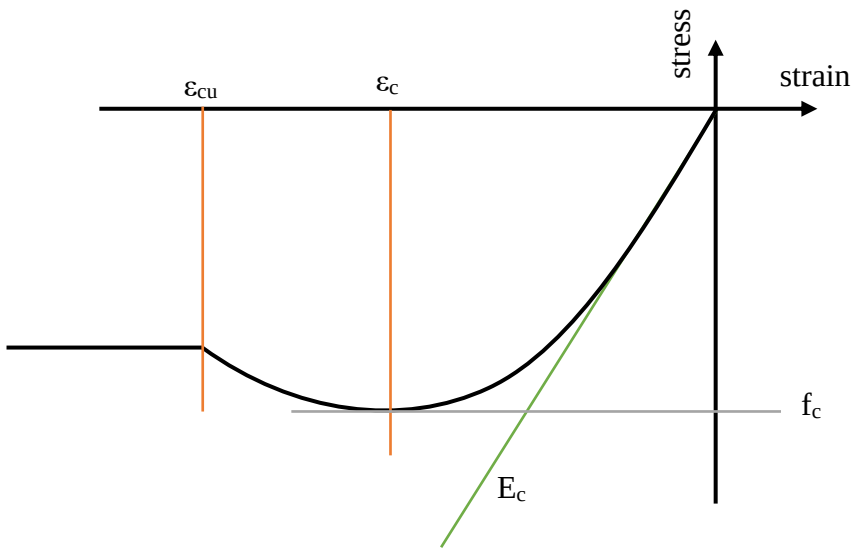

Figure 4-8. Confined Concrete Stress-strain Relation

These properties are (UC Berkeley 2016):

f_c compressive strength of confined concrete = 875.6 ksf,

ε_c strain at maximum strength = 0.0072,

ε_{cu} strain at ultimate strength 0.019,

E_c modulus of elasticity = 524,736 ksf.

An illustration of the non-linear CIP fiber section showing the confined and unconfined concrete and the positions of the longitudinal reinforcement can be seen in Figure 4-9.

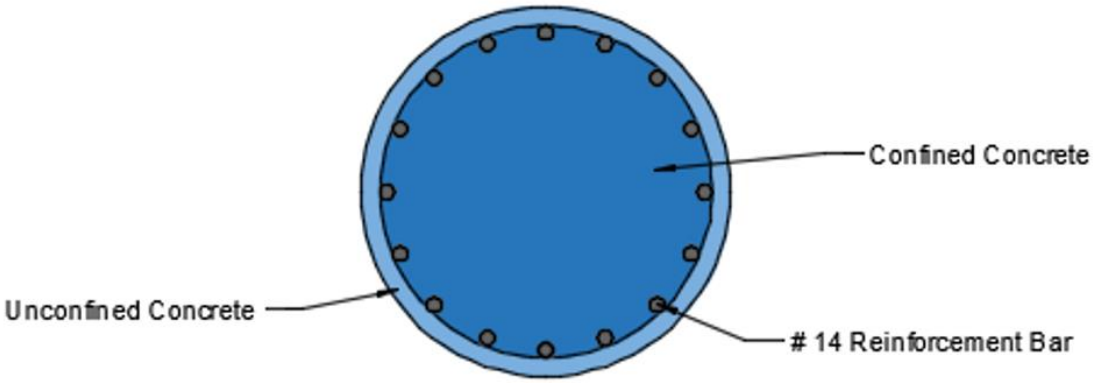

Figure 4-9. Non-linear CIP Fiber Section

4.2.8 Modeling Bond-slip Rotation for Parma Bridge

The procedure to model bond-slip at the base and the top of the columns is the same as that of the column in the UNR study. The moment-curvature input file and the detailed calculations for bond-slip in the Parma bridge can be found in Appendix D.

The *uniaxialMaterial Hysteretic* command in OpenSees requires the stress and strain at the first point of inflection and the ultimate stress and strain on the bilinear approximation of the moment-rotation curve (UC Berkeley 2016). These values are:

s1p = 3583 k-ft Moment at the first point of the envelope in the positive direction,

e1p = 0.0035 Angle at the first point of the envelope in the positive direction,

s2p = 4239 k-ft Moment at the second point of the envelope in the positive direction,

$e2p$ = 0.03 Angle at the second point of the envelope in the positive direction.

4.2.9 Material Properties of Grouted Couplers for Parma Bridge

The method used to determine the material properties of the grouted couplers is the same as that presented in Haber, Saiidi, and Sanders (2015). The calculations for the material properties of the grouted couplers are in Appendix D and the experimental data for those calculations are in Appendix C. For the SSNA No. 14 U-X Grouted Coupler the material properties needed for the *uniaxialMaterial ReinforcingSteel* command are (UC Berkeley 2016):

f_y = 9312.5 ksf yield stress of the coupler,

f_u = 13186.1 ksf ultimate stress at fracture,

E_s = 5707497.6 ksf modulus of elasticity of coupler,

E_{sh} = 378000 ksf slope of the stress-strain curve at strain hardening,

e_{sh} = 0.0019 strain at strain hardening,

e_{ult} = 0.0185 ultimate strain.

The cross-section of the column with the grouted couplers has an area equal to the cross-sectional area of a grouted coupler removed from the fiber section and a section with the area of the reinforcing steel placed in each space. See Figure 4-10.

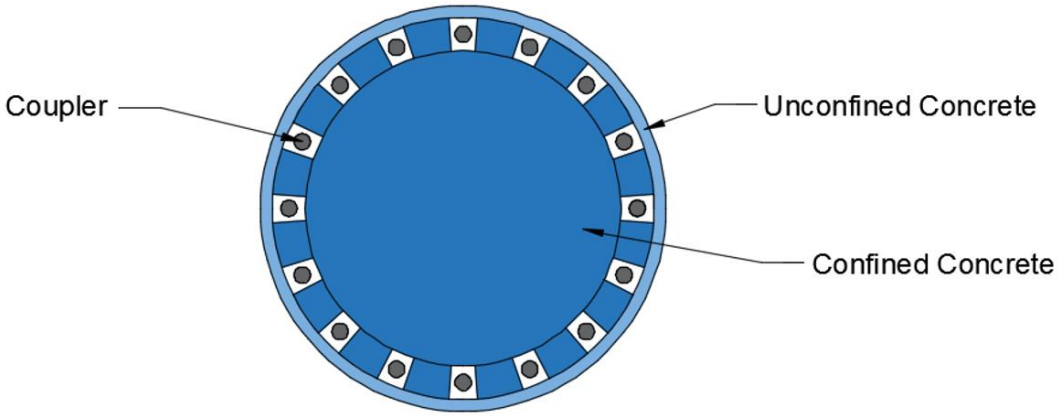

Figure 4-10. OpenSees model of column cross-section with couplers

The input files for the CIP, non-linear CIP, and non-linear with grouted couplers for the Parma bridge are presented in Appendix D.

4.2.10 Results of Computer Analyses of Parma Bridge

Table 4-1 shows a summary of the column displacements, drifts, base shear, and base moment for the transverse and longitudinal loading directions. It should be noted that the transverse loads produce larger displacements and reactions than the longitudinal loads and therefore will control. Also the cracked linear-elastic column produces smaller displacements and larger reactions than the nonlinear columns for the transverse loading. The reverse is the case for the longitudinal loading but the values are closer together for the linear and nonlinear columns. The drift is calculated by dividing the displacement by the column height.

Table 4-1. Parma Bridge Displacements, Drifts, and Column Base Reactions

(Ebrahimpour, et al. 2016)

	Column Model		
	Cracked Linear-elastic	**Nonlinear CIP**	**Nonlinear w/ coupler**
Transverse			
Top of Column Displ., ft	0.315	0.376	0.375
Column Drift, %	1.23	1.46	1.47
Col. Base Shear, k	385.65	271.59	272.40
Col. Base Moment, k-ft	5,443	3,624	3,634
Longitudinal			
Top of Column Displ., ft	0.082	0.081	0.080
Column Drift, %	0.3195	0.3143	0.3135
Col. Base Shear, k	87.58	96.66	98.0
Col. Base Moment, k-ft	1,298	1,347	1,366

The above results for the top of the column displacements are presented graphically in Figures 4-11 and 4-12 as displacement versus percent design load for all three types of columns.

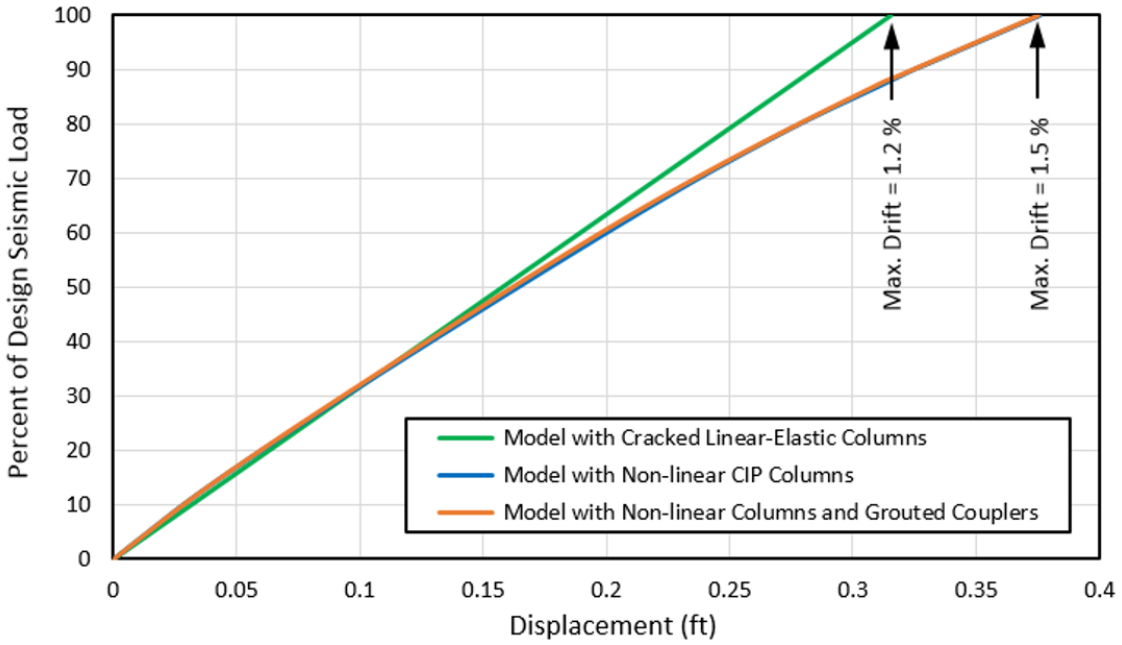

Figure 4-11. Bridge Column Displacements/Drifts under Transverse Load

(Ebrahimpour, et al. 2016)

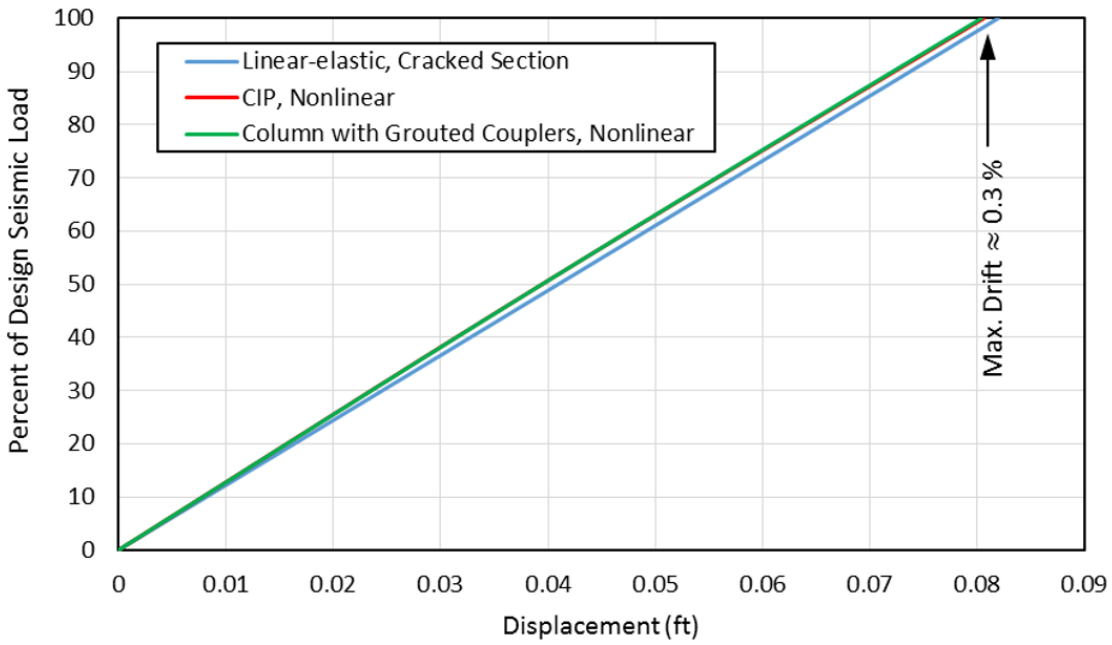

Figure 4-12. Bridge Column Displacements/Drifts under Longitudinal Load (Ebrahimpour, et al. 2016)

Figure 4-13 shows the locations of the most stressed steel reinforcement in the CIP column and the column with grouted couplers for the transverse and longitudinal loads. Figure 4-14 shows the stress-strain values for the most stressed steel bar in the CIP column. The maximum stress and strain for the transverse and longitudinal direction are indicated by a red and a green dot, respectively. Figure 4-15 shows the stress-strain values for the most stressed steel bar and the grouted coupler with the maximum stress-strain in the steel and the grouted couplers indicated by a light red and dark red dot, respectively. The stresses and strains were recorded at the bottom of the CIP column. For the column with couplers these measurements were taken at the bottom of the bottom coupler (for the coupler) and below the bottom coupler at the interface of the column and the footing (for the steel), (Ebrahimpour, et al. 2016)

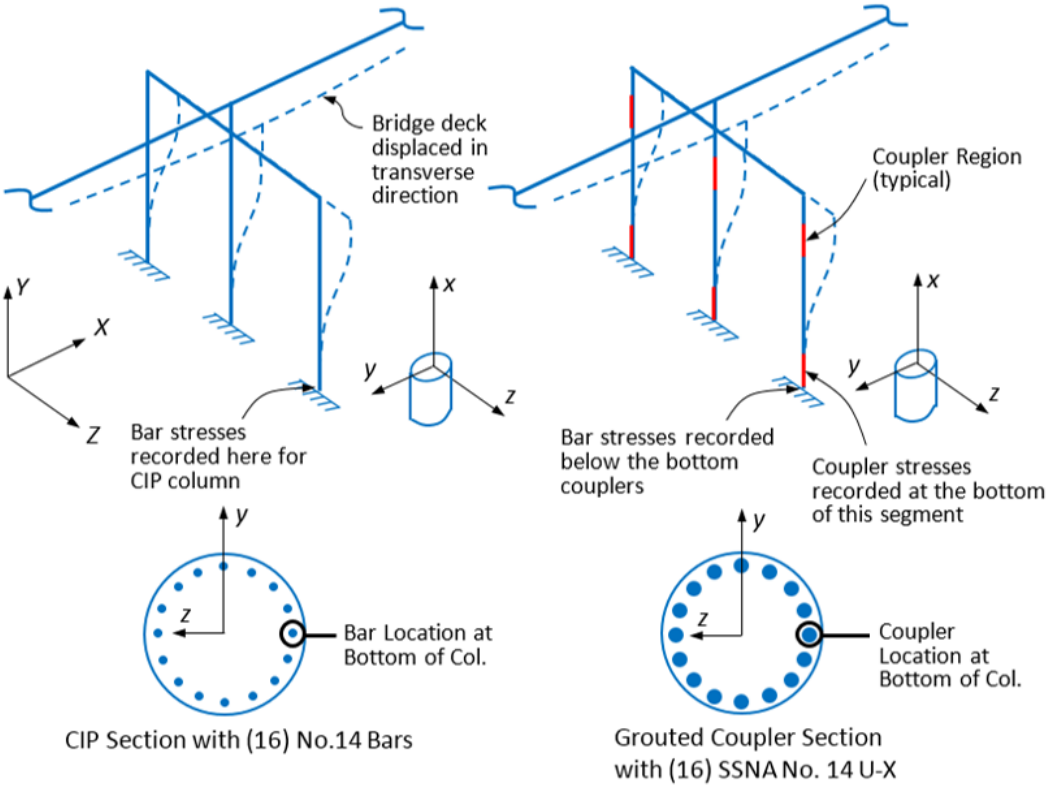

Figure 4-13. Stress-strain Locations: Left CIP Column, Right Column with Couplers (Ebrahimpour, et al. 2016)

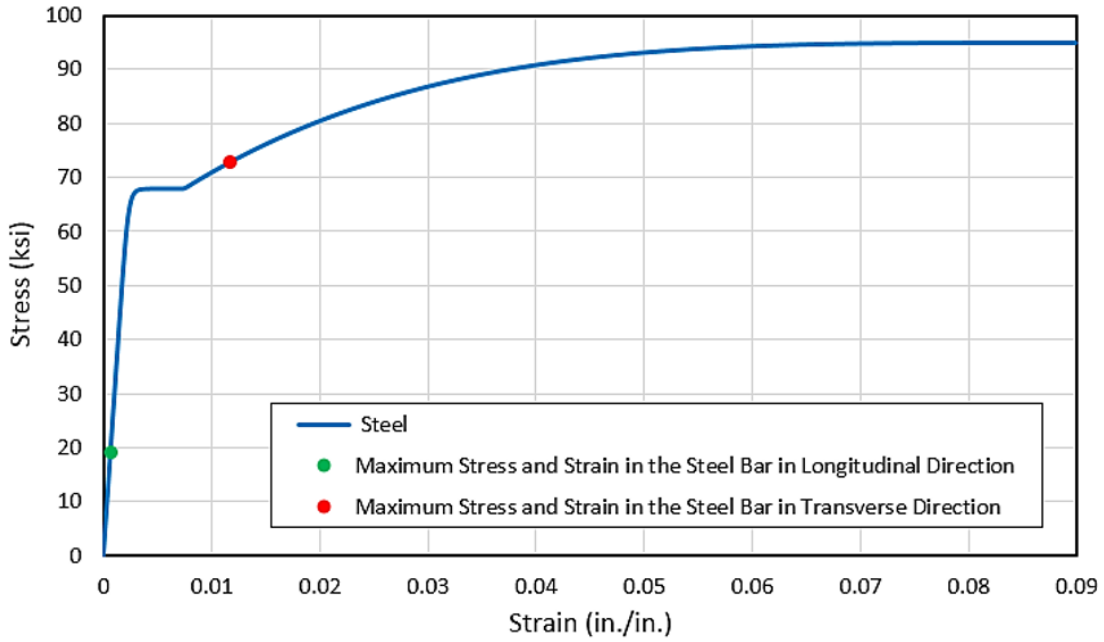

Figure 4-14. The Stress-strain Values in the Most Stressed Steel Bar in the CIP Column (Ebrahimpour, et al. 2016)

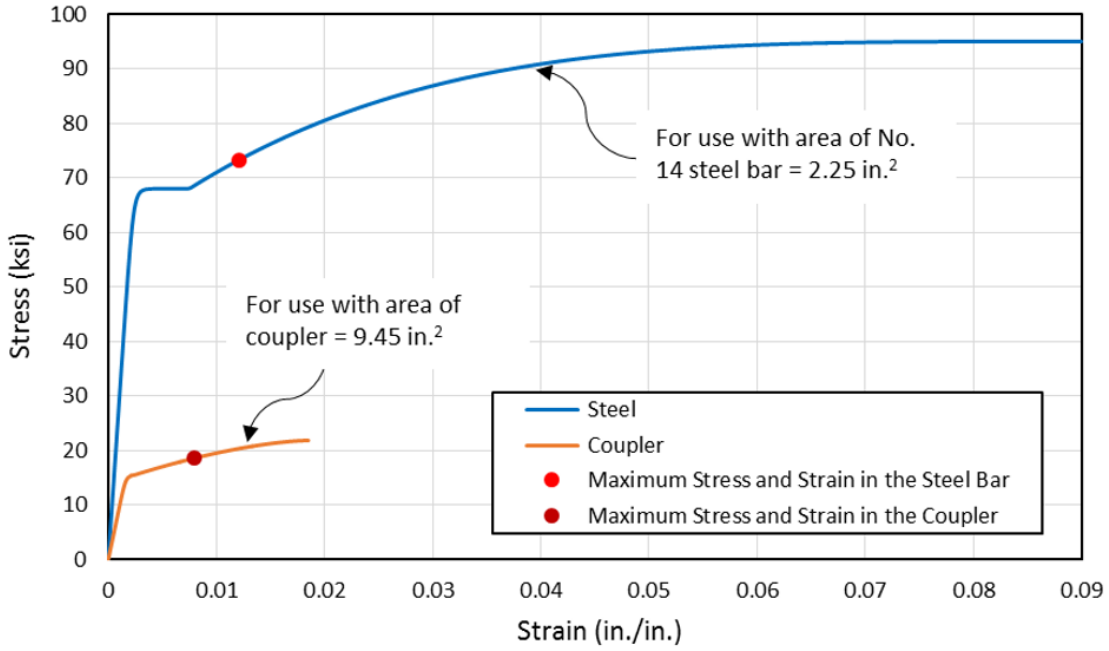

Figure 4-15. The Stress-strain Values in the Most Stressed Steel Bar and Grouted Coupler in the Column with Grouted Couplers under Transverse Loading (Ebrahimpour, et al. 2016)

4.3 Dubois Bridge

4.3.1 Bridge Description

The bridge located near Dubois, ID is on SH-22 and spans I-15, drawings and specifications provided by ITD. The plan and elevation of the bridge can be seen in Figures 4-16 and 4-17, respectively. The bridge at Dubois is a two-span bridge with a four column bent. There are non-integral abutments at each end of the bridge that have eight H-piles as part of the foundation. The superstructure is made up of an 8 inch thick concrete deck that rests on eight steel girders. The substructure is made up of a pier cap, four columns, and their footings all of which are cast-in-place reinforced concrete. The columns are 3.5 feet in diameter and 14.05 feet high.

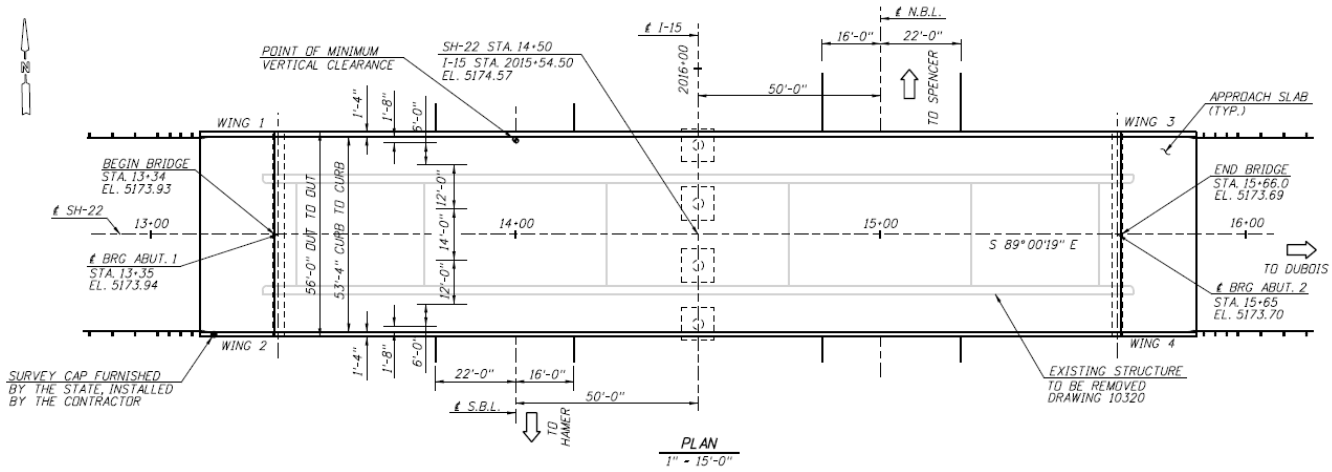

Figure 4-16. Plan View of the SH-22 over I-15 Bridge at Dubois (NTS)

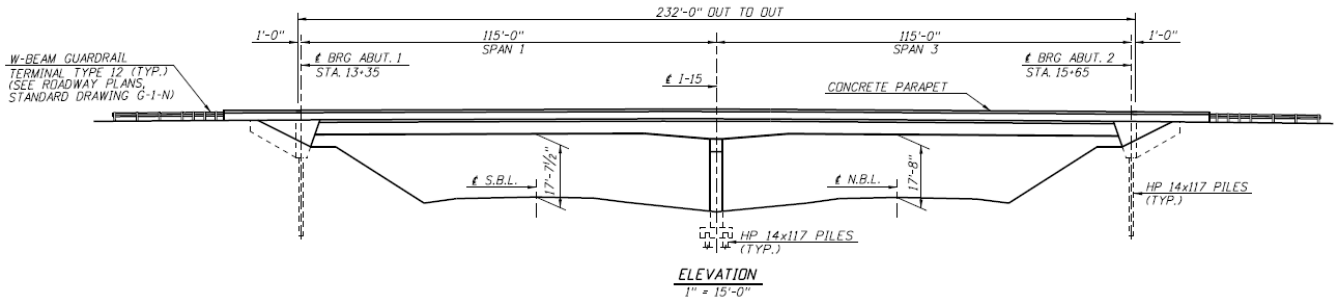

Figure 4-17. Elevation View of the SH-22 over I-15 Bridge at Dubois (NTS)

4.3.2 Linear-elastic Model of Dubois Bridge

The linear-elastic model with CIP columns consists of twenty-four *elasticBeamColumn* elements which have linear-elastic properties. The columns have an element half the depth of the column footings at the base of the column, similar to the FHWA *Seismic Design of Bridges, Design Example No.1* and the node at the base of the footing is fixed in all degrees of freedom. There are extra nodes at the abutments with a *zeroLength* element associated with each of them to model soil stiffness. The bent elements were given a large second area moment of inertia and torsional moment of inertia to prevent any deformation. The linear-elastic columns use a reduced second area moment of inertia to account for a cracked concrete section. An illustration of the model can be seen in Figures D-17 and D-18 in Appendix D.

4.3.3 Nonlinear Models of Dubois Bridge

The nonlinear models have the same number and type of elements in the superstructure and the bent as the linear-elastic model. The elements in the columns of the non-linear models are *nonlinearBeamColumn* elements and *zeroLength* elements are located at the base and top of each column. The footings were removed from these models because the *zeroLength* elements which model bond-slip account for the same displacement as the footing. The longitudinal

reinforcement in the columns of the Dubois bridge consist of 13 Number 11 bars. Figure 4-18 shows the cross-section of the CIP column.

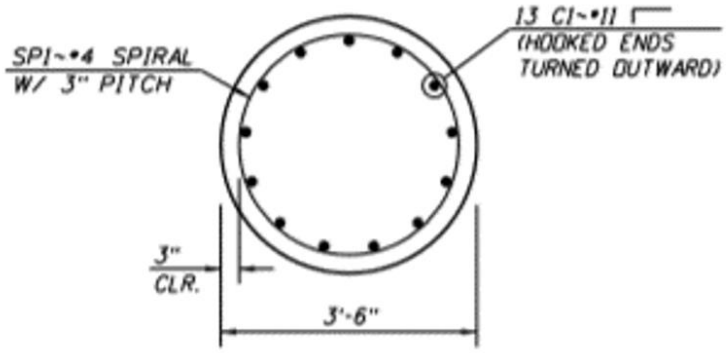

Figure 4-18. Column Detail

The non-linear columns with grouted couplers have a *nonlinearBeamColumn* element located at the top and bottom of the column which represent the grouted couplers. An illustration of the nonlinear CIP and nonlinear with grouted couplers models can be seen in Figures D-25, D-26, D-27, and D-28 in Appendix D.

4.3.4 Estimating Integral Abutment Stiffness Values for Dubois Bridge

The procedure for estimating initial and final abutment stiffness is the same for all the Idaho bridges. The process to determine the final abutment stiffness is outlined in Appendix E. The soil properties at the abutments were provided by ITD in the Phase IV Foundation Investigation Report. For the Dubois bridge, the soil properties at the east and west ends of the bridge are different. To account for the different soil properties the formula for the initial longitudinal abutment stiffness is given as:

$$K_l = \frac{nk_{s_E} + nk_{s_W} + \left(\frac{7.7A}{d}\right)}{2} \quad (4\text{-}13)$$

where:

K_l = the abutments spring stiffness in the longitudinal direction,

n = the number of H-piles in one abutment wall = 8,

k_{sE} = the spring stiffness for one H-pile about the strong axis at the east abutment = 1,092 kip/ft,

k_{sW} = the spring stiffness for one H-pile about the strong axis at the west abutment = 1,392 kip/ft,

A_{awE} = the area of the abutment wall at the east abutment = $H_{awE}\, L_{aw}$ = 469.84 ft^2,

A_{awW} = the area of the abutment wall at the west abutment= $H_{awW}\, L_{aw}$= 469.28 ft^2,

d_E = deflection needed to mobilize full passive resistance = 0.02H_{awE} = 0.1678 ft,

d_W = deflection needed to mobilize full passive resistance = 0.02H_{awW} = 0.1676 ft.

The equations for the transverse direction are the same as those for the Parma bridge. A summary of the initial abutment stiffnesses is:

$$K_{l_E} = 20{,}716\,\frac{kip}{ft},$$

$$K_{l_W} = 20{,}716\,\frac{kip}{ft},$$

$$K_{t_E} = 8\left(684\,\frac{kip}{ft}\right) = 5{,}472\,\frac{kip}{ft},$$

$$K_{t_W} = 8\left(864\,\frac{kip}{ft}\right) = 6{,}912\,\frac{kip}{ft}.$$

The final abutment stiffnesses are:

$$K_{l_E} = 20{,}716 \frac{kip}{ft}$$

$$K_{l_W} = 20{,}716 \frac{kip}{ft}$$

$$K_{t_E} = 5{,}472 \frac{kip}{ft}$$

$$K_{t_W} = 6{,}912 \frac{kip}{ft}$$

4.3.5 Section Properties for Linear-elastic Columns of Dubois Bridge

The procedure to determine the section properties for the Dubois bridge columns are the same as that of the Parma bridge columns. The calculations for the section properties for the Dubois bridge columns can be found in Appendix D. A summary of the section properties follow:

$P/f'_cA_{cg} = 0.0586$

$A_{st}/A_{cg} = 0.141\ ft^2/9.62\ ft^2 = 0.0146$

$I_{eff}/I_{cg} = 0.383$

$I_{ceff} = 0.383 * I_{cg} = 0.383 * 7.366\ ft^4 = 2.821\ ft^4$

$J_{gross} = \pi D^4/32 = \pi(3.5^4)/32 = 14.7\ ft^4$

$J_{eff} = 0.2J_{gross} = 2.95\ ft^4$.

4.3.6 Estimating Seismic Loads for Dubois Bridge

The method of estimating the seismic loads for the Dubois bridge is the same as for the Parma bridge, the single mode spectral method. Because the same seismic conditions were used the values of S_{D1} and S_{DS} are the same. The detailed equations and the tables with the resulting distributed loads (Tables D-18 and D-19) can be found in Appendix D.

4.3.7 Material Properties for Non-linear Models of Dubois Bridge

The specified compressive strength for the unconfined concrete for the Dubois bridge is 4 ksi, therefore the material properties for the unconfined concrete for this bridge is the same as that of the Parma bridge. The longitudinal reinforcement for the Dubois bridge consists of 13 Number 11 bars. The material properties for a Number 11 steel bar, according to Table 8.4.2-1 in the AASHTO *Guide Specifications for LRFD Seismic Bridge Design* are:

f_y = 68 ksi = 9,792 ksf,

f_{su} = 95 ksi = 13,680 ksf,

E_s = 29,000 ksi = 4,176,000 ksf,

E_{sh} = 1247 ksi = 179,568 ksf,

ε_{sh} = 0.0115,

ε_{su} = 0.09.

The material properties for the confined concrete are calculated using the Mander model (Mander, et al. 1988). They are as follows:

f_c compressive strength of confined concrete = 785.9 ksf,

ε_c strain at maximum strength = 0.0056,

ε_{cu} strain at ultimate strength 0.0152,

E_c modulus of elasticity = 524,736 ksf.

4.3.8 Modeling Bond-slip Rotation for Dubois Bridge

As with the Parma bridge, the procedure to model bond-slip at the base and the top of the columns is the same as that of the column in the UNR study. The stress and strain values for the *uniaxialMaterial Hysteretic* command for the Dubois bridge are:

s1p = 1700 k.ft Moment at the first point of the envelope in the positive direction,

e1p = 0.00201 Angle at the first point of the envelope in the positive direction,

s2p = 1947 k.ft Moment at the second point of the envelope in the positive direction,

e2p = 0.01970 Angle at the second point of the envelope in the positive direction.

4.3.9 Material Properties of Grouted Couplers for Dubois Bridge

The procedures for determining the material properties for the grouted couplers used in the Dubois bridge are the same as those used in the Parma bridge. The values for the SSNA SNX11 Grouted Coupler used in the Dubois bridge are:

f_y = 9,685.6 ksf yield stress of the coupler,

f_u = 13,190.7 ksf ultimate stress at fracture,

E_s = 3,992,874.0 ksf modulus of elasticity of coupler,

E_{sh} = 317,216.2 ksf slope of the stress-strain curve at strain hardening,

e_{sh} = 0.00307 strain at strain hardening,

e_{ult} = 0.01648 ultimate strain.

4.3.10 Results of Computer Analyses of Dubois Bridge

Table 4-2 shows a summary of the column displacements, drifts, base shear, and base moment for the transverse and longitudinal loading directions. As with the Parma bridge the transverse loads control. The cracked linear-elastic column has smaller displacements and larger reactions than the nonlinear columns for the transverse loading but the values are closer together for the linear and nonlinear columns. The longitudinal results are smaller and closer together than the transverse.

Table 4-2. Dubois Bridge Displacements, Drifts, and Column Base Reactions (Ebrahimpour, et al. 2016)

	Column Model		
	Cracked Linear-elastic	**Nonlinear CIP**	**Nonlinear w/ coupler**
Transverse			
Top of Column Displ., ft	0.080	0.117	0.123
Column Drift, %	0.57	0.830	0.877
Col. Base Shear, k	347	245.3	245.1
Col. Base Moment, k-ft	2,802	1,749	1,747
Longitudinal			
Top of Column Displ., ft	0.036	0.035	0.035
Column Drift, %	0.26	0.25	0.25
Col. Base Shear, k	109	118	117
Col. Base Moment, k-ft	1,011	991	981

Figure 4-19 shows the stress-strain values for the most stressed steel bar in the CIP column. The maximum stress and strain for the transverse and longitudinal direction are indicated by a red and a green dot, respectively. Figure 4-20 shows the stress-strain values for the most stressed steel bar and the grouted coupler with the maximum stress-strain in the steel and the grouted couplers indicated by a red and brown dot, respectively. The stresses and strains were recorded at the bottom of the CIP column. For the column with couplers these measurements were taken at the bottom of the bottom coupler (for the coupler) and below the bottom coupler at the interface of the column and the footing (for the steel). The OpenSees output results for the three Dubois models are presented in Appendix D. The input files are not presented because of their length.

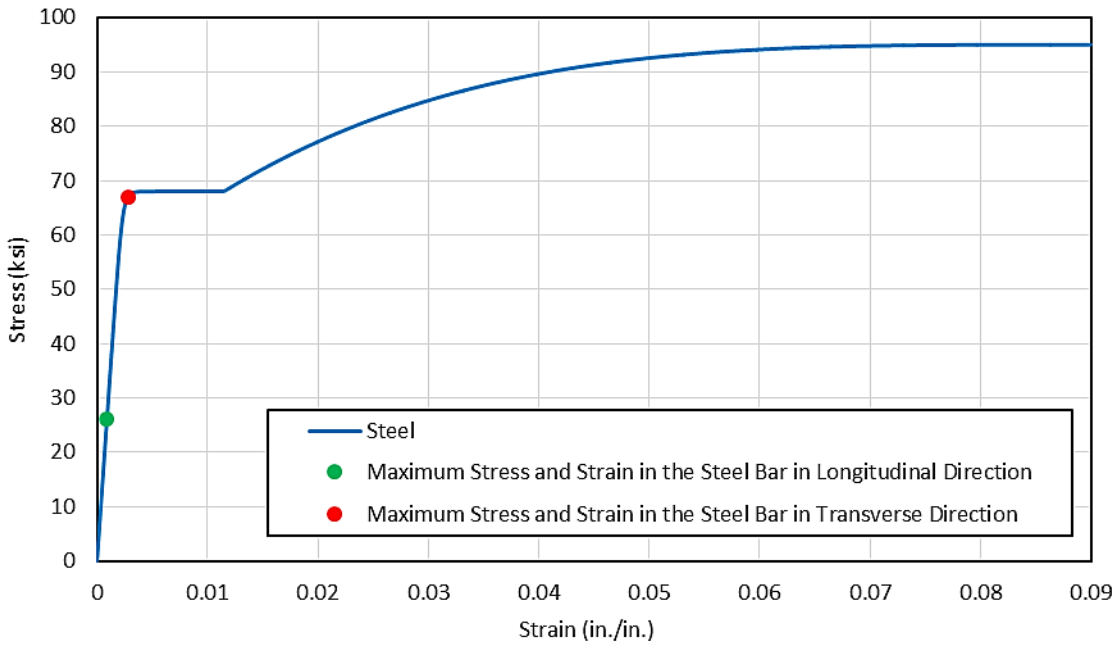

Figure 4-19. The Stress-strain Values in the Most Stressed Steel Bar in the CIP Column (Ebrahimpour, et al. 2016)

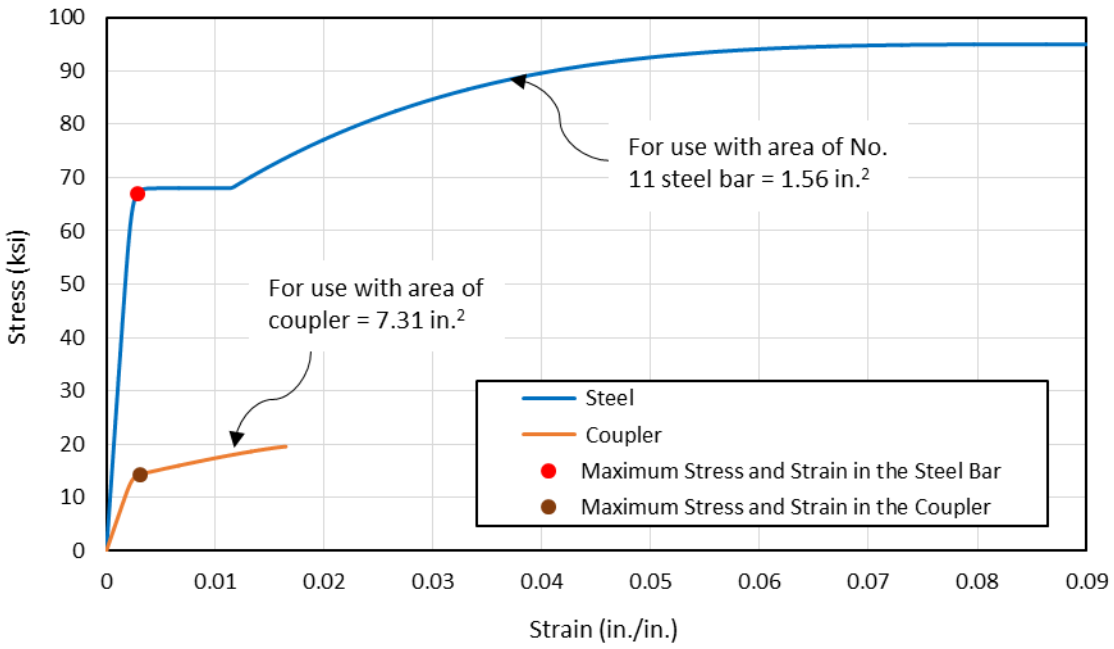

Figure 4-20. The Stress-strain Values in the Most Stressed Steel Bar and Grouted Coupler in the Column with Grouted Couplers under Transverse Loading (Ebrahimpour, et al. 2016)

4.4 Salmon River Bridge

4.4.1 Bridge Description

The third Idaho bridge is on SH-75 and crosses the Salmon River east of Clayton. The plan and elevation of the bridge can be seen in Figures 4-21 and 4-22, respectively. The drawings and specifications were provided by ITD. The bridge near Salmon River is a 260 ft three-span bridge with two piers located at 90 ft and 210 ft from the southwest end of the bridge. The skew in the bridge was removed and the pier caps and abutments were shortened to match the width of the deck to make it easier to model. The superstructure is made up of 8-½ inch thick precast deck panels that rest on five 72 inch prestressed bulb-tee girders. The substructure has two piers, each

with a pier cap and a single oblong column. The column footings are cast-in-place reinforced concrete. The column cross-sections have a major and minor dimension of 9.5 ft and 3.5 ft, respectively. After the skew was removed the major dimension of the column was perpendicular to the length of the bridge. The height of the southwest and northeast columns are 15.469 ft and 15.969 ft, respectively.

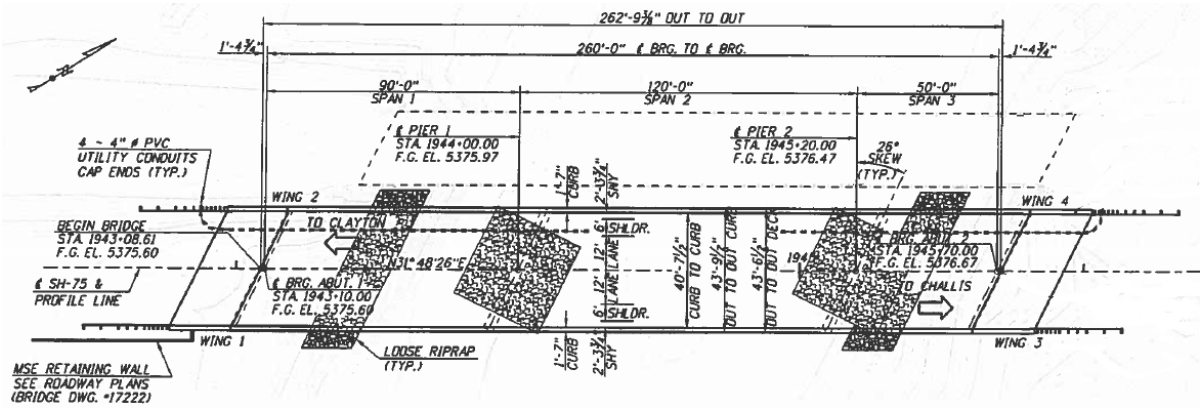

Figure 4-21. Plan View of the Bridge on SH-75 over Salmon River

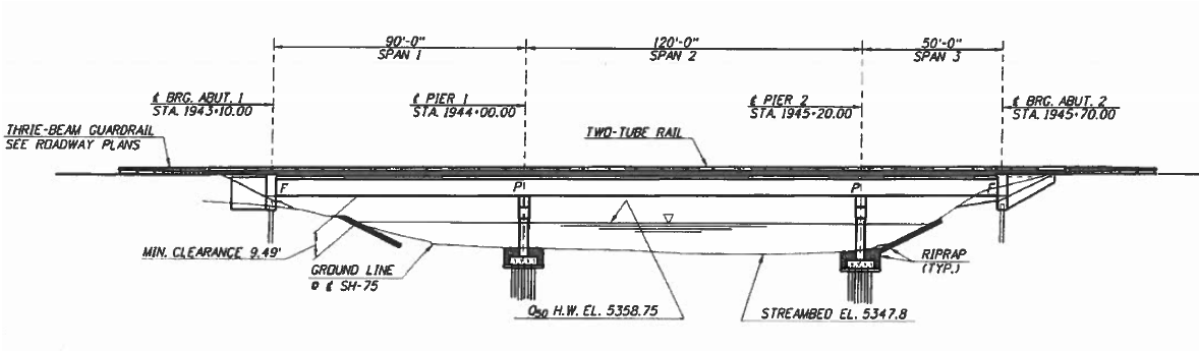

Figure 4-22. Elevation View of the Bridge on SH-75 over Salmon River

The steel reinforcement in the main part of the column consists of 34 number 11 bars within four overlapping number 5 spirals. The columns are connected to the footings with 34

splice sleeves. The transverse reinforcement around the splice sleeves consists of five sets of four overlapping number 5 hoops. See Figures 4-23 and 4-24.

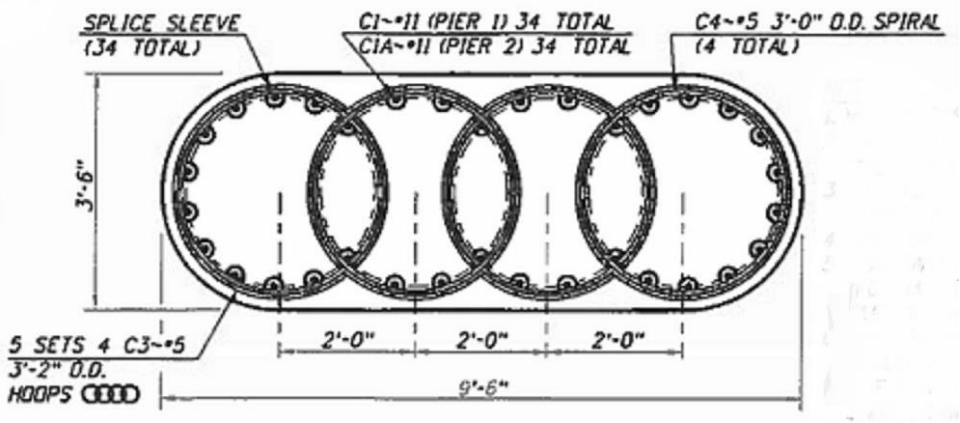

Figure 4-23. Column Section with Steel and Grouted Coupler Locations

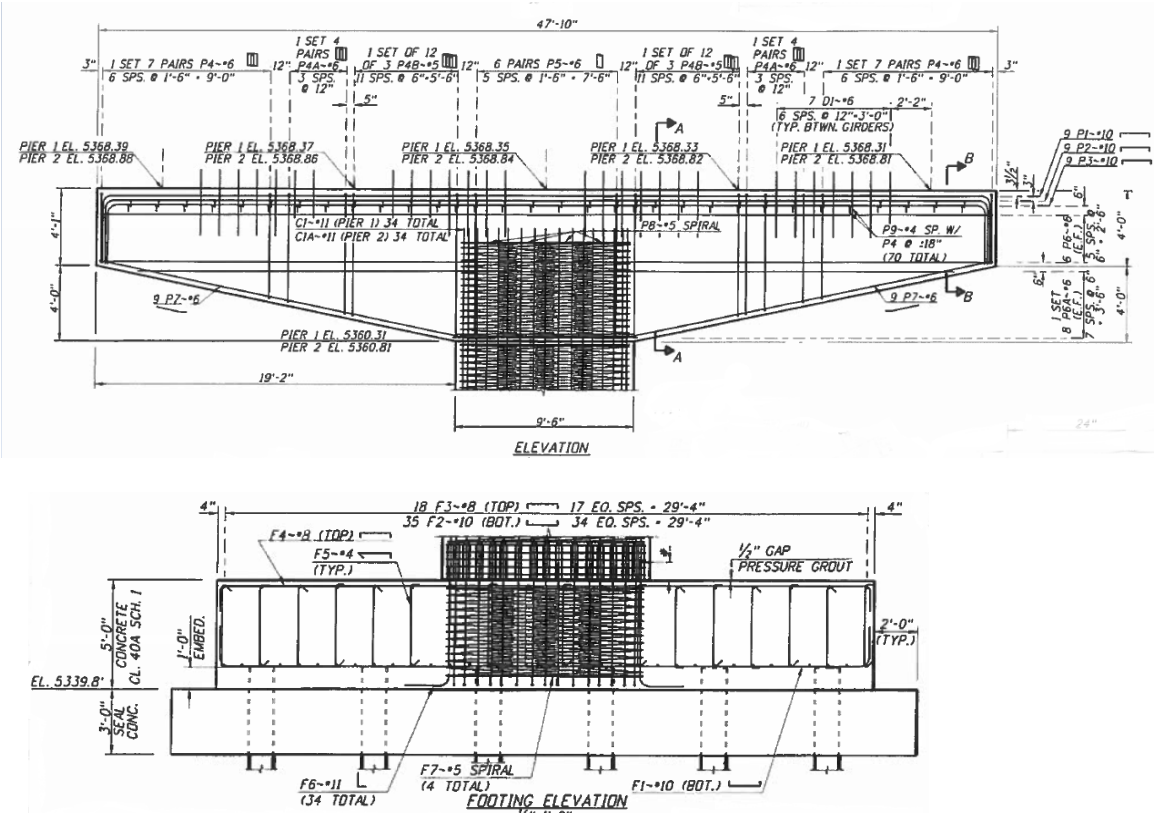

Figure 4-24. Column Cap, Column, and Footing Elevation Views

4.4.2 Linear-elastic Model of Salmon River Bridge

The linear-elastic model consists of nine deck elements and four pier elements for each of the two piers, all of which are *elasticBeamColumn* elements and have linear-elastic properties. There is a *zeroLength* element at each end of the bridge that models the support condition at the abutments. The two top elements of the piers, which represent the column cap and an element that joins the superstructure to the column cap, have very large moments of inertia because bending is prevented by their connection to the superstructure. The bottom element represents the footing and has the same material properties as the column. An illustration of the model can be seen in Figures D-33 and D-34 in Appendix D.

Unlike the other bridges in this study the torsional rigidity of the deck had a significant effect on the displacement of the columns. Therefore, the AASHTO LRFD Specifications' Eq. C 4.6.2.2.1-2. was used to calculate the torsional moment of inertia for the deck. (AASHTO 2014) These calculations are presented in Appendix D.

4.4.3 Nonlinear Models of Salmon River Bridge

The non-linear models have the same number and type of elements in the superstructure and the column cap as the linear-elastic model. The elements in the columns of the non-linear models are *nonlinearBeamColumn* elements with a *zeroLength* element located at the base and top of each column. The footings were removed from these models because the *zeroLength* elements, which model bond-slip, account for the same displacement as the footing.

The non-linear columns with grouted couplers have additional *nonlinearBeamColumn* elements located at the top and bottom of the column which represent the grouted couplers. An illustration of the nonlinear CIP and nonlinear with grouted couplers models can be seen in Figures D-35, D-36, D-40, and D-41 in Appendix D.

4.4.4 Estimating Integral Abutment Stiffness Values for Salmon River Bridge

The soil properties at the abutments of the Salmon River bridge were provided by ITD in the Phase IV Foundation Investigation Report. For the Salmon River bridge, the number of H-piles at the northeast and southwest ends of the bridge are different. Therefore the equation for the longitudinal abutment stiffness was modified to:

$$K_l = \frac{n_s k_s + n_n k_s + (7.7 A_{aw}/d)}{2} \quad (4\text{-}14)$$

Where

K_l = the abutments spring stiffness in the longitudinal direction

n_s = the number of H-piles in the southwest abutment wall =10

n_n = the number of H-piles in the northeast abutment wall = 8

k_s = the initial spring stiffness for one H-pile about the strong axis = 1,392 kip/ft

A_{aw} = the area of the abutment wall = H_{aw} L_{aw} = 495.29 ft^2

d = deflection needed to mobilize full passive resistance = 0.02H_{aw} = 0.23 ft.

The equations for the transverse direction are the same as those for the other Idaho bridges except that the number of H-piles differ at each end of the bridge. A summary of the initial abutment stiffnesses is:

K_l = 20,818.7 kip/ft

K_{ts} = 8,640 kip/ft

K_{tn} = 6,912 kip/ft

The final abutment stiffnesses are:

K_l = 22,672 kip/ft

K_{ts} = 7,200 kip/ft

K_{tn} = 5,760 kip/ft

4.4.5 Section Properties for Linear-elastic Columns of Salmon River Bridge

The procedure to determine the section properties for the Salmon River bridge columns are similar to that of the other Idaho bridges. Because the columns in the Salmon River bridge have different heights and support different lengths of the superstructure of the bridge the axial load ratio and therefore the effective moments of inertia are different for each column. The axial load ratios for the southwest and northeast columns are:

P_s/f'_cA_{cg}= 1,379.55 kips/720 ksf * 30.62 ft^2 = 0.063,

P_n/f'_cA_{cg} = 1,157.16 kips/720 ksf * 30.62 ft^2 = 0.052.

Using the diagram in the AASHTO *Guide Specifications for LRFD Seismic Bridge Design* (2015), see Figure D-32, the elastic stiffness ratios were determined to be:

I_{eff}/I_{cg} = 0.36 Elastic stiffness ratio for the southwest column,

I_{eff}/I_{cg} = 0.35 Elastic stiffness ratio for the northeast column.

Additionally, the moments of inertia for the transverse and longitudinal loadings are different because of the oblong shape of the columns. The calculations for the section properties for the Salmon River bridge columns can be found in Appendix D. A summary of the section properties follow:

For the southwest column,

I_{ceffsy} = 0.36 * I_{cy} = 71.93 ft^4 Effective moment of inertia for a transverse loading,

I_{ceffsz} = 0.36 * I_{cz} = 10.37 ft^4 Effective moment of inertia for a longitudinal loading,

For the northeast column,

$I_{ceffny} = 0.35 * I_{cy} = 69.93$ ft^4 Effective moment of inertia for a transverse loading,

$I_{ceffnz} = 0.35 * I_{cz} = 10.08$ ft^4 Effective moment of inertia for a longitudinal loading.

The effective torsional moment of inertia is 20 percent of the gross torsional moment of inertia. Therefore, the effective torsional moment of inertia is $J_{eff} = 0.2J_{gross} = 18.68$ ft^4.

4.2.6 Estimating Seismic Loads of Salmon River Bridge

The method of estimating the seismic loads for the Salmon River bridge is the same as for the Parma and Dubois bridges, the single mode spectral method. Because the same seismic conditions were used the values of S_{D1} and S_{DS} are the same. The detailed equations and the tables with the resulting distributed loads (Tables D-31 and D-32) can be found in Appendix D.

4.4.7 Material Properties for Non-linear Models of Salmon River Bridge

As previously stated the reinforcement for the main part of the columns consists of 34 number 11 bars attached to four sets of spiral transverse reinforcement. The confined concrete strength was calculated as if for a single circular column with the same cover concrete as the spirals at the base of the column. To make modeling the column cross-section easier the unconfined concrete was assumed to only be the depth of the cover concrete at the base of the columns as shown in Figure 4-25. The value of the compressive strength of the confined concrete used for the sections of the column with the grouted couplers remained the same as that used for

the main part of the columns even though the area of the confined concrete in the sections with the couplers is greater. The differences in the two sections was not enough to result in a significant difference in the compressive strength for their confined concrete.

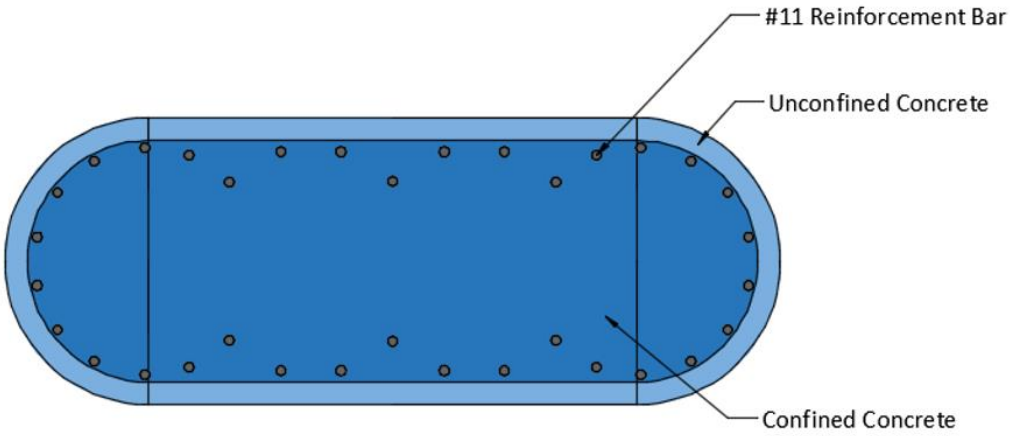

Figure 4-25. Cross-section of the main part of the column showing patch and reinforcement locations

The values needed for the *uniaxialMaterial Concrete01* (unconfined concrete) are:

fpc Maximum compressive strength = 5.0 ksi = 720 ksf,

epsc0 Strain at maximum strength = 0.002,

fpcu Crushing strength = 0.0 ksf, and

epsU Strain at crushing strength = 0.005.

The values needed for the *uniaxialMaterial Concrete04* (confined concrete)

f_c Compressive strength of confined concrete = 966.08 ksf,

ε_c Strain at maximum strength = 0.005418,

ε_{cu} Strain at ultimate strength 0.01475,

E_c Modulus of elasticity = 586,656 ksf.

The material properties for a Number 11 steel bar, according to Table 8.4.2-1 in the AASHTO *Guide Specifications for LRFD Seismic Bridge Design*, 2015, Sec. 8-4, are:

f_y = 68 ksi = 9,792 ksf,

f_{su} = 95 ksi = 13,680 ksf,

E_s = 29,000 ksi = 4,176,000 ksf,

E_{sh} = 1247 ksi = 179,568 ksf,

ε_{sh} = 0.0115,

ε_{su} = 0.09.

4.4.8 Modeling Bond-slip Rotation for Salmon River Bridge

As with the other Idaho bridges, the procedure to model bond-slip at the base and the top of the columns is the same as that of the column in the UNR study. However, because of the oblong shape of the column cross-section the stresses and strains in the reinforcement and the moment reaction differ depending on the direction of the load. Because the moment can only be applied in one direction in the moment-curvature OpenSees file, the orientation of the cross-sections must be turned 90 degrees for each load. The OpenSees input file with both sections are presented in Appendix D.

The stress and strain values for the *uniaxialMaterial Hysteretic* command for the Salmon River bridge are:

$s1p_l$ = 5300 k-ft	moment at the first point of the envelope in the positive direction for longitudinal loading
$e1p_l$ = 0.002	angle at the first point of the envelope in the positive direction for longitudinal loading
$s2p_l$ = 6050 k-ft	moment at the second point of the envelope in the positive direction for longitudinal loading
$e2p_l$ = 0.0128	angle at the second point of the envelope in the positive direction for longitudinal loading
$s1p_t$ = 14800 k-ft	moment at the first point of the envelope in the positive direction for transverse loading
$e1p_t$ = 0.00067	angle at the first point of the envelope in the positive direction for transverse loading
$s2p_t$ = 18300 k-ft	moment at the second point of the envelope in the positive direction for transverse loading
$e2p_t$ = 0.0097	angle at the second point of the envelope in the positive direction for transverse loading

4.4.9 Material Properties of Grouted Couplers for the Salmon River Bridge

The procedures for determining the material properties for the grouted couplers used in the Salmon River bridge are the same as those used in the other Idaho bridges. The values for the SSNA SNX11 Grouted Coupler used in the Salmon River bridge are:

f_y = 9,685.6 ksf — yield stress of the coupler,

f_u = 13,190.7 ksf — ultimate stress at fracture,

E_s = 3,992,874.0 ksf — modulus of elasticity of coupler,

E_{sh} = 317,216.2 ksf — slope of the stress-strain curve at strain hardening,

e_{sh} = 0.00307 — strain at strain hardening,

e_{ult} = 0.01648 — ultimate strain.

4.4.10 Results of Computer Analyses of Salmon River Bridge

The southwest column experiences more displacement at the top of the column in the transverse direction than the northeast column. Therefore, only the results from that column are discussed in this section. Table 4-3 shows a summary of the column displacements, drifts, base shear, and base moment for the transverse and longitudinal loading directions for the southwest column. As with the other bridges the transverse loads control. The cracked linear-elastic column has a larger displacement and smaller column reactions than either nonlinear column in the longitudinal direction. The CIP nonlinear column results are almost identical to the nonlinear with coupler column results in both directions.

Table 4-3. Salmon River Bridge Displacements, Drifts, and Base Reactions for the Southwest Column (Ebrahimpour, et al. 2016)

	Column Model		
	Cracked Linear-elastic	**Nonlinear CIP**	**Nonlinear w/ coupler**
Transverse			
Top of Column Displ., ft	0.063	0.072	0.072
Column Drift, %	0.41	0.47	0.47
Col. Base Shear, k	679	553	551
Col. Base Moment, k-ft	20,560	15,312	15,241
Longitudinal			
Top of Column Displ., ft	0.036	0.036	0.037
Column Drift, %	0.23	0.24	0.24
Col. Base Shear, k	363	433	424
Col. Base Moment, k-ft	3,556	3,691	3,617

The maximum stresses and strains in this bridge occurred at the base of the columns. As shown in Figures 4-26 and 4-27, the maximum stresses and strains in the steel bars and couplers in the transverse direction are greater than that in the longitudinal direction.

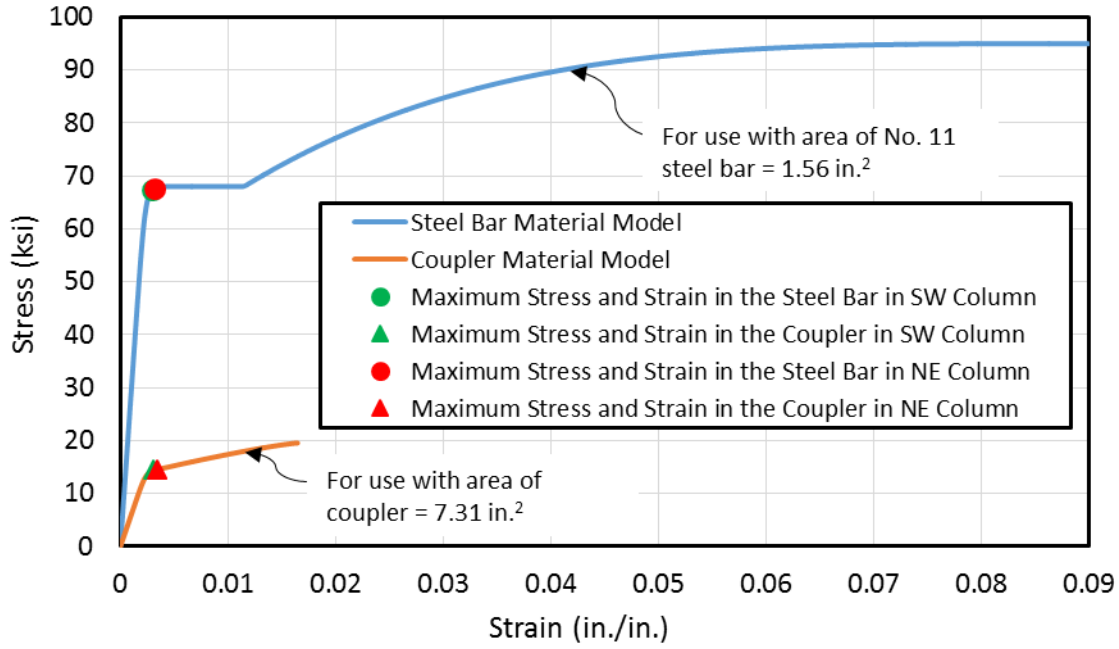

Figure 4-26. The Stress-Strain Values in the Most Stressed Steel Bar and Grouted Coupler in the Column with Grouted Couplers under Transverse Loading (Ebrahimpour, et al. 2016)

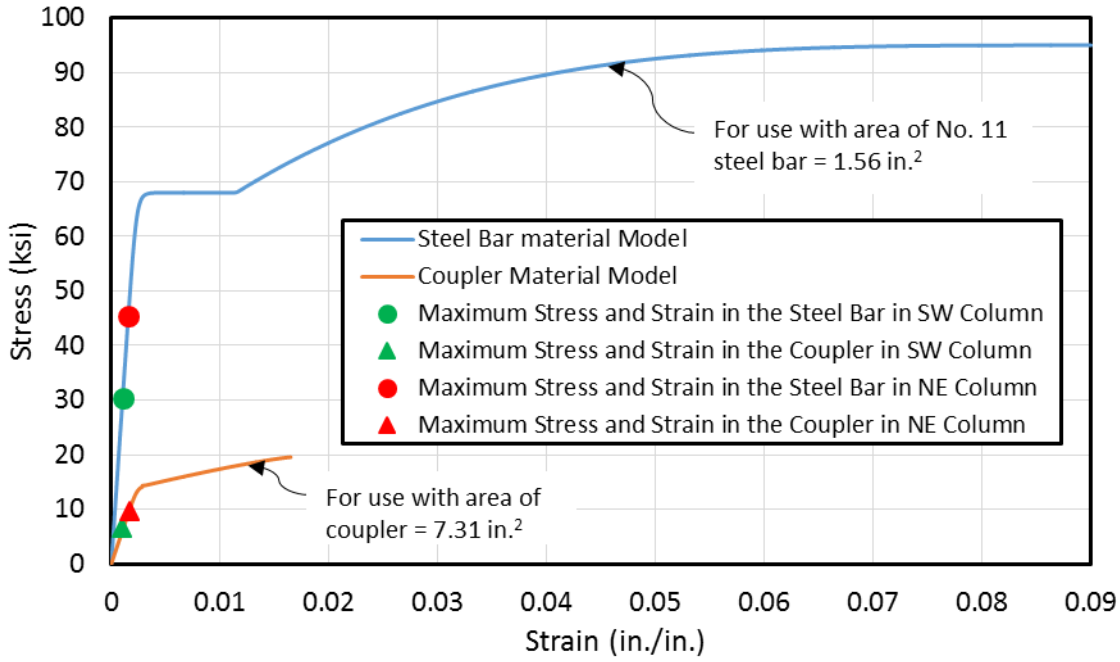

Figure 4-27. The Stress-Strain Values in the Most Stressed Steel Bar and Grouted Coupler in the Column with Grouted Couplers under Longitudinal Loading (Ebrahimpour, et al. 2016)

4.5 Comparison of Results with AASHTO Guide Specifications for LRFD Seismic Bridge Design

In this section the displacement/drift results are compared to the displacement/drift capacity and demand. The AASHTO *Guide Specifications for LRFD Seismic Bridge Design*, Article 4.8.1 presents a formula for the approximation of displacement capacity (Δ_c) for various structure types and Seismic Design Categories (SDC). The bridges in this study were all placed in the most seismically active location in Idaho with soil Site Class D. The structures are considered Type 1 (ductile substructure with essentially elastic superstructure). These conditions place the bridges in SDC C according to The Seismic Guide Table 3.5-1 (AASHTO 2015).

The displacement capacity in inches is:

$$\Delta_C = 0.12\,H_o\{-2.32\ln(x) - 1.22\} \geq 0.12\,H_o \quad (4\text{-}15)$$

Where,

$x = {\Lambda B_o}/{H_o}$, $H_o =$ clear column height in ft,

$B_o =$ column diameter in ft, and

$\Lambda =$ end restraint factor ($\Lambda = 2.0$ for fixed top and bottom and $\Lambda = 1.0$ for fixed-free).

The demand for the linear elastic results is calculated by using the results from the computer analysis and multiplying them by the displacement magnification factor, R_d, as per the Seismic Guide's Article 4.3.3, for each loading direction and adding them together with orthogonal seismic displacements found in Article 4.4 of the Seismic Guide. Since the transverse displacements are larger than the longitudinal, 30% of the longitudinal demand is added to 100% of the transverse demand (AASHTO 2015). The linear magnified demand is:

$$\Delta_{D,\ Linear\ Magnified} = \left(R_d\ \Delta_{D,Linear}\right)_T + 0.3\ \left(R_d\ \Delta_{D,Linear}\right)_L \quad (4\text{-}16)$$

Where,

$\Delta_{D,\ Linear\ Magnified}$ = magnified displacement demand through linear-elastic analysis,

$\left(R_d\ \Delta_{D,Linear}\right)_T$ = magnified transverse displacement demand, and

$\left(R_d\ \Delta_{D,Linear}\right)_L$ = magnified longitudinal displacement demand.

R_d is obtained as follows:

$$R_d = \left(1 - \frac{1}{\mu_D}\right)\frac{T^*}{T} + \frac{1}{\mu_D} \geq 1.0 \text{ for } \frac{T^*}{T} > 1.0 \quad (4\text{-}17)$$

$$R_d = 1.0 \text{ for } \frac{T^*}{T} \leq 1.0 \quad (4\text{-}18)$$

Where,

$T^* = 1.25T_s$,

μ_D= maximum local member displacement demand = 3.0 for SDC C, and

$T_s = \frac{S_{D1}}{S_{DS}}$.

For the nonlinear demand the magnification factor in not needed and the demand is:

$$\Delta_{D,\ Nonlinear} = \left(\Delta_{D,Nonlinear}\right)_T + 0.3\ \left(\Delta_{D,Nonlinear}\right)_L \quad (4\text{-}19)$$

Where,

$\Delta_{D,\ Nonlinear}$ = displacement demand through nonlinear analysis,

$\left(\Delta_{D,\,Nonlinear}\right)_T$ = transverse nonlinear displacement demand, and

$\left(\Delta_{D,\,Nonlinear}\right)_L$ = longitudinal nonlinear displacement demand.

A summary of the capacities and demands for all three bridges are shown in Table 4-4.

Table 4-4. Displacement and Drift Capacity versus Demand for Bridge Columns (Ebrahimpour, et al. 2016)

	Parma	**Dubois**	**Salmon River**
Capacity			
H_o, ft	25.60	14.05	15.47
B_o, ft	3.5	3.5	9.5[b]
Δ_C, ft	0.458	- [a]	0.155
Drift = Δ_C/H_o, %	1.79	- [a]	1.00
Demand, Magnified Linear-elastic Analysis			
Transverse R_d	1.149	1.711	1.420
Longitudinal R_d	1.632	2.077	2.051
$\Delta_{D,\,Linear\,Magnified}$, ft	0.402	0.159	0.112
Drift = $\left(\Delta_{D,\,Linear\,Magnified}\right)/H_o$, %	1.57	1.13	0.72
Demand, Nonlinear Analysis			
$\Delta_{D,\,Nonlinear}$, ft	0.400	0.128	0.082
Drift = $\left(\Delta_{D,\,Nonlinear}\right)/H_o$, %	1.56	0.91	0.53

[a] LRFD Bridge Seismic Guide Article 4.8.1 equations may only be used for clear heights greater than or equal to 15 ft.
[b] Using the transverse direction, thus the major dimension of the oblong cross-section is used.

The capacity of the Parma and Salmon River Bridges, as seen in Table 4-4, exceeds demand. The capacity for the Dubois Bridge, however, could not be calculated. The drift demand using the magnified linear-elastic analysis for the Parma, Dubois, and Salmon River bridges are 1.57, 1.13, and 0.72, respectively. The values using the nonlinear analysis are 1.56, 0.91, and

0.53, respectively. It should be noted that for all three bridges the drift demand values estimated using the magnified linear-elastic analysis are larger than the values from the nonlinear analysis.

Chapter 5 - Analysis of Single Columns with Grouted Couplers under Large Drifts

5.1 Introduction

In this chapter two columns with grouted couplers at the top and bottom of the column, one from the Parma Bridge and one from the Dubois Bridge, were analyzed under large drifts to observe the behavior of the coupler and steel reinforcing bar. Each column had fixed-fixed boundary conditions wherein the bottom of the column is fixed and the top of the column is allowed to translate but not rotate. The fixed-fixed boundary condition was chosen because it more accurately depicted the behavior of columns in a multi-column bent with a rigid cap beam. The loading is as shown in Figure 5-1. The columns were pushed horizontally until the grouted coupler failed.

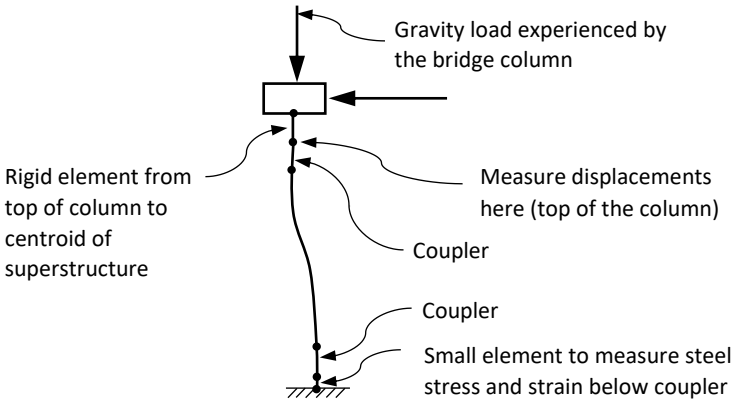

Figure 5-1. Single Column with Fixed-fixed Boundary Conditions (Ebrahimpour, et al. 2016)

5.2 Single Column from Parma Bridge

Figure 5-2 shows the moment reaction at the base of the column versus displacement for a single column from the Parma bridge. In addition to the curve for the nonlinear column with grouted couplers at the top and bottom of the column (see Figure 5-1), the curves for the cracked linear-elastic column and nonlinear cast-in-place (CIP) column are also shown in Figure 5-2. For the nonlinear columns, the points where the steel or the coupler at the extreme location failed (i.e., reached their ultimate values) are noted. Note that in OpenSees once the fiber material (steel or coupler) reaches its ultimate values, the stress remains constant while the strain increases. The displacement in the column with grouted couplers corresponding to the failure of the SSNA No. 14 U-X grouted coupler (used in the Parma bridge model) and the failure of the ASTM A615 steel are 1.126 ft and 1.237 ft, respectively. With the column being 25.6 ft in length, these displacements correspond to drift values of 4.4 percent and 4.8 percent, respectively. Table 5-1 shows the stress and strain values in the most stressed coupler and steel bar for the column in the Parma bridge.

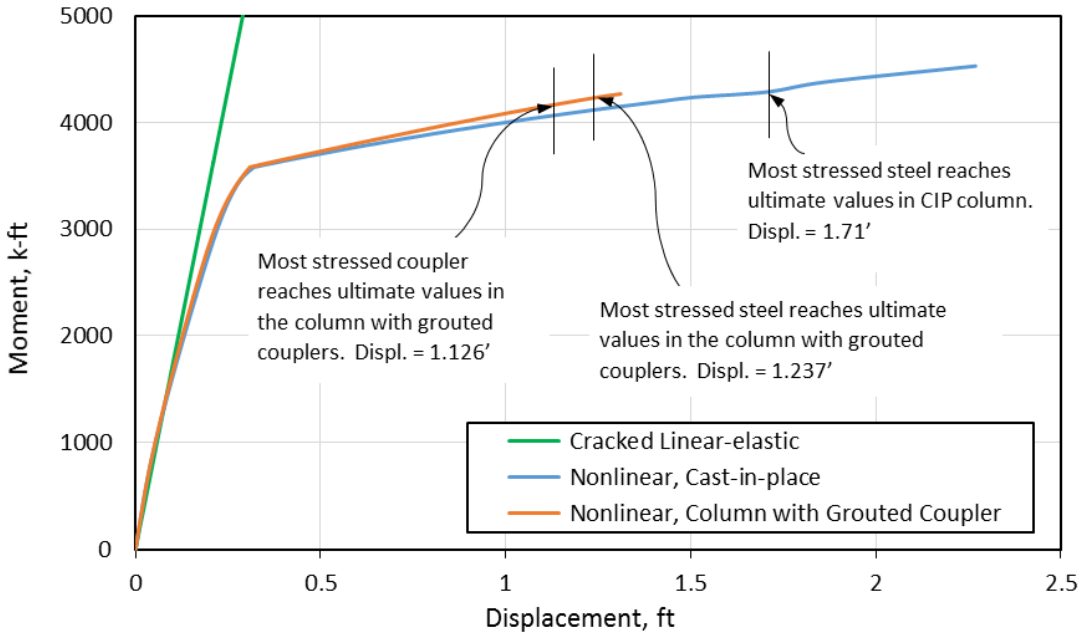

Figure 5-2. Parma Fixed-fixed Column Base Moment versus Top of Column Displacement (Ebrahimpour, et al. 2016)

Table 5-1. Stress and Strain in Coupler Region and Steel Bar for Parma Fixed-fixed Column with Grouted Couplers (Ebrahimpour, et al. 2016)

Column Nonlinear Drift, %	Coupler Region		Steel Bar	
	Stress, ksi	Strain, in./in.	Stress, ksi	Strain, in./in.
0.25	4.50	0.0005	16.32	0.0006
0.5	11.25	0.0012	43.40	0.0015
0.75	15.40	0.0021	65.16	0.0025
1	16.65	0.0044	67.99	0.0045
1.5	18.59	0.0080	73.51	0.0123
2	19.21	0.0094	76.78	0.0156
2.5	19.88	0.0110	80.14	0.0195
3	20.50	0.0126	83.14	0.0236
3.5	21.08	0.0144	86.12	0.0285
4	21.56	0.0165	88.64	0.0338
4.4	21.80[a]	0.0185[a]	90.43	0.0386
4.5	-	-	90.95	0.0402
4.8	-	-	95.00[b]	0.06[b]
4.9	-	-	95.00[c]	0.09[c]

a Ultimate stress and strain values for SSNA No. 14 U-X grouted coupler

b Ultimate stress and strain values for ASTM A615 Grade 60 steel bar

c Ultimate stress and strain values for ASTM A706 Grade 60 steel bar

As shown in Table 5-1, the most stressed coupler reaches its ultimate stress and strain values (i.e., 21.80 ksi and 0.0185 in./in.) at a nonlinear drift value of 4.4 percent.

5.3 Single Column from Dubois Bridge

Table 5-2 shows the stress and strain values in the coupler region and the steel bar for a Dubois column with grouted couplers and fixed-fixed boundary conditions.

Table 5-2. Stress and Strain in Coupler Region and Steel Bar for Dubois Fixed-fixed Column with Grouted Couplers (Ebrahimpour, et al. 2016)

Column Nonlinear Drift, %	Coupler Region		Steel Bar	
	Stress, ksi	Strain, in./in.	Stress, ksi	Strain, in./in.
0.25	7.34	0.0012	33.79	0.0012
0.5	14.12	0.0029	66.25	0.0026
0.75	14.36	0.0030	66.80	0.0028
1	14.40	0.0031	67.24	0.0029
1.5	14.55	0.0035	67.73	0.0032
2	14.78	0.0040	67.92	0.0037
2.5	15.11	0.0047	67.99	0.0044
3	15.60	0.0058	68.00	0.0056
3.5	16.12	0.0070	68.00	0.0088
4	17.37	0.0100	73.59	0.0165
4.5	18.77	0.0137	84.44	0.0294
4.94	19.54[a]	0.0164[a]	87.92	0.0360

[a] Ultimate stress and strain values for SSNA No. SNX11 grouted coupler

As shown in Table 5-2, the most stressed coupler reaches its ultimate stress and strain values (i.e., 19.54 ksi and 0.0164 in./in.) at a nonlinear drift value of 4.9 percent.

5.4 Discussion

The results from the single column analysis indicate that both the Parma and the Dubois columns were able to withstand at least 4 percent of nonlinear drift before the grouted coupler failed. Although both columns have the same diameter of 3.5 ft, there are some differences that would affect their behavior. The factors that may influence the behavior of the two columns considered are: (a) Parma's bridge column aspect ratio (the ratio of column height to diameter) is larger than the Dubois' bridge column aspect ratio; (b) Parma's column has a steel to concrete ratio of 2.90 percent, while Dubois' column has a steel to concrete ratio 1.46 percent; (c) Parma's column resulted in a larger confined concrete compressive strength (about 11 percent higher) than Dubois's; and (d) in the analysis of Parma's column, the SSNA No. 14 U-X grouted coupler was used, while for Dubois's, the SSNA No. SNX 11 grouted coupler was used.

Chapter 6 – Guidelines for the use of Grouted Couplers in Idaho Bridge Columns

6.1 Introduction

Based on the findings in the literature review (Chapter 2), the results of computer modeling of Idaho bridges (Chapters 4 and 5), and the detailed information presented in Appendix F, this chapter provides guidelines for ITD bridge designers when using precast columns with grouted couplers.

NMB Splice Sleeve and Erico Lenton Interlok couplers meet the ACI Type 2 and AASHTO's Full Mechanical Connection (FMC) coupler strength requirements. ACI Type 1 couplers are capable of developing the ultimate strength of the bar in tension (i.e., 1.0 f_u). The AASHTO's FMC couplers must be able to achieve 1.25 times the specified yield stress (i.e., 1.25 f_y) of the coupled bar. The grouted couplers in Table 6-1 meet the ACI and AASHTO strength requirements. (AASHTO 2014, ACI 2014) In addition, using a specified 90 ksi ultimate strength for Grade 60 bars, these couplers are also capable of reaching 1.5 f_y as required by Utah's Structures Design and Detailing Manual (see Appendix F, Section "Key Items Found in the Literature or by Contacting the Manufacturers").(UDOT 2015)

Table 6-1. List of Approved Grouted Couplers (Ebrahimpour, et al. 2016)

ASTM A706 or ASTM A615 Grade 60 Bar Size	NMB Splice Sleeve (ACI 2014)	Erico Lenton Interlok (Erico 2013)
#5	-	LK5
#6	6U-X	LK6
#7	7U-X	LK7
#8	8U-X	LK8
#9	9U-X	LK9
#10	10U-X	LK10
#11	11U-X, SNX11	LK11
#14	14U-X	LK14
#18	-	LK18

6.2 Recommendations for the Idaho Bridge Manual

1. Grouted splice couplers may be used to connect precast columns to footings or cap beams for columns with less than 4 percent drift. Drift is determined by dividing the maximum displacement at the top of the column by its height. Displacements may be obtained through nonlinear analysis (i.e., bridge columns having nonlinear materials for unconfined concrete, confined concrete, and reinforcing steel). Alternatively, the displacements may be obtained by linear-elastic analysis (i.e., using cracked column section) and magnification factors as per AASHTO *Guide Specifications for LRFD Seismic Bridge Design* Article 4.3.3. In both cases, combination of orthogonal seismic displacements are to be used as per Seismic Guide's Article 4.4.(AASHTO 2015)

2. The total length of grouted splice couplers shall not exceed $15d_b$, where d_b is the longitudinal reinforcing bar diameter. See Table 6-1 for a list of approved grouted couplers

3. Grouted couplers in plastic hinge zones must develop 150% of the specified yield strength of the connected reinforcing bar. See Table 6-1 for a list of approved grouted couplers.

4. Minimum clear distance between grouted splice couplers is recommended to be the same as those specified for reinforcing bars. See the typical detail drawings in Figure 6-1. The clear cover for the shear reinforcement over grouted couplers in the precast column shall be 2". See the typical detail drawings in Figure 6-1.

5. Grout for grouted couplers shall be provided by the manufacturer.

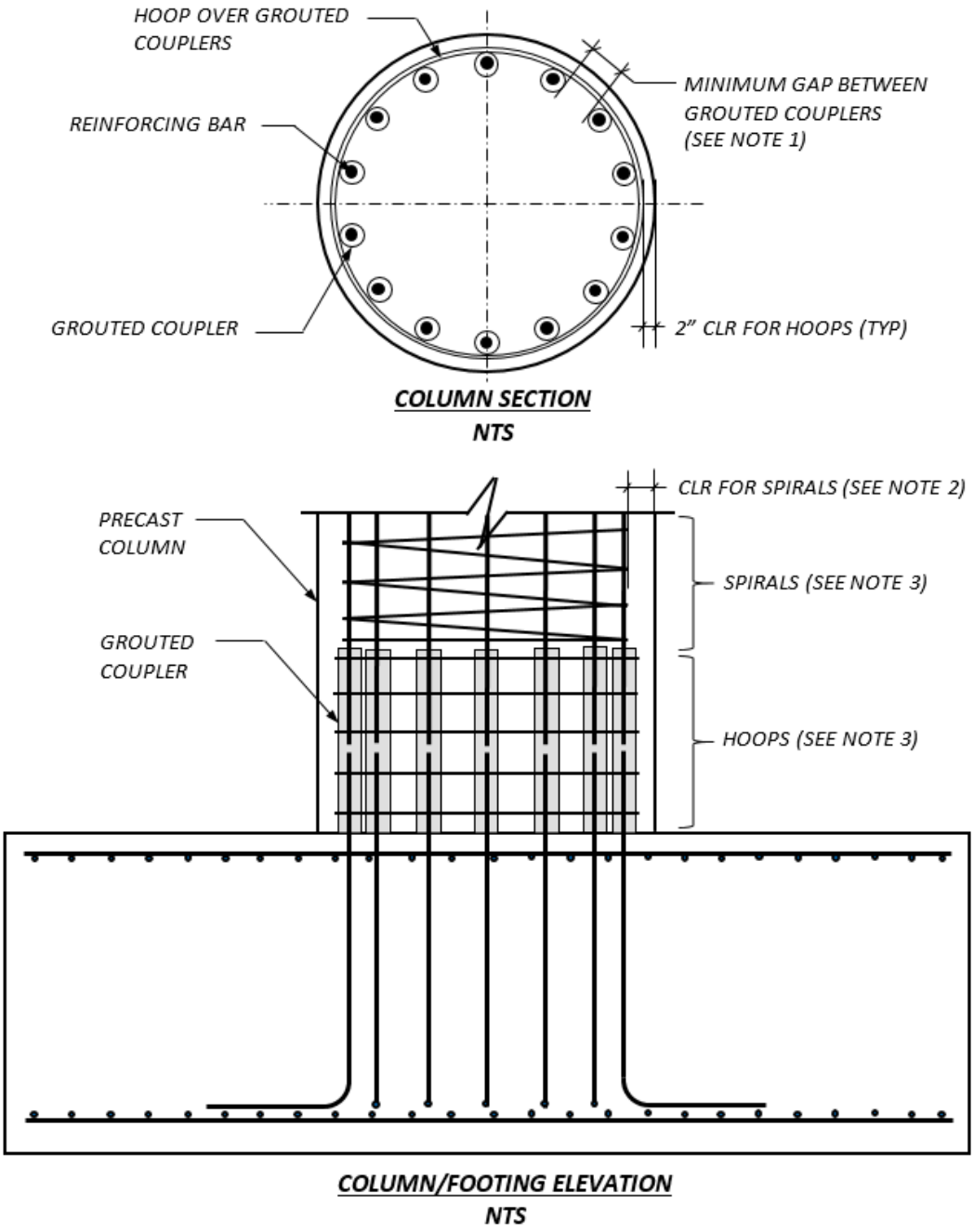

NOTES:

1. LARGER OF (1) 1 IN., (2) 1.33 TIMES MAX. COARSE AGGREGATE SIZE, AND (3) NOMINAL DIAMETER OF CONNECTED REINFORCING.
2. CLEAR COVER FOR SPIRALS = 2" + (DIAM. OF COUPLER – DIAMETER OF BAR)/2
3. FOLLOW THE REQUIREMENTS OF AASHTO LRFD BRIDGE DESIGN SPECIFICATIONS SECTION 5.10.6.

Figure 6-1. Typical Precast Column with Grouted Couplers to Footing Connection Details (Ebrahimpour, et al. 2016)

Chapter 7- Conclusions and Recommendations

7.1 Conclusions

The Idaho Transportation Department (ITD) requested that recommendations for guidelines for the use of grouted couplers in precast concrete columns be made to them based on the analyses of the behavior of three typical highway bridges in Idaho seismic conditions. To accomplish this task four steps were needed: (1) a comprehensive literature review of pertinent research and a survey of current practices of certain western Departments of Transportation (DOT), (2) a verification of the chosen method of analysis. (3) The analysis of the three bridges chosen for this study and a comparison of the results with calculated demand and capacity per the method in the AASHTO *Guide Specifications for LRFD Seismic Bridge Design*. Also an analysis of free-standing columns from two of the bridges was made using large displacements until failure, (4) recommendations for the guidelines to be included in the Idaho Bridge Design Manual were made based on the previously mentioned analysis, current practice, and other research. A brief outline of the first three steps are presented below.

Step 1: Perform a comprehensive literature review. In this step it was concluded that there were two major experimental projects on the behavior of columns with grouted couplers in seismic zones. The data in these projects indicated that grouted couplers could be used in bridge columns if the column drifts were not excessive. However, only one of the sponsors for these projects accepted the recommendations presented to them. The Utah Department of Transportation (UDOT) included a section on the use of grouted couplers in the UDOT *Structures Design and Detailing Manual*.

Step 2: Using OpenSees computer models of the cast-in-place (CIP) column and the column with grouted couplers and no pedestal (GCNP) from the experimental project conducted at the University of Nevada, Reno (UNR) were duplicated. The force-displacement results from the models created in the current study were almost identical to that of the results of the experimental and computer models in the UNR study.

Step 3: In the first part of Step 3 seismic analyses of three Idaho bridges was conducted. The three bridges were the Parma Bridge, the Dubois Bridge, and the Salmon River Bridge. The bridges were modeled in OpenSees and subjected to conditions that would be found in the most seismically active location in Idaho. Each bridge was modeled with three different types of columns: the cracked linear-elastic, the nonlinear cast-in-place (CIP), and the nonlinear with grouted couplers. The grouted couplers were placed within the column and not in the footings or column cap. The results from the computer analyses indicated that in seismic conditions found in Idaho the behavior of columns with grouted couplers was not significantly different from that of the nonlinear CIP columns. It should be noted that the bridges in this study were not specifically designed for the seismic loads that were used but performed well nevertheless. The stresses in the longitudinal reinforcing steel bars and grouted couplers were well within the acceptable range. The highest drift experienced was in the transverse direction of the Parma Bridge at about 1.6 percent when considering a combination of orthogonal displacements. The AASHTO *Guide Specifications for LRFD Seismic Bridge Design* procedures for estimating the magnified linear-elastic drift demand resulted in either the same or larger values compared to the corresponding drift demand values obtained using nonlinear analysis.

In the second part of Step 3 an analysis of single columns taken from two of the bridges, the Parma bridge and the Dubois bridge, was conducted under large drifts. The columns were

pushed until the most stressed coupler in the column reached its ultimate stress. It was found that in both columns the maximum drift was well over 4 percent.

7.2 Recommendations

Step 4: Guidelines for the use of grouted couplers in Idaho bridges were given to the Idaho Transportation Department (ITD) for inclusion in the Idaho Bridge Design Manual. The guidelines are presented in detail in Chapter 6. It was considered that the use of grouted couplers was appropriate if the maximum drift did not exceed 4 percent. The column drift can be obtained by either analyzing the bridge using nonlinear materials in the column, (i.e., unconfined concrete, confined concrete, and reinforcing steel) or by using a cracked linear-elastic column combined with magnification factors using the AASHTO *Guide Specifications for LRFD Seismic Bridge Design*. The procedure to calculate the magnification factor can be found in Chapter 4 in section 4.5. A list of approved grouted couplers and an illustration of a typical column connection using grouted couplers are also shown in Chapter 6.

References

American Association of State Highway and Transportation Officials (AASHTO). (2014). *AASHTO LRFD Bridge Design Specifications,* American Association of State Highway and Transportation Officials, Washington, D. C

American Association of State Highway and Transportation Officials (AASHTO). (2015). *AASHTO Guide Specifications for LRFD Seismic Bridge Design,* Washington, D. C.

ACI Committee 439. (2007). *Types of Mechanical Splices for Reinforcing Bars,* Report No. ACI 439.3R-07, American Concrete Institute, Farmington Hills, MI.

ACI Committee 374. (2013). *Guide for Testing Reinforced Concrete Structural Elements under Slowly Applied Simulated Seismic Loads,* Report No. ACI 374.2R-13, American Concrete Institute, Farmington Hills, MI.

ACI Committee 318. (2014). *Building Code Requirements for Reinforced Concrete,* American Concrete Institute, Detroit, MI.

ASTM International. (2005). *Standard Test Methods for Testing Mechanical Splices for Steel Reinforcing Bars,* Report no. A 1034/A 1034M-05, ASTM International, West Conshohocken, PA.

Bentley Systems, Inc. (2013). *STAAD.Pro V8i Technical Reference Manual,* Exton, PA.

California Department of Transportation (Caltrans). (2015). *Memo to Designers 20-9,* Sacramento, CA.

Ebrahimpour, A., Earles, B. E., Maskey, S., Tangarife, M., Sorensen, A. D. (2016). *Seismic performance of columns with grouted couplers in idaho accelerated bridge construction applications*, Report No. FHWA-ID-16-246, Idaho Transportation Department, Boise, ID.

Erico. (2013). *Instruction Manual Lenton Interlok Rebar Splicing System,* Erico.

Federal Highway Administration. (2017). “Accelerated Bridge Construction.” <www.fhwa.dot.gov/bridge/abc/> (Sept. 25, 2017).

Haber, Z. B., Saiidi, M. S. and Sanders, D. H. (2013). *Precast Column-Footing Connections for Accelerated Bridge Construction in Seismic Zones,* Report No. CCEER 13-08, Center for Civil Engineering Earthquake Research, University of Nevada, Reno.

Haber, Z. B., Saiidi, M. S., and Sanders, D. H. (2015). “Behavior and Simplified Modeling of Mechanical Reinforcing Bar Splices.” *ACI Structural Journal,* Title No. 112-S16, (March-April 2015).

Jansson, P. O. (2008). *Evaluation of Grout-filled Mechanical Splices for Precast Concrete Construction,* Report No. R-1512, Michigan Department of Transportation (MDOT), Lansing, MI.

Mander, J. B., Priestley, M. J. N., and Park, R. (1988). “Theoretical Stress-Strain Model for Confined Concrete”, *Journal of Structural Engineering,* Vol. 114, No. 8 (August 1988): pp. 1804 – 1826.

Marsh, M. L., Buckle, I. G., Kavazanjian, E. (2014). *LRFD Seismic Analysis and Design of Bridges Reference Manual,* Report No. FHWA-NHI-15-004, Federal Highway Administration, Washington, D. C.

Mast, R., Marsh, L, Spry, C., Johnson, S., Griebenow, R., Guarre, J., and Wilson, W. (1996). *Seismic Design of Bridges – Design Example No. 1: Two-Span Continuous CIP Concrete Box Bridge*, FHWA-SA-97-006, U. S. Department of Transportation Federal Highway Administration Central Federal Lands Highway Division.

Pantelides, C. P., Ameli, M. J., Parks, J. E. and Brown, D. N. (2014). *Seismic Evaluation of Grouted Splice Sleeve Connections for Precast RC Bridge Piers in ABC,* Report No. UT-14.09, University of Utah Department of Civil and Environmental Engineering, Salt Lake City, UT.

Splice Sleeve North America, Inc. (SSNA) (2016). *NMB Splice Sleeve Type U-X, SNX11, and A11W Systems for Connecting Reinforcing Bars,* Report ESR-3433, Splice Sleeve North America, Inc.

Tazarv, M. and Saiidi, M. S. (2015). *Design and Construction of Bridge Columns Incorporating Mechanical Bar Splices in Plastic Hinge Zones,* Report No. CCEER 15-07, Center for Civil Engineering Earthquake Research, University of Nevada, Reno.

U. S. Geological Survey (USGS). (2015). "U.S. Seismic Design Maps. U. S. Geological Survey." <http://www.earthquake.usgs.gov/designmaps/us/application.php> (Oct. 1, 2015).

University of California, Berkeley. (2016). "OpenSees; resources for users." <http://opensees.berkeley.edu/OpenSees/user/index.php> (July 20, 2016).

Utah Department of Transportation (UDOT). (2015). *Structures Design and Detailing Manual,* Utah Department of Transportation, Salt Lake City, UT.

Vosooghi, A. and Saiidi M. S. (2010). *Seismic Damage States and Performance Parameters for Bridge Columns; ACI Special Publication Series SP-271, Structural Concrete in Performance-based Seismic Design of Bridges,* American Concrete Institute, Farmington Hills, MI.

Wehbe, N. I., Saiidi, M. S., and Sanders, D. H. (1999). "Seismic Performance of Rectangular Bridge Columns with Moderate Confinement," *ACI Structural Journal.* Vol. 96, No. 2, pp. 248-258.

Wiss, Janney, Elstner Associates, Inc. (2013). *Splice Sleeve North America Laboratory Tests for Conversion of Legacy Report,* Report No. ER-5645, WJE, Inc., Chicago, IL.

Appendix A - Verification of Computer Model Using FHWA Example No. 1

FHWA Seismic Design of Bridges - Example No. 1 with Basic Support Condition

For details of the bridge dimensions and assumptions used, refer to "*Seismic Design of Bridges Design Example No. 1*."

Basic Support Condition

Support stiffness: Rigid
Column stiffness: I_{gross}
Abutment type: Seat type
Restraint of superstructure: Unrestrained longitudinally, restrained (pinned) in the transverse direction.

Superstructure

L = 242 ft	Overall bridge length
A_d = 120 ft^2	Cross-sectional area of superstructure
A_{cb} = 25 ft^2	Cross-sectional area of cap beam
I_{yd} = 51,000 ft^4	Moment of inertia of superstructure cross-sec. about local y-axis
I_{zd} = 575 ft^4	Moment of inertia of superstructure cross-sec. about local z-axis
f_c = 4,000 lb/in^2	Compressive strength of concrete
E_c = 3,600 kip/in^2 = 5.184 x 10^5 kip/ft^2	Young' modulus of elasticity of concrete

Substructure

$I_c = \pi d^4/64 = \pi(4)^4/64$ = 12.57 ft^4	Moment of inertia of one column (about local y- or z-axes)
$A_c = \pi d^2/4 = \pi(4)^2/4$ = 12.57 ft^2	Cross-sectional area of one column

Rigid end zone of the upper part of columns = 2.83 ft. Assign a large stiffness to this zone.

Model of structure

Let's use the same number of nodes and elements as the SAP computer analysis files in the Example 1 Appendix. Except in the upper 2.83 ft of the columns, include a rigid element. In SAP this end condition can be specified. In STAAD and OpenSees, let's add a stiff element at these locations (three locations).

STAAD Model and Results

The STAAD input file and illustrations of the bridge model, its loads, and displacements are presented in this section. Figures A-1 and A-2 show the nodes and elements. Figures A-3 and A-4 show the model under transverse and longitudinal 100 kip/ft loads, respectively. Figures A-5 and A-6 show the displaced shapes of the structure under the transverse and longitudinal loads, respectively.

Input Command File for Basic Support Condition

```
STAAD SPACE
START JOB INFORMATION
ENGINEER DATE 02-Jun-15
END JOB INFORMATION
INPUT WIDTH 79
UNIT FEET KIP
JOINT COORDINATES
1 0 30.17 0; 2 35.5 30.17 0; 3 71 30.17 0; 4 106.5 30.17 0; 5 142 30.17 0;
6 167 30.17 0; 7 192 30.17 0; 8 217 30.17 0; 9 242 30.17 0; 10 142 0 28.375;
11 142 2 28.375; 12 142 27.34 28.375; 13 142 30.17 28.375; 14 142 0 0;
15 142 2 0; 16 142 27.34 0; 17 142 0 -28.375; 18 142 2 -28.375;
19 142 27.34 -28.375; 20 142 30.17 -28.375;
MEMBER INCIDENCES
1 1 2; 2 2 3; 3 3 4; 4 4 5; 5 5 6; 6 6 7; 7 7 8; 8 8 9;
9 10 11; 10 11 12; 11 12 13; 12 14 15; 13 15 16; 14 16 5; 15 17 18; 16 18 19;
17 19 20; 18 20 5; 19 5 13;
DEFINE MATERIAL START
ISOTROPIC CONCRETE
E 518400
POISSON 0.17
DENSITY 0.150336
ALPHA 5e-006
DAMP 0.05
TYPE CONCRETE
STRENGTH FCU 576
END DEFINE MATERIAL
MEMBER PROPERTY AMERICAN
1 TO 8 PRIS AX 120 IX 6000 IY 51000 IZ 575
9 10 12 13 15 16 PRIS AX 12.6 IX 25 IY 12.6 IZ 12.6
11 14 17 PRIS AX 1e+008 IX 1e+008 IY 1e+008 IZ 1e+008
18 19 PRIS AX 25 IX 10000 IY 1e+008 IZ 1e+008
CONSTANTS
MATERIAL CONCRETE ALL
SUPPORTS
10 14 17 FIXED
1 9 FIXED BUT FX MY MZ
LOAD 1 LOADTYPE None TITLE 100 KIP/FT TRANSVERSE
```

```
MEMBER LOAD
1 TO 8 UNI GZ -100
LOAD 2 LOADTYPE None TITLE 100 KIP/FT LONGITUDINAL
MEMBER LOAD
1 TO 8 UNI GX 100
PERFORM ANALYSIS
PRINT JOINT DISPLACEMENTS ALL
FINISH
```

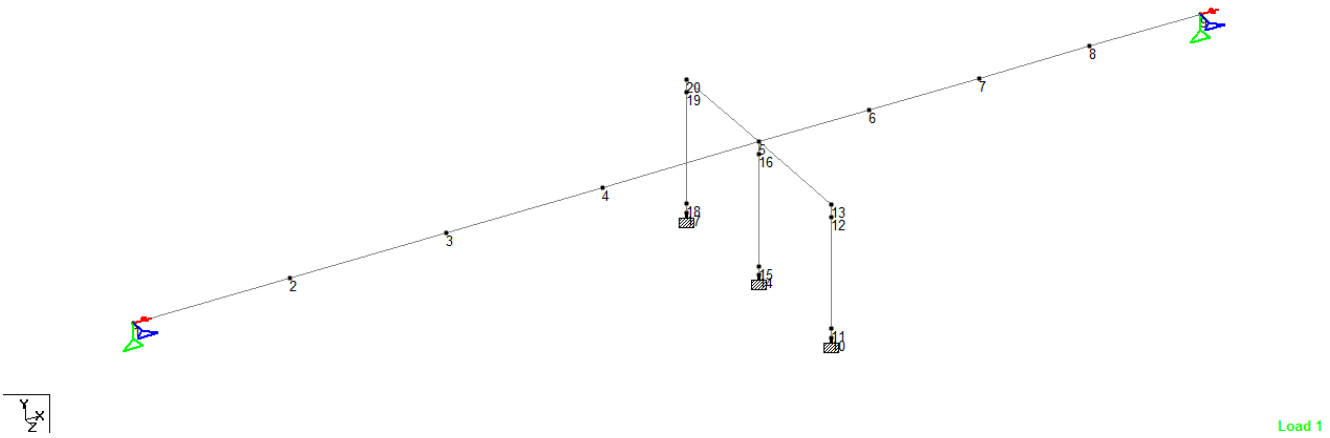

Figure A-1. Bridge model nodes and boundary conditions

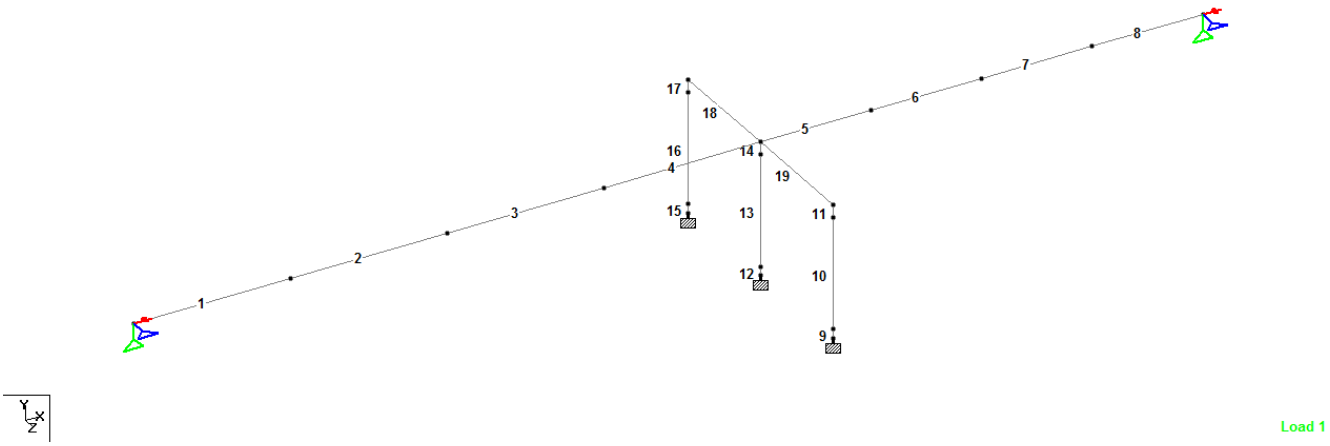

Figure A-2. Bridge model elements

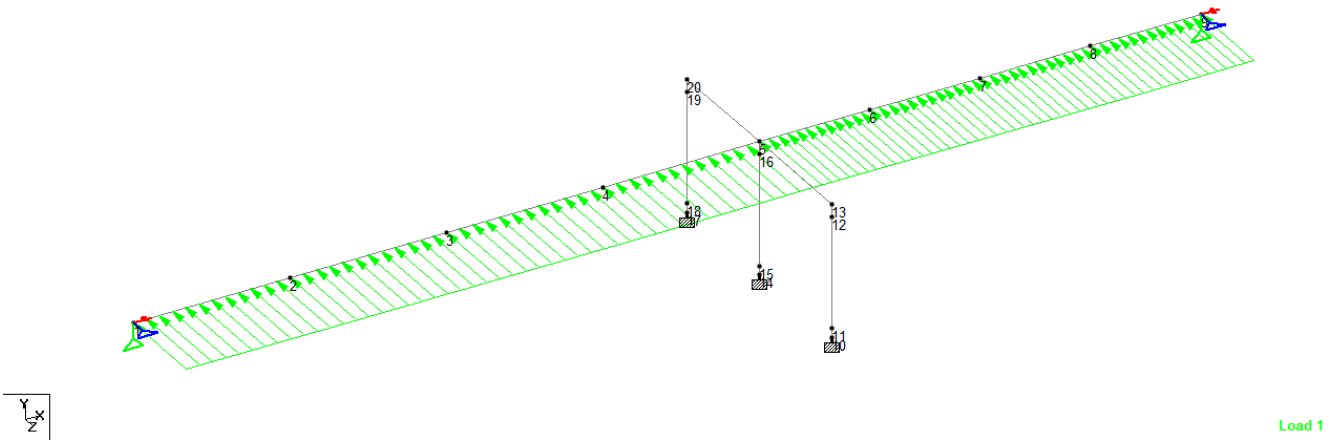

Figure A-3. Bridge model under transverse load of 100 k/ft

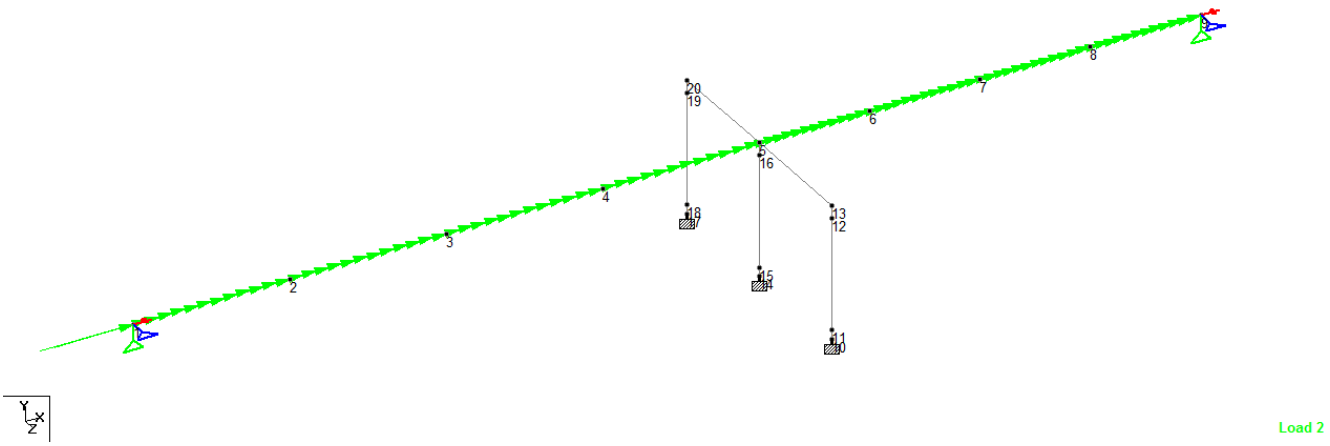

Figure A-4. Bridge model under longitudinal load of 100 k/ft

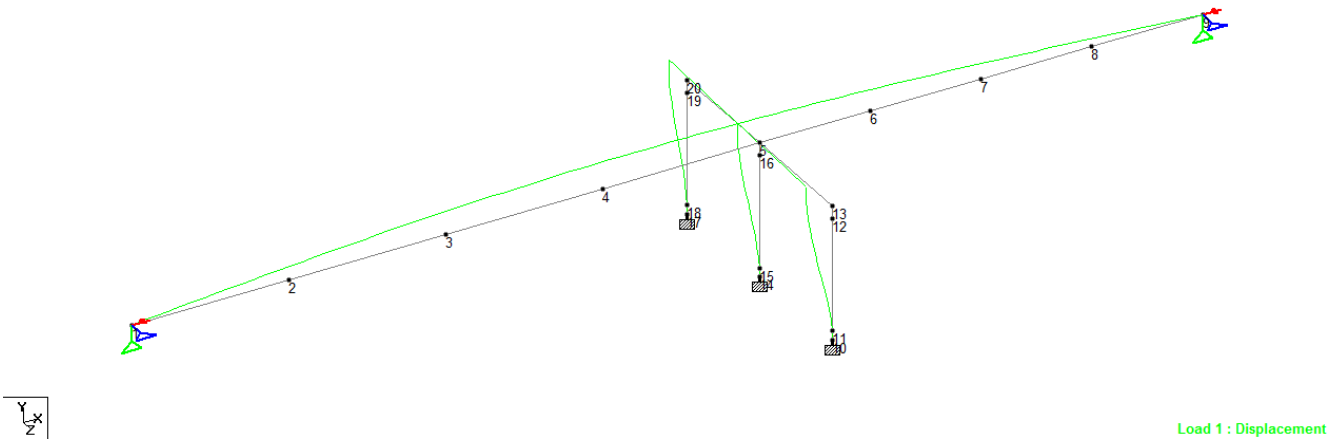

Figure A-5. Displaced shape under transverse load of 100 k/ft

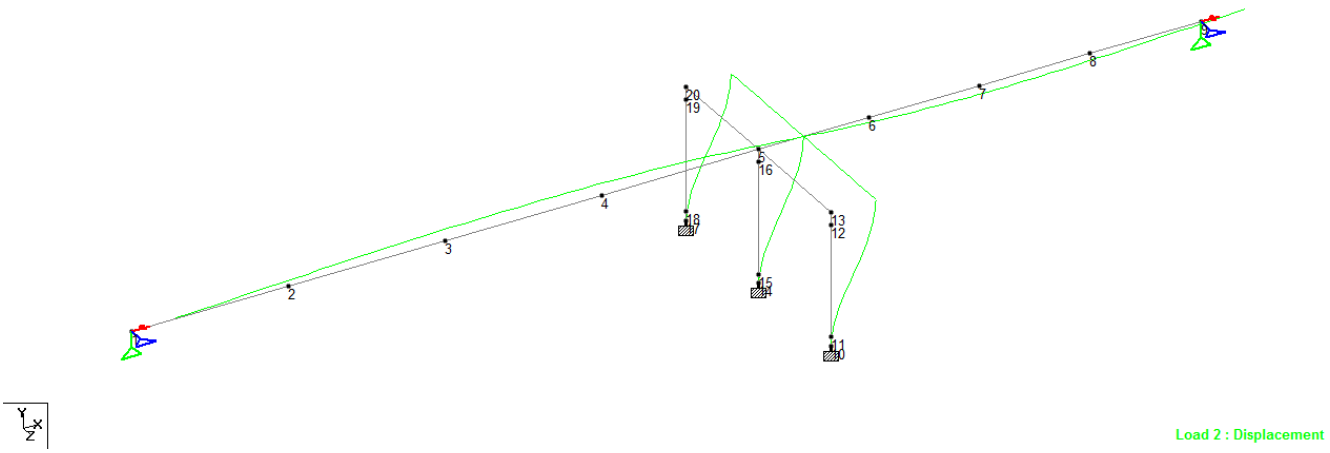

Figure A-6. Displaced shape under longitudinal load of 100 k/ft

STAAD Output Displacements for Basic Support Condition

Table A-1shows the superstructure nodal displacements (dimensions in inch and Radian). Load 1 is transverse, Load 2 is longitudinal.

Table A-1. Portion of the STAAD output file

JOINT DISPLACEMENT (INCH RADIANS) STRUCTURE TYPE = SPACE

JOINT	LOAD	X-TRANS	Y-TRANS	Z-TRANS	X-ROTAN	Y-ROTAN	Z-ROTAN
1	1	0.00000	0.00000	0.00000	0.00000	0.00202	0.00000
	2	30.59186	0.00000	0.00000	0.00000	0.00000	0.01251
2	1	0.00000	0.00000	-0.82583	-0.00002	0.00178	0.00000
	2	30.57970	4.99514	0.00000	0.00000	0.00000	0.01016
3	1	0.00000	0.00000	-1.46215	-0.00003	0.00116	0.00000
	2	30.54324	7.99410	0.00000	0.00000	0.00000	0.00313
4	1	0.00000	0.00000	-1.78553	-0.00005	0.00034	0.00000
	2	30.48246	7.00072	0.00000	0.00000	0.00000	-0.00858
5	1	0.00000	0.00000	-1.74464	-0.00007	-0.00052	0.00000
	2	30.39737	0.01882	0.00000	0.00000	0.00000	-0.02498
6	1	0.00000	0.00000	-1.50313	-0.00005	-0.00108	0.00000
	2	30.43957	-4.90077	0.00000	0.00000	0.00000	-0.00860
7	1	0.00000	0.00000	-1.10576	-0.00003	-0.00155	0.00000
	2	30.46971	-5.60760	0.00000	0.00000	0.00000	0.00310
8	1	0.00000	0.00000	-0.58723	-0.00002	-0.00188	0.00000
	2	30.48779	-3.50593	0.00000	0.00000	0.00000	0.01013
9	1	0.00000	0.00000	0.00000	0.00000	-0.00200	0.00000
	2	30.49382	0.00000	0.00000	0.00000	0.00000	0.01247

OpenSees Model and Results

Geometric transformation

From OpenSees Command Manual: "*The x-axis is a vector given by the two element nodes; The vector vecxz is a vector the user specifies that must not be parallel to the x-axis. The x-axis along with the vecxz Vector define the xz plane. The local y-axis is defined by taking the cross product of the x-axis vector and the vecxz vector (Vy = Vxz X Vx). The local z-axis is then found simply by taking the cross product of the y-axis and x-axis vectors (Vz = Vx X Vy). The section is attached to the element such that the y-z coordinate system used to specify the section corresponds to the y-z axes of the element.*"

The geometric transformations used in OpenSees elements are shown in Figure A-7.

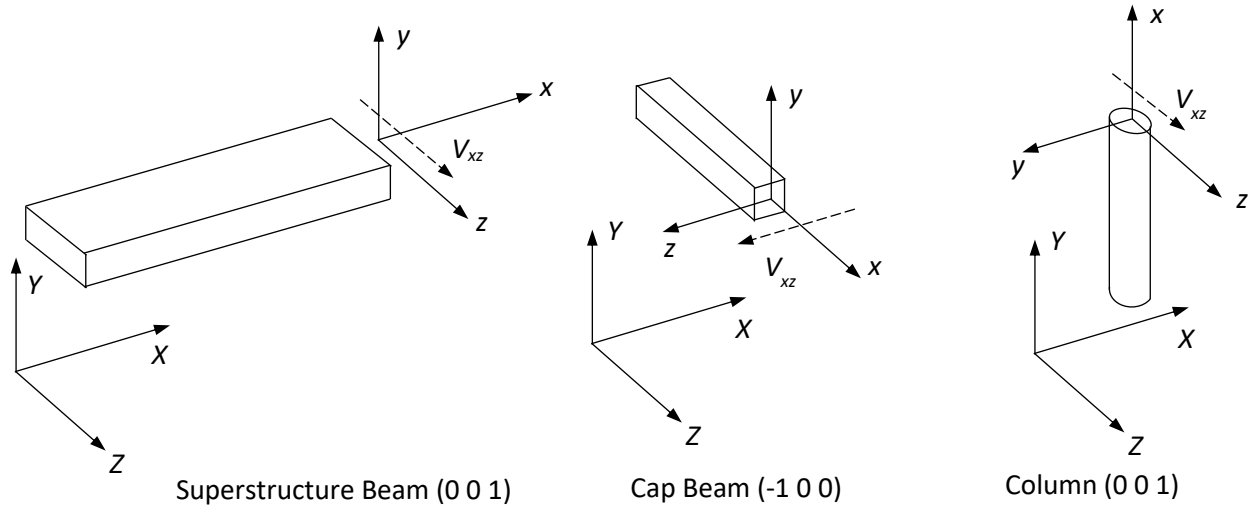

Figure A-7. OpenSees geometric transformation (*XYZ* is global CS and *xyz* is local CS) (Ebrahimpour, et al. 2016)

OpenSees tlc Script

The OpenSees script is shown below. The same node and element numbers are used as those used in the STAAD model.

```
#Clear cached data existing in the program
wipe

#Create Model with 3 dimensions and 6 degrees of freedom
model BasicBuilder -ndm 3 -ndf 6

#Create 6 DOF nodes
#      tag    X       Y        Z
node   1    0.00   30.17     0.000
```

```
node   2   35.50   30.17     0.000
node   3   71.00   30.17     0.000
node   4  106.50   30.17     0.000
node   5  142.00   30.17     0.000
node   6  167.00   30.17     0.000
node   7  192.00   30.17     0.000
node   8  217.00   30.17     0.000
node   9  242.00   30.17     0.000
node  10  142.00    0.00    28.375
node  11  142.00    2.00    28.375
node  12  142.00   27.34    28.375
node  13  142.00   30.17    28.375
node  14  142.00    0.00     0.000
node  15  142.00    2.00     0.000
node  16  142.00   27.34     0.000
node  17  142.00    0.00   -28.375
node  18  142.00    2.00   -28.375
node  19  142.00   27.34   -28.375
node  20  142.00   30.17   -28.375

# Constraints
fix 10  1  1  1  1  1  1
fix 14  1  1  1  1  1  1
fix 17  1  1  1  1  1  1
fix  1  0  1  1  1  0  0
fix  9  0  1  1  1  0  0

# Superstructure main beam elements
geomTransf Linear 1  0 0 1
# element elasticBeamColumn $eleTag $iNode $jNode $A $E $G $J $Iy $Iz $transfTag <-
mass $massDens> <-cMass>
element elasticBeamColumn 1  1  2  120  518400  222000  1e10  51000  575  1
element elasticBeamColumn 2  2  3  120  518400  222000  1e10  51000  575  1
element elasticBeamColumn 3  3  4  120  518400  222000  1e10  51000  575  1
element elasticBeamColumn 4  4  5  120  518400  222000  1e10  51000  575  1
element elasticBeamColumn 5  5  6  120  518400  222000  1e10  51000  575  1
element elasticBeamColumn 6  6  7  120  518400  222000  1e10  51000  575  1
element elasticBeamColumn 7  7  8  120  518400  222000  1e10  51000  575  1
element elasticBeamColumn 8  8  9  120  518400  222000  1e10  51000  575  1

# Substructure column elements
# geomTransf Linear 2  0 0 1
geomTransf PDelta 2  0 0 1; # PDelta may be needed when nonlinear material under
gravity load is used.

element elasticBeamColumn  9  10  11  12.6  518400  222000  25  12.6  12.6  2
element elasticBeamColumn 10  11  12  12.6  518400  222000  25  12.6  12.6  2
element elasticBeamColumn 11  12  13  1e10  518400  222000  1e10  1e10  1e10  2
element elasticBeamColumn 12  14  15  12.6  518400  222000  25  12.6  12.6  2
element elasticBeamColumn 13  15  16  12.6  518400  222000  25  12.6  12.6  2
element elasticBeamColumn 14  16   5   1e10 518400  222000  1e10  1e10  1e10  2

element elasticBeamColumn 15  17  18  12.6  518400  222000  25  12.6  12.6  2
element elasticBeamColumn 16  18  19  12.6  518400  222000  25  12.6  12.6  2
element elasticBeamColumn 17  19  20  1e10  518400  222000  1e10  1e10  1e10  2

# Superstructure cap beam elements
geomTransf Linear 3  -1 0 0
element elasticBeamColumn 18  20  5  25  518400  222000  1e10  1e10  1e10  3
element elasticBeamColumn 19   5  13  25  518400  222000  1e10  1e10  1e10  3

#Create recorder files for displacements
recorder Node -file Nodes1-9DisplTrans.out -time -nodeRange 1 9 -dof 3 disp
```

```
recorder Node -file Nodes1-9DisplLong.out -time -nodeRange 1 9 -dof 1 disp

# 100 lb/ft transverse load
# Create a Plain load pattern with a linear TimeSeries:
# command pattern Plain $tag $timeSeriesTag { $loads }
pattern Plain 1 Linear {
# eleLoad -ele $eleTag1 <$eleTag2 ....> -type -beamUniform $Wy $Wz <$Wx>
  eleLoad -ele 1 2 3 4 5 6 7 8 -type beamUniform 0 100 0
}

# 100 lb/ft longitudinal load
pattern Plain 2 Linear {
# eleLoad -ele $eleTag1 <$eleTag2 ....> -type -beamUniform $Wy $Wz <$Wx>
  eleLoad -ele 1 2 3 4 5 6 7 8 -type beamUniform 0 0 100
}

# Create the system of equations
system BandSPD

# Create the DOF numberer, the reverse Cuthill-McKee algorithm
numberer RCM

# Create the constraint handler, a Plain handler is used as homo constraints
constraints Plain

# Create the integration scheme, the LoadControl scheme using steps of 1.0
integrator LoadControl 1.0

# Create the solution algorithm, a Linear algorithm is created
algorithm Linear

# create the analysis object
analysis Static

analyze 1
```

Comparison of Results

The displacements obtained from STAAD, OpenSees and those given in the FHWA Design Example No. 1 for the superstructure node 5 (directly above the cap beam) are given in Table A-2.

Table A-2. Node 5 Displacements under 100 kip/ft for Basic Support Condition

Displacement	FHWA Example 1	STAAD	OpenSees
Transverse, ft	0.145	0.145	0.145
Longitudinal, ft	2.53	2.53	2.52

FHWA Seismic Design of Bridges-Example No. 1 with Spring Supports

Spring Support Condition

Support stiffness: Springs
Column stiffness: $0.5I_{gross}$
Abutment type: Stub wall
Restraint of superstructure: Restrained longitudinally

Superstructure

L = 242 ft	Overall bridge length
A_d = 120 ft^2	Cross-sectional area of superstructure
A_{cb} = 25 ft^2	Cross-sectional area of cap beam
I_{yd} = 51,000 ft^4	Moment of inertia of superstructure cross-sec. about local y-axis
I_{zd} = 575 ft^4	Moment of inertia of superstructure cross-sec. about local z-axis
f_c = 4,000 lb/in^2	Compressive strength of concrete
E_c = 3,600 kip/in^2 = 5.184 x 10^5 kip/ft^2	Young' modulus of elasticity of concrete

Substructure

$I_c = \pi d^4/64 = \pi(4)^4/64$ = 12.57 ft^4	Moment of inertia of one column (about local y- or z-axes)
$A_c = \pi d^2/4 = \pi(4)^2/4$ = 12.57 ft^2	Cross-sectional area of one column

Rigid end zone of the upper part of columns = 2.83 ft. Assign a large stiffness to this zone.

Soil Spring Constants

$K_a = k_a/2$ = 166000/2 = 83000 kip/ft	Soil spring constant at abutments (half the value to account for the opposing spring) in the x direction
K_w = 53000 kip/ft	Soil spring constant at wingwalls in the z direction

K_r = 4,800,000 kip/ft/radian / 57.296 radians/degrees = 83776 kip/ft/degree

Rotational soil spring constant for columns about the x and z axes

A large spring constant (1e12) was used for all other DOF's except the ones about the y and z axes of the abutments, which were assigned a value of zero.

Model of Structure

The same number of nodes and elements as were used in the SAP computer analysis files in the Example 1 Appendix are used for the STAAD and OpenSees models, with some exceptions. OpenSees requires an extra node and corresponding zeroLength element to model springs. These are located at the abutments and the bases of the columns. In SAP the upper 2.83 ft of the columns were specified as being rigid. In STAAD and OpenSees a rigid element of that length was included to simulate this condition.

STAAD Model and Results

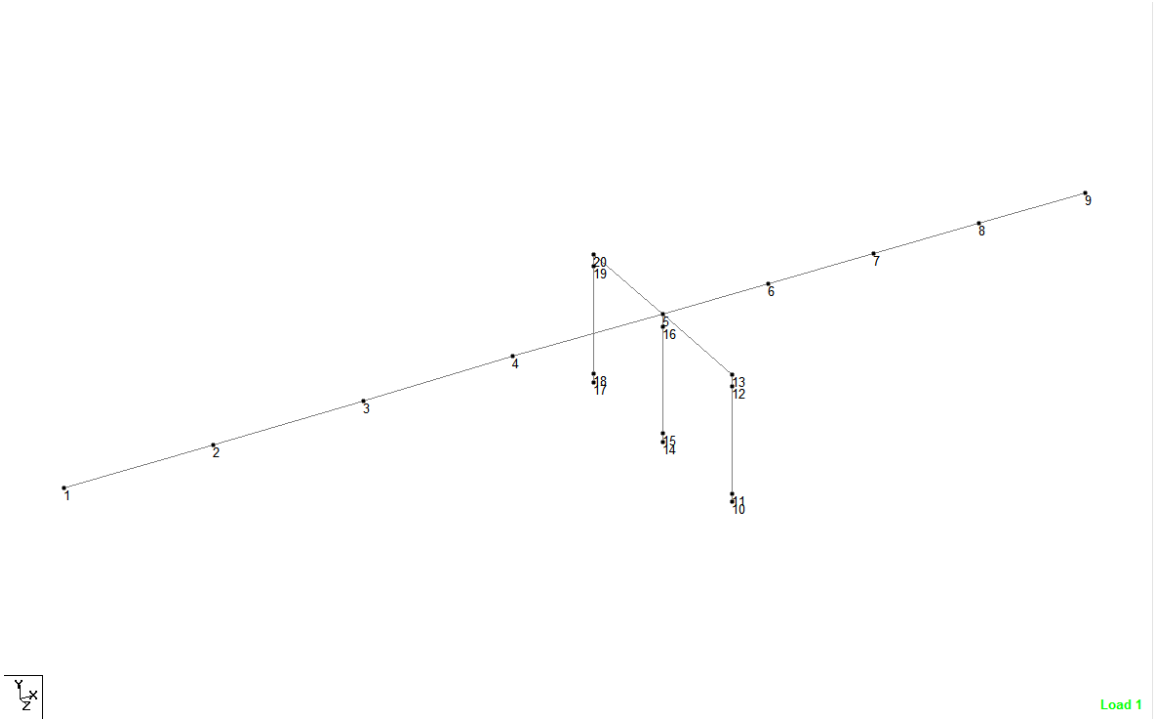

Figure A-8. Bridge model with node numbers

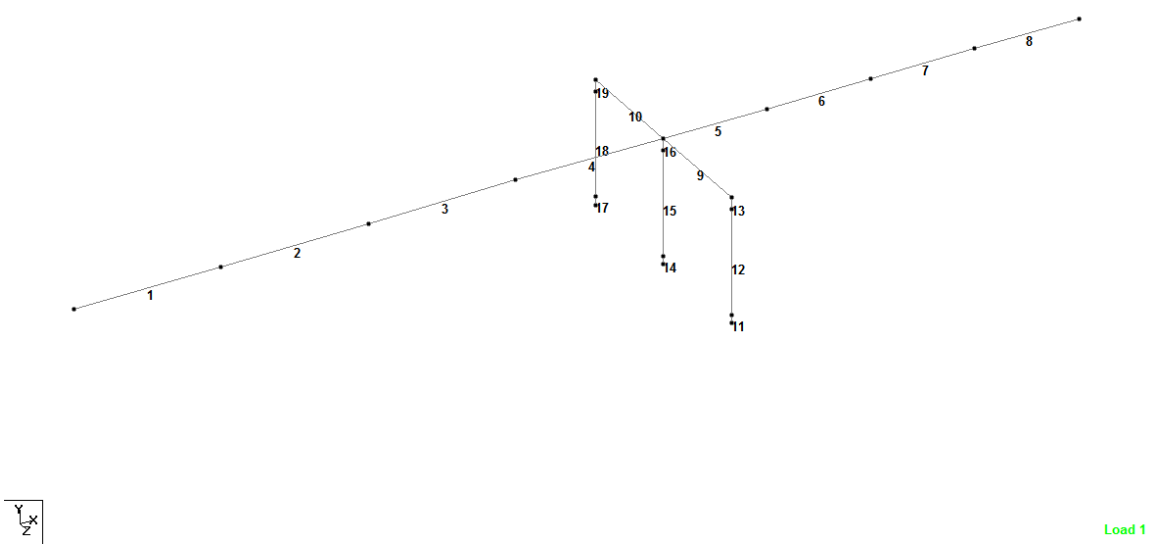

Figure A-9. Bridge model with member numbers

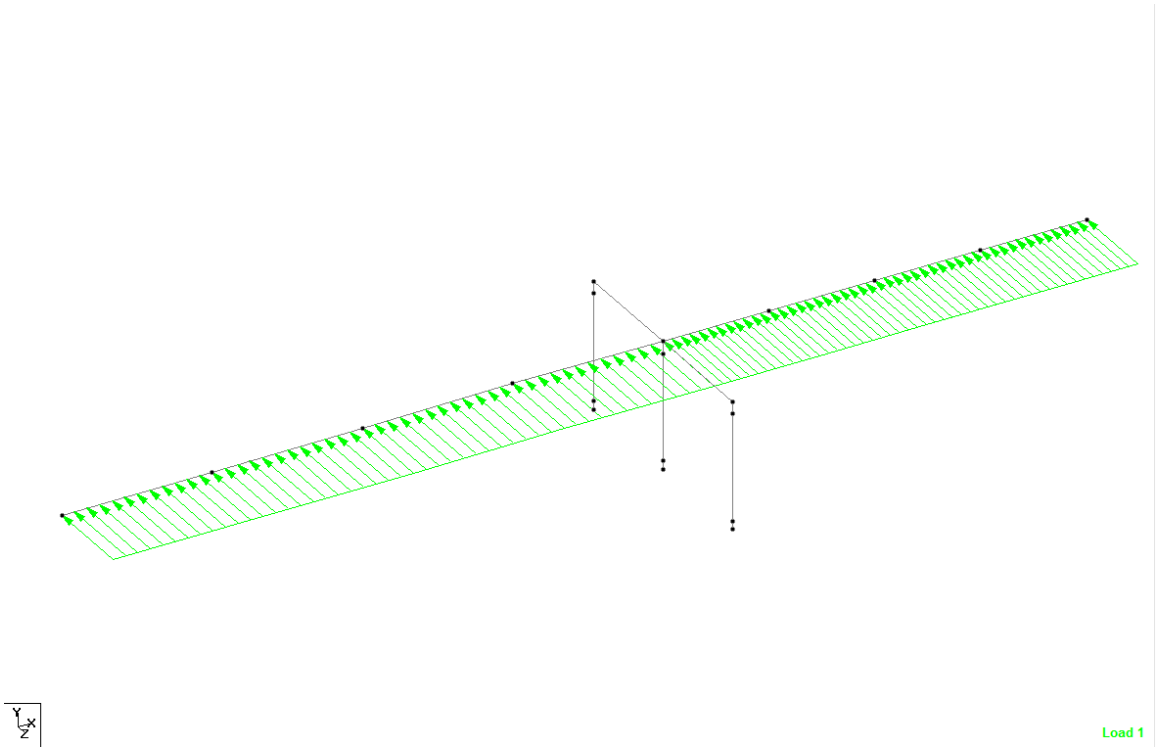

Figure A-10. Bridge model under transverse load of 100 k/ft

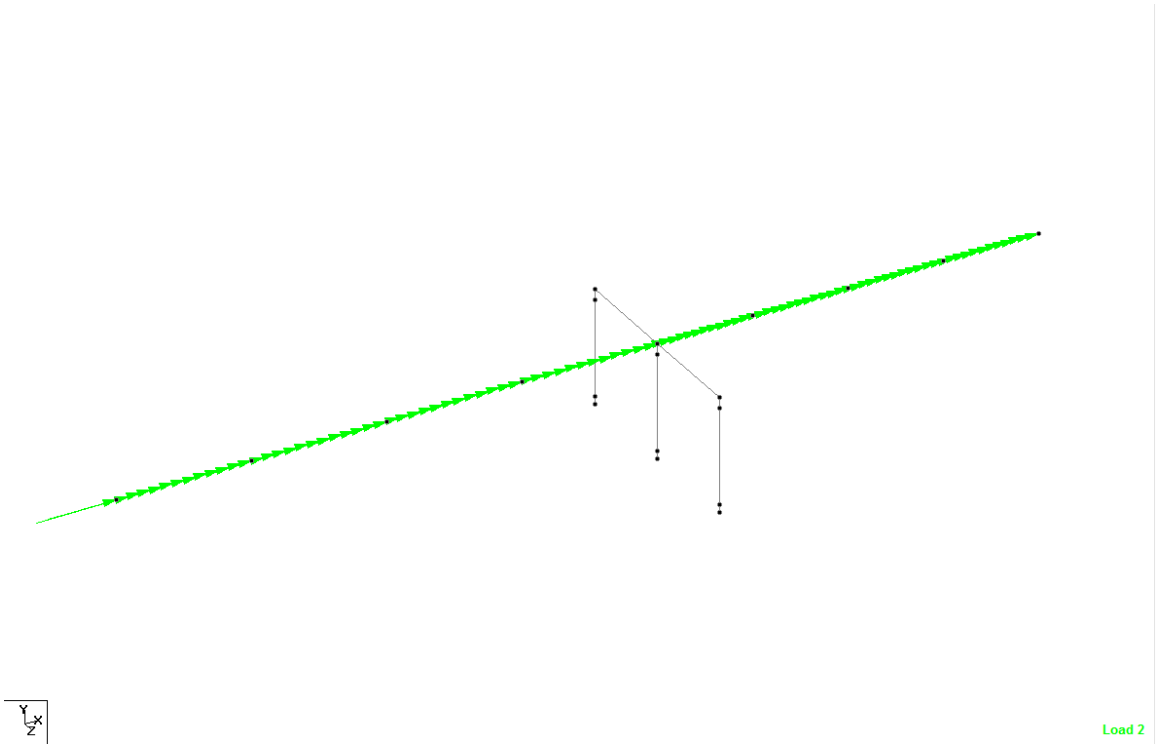

Figure A-11. Bridge model under longitudinal load of 100 k/ft

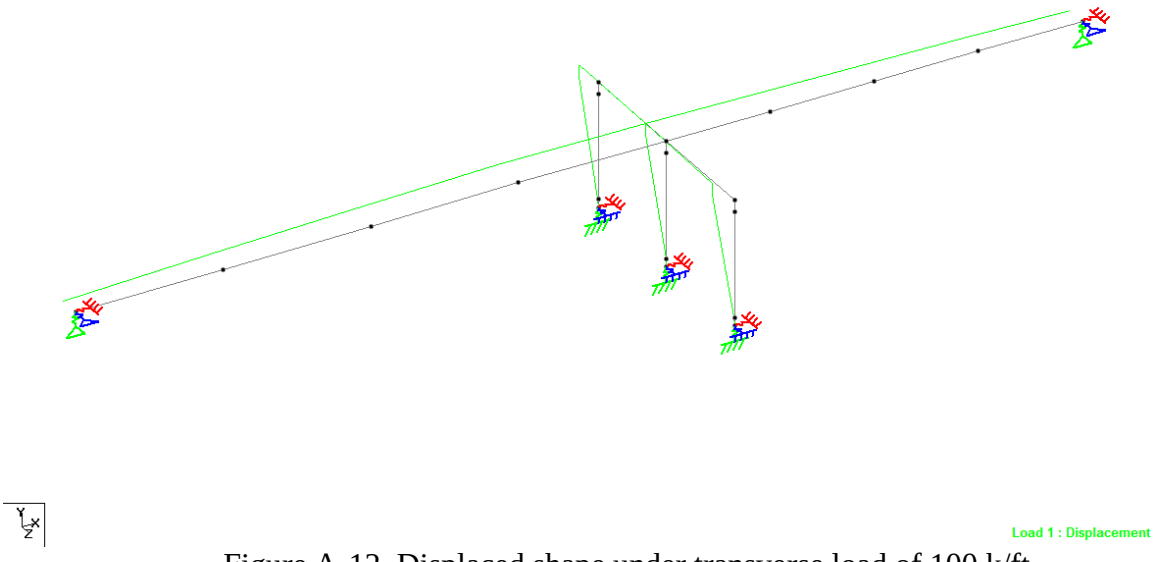

Figure A-12. Displaced shape under transverse load of 100 k/ft

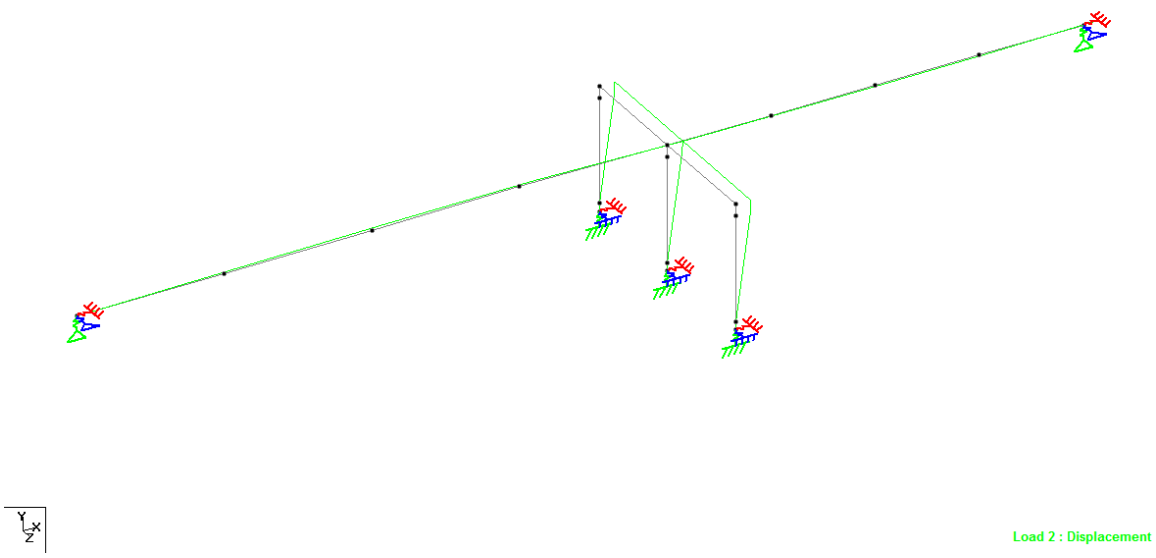

Figure A-13. Displaced shape under longitudinal load of 100 k/ft

Input Command File for Spring Support Condition

```
STAAD SPACE
START JOB INFORMATION
ENGINEER DATE 10-Jun-15
END JOB INFORMATION
INPUT WIDTH 79
UNIT FEET KIP
JOINT COORDINATES
1 0 30.17 0; 2 35.5 30.17 0; 3 71 30.17 0; 4 106.5 30.17 0; 5 142 30.17 0; 6 167 30.17
0; 7 192 30.17 0;
8 217 30.17 0; 9 242 30.17 0; 10 142 0 28.375; 11 142 2.0 28.375; 12 142 27.34 28.375;
13 142 30.17 28.375; 14 142 0 0; 15 142 2 0; 16 142 27.34 0;
17 142 0 -28.375; 18 142 2 -28.375; 19 142 27.34 -28.375;
20 142 30.17 -28.375;
MEMBER INCIDENCES
1 1 2; 2 2 3; 3 3 4; 4 4 5; 5 5 6; 6 6 7; 7 7 8; 8 8 9; 9 13 5; 10 5 20;
11 10 11; 12 11 12; 13 12 13; 14 14 15; 15 15 16; 16 16 5; 17 17 18; 18 18 19;
19 19 20;
DEFINE MATERIAL START
ISOTROPIC CONCRETE
E 518400
POISSON 0.17
DENSITY 0.150336
ALPHA 5e-006
DAMP 5e-005
TYPE CONCRETE
STRENGTH FCU 576
END DEFINE MATERIAL
```

```
MEMBER PROPERTY AMERICAN
1 TO 8 PRIS AX 120 IX 6000 IY 51000 IZ 575
11 12 14 15 17 18 PRIS AX 12.6 IX 25 IY 6.3 IZ 6.3
13 16 19 PRIS AX 1e+008 IX 1e+008 IY 1e+008 IZ 1e+008
9 10 PRIS AX 25 IX 10000 IY 1e+008 IZ 1e+008
CONSTANTS
MATERIAL CONCRETE ALL
SUPPORTS
1 9 FIXED BUT MY MZ KFX 83000 KFY 1e+012 KFZ 53000 KMX 1e+012
10 14 17-
FIXED BUT KFX 1e+012 KFY 1e+012 KFZ 1e+012 KMX 83776 KMY 1e+012 KMZ 83776
LOAD 1 LOADTYPE None  TITLE 100 KIP/FT TRANSVERSE
MEMBER LOAD
1 TO 8 UNI GZ -100
LOAD 2 LOADTYPE None  TITLE 100 KIP/FT LONGITUDINAL
MEMBER LOAD
1 TO 8 UNI GX 100
PERFORM ANALYSIS
PRINT JOINT DISPLACEMENTS ALL
FINISH
```

Table A-3. Portion of the STAAD output file, spring support condition

JOINT DISPLACEMENT (INCH RADIANS) STRUCTURE TYPE = SPACE

JOINT	LOAD	X-TRANS	Y-TRANS	Z-TRANS	X-ROTAN	Y-ROTAN	Z-ROTAN
1	1	0.00000	0.00000	-2.56184	0.00000	0.00197	0.00000
	2	1.69808	0.00000	0.00000	0.00000	0.00000	0.00044
2	1	0.00000	0.00000	-3.36641	-0.00003	0.00173	0.00000
	2	1.76635	0.17580	0.00000	0.00000	0.00000	0.00035
3	1	0.00000	0.00000	-3.98328	-0.00006	0.00112	0.00000
	2	1.81032	0.27502	0.00000	0.00000	0.00000	0.00008
4	1	0.00000	0.00000	-4.29104	-0.00022	0.00030	0.00000
	2	1.83038	0.23174	0.00000	0.00000	0.00000	-0.00030
5	1	0.00000	0.00000	-4.23816	-0.00008	-0.00054	0.00000
	2	1.82357	0.00050	0.00000	0.00000	0.00000	-0.00081
6	1	0.00000	0.00000	-3.99260	-0.00006	-0.00109	0.00000
	2	1.80926	-0.15960	0.00000	0.00000	0.00000	-0.00028
7	1	0.00000	0.00000	-3.59419	-0.00004	-0.00155	0.00000
	2	1.78290	-0.18258	0.00000	0.00000	0.00000	0.00010
8	1	0.00000	0.00000	-3.07664	-0.00002	-0.00187	0.00000
	2	1.74448	-0.11414	0.00000	0.00000	0.00000	0.00033
9	1	0.00000	0.00000	-2.49139	0.00000	-0.00199	0.00000
	2	1.69400	0.00000	0.00000	0.00000	0.00000	0.00041

OpenSees Model and Results

The geometric transformation of the elements are the same as those in Figure A-7. To define the zeroLength elements that are used to create the springs at the abutments and column bases additional nodes are needed. The nodes at the abutments are, 1 and 11. The nodes at the column bases are 12, 17, and 21. The zeroLength elements at the abutments are 20 and 21 and the elements at the column bases are 22, 23, and 24. See Figures A-14 and A-15.

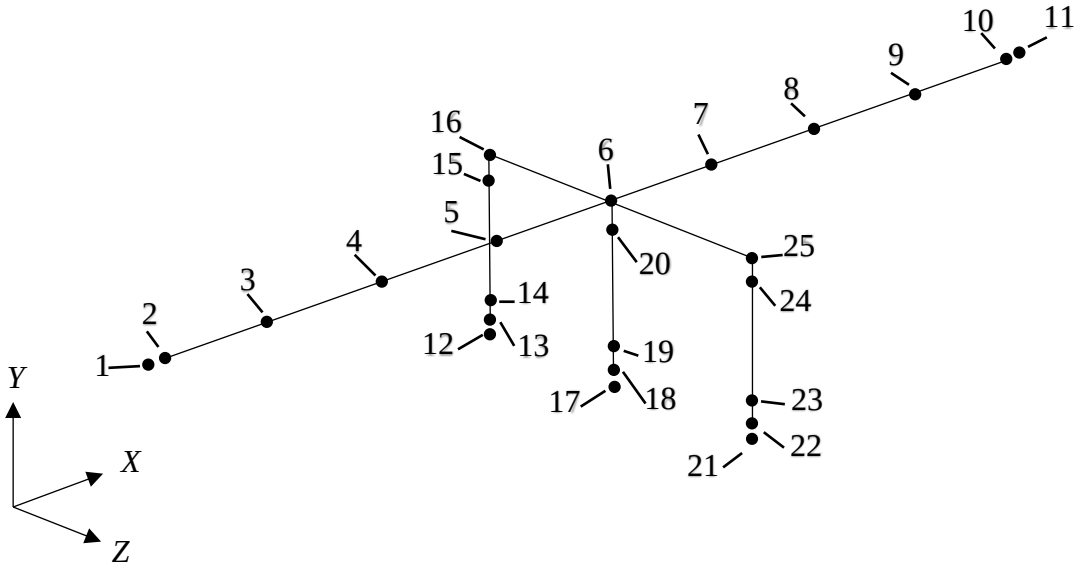

Figure A-14. OpenSees model with node numbers

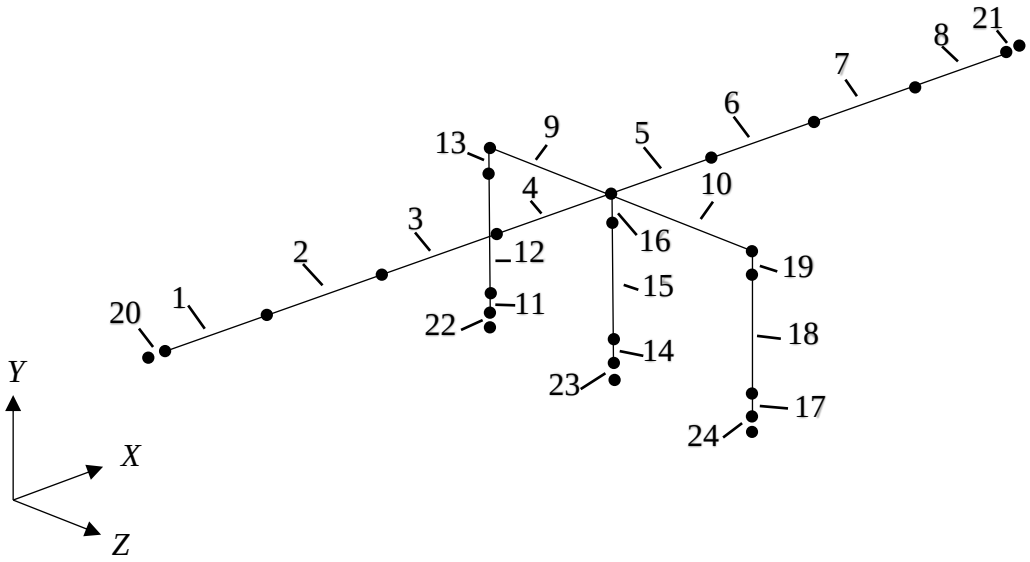

Figure A-15. OpenSees model with element numbers

OpenSees tlc Script

```
#Design example No. 1-Seismic Design of Bridges

wipe

#Create model with 3 dimensions and 6 DOF

model BasicBuilder -ndm 3 -ndf 6

#Create 6 DOF nodes

#Bridge deck nodes
#       tag          x           y           z

node     1          0.0        30.17        0.0
node     2          0.0        30.17        0.0
node     3         35.5        30.17        0.0
node     4         71.0        30.17        0.0
node     5        106.5        30.17        0.0
node     6        142.0        30.17        0.0
node     7        167.0        30.17        0.0
node     8        192.0        30.17        0.0
node     9        217.0        30.17        0.0
node    10        242.0        30.17        0.0
node    11        242.0        30.17        0.0

#Column and bent nodes

node    12        142.0         0.0        28.37
node    13        142.0         0.0        28.37
node    14        142.0         2.0        28.37
node    15        142.0        27.34       28.37
node    16        142.0        30.17       28.37
node    17        142.0         0.0         0.0
node    18        142.0         0.0         0.0
node    19        142.0         2.0         0.0
node    20        142.0        27.34        0.0
node    21        142.0         0.0       -28.37
node    22        142.0         0.0       -28.37
node    23        142.0         2.0       -28.37
node    24        142.0        27.34      -28.37
node    25        142.0        30.17      -28.37

#Specify geometric transformation

geomTransf Linear 1  0  0  1
geomTransf Linear 2 -1  0  0
geomTransf PDelta 3  0  0  1

# Fix column bases in the x, y, and z directions and abutments about the y axis

fix 12 1 1 1 1 1 1
fix 17 1 1 1 1 1 1
fix 21 1 1 1 1 1 1
fix  1 1 1 1 1 1 1
fix 11 1 1 1 1 1 1

# Create deck elements
```

```
# element elasticBeamColumn $eleTag $iNode $jNode $A $E $G $J $Iy $Iz $transfTag

element elasticBeamColumn 1  2  3  120  518400  222000  1e10  51000  575  1
element elasticBeamColumn 2  3  4  120  518400  222000  1e10  51000  575  1
element elasticBeamColumn 3  4  5  120  518400  222000  1e10  51000  575  1
element elasticBeamColumn 4  5  6  120  518400  222000  1e10  51000  575  1
element elasticBeamColumn 5  6  7  120  518400  222000  1e10  51000  575  1
element elasticBeamColumn 6  7  8  120  518400  222000  1e10  51000  575  1
element elasticBeamColumn 7  8  9  120  518400  222000  1e10  51000  575  1
element elasticBeamColumn 8  9 10  120  518400  222000  1e10  51000  575  1

# Create cap beam elements

element elasticBeamColumn  9 16  6  25  518400  222000  1e10  1e10  1e10  2
element elasticBeamColumn 10  6 25  25  518400  222000  1e10  1e10  1e10  2

# Create column elements

element elasticBeamColumn 11 13 14  12.6  518400  222000  25.1  6.3  6.3  3
element elasticBeamColumn 12 14 15  12.6  518400  222000  25.1  6.3  6.3  3
element elasticBeamColumn 13 15 16  1000  518400  222000  1e12  1e12  1e12  3
element elasticBeamColumn 14 18 19  12.6  518400  222000  25.1  6.3  6.3  3
element elasticBeamColumn 15 19 20  12.6  518400  222000  25.1  6.3  6.3  3
element elasticBeamColumn 16 20  6  1000  518400  222000  1e12  1e12  1e12  3
element elasticBeamColumn 17 22 23  12.6  518400  222000  25.1  6.3  6.3  3
element elasticBeamColumn 18 23 24  12.6  518400  222000  25.1  6.3  6.3  3
element elasticBeamColumn 19 24 25  1000  518400  222000  1e12  1e12  1e12  3

# Create spring elements

uniaxialMaterial Elastic 1 83e3;   # Translational stiffness along local x axis of the
abutments, kip/ft
uniaxialMaterial Elastic 2 1e12;   # Translational stiffness along local y axis of the
abutments, kip/ft
uniaxialMaterial Elastic 3 52e3;   # Translational stiffness along local z axis of the
abutments, kip/ft
uniaxialMaterial Elastic 4 1e12;   # Rotational stiffness about local x axes of the
abutments, kip.ft/radian
uniaxialMaterial Elastic 5 0;      # Rotational stiffness about local y axis of the
abutments, kip.ft/radian
uniaxialMaterial Elastic 6 0;      # Rotational stiffness about the local z axis of
the abutment, kip.ft/radian
uniaxialMaterial Elastic 7 1e12;    # Translational stiffness along local x axis of
the columns, kip/ft
uniaxialMaterial Elastic 8 1e12;    # Translational stiffness along local y axis of
the columns, kip/ft
uniaxialMaterial Elastic 9 1e12;    # Translational stiffness along local z axis of
the columns, kip/ft
uniaxialMaterial Elastic 10 4.8e6;   # Rotational stiffness about local x axes of the
columns, kip.ft/radian
uniaxialMaterial Elastic 11 1e12;    # Rotational stiffness about local y axis of the
coumns, kip.ft/radian
uniaxialMaterial Elastic 12 4.8e6;   # Rotational stiffness about local z axis of the
columns, kip.ft/radian

# Spring elements using above stiffness values
# element zeroLength $eleTag $iNode $jNode -mat $matTag1 $matTag2 ... -dir $dir1 $dir2
...

element zeroLength 20  1  2 -mat 1 2 3 4 5 6 -dir 1 2 3 4 5 6
element zeroLength 21 10 11 -mat 1 2 3 4 5 6 -dir 1 2 3 4 5 6
element zeroLength 22 12 13 -mat 7 8 9 10 11 12 -dir 1 2 3 4 5 6
element zeroLength 23 17 18 -mat 7 8 9 10 11 12 -dir 1 2 3 4 5 6
```

```
element zeroLength 24 21 22 -mat 7 8 9 10 11 12 -dir 1 2 3 4 5 6

# Create recorder files

recorder Node -file Nodes1-11DisplTrans.out -time -nodeRange 1 11 -dof 3 disp
recorder Node -file Nodes1-11DisplLong.out -time -nodeRange 1 11 -dof 1 disp

# Create load pattern
# 100 kip/ft transverse load
pattern Plain 1 Linear {
# eleLoad -ele $eleTag1 <$eleTag2 ....> -type -beamUniform $Wy $Wz <$Wx>
  eleLoad -ele 1 2 3 4 5 6 7 8 -type beamUniform 0 -100 0
}

# 100 kip/ft longitudinal load
pattern Plain 2 Linear {
# eleLoad -ele $eleTag1 <$eleTag2 ....> -type -beamUniform $Wy $Wz <$Wx>
  eleLoad -ele 1 2 3 4 5 6 7 8 -type beamUniform 0 0 100
}


constraints Plain

numberer RCM

system BandSPD

algorithm Linear

integrator LoadControl 1.0

analysis Static

analyze 1
```

Table A-4. Center Deck Node Displacements under 100 kip/ft, Spring Support Condition

Displacement	FHWA Example 1	STAAD	OpenSees
Transverse, ft	0.357	0.353	0.356
Longitudinal, ft	0.152	0.152	0.152

Appendix B - Single Column Computer Models

Cast-in-place Column

Appendix B presents the procedure and OpenSees input files for modeling the cast-in-place (CIP) column used in the University of Nevada, Reno (UNR) study. This includes the procedure for determining the bond slip parameters, the moment-curvature input file, the cyclic push-pull input file, and the pushover input file.

Procedure for Determining Bond-Slip Model Parameters

The steps below are for estimating the bond-slip moment-rotation values that are used in the Opensees input file developed by Idaho State University (ISU) for the UNR's CIP column.

Run the moment-curvature input file given in the next section. This input file is for the UNR's CIP column. Figure B-1 shows the column rebar stressed in the direction the UNR report calls the "push" direction. (Haber, et al. 2013) The program is set up with a tributary weight of 208 kip in compression and a displacement-controlled moment is applied such that the bar at (9.375", 0") is in compression and the two bars at (-8.955", 2.641") and at (-8.995", -2.641") are in tension.

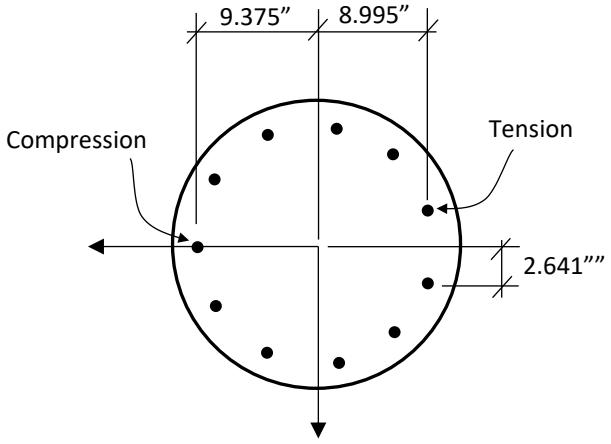

Figure B-1. UNR's CIP Column Cross-section (Column Diameter = 2.0 ft)

(Ebrahimpour, et al. 2016)

1. Using the relationships below create Table B-1 in a spreadsheet.

$$\delta_{slip} = \begin{cases} \frac{\varepsilon_s L_1}{2} & if \ \ \varepsilon_s \leq \varepsilon_y \\ \frac{\varepsilon_y L_{1y}}{2} + \frac{(\varepsilon_s + \varepsilon_y) L_2}{2} & if \ \ \varepsilon_s > \varepsilon_y \end{cases} \quad \text{(B-1)}$$

Where, δ_{slip} is the slip in the extreme tension bar as shown in Figure B-2. ε_s is the steel tensile strain in the extreme location (see Figure B-1) and ε_y is the steel yield strain. Lengths L_1 and L_2 are determined using the following relationships.

$$L_1 = \frac{f_s d_b}{4u} \quad \text{(B-2)}$$

$$L_2 = \frac{(f_s - f_y)\, d_b}{4u} \quad \text{(B-3)}$$

$$u = \frac{9.5\sqrt{f_c'}}{d_b} \leq 800 \ \ psi \quad \text{(B-4)}$$

Where, f_s = stress in the extreme tension steel, d_b= diameter of the bar = 1 in., f_y =steel yield strength = 66.8 ksi, and f_c' = core concrete compressive strength = 4,446 psi. The yellow cells in Table B-1 in the ε_s column indicates that the second part of of the equation for δ_{slip} controlled. As shown in Figure B-2, once the slip is known, the bond-slip rotation at the base of the column corresponding to each value of moment is determined by:

$$\theta_{slip} = tan^{-1}\left(\frac{\delta_{slip}}{c - d}\right) \quad \text{(B-5)}$$

Where, c = distance to the neutral axis from the compression edge obtained from the moment-curvature analysis (see Figure B-2) and d = column diameter. With steel tensile strain (ε_t) and compressive strain (ε_c) known, and the dimensions given in Figure B-1, the formula for c is:

$$c = 2.65 + \frac{|\varepsilon_c|}{(\varepsilon_t - \varepsilon_c)}(18.37) \ \ in. \quad \text{(B-6)}$$

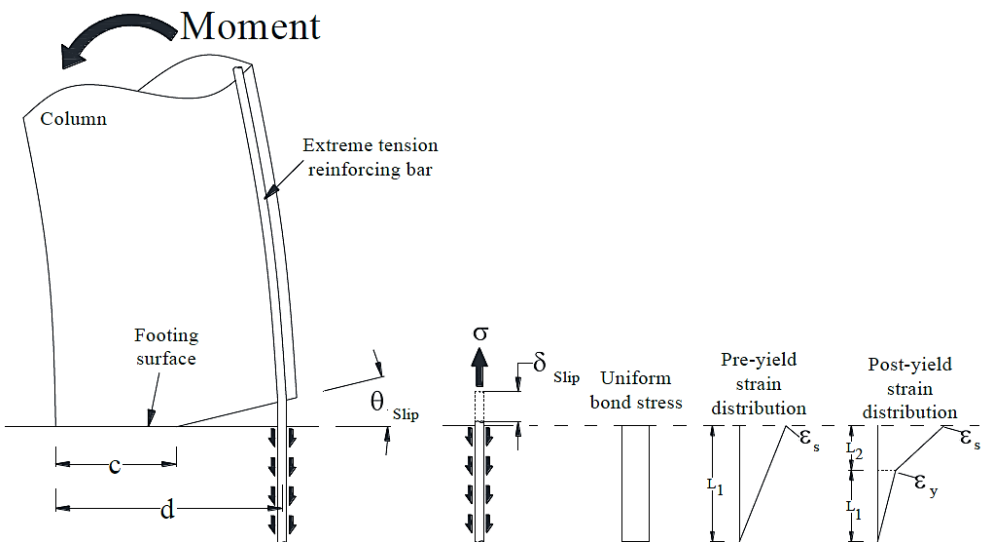

Figure B-2. Schematic for Determining the Bond-Slip Rotation (Wehbe, et al. 1999)

Table B-1. Spreadsheet File for Determining Bond-slip Moment-rotation

Comp. Strain	Tensile Stress f_s (ksi)	Tensile Strain, ε_s	Neutral Axis, c (in.)	u (ksi)	L_1 (in)	L_2 (in)	δ_{slip} (in)	θ (Rad)	Moment (Kip-in)
-0.0002126	0.0168168	5.779E-07	20.945	0.633	0.007	-26.357	0.000000	0.000	-847.203
-0.0003017	3.62425	1.246E-04	15.627	0.633	1.430	-24.933	0.000089	0.000	-1332.41
-0.0003767	7.64222	2.627E-04	13.448	0.633	3.016	-23.348	0.000396	0.000	-1665.86
-0.0004455	11.8409	4.071E-04	12.223	0.633	4.673	-21.691	0.000951	0.000	-1954.24
-0.0005115	16.1171	5.543E-04	11.441	0.633	6.361	-20.003	0.001763	0.000	-2224.53
-0.0005750	20.4638	7.040E-04	10.884	0.633	8.076	-18.287	0.002843	0.000	-2481.7
-0.0006379	24.8259	8.542E-04	10.478	0.633	9.798	-16.566	0.004185	0.000	-2732.83
-0.0007003	29.1975	1.005E-03	10.170	0.633	11.523	-14.840	0.005790	0.000	-2978.92
-0.0007628	33.5669	1.156E-03	9.929	0.633	13.248	-13.116	0.007655	-0.001	-3220.96
-0.0008251	37.9312	1.306E-03	9.736	0.633	14.970	-11.394	0.009779	-0.001	-3458.91
-0.0008874	42.2724	1.457E-03	9.577	0.633	16.684	-9.680	0.012157	-0.001	-3692.85
-0.0009499	46.5528	1.608E-03	9.447	0.633	18.373	-7.991	0.014771	-0.001	-3922.47
-0.0010125	50.7061	1.758E-03	9.337	0.633	20.012	-6.352	0.017595	-0.001	-4146.4
-0.0010751	54.6136	1.909E-03	9.243	0.633	21.554	-4.810	0.020574	-0.001	-4362.01
-0.0011372	58.0976	2.060E-03	9.159	0.633	22.929	-3.435	0.023618	-0.002	-4565.4
-0.0011984	60.9676	2.212E-03	9.080	0.633	24.062	-2.302	0.026613	-0.002	-4752.02
-0.0012581	63.1125	2.365E-03	9.003	0.633	24.908	-1.455	0.026063	-0.002	-4918.49
-0.0013162	64.5645	2.521E-03	8.927	0.633	25.482	-0.882	0.027332	-0.002	-5064.34
-0.0013725	65.4747	2.677E-03	8.851	0.633	25.841	-0.523	0.028158	-0.002	-5190.85
-0.0014272	66.0182	2.836E-03	8.775	0.633	26.055	-0.309	0.028667	-0.002	-5299.95
-0.0014803	66.336	2.996E-03	8.700	0.633	26.181	-0.183	0.028975	-0.002	-5393.32
-0.0015318	66.5211	3.158E-03	8.626	0.633	26.254	-0.110	0.029160	-0.002	-5471.33
-0.0015830	66.6293	3.320E-03	8.557	0.633	26.296	-0.067	0.029271	-0.002	-5535.95
-0.0016334	66.6936	3.482E-03	8.490	0.633	26.322	-0.042	0.029339	-0.002	-5591.77
-0.0016840	66.7324	3.645E-03	8.430	0.633	26.337	-0.027	0.029381	-0.002	-5639.82
-0.0017344	66.7562	3.808E-03	8.374	0.633	26.347	-0.017	0.029407	-0.002	-5682.04
-0.0017847	66.7711	3.970E-03	8.322	0.633	26.352	-0.011	0.029424	-0.002	-5720.06
-0.0018355	66.7807	4.133E-03	8.275	0.633	26.356	-0.008	0.029436	-0.002	-5755.1
-0.0018870	66.7868	4.294E-03	8.233	0.633	26.359	-0.005	0.029443	-0.002	-5786.96
-0.0019386	66.7909	4.456E-03	8.194	0.633	26.360	-0.004	0.029448	-0.002	-5817.16
-0.0019902	66.7936	4.618E-03	8.158	0.633	26.361	-0.003	0.029452	-0.002	-5845.76
-0.0020418	66.8006	4.779E-03	8.124	0.633	26.364	0.000	0.029461	-0.002	-5872.75
-0.0020936	66.8423	4.940E-03	8.093	0.633	26.381	0.017	0.029521	-0.002	-5897.78
-0.0021456	66.9498	5.102E-03	8.064	0.633	26.423	0.059	0.029679	-0.002	-5921.16
Missing lines in the Excel file ⋮									

2. Plot moment versus rotation curve as shown in Figure B-3. This graph is drawn using the last two columns of Table B-1, but the signs have been changed.

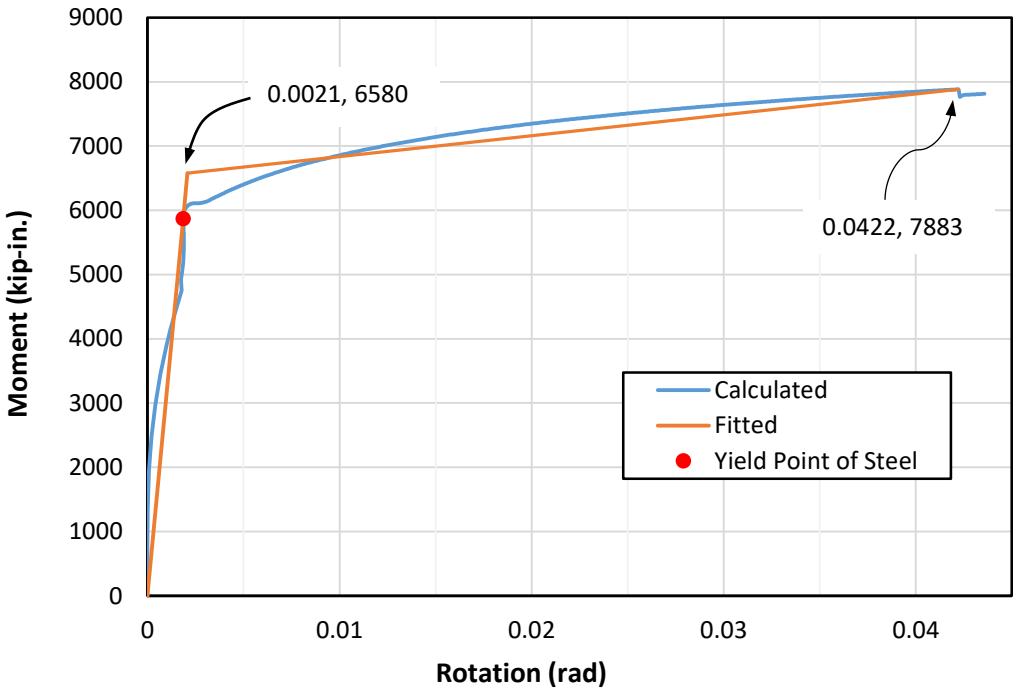

Figure B-3. Bond-Slip Moment versus Rotation (Ebrahimpour, et al. 2016)

3. Fit two straight lines. The first line starts at (0, 0) and crosses the moment corresponding to the yield tensile stress in the tension bar (see the orange cells in Table B-1 corresponding to steel tensile stress of 66.8 ksi). Extend the first line beyond this point. Then, draw the second line by balancing the area between the calculated and the second line after the first yield point.

Using the above approach, the ISU's fitted lines correspond to the points shown in Figure B-3. These points are 6,580 kip-in. and 0.0021 radian and 7,883 kip-in. and 0.0422 radian. The corresponding values for the UNR project were 6,746 kip-in. and 0.0028 radian and 7,859 kip-in. and 0.0452 radian. Since the longitudinal steel reinforcement in the UNR columns were not symmetrically placed (see Figure B-1), the values obtained in Figure B-3 are for direction that UNR report calls "push" direction. Since the "push" and "pull" values are within 5 percent, we used the ISU "push" values in our computer models of the UNR column.

Moment-Curvature Input File for UNR's CIP Column

```
#Create uniaxial materials for Concrete and Steel
uniaxialMaterial Concrete01  1  -4.446   -0.002  0  -0.005
uniaxialMaterial Concrete04  2  -6.944     -0.0076  -0.0318  3801
uniaxialMaterial ReinforcingSteel  3  66.8   111.3   29000   1247   0.005   0.09

#Create fiber section with Defined Concrete and Rebar

section Fiber  1  {
patch circ 1 44  2  0  0  10.25  12.0  0  360
patch circ 2 44  10  0  0  0  10.25  0  360
layer circ 3  11  0.79  0  0  9.375
}

#Create nodes
#       tag   x     y
node     1    0.0   0.0
node     2    0.0   0.0

#Fix node 1
fix  1  1  1  1
fix  2  0  1  0

element zeroLengthSection 1 1 2 1
recorder Node -file MomentSection1Corrected.out -node 1 -dof 3 reaction
recorder Element -file TensStrain.out -ele 1 section fiber -8.955 2.641 stressStrain
recorder Element -file CompStrain-steel.out -ele 1 section fiber  9.375 0 3
stressStrain
recorder Element -file CompStrain-concrete.out -ele 1 section fiber  9.375 0 2
stressStrain

pattern Plain 1 "Constant" {
load 2  -208 0  0
}

integrator LoadControl 0.0
system SparseGeneral -piv
test NormUnbalance 1.0e-9 10
numberer Plain
constraints Plain
algorithm Newton
analysis Static
analyze 1

pattern Plain 2 "Linear" {
load 2  0.0  0.0  -1.0
}
integrator DisplacementControl 2  3  .000011515
analyze 500
```

OpenSees Input File for CIP Column Cyclic Push-Pull

```
#Clear cached data existing in the program
wipe

#Create Model with 3 dimensions and 6 degrees of freedom
model BasicBuilder -ndm 3 -ndf 6
#Create 6 DOF nodes

#       tag   x     y     z
```

```
node     1    0.0   0.0   0.0
node     2    0.0   0.0   0.0
node     3    0.0   96.0  0.0
node     4    0.0   108.0 0.0
node     5    0.0   120.0 0.0
node     6    -27.0 108.0 0.0

#Specifify geometric transoformation
geomTransf Linear 1  0  0  1

#Fix node 1
fix  1  1  1  1  1  1  1
fix  2  1  1  1  0  0  0

#Create uniaxial materials for Concrete and Steel
uniaxialMaterial Concrete01  1  -4.446   -0.002  0  -0.005
uniaxialMaterial Concrete04  2  -6.944     -0.0076  -0.0318  3801
uniaxialMaterial ReinforcingSteel  3  66.8   111.3   29000   1247   0.005   0.09

#Create hysteretic material to model Bond-Slip
uniaxialMaterial Hysteretic 4  6580  0.002079  7883  0.04223  -6580  -0.002079   -7883
-0.04223    1  1  0  0  0.35

#Create fiber section with Defined Concrete and Rebar
section Fiber  1  {
patch circ 1 44  2  0  0  10.25  12.0  0  360
patch circ 2 44  10  0  0  0  10.25  0  360
layer circ 3  11  0.79  0  0  9.375
}

#Create zero length element between nodes 1 and 2
element zeroLength 1  1  2  -mat 4 4 4 -dir 4  5  6

#Create nonlinear beam column between nodes 2 and 3
element nonlinearBeamColumn  2  2  3  9  1  1

#Create elastic beam column elements for the loading head
element elasticBeamColumn 3  3  4  1080  3656  1523.3  365880  122880  243000  1
element elasticBeamColumn 4  4  6  768  3656  1523.3  88704  51840  36864  1
element elasticBeamColumn 5  4  5  1080  3656  1523.3  365880  122880  243000  1

#Set up time series

timeSeries Linear 1

#Create two recorder files: displacements and reactions
recorder Node  -file ColumnDispCIPISU08272015.out -time -node 4 -dof 1 6 disp
recorder Node  -file ColumnreactionCIPISU08272015.out -time -node 2 -dof 1 reaction
recorder Node  -file ColumnmomentCIPISU08272015.out -time -node 1  -dof  6 reaction

#Set loading pattern for vertical loading
pattern Plain 1 1 {
load 5  0  -208  0  0  0  0
}

#Perform Following Analysis Commands for Vertical Loading
constraints Plain
numberer Plain
system BandGeneral
test NormDispIncr  1.0e-8  6
algorithm Newton
integrator LoadControl 1
analysis Static
```

```
analyze 1

#Reset time to perform pushover analysis
loadConst -time 0.0
pattern Plain  2  1  {
load 6 -200  0  0  0  0  0
}

constraints Plain
numberer Plain
system BandGeneral
test EnergyIncr  1.0e-8  8  0
algorithm Newton
analysis Static

integrator DisplacementControl  6  1  .009
analyze 30
integrator DisplacementControl  6  1  -.009
analyze 60
integrator DisplacementControl  6  1  .009
analyze 30
integrator DisplacementControl  6  1  .018
analyze 30
integrator DisplacementControl  6  1  -.018
analyze 60
integrator DisplacementControl  6  1  .018
analyze 30
integrator DisplacementControl  6  1  .027
analyze 30
integrator DisplacementControl  6  1  -.027
analyze 60
integrator DisplacementControl  6  1  .027
analyze 30
integrator DisplacementControl  6  1  .036
analyze 30
integrator DisplacementControl  6  1  -.036
analyze 60
integrator DisplacementControl  6  1  .036
analyze 30
integrator DisplacementControl  6  1  .1008
analyze 20
integrator DisplacementControl  6  1  -.1008
analyze 40
integrator DisplacementControl  6  1  .1008
analyze 20
integrator DisplacementControl  6  1  .108
analyze 30
integrator DisplacementControl  6  1  -.108
analyze 60
integrator DisplacementControl  6  1  .108
analyze 30
integrator DisplacementControl  6  1  .144
analyze 30
integrator DisplacementControl  6  1  -.144
analyze 60
integrator DisplacementControl  6  1  .144
analyze 30
integrator DisplacementControl  6  1  .18
analyze 30
integrator DisplacementControl  6  1  -.18
analyze 60
integrator DisplacementControl  6  1  .18
analyze 30
```

```
integrator DisplacementControl  6  1  .216
analyze 30
integrator DisplacementControl  6  1  -.216
analyze 60
integrator DisplacementControl  6  1  .216
analyze 30
integrator DisplacementControl  6  1  .252
analyze 30
integrator DisplacementControl  6  1  -.252
analyze 60
integrator DisplacementControl  6  1  .252
analyze 30
integrator DisplacementControl  6  1  .288
analyze 30
integrator DisplacementControl  6  1  -.288
analyze 60
integrator DisplacementControl  6  1  .288
analyze 30
integrator DisplacementControl  6  1  .36
analyze 30
integrator DisplacementControl  6  1  -.36
analyze 60
integrator DisplacementControl  6  1  .36
analyze 30
```

OpenSees Input File for the CIP Column Pushover

```
#Clear cached data existing in the program
wipe

#Create Model with 3 dimensions and 6 degrees of freedom
model BasicBuilder -ndm 3 -ndf 6

#Create 6 DOF nodes
#       tag   x     y     z
node     1    0.0   0.0   0.0
node     2    0.0   0.0   0.0
node     3    0.0   96.0  0.0
node     4    0.0   108.0 0.0
node     5    0.0   120.0 0.0
node     6    -27.0 108.0 0.0

#Specifify geometric transoformation
geomTransf Linear 1  0  0  1

#Fix node 1
fix  1  1  1  1  1  1  1
fix  2  1  1  1  0  0  0

#Create uniaxial materials for Concrete and Steel
uniaxialMaterial Concrete01  1  -4.446   -0.002  0  -0.005
uniaxialMaterial Concrete04  2  -6.944     -0.0076  -0.0318  3801
uniaxialMaterial ReinforcingSteel  3  66.8   111.3   29000   1247   0.005   0.09

#Create hysteretic material to model Bond-Slip
uniaxialMaterial Hysteretic 4  6580  0.002079  7883  0.04223  -6580  -0.002079   -7883
-0.04223    1  1  0  0  0.35

#Create fiber section with Defined Concrete and Rebar

section Fiber  1  {
```

```
patch circ 1 44  2  0  0  10.25  12.0  0  360
patch circ 2 44  10  0  0  0  10.25  0  360
layer circ 3  11  0.79  0  0  9.375
}

#Create zero length element between nodes 1 and 2
element zeroLength 1  1  2  -mat 4 4 4 -dir 4  5  6

#Create nonlinear beam column between nodes 2 and 3
element nonlinearBeamColumn  2  2  3  9  1  1

#Create elastic beam column elements for the loading head
element elasticBeamColumn 3  3  4  1080  3656  1523.3  365880  122880  243000  1
element elasticBeamColumn 4  4  6  768  3656  1523.3  88704  51840  36864  1
element elasticBeamColumn 5  4  5  1080  3656  1523.3  365880  122880  243000  1

#Set up time series
timeSeries Linear 1

#Create two recorder files: displacements and reactions
recorder Node  -file ColumnDispCIPPushoverISU08272015.out -time -node 4 -dof 1 6 disp
recorder Node  -file ColumnreactionCIPPushoverISU08272015.out -time -node 2 -dof 1
reaction
recorder Node  -file ColumnmomentCIPPushoverISU08272015.out -time -node 1  -dof  6
reaction

#Set loading pattern for vertical loading
pattern Plain 1 1 {
load 5  0  -208  0  0  0  0
}

#Perform Following Analysis Commands for Vertical Loading
constraints Plain
numberer Plain
system BandGeneral
test NormDispIncr  1.0e-8  6
algorithm Newton
integrator LoadControl 1
analysis Static
analyze 1

#Reset time to perform pushover analysis
loadConst -time 0.0

pattern Plain  2  1  {
load 6 -200  0  0  0  0  0
}

constraints Plain
numberer Plain
system BandGeneral
test EnergyIncr  1.0e-8  8  0
algorithm Newton
analysis Static
integrator DisplacementControl  6  1  .108
analyze 100
```

GCNP Column

This section of Appendix B presents the cyclic push-pull input file and the pushover input file for the UNR's GCNP column.

OpenSees Input File for GCNP Column Cyclic Push-Pull

```
#Clear cached data existing in the program
wipe

#Create Model with 3 dimensions and 6 degrees of freedom
model BasicBuilder -ndm 3 -ndf 6

#Create 6 DOF nodes
#       tag   x     y     z
node     1    0.0   0.0   0.0
node     2    0.0   0.0   0.0
node     3    0.0   14.5  0.0
node     4    0.0   108.0 0.0

#Specifify geometric transoformation
geomTransf Linear 1  0  0  1

#Fix node 1
fix  1  1  1  1  1  1  1
#Fix node 2 except for rotation
fix  2  1  1  1  0  0  0

#Create unconfined concrete
uniaxialMaterial Concrete01  1  -4.228   -0.002  0  -0.005

#Create confined concrete in precast shell
uniaxialMaterial Concrete04  2  -6.704     -0.0079  -0.0328  3706

#Create confined SCC in core of precast shell
uniaxialMaterial Concrete04  3  -7.543    -0.0071   -0.0296  4029

#Create reinforcing steel
uniaxialMaterial ReinforcingSteel  4  66.8   111.3   29000   1247   0.005   0.09

#Create Sleeve Section modeled as reinforcing steel
uniaxialMaterial ReinforcingSteel  7  79.4   110.5   35179   4116   0.0033   0.0170

#Create hysteretic material to model Bond-Slip at footing interface
uniaxialMaterial Hysteretic 5  6580  .002079  7883  .04223  -6580  -0.002079  -7883  -
0.04223   1  1  0  0  0.35

#Create fiber section for Column Shaft
section Fiber  1  {
patch circ 1 44  2  0  0  10.25  12.0   0  360
patch circ 2 44  3  0  0  7      10.25  0  360
patch circ 3 44  7  0  0  0      7      0  360
layer circ 4  11  0.79  0  0  9.375
}

section Fiber 2 {
patch circ  1  44  2  0  0  10.25  12.0   0  360
patch circ  2  4  3  0  0  7      10.25  5.02  27.71
patch circ  2  4  3  0  0  7      10.25  37.75  60.44
patch circ  2  4  3  0  0  7      10.25  70.48  93.17
patch circ  2  4  3  0  0  7      10.25  103.21  125.9
patch circ  2  4  3  0  0  7      10.25  135.94  158.63
patch circ  2  4  3  0  0  7      10.25  168.67  191.36
```

```
patch circ  2  4  3  0  0  7      10.25  201.4  224.09
patch circ  2  4  3  0  0  7      10.25  234.13  256.82
patch circ  2  4  3  0  0  7      10.25  266.86  289.55
patch circ  2  4  3  0  0  7      10.25  299.59  322.28
patch circ  2  4  3  0  0  7      10.25  332.32  355.01
patch circ  3  44  7  0  0  0      7      0  360
layer circ  7  11  0.79  0  0  9.375
}

#Create zero length element between nodes 1 and 2
element zeroLength 1  1  2  -mat 5 5 5 -dir 4  5  6

#Create element between nodes 2 and 3
element nonlinearBeamColumn 2  2  3  5  2  1

#Create nonlinear beam column between nodes 3 and 4
element nonlinearBeamColumn 3  3  4  5  1  1

#Set up time series
timeSeries Linear 1

#Create two recorder files: displacements and reactions
recorder Node  -file ColumnDisp09222015.out -node 4 -dof 1 disp
recorder Node  -file ColumnReaction09222015.out -node 2 -dof 1 reaction

#Set loading pattern for vertical loading
pattern Plain 1 1 {
load 4  0  -208  0  0  0  0
}

#Perform Following Analysis Commands for Vertical Loading
constraints Plain
numberer Plain
system BandGeneral
test NormDispIncr  1.0e-8  6
algorithm Newton
integrator LoadControl 1
analysis Static
analyze 1

#Reset time to perform pushover analysis
loadConst -time 0.0
pattern Plain  2  1  {
load 4  200  0  0  0  0  0
}

constraints Plain
numberer Plain
system BandGeneral
test EnergyIncr  1.0e-8  8  0
algorithm Newton
analysis Static
integrator DisplacementControl  4  1  .009
analyze 30
integrator DisplacementControl  4  1  -.009
analyze 60
integrator DisplacementControl  4  1  .009
analyze 30
integrator DisplacementControl  4  1  .009
analyze 30
integrator DisplacementControl  4  1  -.009
analyze 60
integrator DisplacementControl  4  1  .009
```

```
analyze 30
integrator DisplacementControl  4  1  .018
analyze 30
integrator DisplacementControl  4  1  -.018
analyze 60
integrator DisplacementControl  4  1  .018
analyze 30
integrator DisplacementControl  4  1  .018
analyze 30
integrator DisplacementControl  4  1  -.018
analyze 60
integrator DisplacementControl  4  1  .018
analyze 30
integrator DisplacementControl  4  1  .027
analyze 30
integrator DisplacementControl  4  1  -.027
analyze 60
integrator DisplacementControl  4  1  .027
analyze 30
integrator DisplacementControl  4  1  .027
analyze 30
integrator DisplacementControl  4  1  -.027
analyze 60
integrator DisplacementControl  4  1  .027
analyze 30
integrator DisplacementControl  4  1  .036
analyze 30
integrator DisplacementControl  4  1  -.036
analyze 60
integrator DisplacementControl  4  1  .036
analyze 30
integrator DisplacementControl  4  1  .036
analyze 30
integrator DisplacementControl  4  1  -.036
analyze 60
integrator DisplacementControl  4  1  .036
analyze 30
integrator DisplacementControl  4  1  .1008
analyze 20
integrator DisplacementControl  4  1  -.1008
analyze 40
integrator DisplacementControl  4  1  .1008
analyze 20
integrator DisplacementControl  4  1  .1008
analyze 20
integrator DisplacementControl  4  1  -.1008
analyze 40
integrator DisplacementControl  4  1  .1008
analyze 20
integrator DisplacementControl  4  1  .108
analyze 30
integrator DisplacementControl  4  1  -.108
analyze 60
integrator DisplacementControl  4  1  .108
analyze 30
integrator DisplacementControl  4  1  .108
analyze 30
integrator DisplacementControl  4  1  -.108
analyze 60
integrator DisplacementControl  4  1  .108
analyze 30
integrator DisplacementControl  4  1  .144
analyze 30
```

```
integrator DisplacementControl  4  1  -.144
analyze 60
integrator DisplacementControl  4  1  .144
analyze 30
integrator DisplacementControl  4  1  .144
analyze 30
integrator DisplacementControl  4  1  -.144
analyze 60
integrator DisplacementControl  4  1  .144
analyze 30
integrator DisplacementControl  4  1  .18
analyze 30
integrator DisplacementControl  4  1  -.18
analyze 60
integrator DisplacementControl  4  1  .18
analyze 30
integrator DisplacementControl  4  1  .18
analyze 30
integrator DisplacementControl  4  1  -.18
analyze 60
integrator DisplacementControl  4  1  .18
analyze 30
integrator DisplacementControl  4  1  .216
analyze 30
integrator DisplacementControl  4  1  -.216
analyze 60
integrator DisplacementControl  4  1  .216
analyze 30
integrator DisplacementControl  4  1  .216
analyze 30
integrator DisplacementControl  4  1  -.216
analyze 60
integrator DisplacementControl  4  1  .216
analyze 30
```

OpenSees Input File for the GCNP Column Pushover

```
#Clear cached data existing in the program
wipe

#Create Model with 3 dimensions and 6 degrees of freedom
model BasicBuilder -ndm 3 -ndf 6

#Create 6 DOF nodes
#       tag   x     y     z
node     1    0.0   0.0   0.0
node     2    0.0   0.0   0.0
node     3    0.0   14.5  0.0
node     4    0.0   108.0 0.0

#Specifify geometric transoformation
geomTransf Linear 1  0  0  1

#Fix node 1
fix  1  1  1  1  1  1  1

#Fix node 2 except for rotation
fix  2  1  1  1  0  0  0
#Create unconfined concrete
uniaxialMaterial Concrete01  1  -4.228   -0.002  0  -0.005
```

```
#Create confined concrete in precast shell
uniaxialMaterial Concrete04  2  -6.704     -0.0079  -0.0328  3706

#Create confined SCC in core of precast shell
uniaxialMaterial Concrete04  3  -7.543    -0.0071   -0.0296  4029

#Create reinforcing steel
uniaxialMaterial ReinforcingSteel  4  66.8   111.3   29000   1247   0.005   0.09

#Create Sleeve Section modeled as reinforcing steel
uniaxialMaterial ReinforcingSteel  7  79.4   110.5   35179   4116   0.0033   0.0170

#Create hysteretic material to model Bond-Slip at footing interface
uniaxialMaterial Hysteretic 5  6580  .002079  7883  .04223  -6580  -0.002079  -7883  -
0.04223   1  1  0  0  0.35

#Create fiber section for Column Shaft
section Fiber  1  {
patch circ 1 44  2  0  0  10.25  12.0   0  360
patch circ 2 44  3  0  0  7      10.25  0  360
patch circ 3 44  7  0  0  0      7      0  360
layer circ 4  11  0.79  0  0  9.375
}

section Fiber 2 {
patch circ  1  44  2  0  0  10.25  12.0   0  360
patch circ  2  4  3  0  0  7      10.25  5.02  27.71
patch circ  2  4  3  0  0  7      10.25  37.75  60.44
patch circ  2  4  3  0  0  7      10.25  70.48  93.17
patch circ  2  4  3  0  0  7      10.25  103.21  125.9
patch circ  2  4  3  0  0  7      10.25  135.94  158.63
patch circ  2  4  3  0  0  7      10.25  168.67  191.36
patch circ  2  4  3  0  0  7      10.25  201.4  224.09
patch circ  2  4  3  0  0  7      10.25  234.13  256.82
patch circ  2  4  3  0  0  7      10.25  266.86  289.55
patch circ  2  4  3  0  0  7      10.25  299.59  322.28
patch circ  2  4  3  0  0  7      10.25  332.32  355.01
patch circ  3  44  7  0  0  0      7      0  360
layer circ  7  11  0.79  0  0  9.375
}

#Create zero length element between nodes 1 and 2
element zeroLength 1  1  2  -mat 5 5 5 -dir 4  5  6

#Create element between nodes 2 and 3
element nonlinearBeamColumn 2  2  3  5  2  1

#Create nonlinear beam column between nodes 3 and 4
element nonlinearBeamColumn 3  3  4  5  1  1

#Set up time series
timeSeries Linear 1

#Create two recorder files: displacements and reactions
recorder Node  -file ColumnDispSmallArea09302015.out -node 4 -dof 1 disp
recorder Node  -file ColumnReactionSmallArea09302015.out -node 2 -dof 1 reaction

#Set loading pattern for vertical loading
pattern Plain 1 1 {
load 4  0  -208  0  0  0  0
}
```

```
#Perform Following Analysis Commands for Vertical Loading
constraints Plain
numberer Plain
system BandGeneral
test NormDispIncr  1.0e-8  6
algorithm Newton
integrator LoadControl 1
analysis Static
analyze 1

#Reset time to perform pushover analysis
loadConst -time 0.0
pattern Plain  2  1  {
load 4  200  0  0  0  0  0
}

constraints Plain
numberer Plain
system BandGeneral
test EnergyIncr  1.0e-8  8  0
algorithm Newton
analysis Static
integrator DisplacementControl  4  1  .0648
analyze 100
```

Appendix C - Grouted Coupler Experimental Data

The stress-strain data needed to model the grouted couplers used in the this project are presented in this appendix. The data was obtained by processing the laboratory test data provided in a report that was prepared for Splice Sleeve North America (SSNA), Inc. (Wiss, Janney, Elstner Associates, Inc. 2013) The report was obtained from SSNA, Inc. For this project only the stress-strain data pertaining to the 8U-X, SNX11, and 14U-X (which are used with the No. 8, No. 11, and No. 14 reinforcing bars) was needed. Table C-1 shows the dimensions for these couplers. The experimental set up is shown in Figure C-1.

A typical example of cyclic test experimental data in Appendix E of the test report for SSNA grouted couplers is shown in Figure C-2. For each of the three couplers used in this project, we had data for five specimens that were used with ASTM A615 Grade 60 steel bars. The data provided the force versus elongation of the coupler region (called "slip" in the test report) as shown in Figure C-1(b). The effective stress in the coupler is found by dividing the force by the area of the grouted coupler. The average strain of the coupler is obtained by dividing elongation of the coupler region by the length of the coupler region. Tables C-2 to C-4 show the stress-strain data needed for OpenSees' *ReinforcingSteel* uniaxial material used to model the grouted couplers. The graphs of the data are shown in Figures C-3 to C-5 along with the best fit curves.

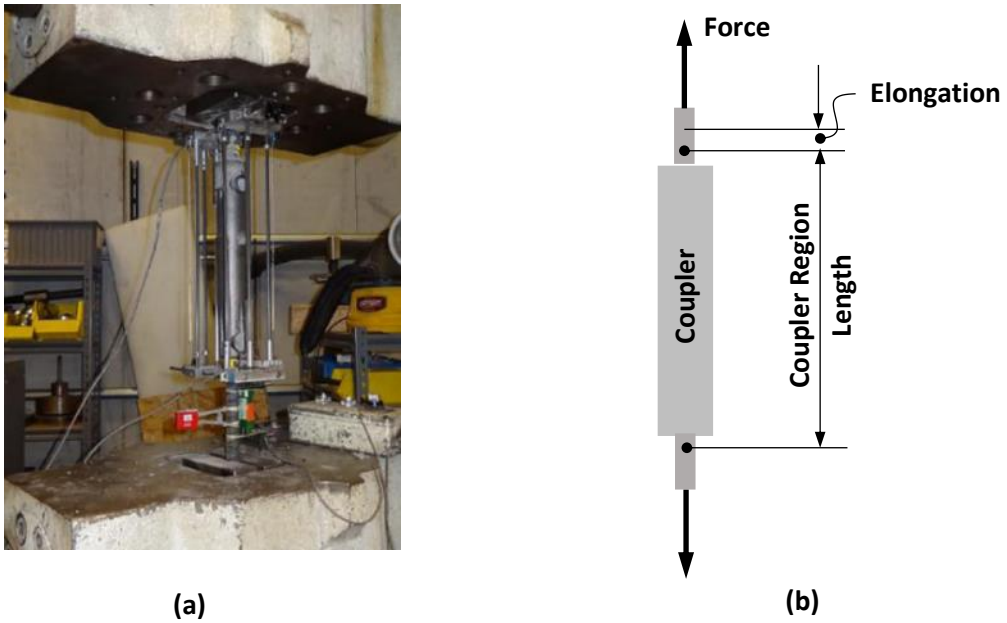

Figure C-1. (a) Experimental Set-up for Testing Grouted Coupler, and (b) Schematic Describing Coupler Region and the Elongation (Slip) (Wiss, Janney, Elstner Associates, Inc. 2013)

Table C-1. Measured Grouted Coupler Sleeve Dimensions

(Wiss, Janney, Elstner Associates, Inc. 2013)

Bar Size	Coupler Type	Diameter (mm)	Overall Length (mm)	Wall Thickness (mm)
6	U-X	51.8	285.1	4.73
8	U-X	63.7	369.6	4.71
10	U-X	72.6	455.3	5.45
14	U-X	88.1	620.4	8.08
11	SNX	77.5	485.9	6.53

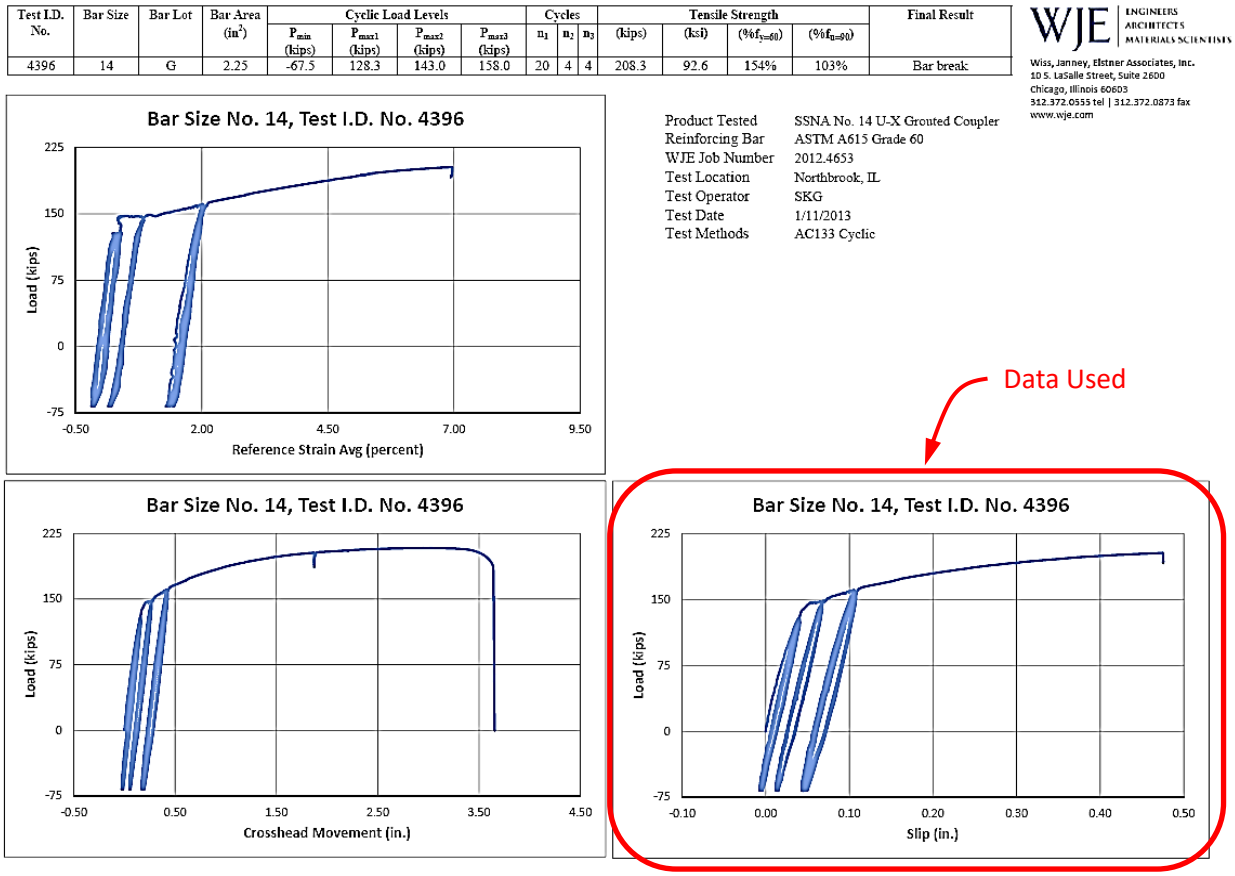

Figure C-2. Typical Cyclic Test Experimental Data (Ebrahimpour, et al. 2016)

Table C-2. Stress-Strain Data for SSNA 8U-X (Ebrahimpour, et al. 2016)

Test I.D.	Yield Stress (ksi)	Ultimate Stress (ksi)	Modulus of Elasticity (ksi)	Strain Hardening Modulus (ksi)	Initial Strain Hardening Strain (in./in.)	Ultimate Strain (in./in.)
4382	12.6	17.714	5,814	720.7	0.003361	0.0169
4383	12.7	17.714	5,548	705.5	0.003285	0.0170
4384	12.6	17.471	5,078	651.6	0.003361	0.0175
4385	12.6	17.713	5,708	664.7	0.003065	0.0166
4386	12.8	17.714	5,981	564.4	0.003285	0.0170
Average	**12.7**	**17.665**	**5,626**	**661.4**	**0.003271**	**0.0170**

Note: Sleeve area = 4.94 in^2

Table C-3. Stress-Strain Data for SSNA SNX11 (Ebrahimpour, et al. 2016)

Test I.D.	Yield Stress (ksi)	Ultimate Stress (ksi)	Modulus of Elasticity (ksi)	Strain Hardening Modulus (ksi)	Initial Strain Hardening Strain (in./in.)	Ultimate Strain (in./in.)
4402	14.5	19.67	5,259	722.5	0.0044	0.0161
4403	14.0	19.37	5,978	713.7	0.0046	0.0169
4404	13.8	19.37	5,838	669.4	0.0043	0.0167
4405	14.6	19.38	6,106	707.0	0.0041	0.0151
4406	14.2	19.94	6,398	682.0	0.0037	0.0176
Average	**14.2**	**19.54**	**5,916**	**698.9**	**0.0042**	**0.0165**

Note: Sleeve area = 7.31 in^2

Table C-4. Stress-Strain Data for SSNA SNX14 (Ebrahimpour, et al. 2016)

Test I.D.	Yield Stress (ksi)	Ultimate Stress (ksi)	Modulus of Elasticity (ksi)	Strain Hardening Modulus (ksi)	Initial Strain Hardening Strain (in./in.)	Ultimate Strain (in./in.)
4396	15.2	21.70	8,324	704.1	0.0020	0.0196
4397	15.7	21.70	8,472	714.7	0.0020	0.0186
4398	15.4	22.23	8,472	721.8	0.0018	0.0179
4399	15.3	21.70	8,206	776.8	0.0020	0.0183
4400	15.3	21.70	9,591	761.2	0.0017	0.0180
Average	**15.4**	**21.80**	**8,613**	**735.7**	**0.0019**	**0.0185**

Note: Sleeve area = 9.45 in^2

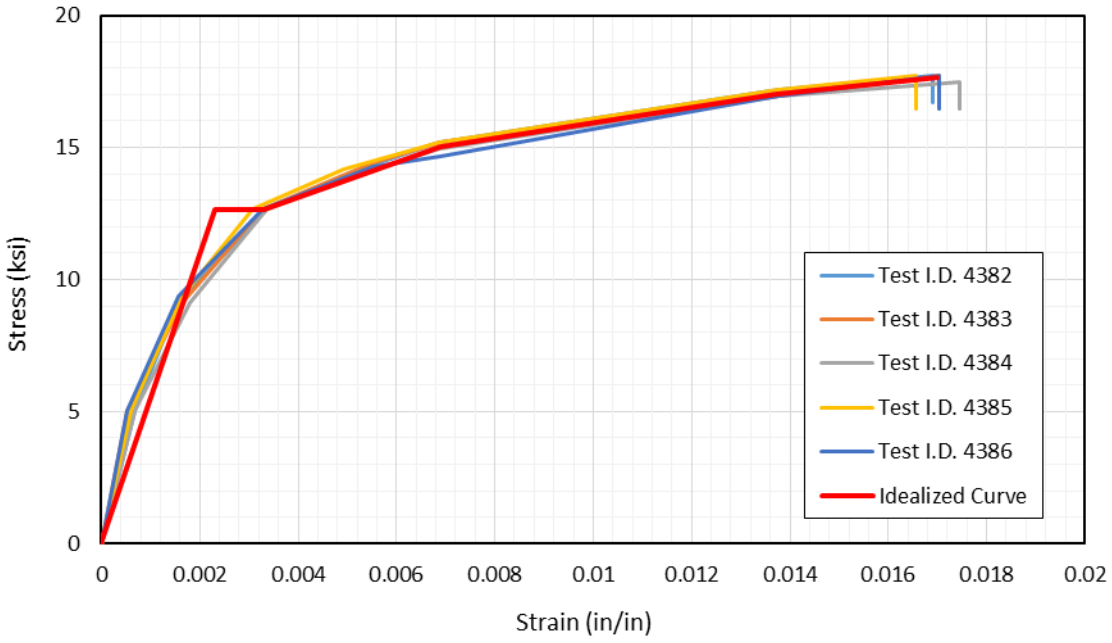

Figure C-3. Stress-Strain Relationship for SSNA 8U-X (Ebrahimpour, et al. 2016)

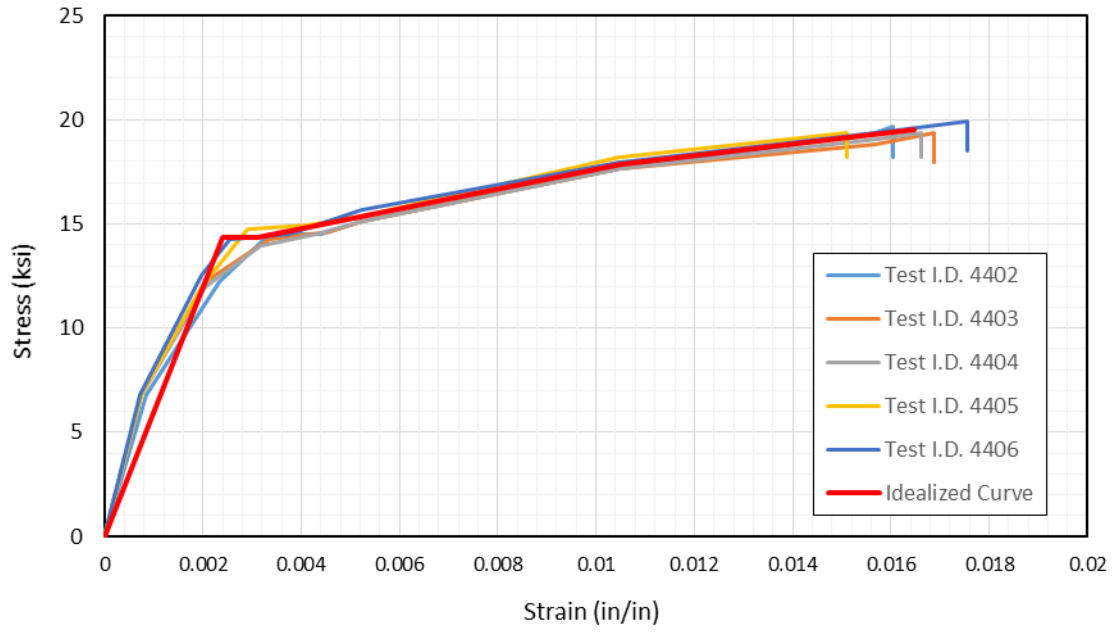

Figure C-4. Stress-Strain Relationship for SSNA SNX11 (Ebrahimpour, et al. 2016)

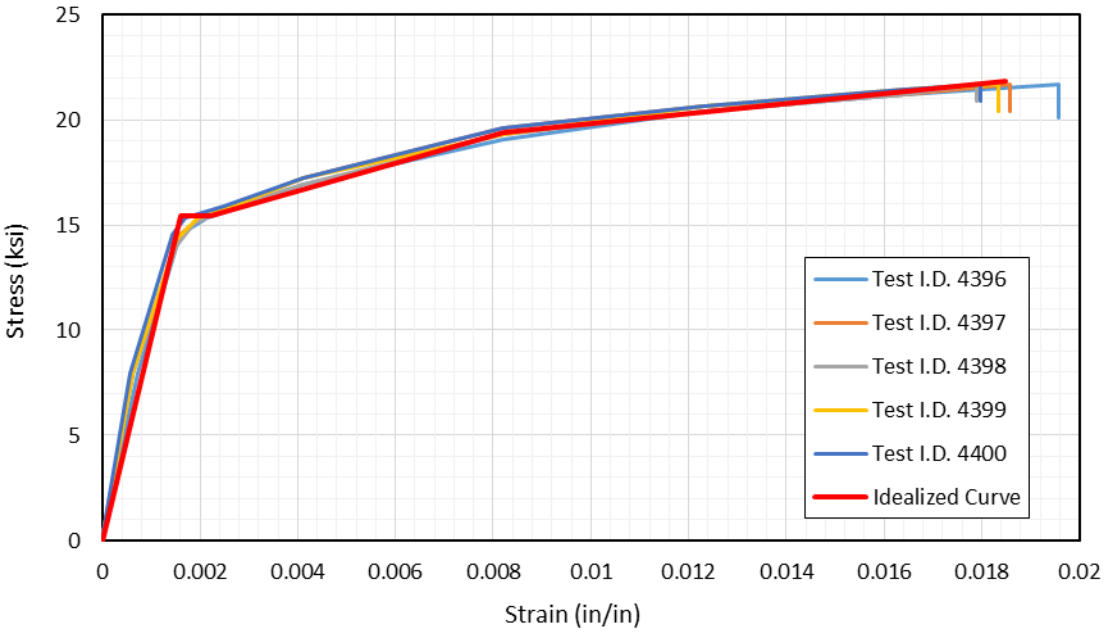

Figure C-5. Stress-Strain Relationship for SSNA 14U-X (Ebrahimpour, et al. 2016)

Appendix D - Computer Models of Idaho Bridges and Output Data

Two-Span Bridge on US95 at Parma, Idaho

The bridge at Parma is a two-span bridge with a three column bent. The skew in the bridge was removed for ease of modeling. The overall dimensions of the bridge were maintained and the bent and abutment lengths were shortened to match the deck width. The superstructure is made up of an 8 inch thick deck that rests on 5 prestressed WF66G girders. The substructure is made up of a pier cap, three columns, and their footings all of which are cast-in-place. The drawings and specifications were provided by ITD.

Spring Support Condition

Support stiffness:	Springs at abutments, fixed column bases
Abutment type:	Integral
Restraint of superstructure:	Abutments with springs in longitudinal and transverse directions, unrestrained rotation about the C. L. abutment.

Soil Spring Stiffness

Each abutment wall has eight 14X89 H-piles. Each H-pile is oriented with its strong axis parallel to the abutment wall length and its weak axis perpendicular to the abutment wall length. The dimensions of one wall are:

H_{aw} = 10.67’	Height of abutment wall
L_{aw} = 42’	Length of abutment wall

The soil spring stiffness for the H-piles were derived from the Phase IV Foundation Investigation Report. Figures D-1 and D-2 show force and deflection up to 48 ft of depth for one H-pile. Since spring stiffness equals force divided by deflection ($K = F/d$) the spring stiffness can be estimated by determining the force at 1 in of deflection. About the strong axis the force at 1 in of deflection is 95 kip, and about the weak axis the force at 1 in of deflection is 57.5 kip.

k_s = 95 kip/in = 1,140 kip/ft.

k_w = 57.5 kip/in = 690 kip/ft.

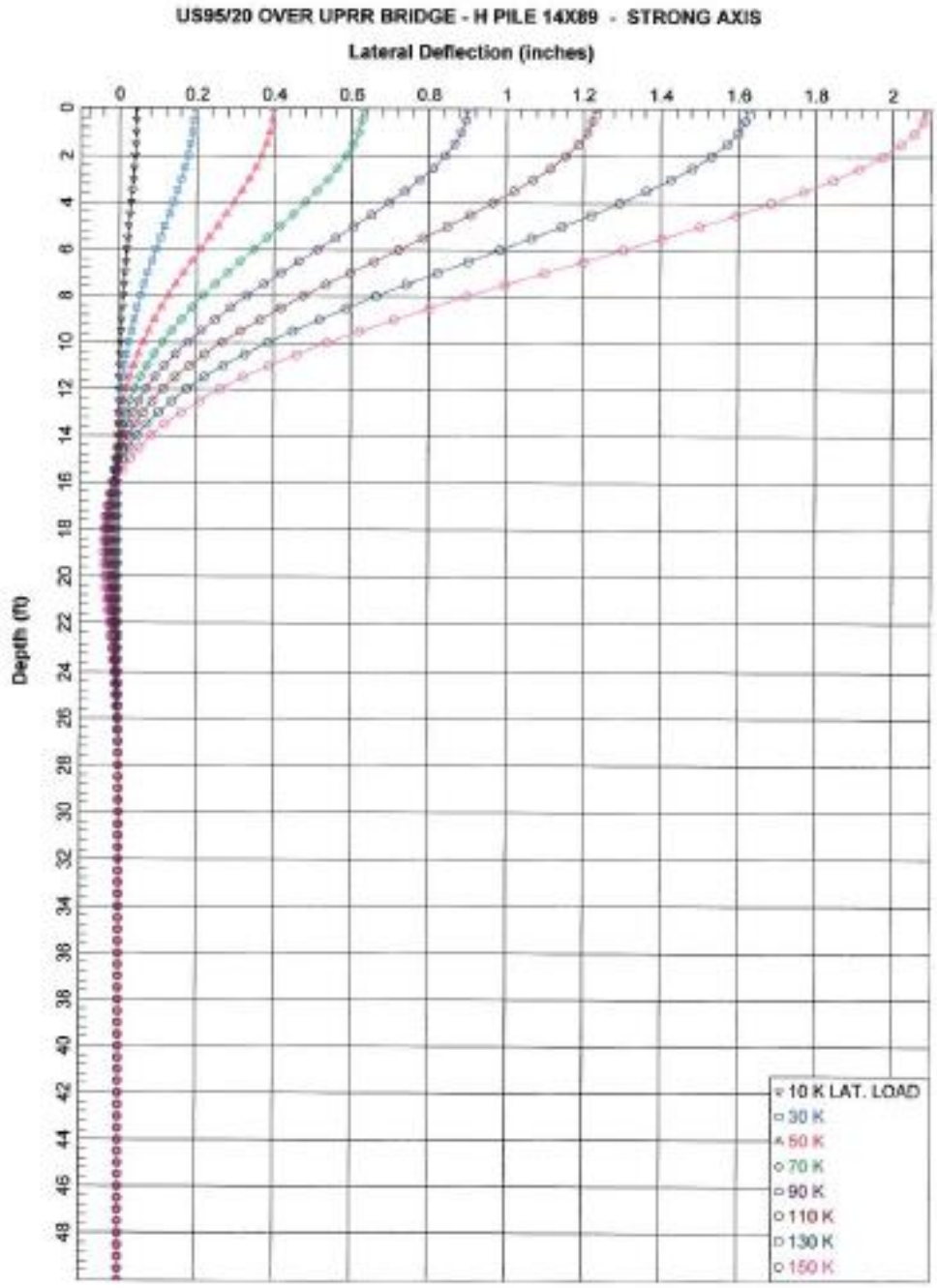

Figure D-1. Lateral Deflection vs. Depth of an H-Pile about the Strong Axis

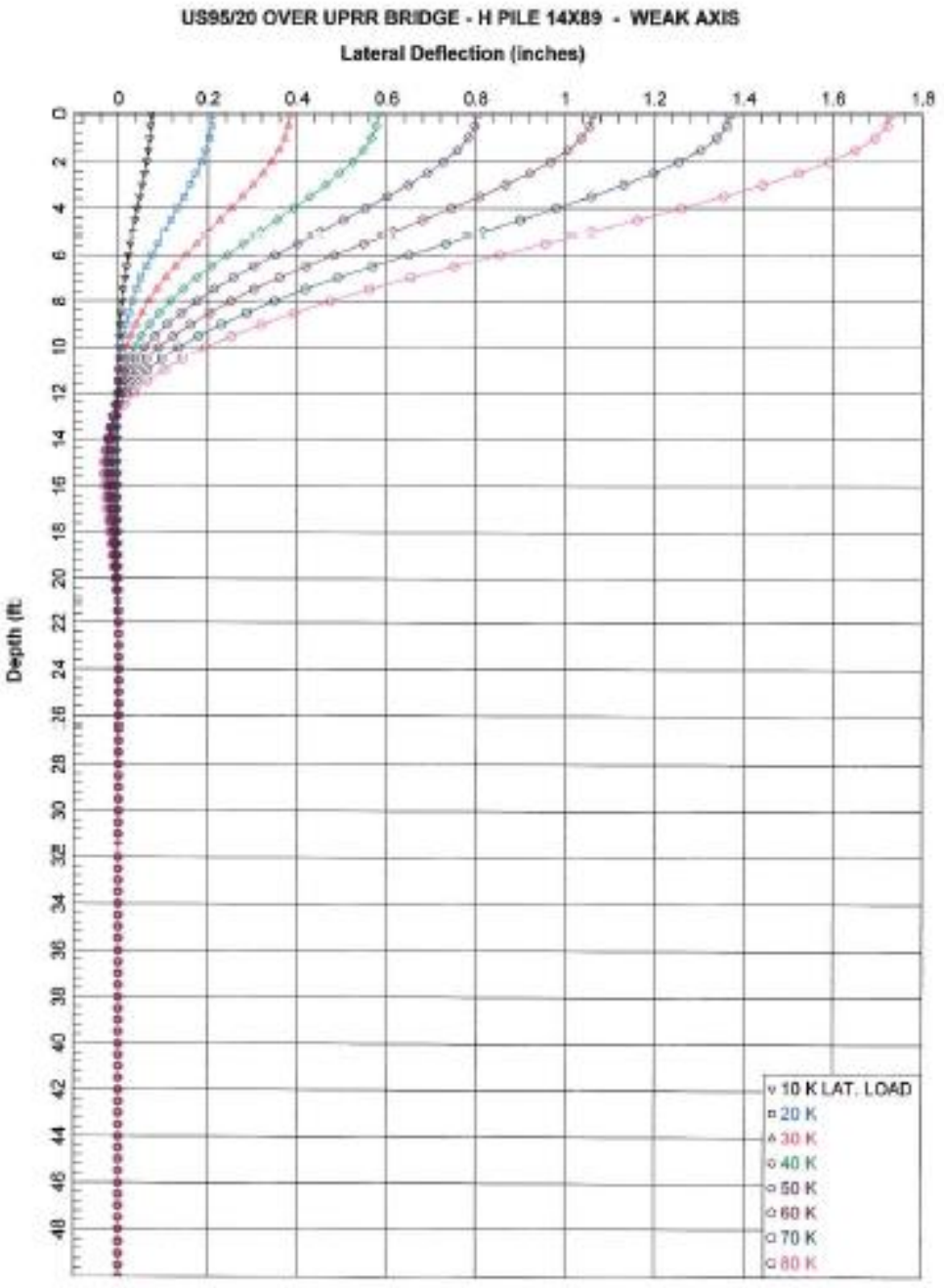

Figure D-2. Lateral Deflection vs. Depth of an H-Pile about the Weak Axis

The initial value due to abutments spring stiffness in the longitudinal direction is calculated by

$$K_l = \frac{2nk_s + (7.7A_{aw}/d)}{2} \quad \text{(D-1)}$$

Where

K_l = The abutments spring stiffness in the longitudinal direction
n = The number of H-piles in one abutment wall = 8
k_s = The spring stiffness for one H-pile about the strong axis = 1,140 kip/ft
A_{aw} = The area of the abutment wall = $H_{aw}\, L_{aw}$ = 448 ft^2
d = deflection needed to mobilize full passive resistance = 0.02H_{aw} = 0.2134 ft.

Initial value for the soil spring stiffness in the transverse direction is calculated by

$K_t = nk_w$

Where:
K_t = The spring stiffness in the transverse direction
k_w = The spring stiffness for one H-pile about the weak axis = 690 kip/ft

K_l = 17,202 kip/ft	Spring stiffness at abutments in the longitudinal direction
K_t = 5,520 kip/ft	Spring stiffness at abutments in the transverse direction

A large spring stiffness (1e12) was used for all other DOF's except the rotation about the C. L. abutments, which were assigned a value of zero.

Superstructure

Properties of the superstructure and its elements are as follows

L = 282'-2⅜"	Overall length of bridge
A_{Sup} = 58.40 ft^2	Cross-sectional area of superstructure without parapets
A_{gSup} = 62.50 ft^2	Gross cross-sectional area of superstructure including parapets for weight calculations
f'_{cCIP} = 4.0 ksi	Compressive strength of cast-in-place concrete
$f'_{cPrestressed}$ = 8.0 ksi	Compressive strength of prestressed concrete

$E_{CIP} = 33000*0.145^{1.5}\sqrt{f'_{cCIP}} = 33000(0.145^{1.5})\sqrt{4.0} = 3{,}644$ ksi

Modulus of elasticity of cast-in-place concrete

$E_{Prestressed} = 33000(0.14+0.001f'_{cPrestressed})^{1.5}\sqrt{f'_c} = 33000(0.14+(0.001*8.0))^{1.5}\sqrt{8.0} = 5314.37$ ksi

Modulus of elasticity of prestressed concrete

$n = E_{Prestressed}/E_{CIP} = 5314/3644 = 1.458$

Modular ratio of elasticity

The moments of inertia of the superstructure were determined by calculating the moments of inertia of the prestressed girders and the transformed moment of inertia of the deck and using the parallel axis theorem,

$$I_s = \sum I_o + Ad^2. \quad \text{(D-2)}$$

Where:

I_s = the moment of inertia of the superstructure

I_o = the moment of inertia of a section (girder or deck) of the superstructure

A = the area of a section of the superstructure

d = the distance from the centroid of the section to the centroid of the superstructure

$A_{Girder} = 6.08\ ft^2$ Cross-sectional area of one girder

$I_{yGirder} = 3.48\ ft^4$ Moment of inertia of one girder about the y axis

$I_{zGirder} = 27.14\ ft^4$ Moment of inertia of one girder about the z axis

The transformed moment of inertia and area for the deck was calculated by dividing the value of I_{zDeck}, I_{yDeck} and A_{Deck} by the modular ratio, n. The parapets on the outside edge of the deck were not included in these calculations.

$A_{tDeck} = 19.2\ ft^2$ Transformed area of deck

$I_{yDeck} = 2823\ ft^4$ Transformed moment of inertia of the deck about the y axis

$I_{zDeck} = 0.7113\ ft^4$ Transformed moment of inertia of the deck about the z axis

$d_{zGirder} = 1.20$ ft Distance from the centroid of the girder to the centroid of the superstructure along the y-axis

$d_{zDeck} = 1.90$ ft Distance from the centroid of the deck to the centroid of the superstructure along the y-axis

$d_{yGirder1,5} = 17.5$ ft Distance from the centroid of the first and fifth girders to the centroid of the superstructure along the z-axis

$d_{yGirder2,4} = 8.75$ ft Distance from the centroid of the second and fourth girders to the centroid of the superstructure along the z-axis

$d_{yGirder3}$ = 0 ft Distance from the centroid of the third girder to the centroid of the superstructure along the z-axis

d_{yDeck} = 0 ft Distance from the centroid of the deck to the centroid of the superstructure along the z-axis

$$I_{ySup} = 2823ft^4 + 5(3.48ft^4) + 6.08ft^2[2(17.2ft)^2 + 2(8.75ft)^2] = 7495.5ft^4$$

Transformed moment of inertia of the superstructure about the y axis

$$I_{zSup} = 0.7113ft^4 + 19.20ft^2(1.90ft)^2 + 5[27.14ft^4 + 6.08ft^2(1.20ft)^2] = 249.3ft^4$$

Transformed moment of inertia of the superstructure about the z axis

$$A_{tSup} = A_{tDeck} + \sum A_{Girder} = 19.2ft^2 + 5(6.08ft^2) = 49.6ft^2$$

Transformed area of the superstructure

The modulus of rigidity, *G*, for the cast-in-place and prestressed concrete are calculated by

$$G = \frac{E}{2(1+\nu)}$$

Where:

ν = Poisson's ratio, typically from 0.15 - 0.2.

$G_{prestressed}$ = 5314.37/2(1+0.2) = 2,214.3 ksi =318,862.2 ksf

G_{CIP} = 3644/2(1+0.2) = 1,518.3 ksi = 218,640 ksf

Substructure

Properties of the substructure and its elements are as follows

L_p = 42'-0"	Length of pier cap
A_{pyz} = 25.23 ft^2	Cross-sectional area of pier cap in the x-y plane
I_{pz} = 60.9 ft^4	Moment of inertia about the z axis
L_c = 25'-7.75"	Column height
D_c = 3'-6"	Column diameter
A_{cg} = 9.62 ft^2	Cross-sectional area of one column
I_{cg} = πd^4/64 = 7.366 ft^4	Gross moment of inertia of one column

Column Reinforcement

The columns are reinforced with 16 #10 two-bar bundles and a #5 spiral with a 3 in pitch. There is 1.5 in of cover concrete as shown in Figure E-D.

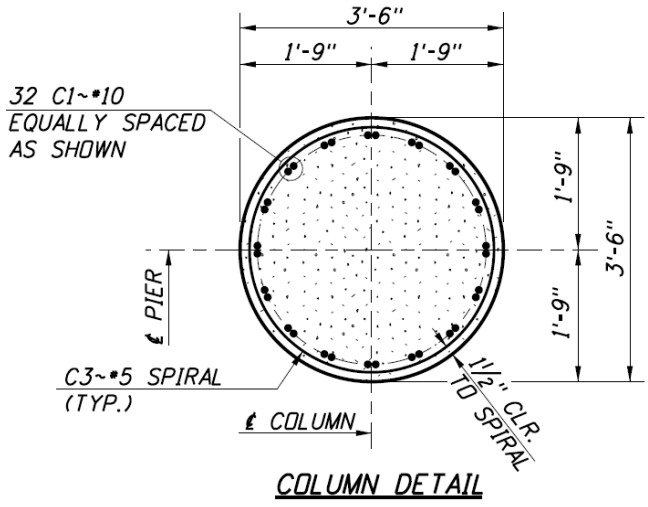

Figure D-3. Reinforced column detail

To accommodate the grouted couplers 16 single reinforcing bars need to be used instead of the two-bar bundles. A #14 bar has the closest cross-sectional area to that of the two #10 bars.

A_{r10} = 1.270 in^2	Cross-sectional area of a #10 bar
A_{r14} = 2.25 in^2 = 0.015625 ft^2	Cross-sectional area of a #14 bar
d_{r14} = 1.693 in = 0.141083 ft	Diameter of a #14 reinforcing bar
d_s = 0.625”	Diameter of spiral reinforcing
A_{st14} = 16A_{r14} = 0.25 ft^2	Total longitudinal steel in one column with #14 bars
R_{14} = 1.502 ft	Distance from the center of the column to the center of the #14 bars

Effective Moment of Inertia and Torsional Moment of Inertia of the Columns

For the effective moment of inertia the gross moment of inertia is multiplied by the Elastic Stiffness Ratio (I_{eff}/I_{cg}). This is obtained from Figure D-4 with the Axial Load Ratio and the ratio of reinforcing steel to concrete.

$Axial\ Load\ Ratio = P/f'_cA_{cg}$

Where

P = The axial load to the column from the self-weight of the bridge = 627.07 kips

The axial load on one column is from half the weight of each span divided by three plus the weight on the node in the pier cap above the column plus half the weight of one column. The dead load to each node is given in Table D-1.

P/f'_cA_{cg} = 0.113

A_{st}/A_{cg} =0.25 ft^2/9.62 ft^2 = 0.029

I_{eff}/I_{cg} = 0.57

I_{ceff} = 0.57 * I_{cg} = 4.199 ft^4 Effective moment of inertia of one column

Table D-1. Weight of Structure to nodes from deck, pier cap, and top half of columns

Secition	X-sec. Area (ft^2)	Length (ft)	Weight of concrete (kips/ft^3)	Weight of diaphragms (kips)	Weight of deck forms and future wearing surface (klf)	Weight to node (kips)
Deck						
node 1	62.5	17.629	0.15	0	1.89	198.585
node 2	62.5	35.275	0.15	20.754	1.89	418.127
node 3	62.5	35.275	0.15	20.754	1.89	418.127
node 4	62.5	35.275	0.15	20.754	1.89	418.127
node 5	62.5	35.275	0.15	0	1.89	397.373
node 6	62.5	35.275	0.15	20.754	1.89	418.127
node 7	62.5	35.275	0.15	20.754	1.89	418.127
node 8	62.5	35.275	0.15	20.754	1.89	418.127
node 9	62.5	17.629	0.15	0	1.89	198.585
Pier cap						
node 13	25.23	13.339	0.15	N/A	N/A	50.481
node 17	25.23	15.322	0.15	N/A	N/A	57.986
node 21	25.23	13.339	0.15	N/A	N/A	50.481
Top half of columns						
node 12	9.62	12.823	0.15	N/A	N/A	18.504
node 16	9.62	12.823	0.15	N/A	N/A	18.504
node 20	9.62	12.823	0.15	N/A	N/A	18.504
				Total		3517.766
				w(x) kip/ft		12.466

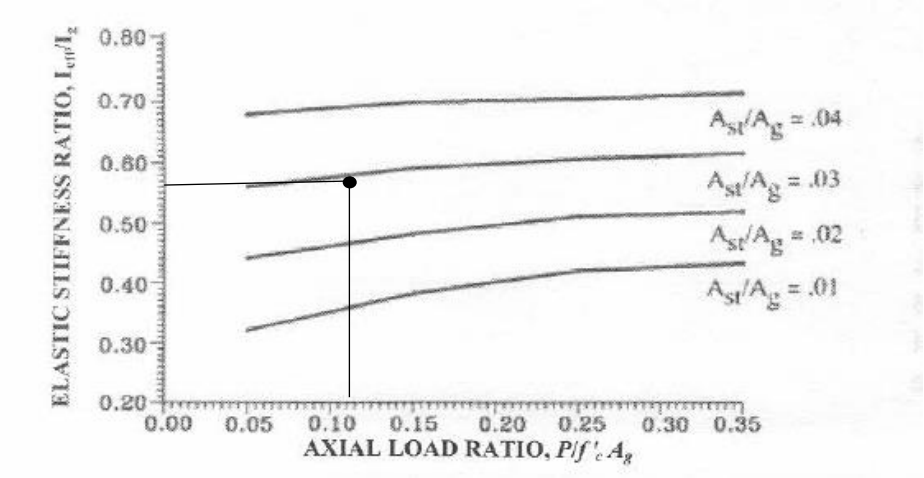

Figure D-4. Elastic Stiffness Ratio (AASHTO *Guide Specifications for LRFD Seismic Bridge Design* (2011), p.5-19)

$J_{gross} = \frac{\pi D^4}{32}$ =π(3.5^4)/32 = 14.7 ft^4

Gross torsional moment of inertia

$J_{eff} = 0.2J_{gross}$ = 2.95 ft^4 Effective torsional moment of inertia

Linear Elastic Model of the Structure

Each span of the superstructure is modeled as four elements (35.275' each) attached end to end from south to north. A rigid element with a large moment of inertia attaches the superstructure to the pier bent at the midpoint of both. This element starts at the center of gravity of the pier bent and ends at the center of gravity of the superstructure (6.154'). At the top of each column there is another rigid element that starts at the top of the column and ends at the center of gravity of the pier bent (2.701'). The footings of the columns are modeled as an element at the bottom of the columns with the same properties as the columns, except that they are rigid, and are half the depth of the footings in length (2.0'). To model the spring support condition an extra node and zeroLength element is assigned to the abutment ends of the superstructure.

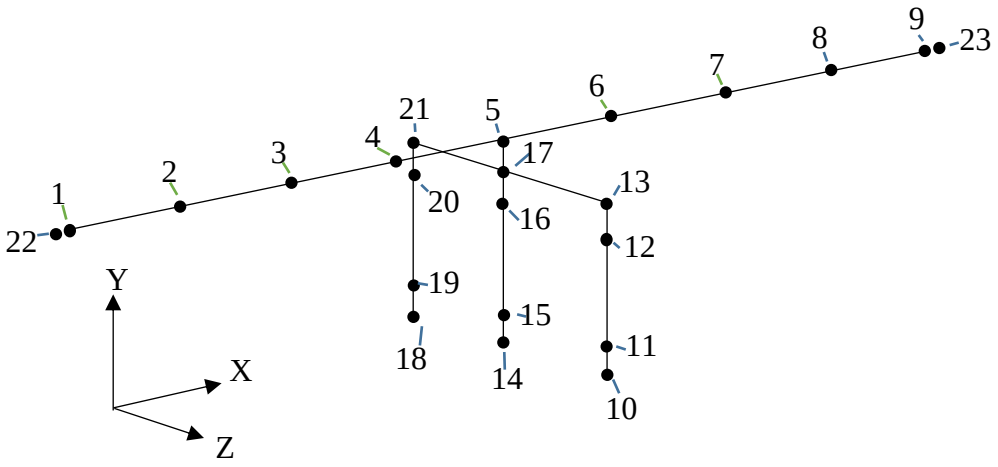

Figure D-5. Bridge model with node numbers

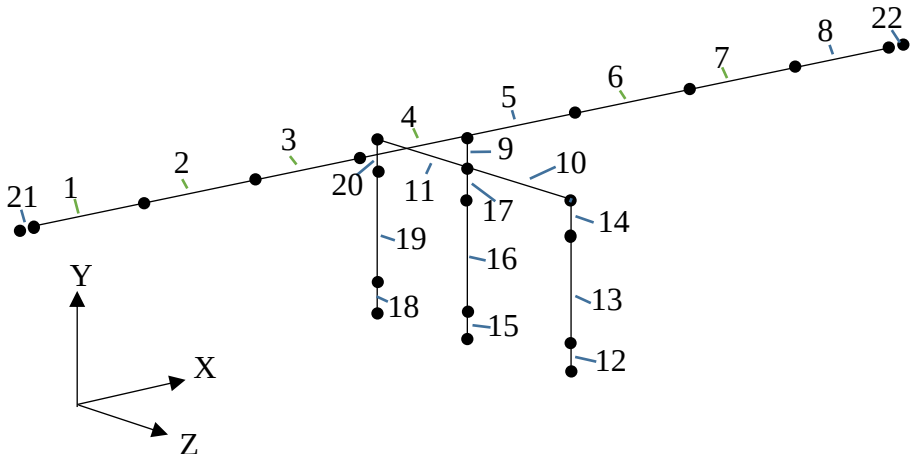

Figure D-6. Bridge model with element numbers

Geometric transformation

From OpenSees Command Manual: "*The x-axis is a vector given by the two element nodes; The vector vecxz is a vector the user specifies that must not be parallel to the x-axis. The x-axis along with the vecxz Vector define the xz plane. The local y-axis is defined by taking the cross product of the x-axis vector and the vecxz vector (Vy = Vxz X Vx). The local z-axis is then found simply by taking the cross product of the y-axis and x-axis vectors (Vz = Vx X Vy). The section is attached to the element such that the y-z coordinate system used to specify the section corresponds to the y-z axes of the element.*"

The geometric transformations used in OpenSees elements are shown in Figure D-7.

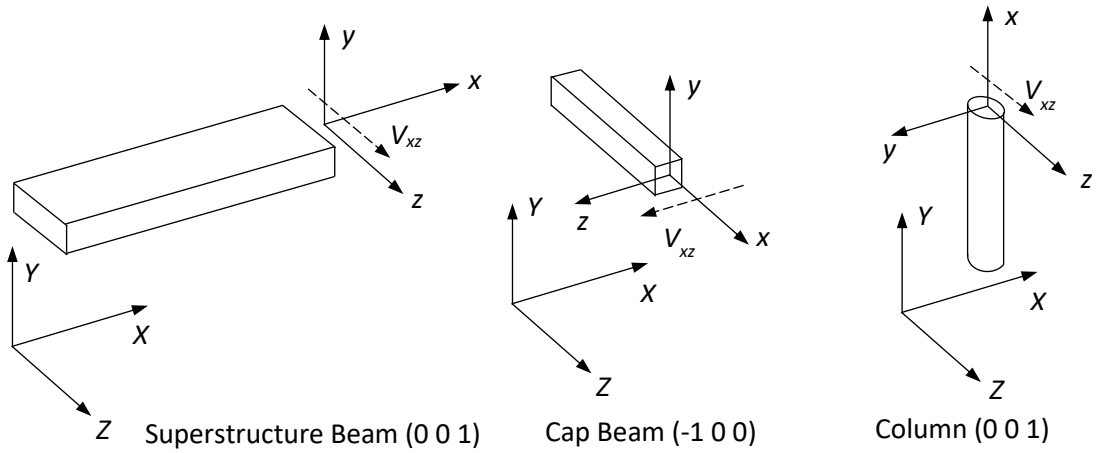

Figure D-7. OpenSees geometric transformation (*XYZ* is global CS and *xyz* is local CS) (Ebrahimpour, et al. 2016)

Calculation of Seismic Loads

The bridge will be subject to more seismically active conditions than that found near Parma, ID. Montpelier, ID is the most seismically active city in Idaho where there might be a bridge. Figure D-8 shows the Design Maps Summary Report for Montpelier, ID.

USGS Design Maps Summary Report

User-Specified Input

Building Code Reference Document	2009 AASHTO Guide Specifications for LRFD Seismic Bridge Design (which utilizes USGS hazard data available in 2002)
Site Coordinates	42.32204°N, 111.29481°W
Site Soil Classification	Site Class D – "Stiff Soil"

USGS-Provided Output

PGA =	0.322 g	A_s =	0.379 g
S_S =	0.758 g	S_{DS} =	0.907 g
S_1 =	0.258 g	S_{D1} =	0.486 g

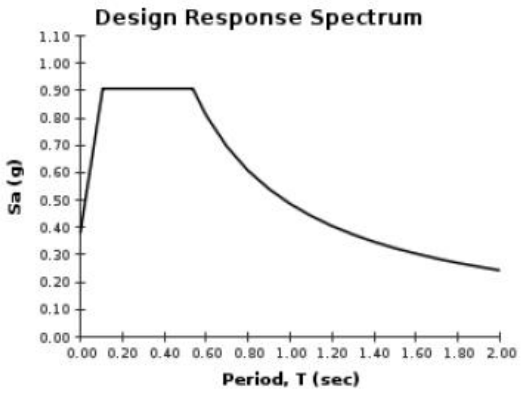

Figure D-8. USGS Design Maps Summary Report (USGS 2015)

To calculate the seismic loads on the deck of the bridge the displacements at the deck nodes from a uniformly distributed load of 10 kip/ft in the longitudinal and transverse direction are determined and used to calculate the factors α, β, and γ. The factors are used to calculate the loads (*pe (x)*) at the nodes on the deck. The distributed seismic loads on each element is the average of the loads on the nodes. These loads are shown in column 9 of Tables D-2 and D-3. (Mast, et al. 1996)

$$\alpha = \int_0^L v_s(x)\, dx \tag{D-3}$$

$$\beta = \int_0^L w(x) v_s(x) dx \tag{D-4}$$

$$\gamma = \int_0^L w(x) v_s\,(x)^2 dx \tag{D-5}$$

Where

$v_x\,(x)$ = Displacement due to a uniformly distributed load of 10 kip/ft.
$w(x)$ = Weight of the bridge per unit length = 12.466 kip/ft
dx = Tributary length
L = Total length of bridge

$p_e(x) = \beta C_{sm} w(x) * v_s(x)/\gamma$

Where

$C_{sm} = S_{DS}$ = 0.907 for $T_o < T_m < T_s$ and
$C_{sm} = S_{D1}/T_m$ = 0.887 for $T_m > T_s$

Where

$T_m = 2\pi\sqrt{\gamma/P_0 g\alpha}$ = 0.344s for longitudinal loads
$T_m = 2\pi\sqrt{\gamma/P_o g\alpha}$ = 0.548s for transverse loads
$T_s = S_{D1}/S_{DS}$ = 0.5358
$T_o = 0.2T_s$ = 0.1072
g = 32.2 ft/s^2
P_o = 10 kip/ft

Table D-2. Calculation of Seismic Loads in the Longitudinal Direction

Nodes	x (ft)	dx (ft)	vs(x) (ft)	α(x) (ft^2)	β(x) (k-ft)	γ(x) (k-ft^2)	pe(x) (k/ft)	ave. (k/ft)
1	0.00	0.00	0.0753	0.000	0.000	0.000	11.084	
2	35.27	35.27	0.0764	2.676	33.360	2.531	11.237	11.161
3	70.55	35.27	0.0771	2.707	33.746	2.590	11.342	11.290
4	105.82	35.27	0.0775	2.726	33.987	2.627	11.399	11.370
5	141.01	35.27	0.0775	2.734	34.084	2.642	11.407	11.403
6	176.37	35.27	0.0775	2.734	34.084	2.642	11.399	11.403
7	211.65	35.27	0.0771	2.726	33.987	2.627	11.342	11.370
8	246.91	35.27	0.0764	2.707	33.746	2.590	11.237	11.290
9	282.18	35.27	0.0753	2.676	33.360	2.531	11.084	11.161
Totals		282.19		21.687	270.354	20.779		

Table D-3. Calculation of Seismic Loads in the Transverse Direction

Nodes	x (ft)	dx (ft)	vs(x) (ft)	α(x) (ft^2)	β(x) (k-ft)	γ(x) (k-ft^2)	pe(x) (k/ft)	ave. (k/ft)
1	0	0	-0.188	0.000	0.000	0.000	10.611	
2	35.27	35.27	-0.192	-6.703	-83.563	15.880	10.789	10.700
3	70.55	35.27	-0.197	-6.856	-85.464	16.611	11.098	10.943
4	105.82	35.27	-0.201	-7.022	-87.534	17.425	11.319	11.208
5	141.01	35.27	-0.202	-7.111	-88.646	17.871	11.383	11.351
6	176.37	35.27	-0.201	-7.111	-88.652	17.873	11.320	11.352
7	211.65	35.27	-0.197	-7.023	-87.549	17.431	11.100	11.210
8	246.91	35.27	-0.192	-6.857	-85.484	16.618	10.792	10.946
9	282.18	35.27	-0.189	-6.705	-83.586	15.889	10.614	10.703
Totals		282.19		-55.389	-690.478	135.597		

Linear Elastic OpenSees tlc Script for Seismic Load in Transverse Direction

```
#Two-span Bridge on US95 at Parma, Idaho

wipe

#Create model with 3 dimensions and 6 DOF

model BasicBuilder -ndm 3 -ndf 6

#Units are kips and feet
```

```
#Create 6 DOF nodes

#Superstructure nodes
#       tag         x             y            z

node     1         0.0         36.459         0.0
node     2        35.275       36.459         0.0
node     3        70.549       36.459         0.0
node     4       105.824       36.459         0.0
node     5       141.009       36.459         0.0
node     6       176.374       36.459         0.0
node     7       211.648       36.459         0.0
node     8       246.914       36.459         0.0
node     9       282.179       36.459         0.0

#Substructure nodes

node    10       141.009        0.0          15.322
node    11       141.009        2.0          15.322
node    12       141.009       27.646        15.322
node    13       141.009       30.347        15.322
node    14       141.009        0.0           0.0
node    15       141.009        2.0           0.0
node    16       141.009       27.646         0.0
node    17       141.009       30.347         0.0
node    18       141.009        0.0         -15.322
node    19       141.009        2.0         -15.322
node    20       141.009       27.646       -15.322
node    21       141.009       30.347       -15.322

#Spring support nodes

node    22         0.0         36.459         0.0
node    23       282.179       36.459         0.0

#Specify geometric transformation

geomTransf Linear 1  0  0  1
geomTransf Linear 2 -1  0  0
geomTransf PDelta 3  0  0  1

# Fix column bases and abutments in all DOF's

fix 22 1 1 1 1 1 1
fix 23 1 1 1 1 1 1
fix 10 1 1 1 1 1 1
fix 14 1 1 1 1 1 1
fix 18 1 1 1 1 1 1


# Create deck elements

# element elasticBeamColumn $eleTag $iNode $jNode $A $E $G $J $Iy $Iz $transfTag

element elasticBeamColumn 1  1  2  49.60  765269.3  318862.2  1e10  7495.5  244.3  1
element elasticBeamColumn 2  2  3  49.60  765269.3  318862.2  1e10  7495.5  244.3  1
element elasticBeamColumn 3  3  4  49.60  765269.3  318862.2  1e10  7495.5  244.3   1
element elasticBeamColumn 4  4  5  49.60  765269.3  318862.2  1e10  7495.5  244.3  1
element elasticBeamColumn 5  5  6  49.60  765269.3  318862.2  1e10  7495.5  244.3  1
element elasticBeamColumn 6  6  7  49.60  765269.3  318862.2  1e10  7495.5  244.3  1
element elasticBeamColumn 7  7  8  49.60  765269.3  318862.2  1e10  7495.5  244.3  1
element elasticBeamColumn 8  8  9  49.60  765269.3  318862.2  1e10  7495.5  244.3  1
```

```
# Create pier bent elements

element elasticBeamColumn  9  5 17  196.00   524736  218640 1e10  1e10  1e10  3
element elasticBeamColumn 10 13 17   25.23   524736  218640 1e10  1e10  1e10  2
element elasticBeamColumn 11 17 21   25.23   524736  218640 1e10  1e10  1e10  2

# Create column elements

element elasticBeamColumn 12 10 11  9.62  524736  218640 1e10  4.199  4.199 3
element elasticBeamColumn 13 11 12 9.62  524736  218640 2.95  4.199  4.199 3
element elasticBeamColumn 14 12 13  1e10  524736  218640 1e10  1e10  1e10  3
element elasticBeamColumn 15 14 15 9.62  524736  218640 1e10  4.199  4.199 3
element elasticBeamColumn 16 15 16 9.62  524736  218640 2.95  4.199  4.199 3
element elasticBeamColumn 17 16 17  1e10  524736  218640 1e10  1e10  1e10  3
element elasticBeamColumn 18 18 19 9.62  524736  218640 1e10  4.199  4.199 3
element elasticBeamColumn 19 19 20 9.62  524736  218640 2.95  4.199  4.199 3
element elasticBeamColumn 20 20 21  1e10  524736  218640 1e10  1e10  1e10  3

# Create spring elements

# Initial abutment stiffnesses to be used with the uniform loads to determine the
seismic loads

#uniaxialMaterial Elastic 1 17.202e3;   # Translational stiffness  of the abutments
along x axis, kip/ft
#uniaxialMaterial Elastic 3 5.52e3;   # Translational stiffness of the abutments along
z axis, kip/ft

# Final abutment stiffnesses

uniaxialMaterial Elastic 1 17.042e3;   # Translational stiffness  of the abutments
along x axis, kip/ft
uniaxialMaterial Elastic 2 1e12;   # Translational stiffness of the abutments along y
axis, kip/ft
uniaxialMaterial Elastic 3 3.2e3;   # Translational stiffness of the abutments along z
axis, kip/ft
uniaxialMaterial Elastic 4 1e12;   # Rotational stiffness of the abutments about x
axes, kip.ft/radian
uniaxialMaterial Elastic 5 1e12;      # Rotational stiffness of the abutments about y
axes, kip.ft/radian
uniaxialMaterial Elastic 6 0;      # Rotational stiffness of the abutments about z
axes, kip.ft/radian


# Spring elements using above stiffness values
# element zeroLength $eleTag $iNode $jNode -mat $matTag1 $matTag2 ... -dir $dir1 $dir2
...

element zeroLength 21 22  1 -mat 1 2 3 4 5 6 -dir 1 2 3 4 5 6
element zeroLength 22  9 23 -mat 1 2 3 4 5 6 -dir 1 2 3 4 5 6

# Create recorder files

recorder Node -file Nodes1-9DisplLong_Parma_elastic.out -time -nodeRange 1 9 -dof 1
disp
recorder Node -file Nodes1-9DispTrans_Parma_elastic.out -time -nodeRange 1 9 -dof 3
disp
recorder Node -file Node22_Reaction_Parma_eleastic_long.out -time -node 22 -dof 1
reaction
recorder Node -file Node23_Reaction_Parma_eleastic_long.out -time -node 23 -dof 1
reaction

# Assign gravity loads
```

```
pattern Plain 1 Constant {
#    tag    FX       FY       FZ   MX   MY   MZ
load  1     0.0    -198.585  0.0  0.0  0.0  0.0
load  2     0.0    -418.127  0.0  0.0  0.0  0.0
load  3     0.0    -418.127  0.0  0.0  0.0  0.0
load  4     0.0    -418.127  0.0  0.0  0.0  0.0
load  5     0.0    -397.373  0.0  0.0  0.0  0.0
load  6     0.0    -418.127  0.0  0.0  0.0  0.0
load  7     0.0    -418.127  0.0  0.0  0.0  0.0
load  8     0.0    -418.127  0.0  0.0  0.0  0.0
load  9     0.0    -198.585  0.0  0.0  0.0  0.0
load 13     0.0     -68.98   0.0  0.0  0.0  0.0
load 17     0.0     -76.49   0.0  0.0  0.0  0.0
load 21     0.0     -68.98   0.0  0.0  0.0  0.0
}
constraints Plain

numberer Plain

system BandGeneral

test NormDispIncr 1.0e-8  6

algorithm Newton

integrator LoadControl 1

analysis Static

analyze 1

#Reset time to perform pushover analysis

loadConst -time 0.0


# Create load pattern for horizontal loading
#The 10 kip/ft load should be activated when placing a uniform load of 10 kip/ft in
the longitudinal or transverse direction
#These loads should be used with the initial abutment stiffnesses
#pattern Plain 2 Linear {
# eleLoad -ele $eleTag1 <$eleTag2 ....> -type -beamUniform $Wy $Wz <$Wx>
# eleLoad -ele 1 2 3 4 5 6 7 8 -type beamUniform 0 0 10
#}

#pattern Plain 3 Linear {
# eleLoad -ele $eleTag1 <$eleTag2 ....> -type -beamUniform $Wy $Wz <$Wx>
# eleLoad -ele 1 2 3 4 5 6 7 8 -type beamUniform 0 -10 0
#}

#Transverse seismic loads

pattern Plain 4 Linear {
eleLoad -ele 1 -type beamUniform 0 10.7 0
}

pattern Plain 5 Linear {
eleLoad -ele 1 -type beamUniform 0 10.943 0
}

pattern Plain 6 Linear {
eleLoad -ele 2 -type beamUniform 0 11.208 0
```

```
}

pattern Plain 7 Linear {
eleLoad -ele 2 -type beamUniform 0 11.351 0
}

pattern Plain 8 Linear {
eleLoad -ele 3 -type beamUniform 0 11.352 0
}

pattern Plain 9 Linear {
eleLoad -ele 3 -type beamUniform 0 11.21 0
}

pattern Plain 10 Linear {
eleLoad -ele 4 -type beamUniform 0 10.946 0
}

pattern Plain 11 Linear {
eleLoad -ele 4 -type beamUniform 0 10.703 0
}
# The following eight loading patterns should be activated instead of the previous
eight, when loading in the longitudinal direction

#pattern Plain 12 Linear {
#eleLoad -ele 5 -type beamUniform 0 0 11.205
#}

#pattern Plain 13 Linear {
#eleLoad -ele 5 -type beamUniform 0 0 11.294
#}

#pattern Plain 14 Linear {
#eleLoad -ele 6 -type beamUniform 0 0 11.351
#}

#pattern Plain 15 Linear {
#eleLoad -ele 6 -type beamUniform 0 0 11.375
#}

#pattern Plain 16 Linear {
#eleLoad -ele 7 -type beamUniform 0 0 11.375
#}

#pattern Plain 17 Linear {
#eleLoad -ele 7 -type beamUniform 0 0 11.351
#}

#pattern Plain 18 Linear {
#eleLoad -ele 8 -type beamUniform 0 0 11.294
#}

#pattern Plain 19 Linear {
#eleLoad -ele 8 -type beamUniform 0 0 11.205
#}

constraints Plain

numberer Plain

system BandGeneral

test NormDispIncr  1.0e-8  6
```

```
algorithm Newton

integrator LoadControl 1

analysis Static

analyze 1
```

Determination of Final Soil Spring Stiffness

The final estimations of the bridge transverse and longitudinal abutment stiffness values are accomplished with an iterative process. In the longitudinal direction the backfill behind the abutment wall as well as the embedded piles resist the seismic forces at the ends of the deck. The following procedure is used to achieve a correlation between these.

1. Determine the displacements and OpenSees reactions at the end nodes of the deck.
2. Add the OpenSees reactions from both abutments. This sum is the total longitudinal demand force on an abutment.
3. Determine the force that each pile resists based on the displacements and multiply it by the total number of piles from both abutments.
4. Determine the abutment wall force by subtracting the pile resistance from the total demand on the abutment.
5. Compare the displacement at the end nodes to $0.02H_{aw}$.
    a. If it is greater – the wall force is $7.7A_{aw}$.
    b. If it is smaller – the wall force is calculated by a linear interpolation

$$F = \Delta\left(\frac{7.7A_{aw}}{0.02H_{aw}}\right) \quad \text{(D-6)}$$

        i. F = the wall capacity,
        ii. Δ = the displacement of the end node.
6. Compare the abutment demand to the abutment capacity (i.e., sum of the forces of the piles and the backfill force).
    a. If it is greater, increase abutment stiffness.
    b. If it is smaller, decrease abutment stiffness.
7. Repeat process until the combined backfill force and pile force is within 10% of the value of the longitudinal demand force.

Table D-4. Results of Estimation of Longitudinal Abutment Stiffness

	Longitudinal Displacement (ft)					
Iteration	node 1	node 10	Total Demand (kip)	Total Capacity (kip)	K_l(kip/ft)	Corellation (%)
1	0.0852	0.0852	2931.07	2913.619	17,202	0.5954
2	0.0859	0.0859	2928.49	2925.328	17,042	0.108

The transverse abutment stiffness values depend only on the resistance of the piles in one abutment wall. The procedure is simple because the abutments are similar and there are no wingwalls.

1. Determine the displacements and OpenSees reactions at the end nodes of the deck. The OpenSees reactions are the demand forces on each abutment.
2. Based on the displacements determine the force that one pile resists.
3. Multiply the force that one pile resists by the number of piles in each abutment.
4. Compare the total force that the piles from one abutment resist to the demand.
    a. If it is greater, increase abutment stiffness.
    b. If it is smaller, decrease abutment stiffness.
5. Repeat procedure until the pile resistance is within 10% of the abutment demand.

Table D-5. Results of Estimation of Transverse Abutment Stiffness

	Transverse Displacement (ft)		Demand (kip)				
Iteration	node 1	node 10	node 22	node 23	Total Capacity (kip)	K_t (kip/ft)	Correlation (%)
1	0.2082	0.2082	1149.01	1149.45	768	5,520	33.19
2	0.2312	0.2313	1109.73	1110.17	808	4,800	27.22
3	0.2636	0.2637	1054.44	1054.88	872	4,000	17.34
4	0.3066	0.3067	981.132	981.551	936	3,200	4.64

The final estimation for the abutment stiffness values are

K_l = 17,042 kips/ft Longitudinal abutment stiffness

K_t = 3,200 kips/ft Transverse abutment stiffness

As a check, the final abutment stiffness values were used in the OpenSees program with the uniformly distributed load used for calculating the seismic loads to see how the new stiffness

values would affect the calculation of the seismic loads. The results are shown in the Tables D-6 and D-7. The difference in the transverse values was less than 2% and the difference in the longitudinal values was less than 0.01%. The final stiffness values were softer than the initial values and this produced less of a difference in the seismic forces from the end of the deck to the center so that the characteristic trapezoidal shape of the seismic forces was flatter than before.

Table D-6. Comparison of Updated and Original Longitudinal Design Loads

Updated Design Loads (kip/ft)	Original Design Loads (kip/ft)
11.162	11.161
11.290	11.29
11.370	11.37
11.402	11.403
11.402	11.403
11.370	11.37
11.290	11.29
11.162	11.161

Table D-7. Comparison of Updated and Original Transverse Design Loads

Updated Design Loads (kip/ft)	Original Design Loads (kip/ft)
10.914	10.7
11.022	10.943
11.123	11.208
11.162	11.351
11.163	11.352
11.126	11.21
11.025	10.946
10.917	10.703

Linear-elastic Analysis Results

Tables D-8 and D-9 show the displacements and column base reactions for the longitudinal and transverse directions, respectively.

Table D-8. Displacements and Column Base Reactions for Seismic Loads in the Longitudinal Direction

Nodes	Displacement (ft.)
Deck	
1	0.08589
2	0.08707
3	0.08788
4	0.08832
5	0.08838
6	0.08832
7	0.08788
8	0.08707
9	0.08589
Top of the Columns	
12	0.08195
16	0.08195
20	0.08195

Columns	Shear (k)	Axial (k)	Moment (k-ft)
1	-87.578	752.152	1297.780
2	-87.578	752.152	1297.780
3	-87.578	752.152	1297.780

Table D-9. Displacements and Column Base Reactions for Seismic Loads in the Transverse Direction

Nodes	Displacement (ft.)
Deck	
1	0.30660
2	0.30909
3	0.31297
4	0.31512
5	0.31539
6	0.31518
7	0.31307
8	0.30921
9	0.30674
Top of the Columns	
12	0.31494
16	0.31539
20	0.31494

Columns	Shear (k)	Axial (k)	Moment (k-ft)
1	-385.104	752.175	-5434.940
2	-385.650	752.136	-5442.630
3	-385.105	752.097	-5434.940

The drift in the longitudinal and transverse directions for top of the columns are shown in Table D-10.

Table D-10. Calculated Drift for Top of the Columns

Node	12	16	20
Long. drift (%)	0.3195	0.3195	0.3195
Trans. drift (%)	1.2280	1.2298	1.2280

Nonlinear CIP Model of the Structure

The non-linear model of the bridge superstructure and the column bent is the same as that of the linear elastic model. The columns are modeled with a nonlinearBeamColumn and a fiber section which describes the dimensions and properties of the reinforcing steel in the column. Additionally a zeroLength element is placed at the top and bottom of the columns to model bond-slip at the column-footing and column-bent interfaces and the footing is removed from the model.

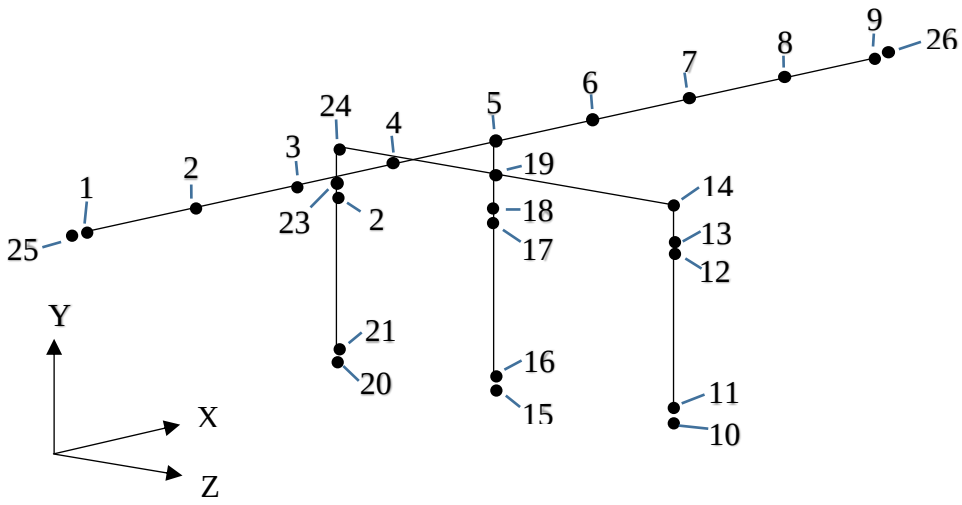

Figure D-9. Nonlinear cast-in-place bridge model with node numbers

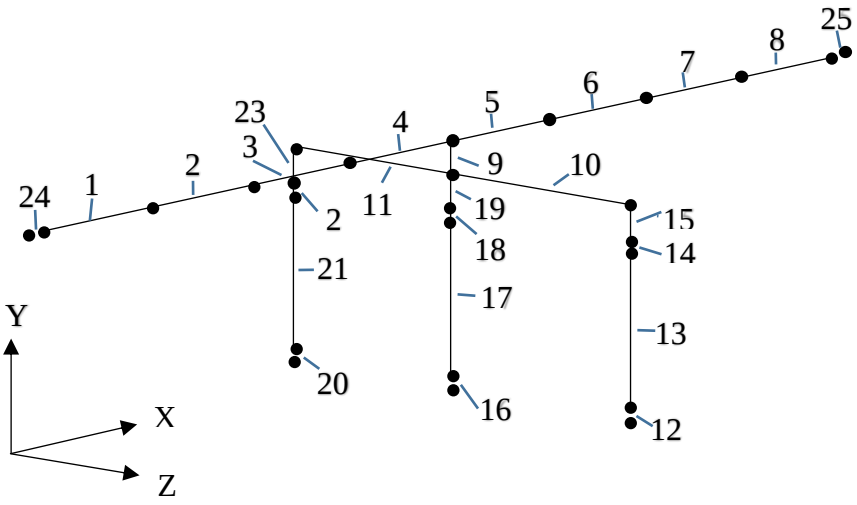

Figure D-10. Nonlinear cast-in-place bridge model with element numbers

The following dimensions are required for modeling the fiber section.

d_{r14} = 1.693 in = 0.141083 ft Diameter of a #14 reinforcing bar

d_s = 0.625”	Diameter of spiral reinforcing
R_{14} = 1.502 ft	Distance from the center of the column to the center of the #14 bars

An illustration of the OpenSees model of the nonlinear fiber section can be seen in the Figure D-11.

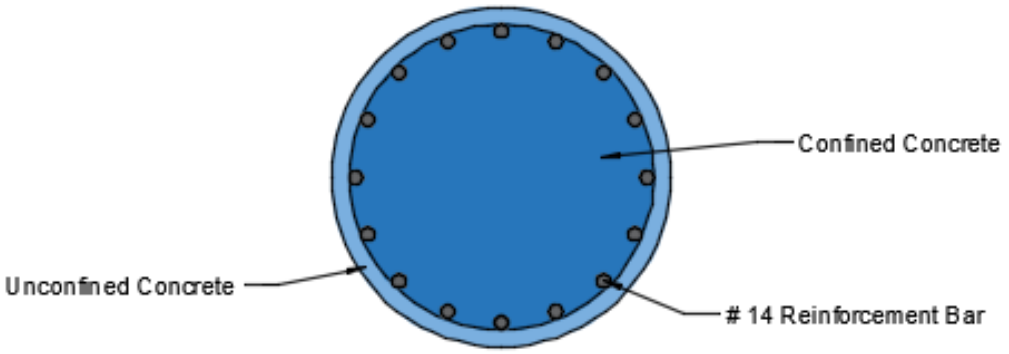

Figure D-11. Nonlinear Fiber Section

Material Properties

Unconfined Concrete

As previously determined the modulus of elasticity, *E*, and the modulus of rigidity, *G*, for cast-in-place concrete are:

E_{CIP} = 3,644 ksi = 524,736 ksf	Modulus of elasticity of cast-in-place concrete
G_{CIP} = 218,640 ksf	Modulus of rigidity of cast-in-place concrete

Peak strain for 4000 psi concrete is 0.002 and ultimate strain is 0.005.

Reinforcing Steel

The grade of the steel is specified in the plans. For the Parma Bridge the steel is Grade 60. The following properties are found in Table 8.4.2-1 in the AASHTO *Guide Specifications for LRFD Seismic Bridge Design*, 2011, Sec. 8-4.

f_y = 68 ksi = 9,792 ksf

f_u = 95 ksi = 13,680 ksf

The strain for a #14 bar at strain hardening is

e_{sh} = 0.0075

The ultimate strain is

e_u = 0.09

The modulus of elasticity for steel is

E = 29,000 ksi = 4,176,000 ksf

The slope of the line at strain hardening is

E_{sh} = 1247 ksi = 179,568 ksf

Confined Concrete Strength Using Theoretical Stress-Strain Model Developed by Mander et al.

AASHTO Guide Specifications for LRFD Seismic Bridge Design, 2011, Sec. 8.4.4, Concrete Modeling, specifies that confined concrete should be modeled based on Mander's stress-stain model. It also indicates in equation (8.4.4-1) that the compressive strength of confined concrete could be estimated by $f'_{ce} \geq 1.3 f'_c$.

From Mander, et al. (1988a) the compressive strength of confined concrete in a circular column was determined by equation 29:

$$f'_{cc} = f'_{co}\left(-1.254 + 2.254\sqrt{1 + \frac{7.94 f'_l}{f'_{co}}} - 2\frac{f'_l}{f'_{co}}\right) \quad \text{(D-7)}$$

Where:

f'_{cc} = The confined compressive strength of concrete,

f'_{co}=The unconfined compressive strength of concrete = 4.0 ksi, and

f'_l= The lateral pressure from the transverse reinforcement and is given by equation 19.

$$f'_l = \frac{1}{2} k_e \rho_s f_{yh} \quad \text{(D-8)}$$

Where:

k_e= The Confinement Effectiveness Coefficient given by equation 15,

ρ_s=The ratio of the volume of transverse confining steel to the volume of the confined concrete core, defined by equation 17, and

f_{yh}= The yield strength of the horizontal reinforcing = 68 ksi.

The Confinement Effectiveness Coefficient for circular spirals is:

$$k_e = \frac{1-\frac{s'}{2d_s}}{1-\rho_{cc}} \quad \text{(D-9)}$$

Where:

s'= The clear vertical spacing between spirals = 2.375 in,

d_s=The diameter of spirals between bar centers = 37.307 in, and

ρ_{cc} =The ratio of the area of the longitudinal steel to the area of the confined concrete.

The ratio of the volume of transverse confining steel to the volume of confined concrete core can be determined by:

$$\rho_s = \frac{4A_{sp}}{d_s s} \quad \text{(D-10)}$$

Where:

A_{sp}=The area of the transverse reinforcing bar = 0.3068 in^2 and

s=The center to center spacing between spirals, or pitch = 3 in.

The ratio of the area of the longitudinal steel to the area of the confined concrete (ρ_{cc}) can be given by:

$$\rho_{cc} = \frac{A_{st}}{A_c} \quad \text{(D-11)}$$

Where:

A_{st}= The area of longitudinal steel = 36 in^2 and

A_c= Area of the core of the section enclosed by the center lines of the perimeter

spiral = 1,093 in^2.

In summary:

ρ_s = 0.011

ρ_{cc} = 0.0329

k_e = 1.0011

f'_l = 0.3622 ksi

f'_{cc} = 6.08 ksi = 875.6 ksf

The strain at maximum strength can be calculated by equation 5:

$$\varepsilon_{cc} = \varepsilon_{co}\left[1 + 5\left(\frac{f'_{cc}}{f'_{co}} - 1\right)\right] \quad \text{(D-12)}$$

Where:

ε_{co} = The strain at maximum strength of unconfined concrete = 0.002.

ε_{cc} = 0.0072

From Paulay and Priestley (1992) the ultimate strain ε_{cu} is defined as the strain at the first fracture of the transverse reinforcement. The following equation can be used to calculate ε_{cu}.

$$\varepsilon_{cu} = 0.004 + \frac{1.4\rho_s f_{yh}\varepsilon_{sm}}{f'_{cc}} \quad \text{(D-13)}$$

Where:

ε_{sm} = The strain of the transverse reinforcement at peak stress = 0.09

ε_{cu} = 0.019

Modeling Bond-slip

To model the bond-slip of the reinforcing steel at the interfaces between the footing and column and the bent and the column a zeroLength element with hysteretic material properties is used. The uniaxialMaterial Hysteretic command in OpenSees requires values from a moment-curvature analysis of the cross-section of the column. A zeroLength element with the same cross-section as that of the reinforced column was created in a separate tcl file to analyze the material's behavior. An axial load equal to the average axial load seen by the columns and a moment of 1 kip-in was applied to the element. The stresses and strains in the reinforcing steel on the tension and compression side of the section as well as the concrete at the same location were recorded. The reaction was also recorded. The slip can be calculated using equations from Section 8.2.3.1 in the Haber report.

$$\delta_{slip} = \begin{cases} \frac{\varepsilon_s L_1}{2} & if \;\; \varepsilon_s \le \varepsilon_y \\ \frac{\varepsilon_y L_1}{2} + \frac{(\varepsilon_s + \varepsilon_y)L_2}{2} & if \;\; \varepsilon_s > \varepsilon_y \end{cases} \quad \text{(D-14)}$$

Where:

ε_s = strain in the reinforcing steel on the tension side of the column

ε_y = yield strain of the reinforcing steel

L_1 and L_2 can be determined by

$$L_1 = \frac{f_s d_b}{4u} \quad \text{(D-15)}$$

$$L_2 = \frac{(f_s - f_y) d_b}{4u} \quad \text{(D-16)}$$

Where:

f_s = stress in the reinforcing steel on the tension side of the column

f_y = maximum stress of the reinforcing steel

d_b = diameter of one reinforcing bar

u can be calculated by

$$u = \frac{9.5\sqrt{f'_c}}{d_b} \leq 800\ psi \quad \text{(D-17)}$$

Where:

f'_c = the compressive strength of concrete

Once the slip is found the rotation of the column that corresponds to each moment is calculated by

$$\theta_{slip} = tan^{-1}\left(\frac{\delta_{slip}}{c-d}\right) \quad \text{(D-18)}$$

Where:

c = neutral axis location determined from moment-curvature analysis

d = column diameter

A graph of the moment vs. rotation with an idealized bilinear curve for the Parma Bridge is shown in Figure D-12.

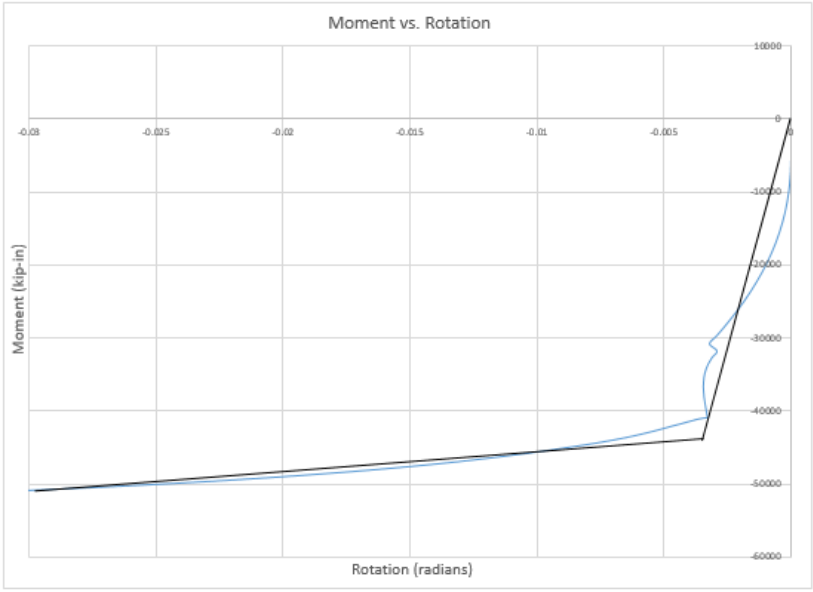

Figure D-12. Moment vs. Rotation

The uniaxialMaterial Hysteretic command in OpenSees requires the stress and strain at the first point of inflection and the ultimate stress and strain on the bilinear approximation of the moment-rotation curve. These values are

s1p = 3583 k.ft Moment at the first point of the envelope in the positive direction

e1p = 0.0035 Angle at the first point of the envelope in the positive direction

s2p = 4239 k.ft Moment at the second point of the envelope in the positive direction

e2p = 0.03 Angle at the second point of the envelope in the positive direction

Because of the symmetry of the column the moments and rotations in the negative direction are the same as those in the positive direction.

Moment-curvature OpenSees tlc Script

```
#Clear cached data existing in the program

wipe

#Values in kips and feet

#Create Model with 2 dimensions and 3 degrees of freedom

model BasicBuilder -ndm 2 -ndf 3

#Create 3 DOF nodes

#       tag   x     y
```

```
node     1    0.0   0.0
node     2    0.0   0.0

#Fix node 1 in all DOF and node 2 in the y direction

fix  1  1  1  1

fix  2  0  1  0


#Create uniaxial materials for Concrete and Steel

# uniaxialMaterial Concrete01 $matTag $fpc $epsc0 $fpcu $epsU

uniaxialMaterial Concrete01  1  -4.0  -0.002  0  -0.005

# uniaxialMaterial Concrete04 $matTag $fc $ec $ecu $Ec <$ft $et> <$beta>

uniaxialMaterial Concrete04  2  -6.08   -0.0072  -0.019  3644

# uinaxialMaterial ReinforcingSteel $matTag $fy $fu $Es $Esh $esh $eult

uniaxialMaterial ReinforcingSteel  3  68   95   29000   1247   0.0075   0.09


#Create fiber section with Defined Concrete and Rebar

section Fiber  1  {
#patch circ $matTag $numSubdivCirc $numSubdivRad $yCenter $zCenter $intRad $extRad
<$startAng endAng>
patch circ 2  44  10  0  0  0  18.875  0  360
patch circ 1 44 2  0  0  18.875 21 0  360
#layer circ $matTag $numBar $areaBar $yCenter $zCenter $radius <$startAng $endAng>
layer circ 3  16  2.25  0  0  18.0285 0 360
}

#Create zero length element between nodes 1 and 2

element zeroLengthSection 1  1  2  1


#Set up time series

timeSeries Linear 1

#Create recorder files: displacements and reactions

recorder Node  -file MomentSection1Corrected-Parma.out -node 1 -dof 3 reaction
recorder Element  -file TensionStrainCorrected_steel-Parma.out -ele 1 section fiber -
18.0285 0 3 stressStrain
recorder Element  -file TensionStrainCorrected_concrete-Parma.out -ele 1 section fiber
-18.0285 0 2 stressStrain
recorder Element  -file CompressiveStrainCorrected-steel-Parma.out -ele 1 section
fiber 18.0285 0 3 stressStrain
recorder Element  -file CompressiveStrainCorrected-concrete-Parma.out -ele 1 section
fiber 18.0285 0 2 stressStrain


pattern Plain 1 Constant {
load 2  -622  0  0
}

integrator LoadControl 0.0
```

```
system SparseGeneral -piv
test NormUnbalance 1.0e-9 10
numberer Plain
constraints Plain
algorithm Newton
analysis Static
analyze 1


pattern Plain 2 Linear {
load 2 0.0 0.0 -1.0
}

integrator DisplacementControl 2 3 0.000005
analyze 500
```

Nonlinear Cast-in-place OpenSees tlc Script for Seismic Load in Transverse Direction

```
#Two-span Bridge on US95 at Parma, Idaho

wipe

#Create model with 3 dimensions and 6 DOF

model BasicBuilder -ndm 3 -ndf 6

#Units are kips and feet

#Create 6 DOF nodes

#Superstructure nodes
#       tag          x             y            z

node     1          0.0         34.459         0.0
node     2        35.275        34.459         0.0
node     3        70.549        34.459         0.0
node     4       105.824        34.459         0.0
node     5       141.009        34.459         0.0
node     6       176.374        34.459         0.0
node     7       211.648        34.459         0.0
node     8       246.914        34.459         0.0
node     9       282.179        34.459         0.0

#Substructure nodes

node    10       141.009         0.0          15.322
node    11       141.009         0.0          15.322
node    12       141.009        25.646        15.322
node    13       141.009        25.646        15.322
node    14       141.009        28.347        15.322
node    15       141.009         0.0           0.0
node    16       141.009         0.0           0.0
node    17       141.009        25.646         0.0
node    18       141.009        25.646         0.0
node    19       141.009        28.347         0.0
node    20       141.009         0.0         -15.322
node    21       141.009         0.0         -15.322
node    22       141.009        25.646       -15.322
node    23       141.009        25.646       -15.322
node    24       141.009        28.347       -15.322
```

```
#Spring support nodes

node    25         0.0         34.459         0.0
node    26       282.179       34.459         0.0

#Specify geometric transformation

geomTransf Linear 1  0  0  1
geomTransf Linear 2 -1  0  0
geomTransf PDelta 3  0  0  1

# Fix column bases and abutments in all DOF's

fix 25 1 1 1 1 1 1
fix 26 1 1 1 1 1 1
fix 10 1 1 1 1 1 1
fix 15 1 1 1 1 1 1
fix 20 1 1 1 1 1 1

#Create uniaxial materials for concrete and steel

# uniaxialMaterial Concrete01 $matTag $fpc $epsc0 $fpcu $epsU

uniaxialMaterial Concrete01  1  -576.0  -0.002  0  -0.005

# uniaxialMaterial Concrete04 $matTag $fc $ec $ecu $Ec <$ft $et> <$beta>

uniaxialMaterial Concrete04 2  -875.6  -0.0072  -0.019  524736

# uinaxialMaterial ReinforcingSteel $matTag $fy $fu $Es $Esh $esh $eult

uniaxialMaterial ReinforcingSteel  3  9792  13680  4176000  179568  0.0075  0.09

#Create hysteretic uniaxial material to model bond-slip

# uniaxialMaterial Hysteretic $matTag $s1p $e1p $s2p $e2p $s1n $e1n $s2n $e2n $pinchX
$pinchY $damage1 $damage2 <$beta>

uniaxialMaterial Hysteretic 4  3583  .0035  4239  .03  -3583  -0.0035   -4239.0  -.03
1  1  0  0  0.35

uniaxialMaterial Elastic 5  1e12

#Create fiber section with Defined Concrete and Rebar

section Fiber  1  {
#patch circ $matTag $numSubdivCirc $numSubdivRad $yCenter $zCenter $intRad $extRad
<$startAng endAng>
patch circ 2  44  10  0  0  0  1.573  0  360
patch circ 1 44 2  0  0  1.573 1.75 0  360
#layer circ $matTag $numBar $areaBar $yCenter $zCenter $radius <$startAng $endAng>
layer circ 3  16  0.015625  0  0  1.502 0 360
}

# Define shear stiffness (GJ) elastic material

set Gc 218640
set Jc  2.95
set GJ [expr $Gc*$Jc]
uniaxialMaterial Elastic 6  $GJ

section Aggregator 2  6 T -section  1
```

```
# Create deck elements

# element elasticBeamColumn $eleTag $iNode $jNode $A $E $G $J $Iy $Iz $transfTag

element elasticBeamColumn 1  1  2  49.60  765269.3  318862.2  1e10  7493.7  242.06  1
element elasticBeamColumn 2  2  3  49.60  765269.3  318862.2  1e10  7493.7  242.06  1
element elasticBeamColumn 3  3  4  49.60  765269.3  318862.2  1e10  7493.7  242.06  1
element elasticBeamColumn 4  4  5  49.60  765269.3  318862.2  1e10  7493.7  242.06  1
element elasticBeamColumn 5  5  6  49.60  765269.3  318862.2  1e10  7493.7  242.06  1
element elasticBeamColumn 6  6  7  49.60  765269.3  318862.2  1e10  7493.7  242.06  1
element elasticBeamColumn 7  7  8  49.60  765269.3  318862.2  1e10  7493.7  242.06  1
element elasticBeamColumn 8  8  9  49.60  765269.3  318862.2  1e10  7493.7  242.06  1

# Create pier bent elements

element elasticBeamColumn  9  5 19  196.00   524736  218640  1e10  1e10  1e10  3
element elasticBeamColumn 10 14 19   25.23   524736  218640  1e10  1e10  60.9  2
element elasticBeamColumn 11 19 24   25.23   524736  218640  1e10  1e10  60.9  2

# Create column elements

# element nonlinearBeamColumn $eleTag $iNode $jNode $numintgrPts $secTag $transfTag
# element zeroLength $eleTag $iNode $jNode -mat $matTag1 $matTag2 ... -dir $dir1 $dir2
...

element zeroLength 12 10  11 -mat 5 5 5 4 4 4 -dir 1 2 3 4 5 6
element nonlinearBeamColumn 13 11 12 9 2 3
element zeroLength 14  12  13 -mat 5 5 5 4 4 4 -dir 1 2 3 4 5 6
element elasticBeamColumn 15  13  14  1e10  524736  218640  1e10  1e10  1e10  3
element zeroLength 16  15  16 -mat 5 5 5 4 4 4 -dir 1 2 3 4 5 6
element nonlinearBeamColumn 17  16  17 9 2 3
element zeroLength 18  17  18 -mat 5 5 5 4 4 4 -dir 1 2 3 4 5 6
element elasticBeamColumn 19  18  19  1e10  524736  218640  1e10  1e10  1e10  3
element zeroLength 20  20  21 -mat 5 5 5 4 4 4 -dir 1 2 3 4 5 6
element nonlinearBeamColumn 21  21  22 9 2 3
element zeroLength 22  22  23 -mat 5 5 5 4 4 4 -dir 1 2 3 4 5 6
element elasticBeamColumn 23  23  24  1e10  524736  218640  1e10  1e10  1e10  3

# Create spring elements

uniaxialMaterial Elastic 7 17.202e3;   # Translational stiffness along X axis of the
abutments, kip/ft
uniaxialMaterial Elastic 8 1e12;   # Translational stiffness along Y axis of the
abutments, kip/ft
uniaxialMaterial Elastic 9 3.2e3;   # Translational stiffness along Z axis of the
abutments, kip/ft
uniaxialMaterial Elastic 10 1e12;   # Rotational stiffness about X axes o10f the
abutments, kip.ft/radian
uniaxialMaterial Elastic 11 1e12;      # Rotational stiffness about Y axis of the
abutments, kip.ft/radian
uniaxialMaterial Elastic 12 0;      # Rotational stiffness about the Z axis of the
abutment, kip.ft/radian


# Spring elements using above stiffness values
# element zeroLength $eleTag $iNode $jNode -mat $matTag1 $matTag2 ... -dir $dir1 $dir2
...

element zeroLength 24 25  1 -mat 7 8 9 10 11 12 -dir 1 2 3 4 5 6
element zeroLength 25  9 26 -mat 7 8 9 10 11 12 -dir 1 2 3 4 5 6

# Create recorder files
```

```
recorder Node -file Nodes1-9_NonLin_Disp_Long_Parma.out -time -nodeRange 1 9 -dof 1
disp
recorder Node -file Nodes1-9_NonLin_Disp_Trans_Parma.out -time -nodeRange 1 9 -dof 3
disp
recorder Node -file Column_1_Reaction_Parma.out -time -node 10 -dof 1 2 3 4 5 6
reaction
recorder Node -file Column_2_Reaction_Parma.out -time -node 15 -dof 1 2 3 4 5 6
reaction
recorder Node -file Column_3_Reaction_Parma.out -time -node 20 -dof 1 2 3 4 5 6
reaction

# Assign gravity loads

pattern Plain 1 Constant {
#    tag    FX       FY      FZ   MX   MY   MZ
load  1     0.0    -198.585  0.0  0.0  0.0  0.0
load  2     0.0    -418.127  0.0  0.0  0.0  0.0
load  3     0.0    -418.127  0.0  0.0  0.0  0.0
load  4     0.0    -418.127  0.0  0.0  0.0  0.0
load  5     0.0    -397.373  0.0  0.0  0.0  0.0
load  6     0.0    -418.127  0.0  0.0  0.0  0.0
load  7     0.0    -418.127  0.0  0.0  0.0  0.0
load  8     0.0    -418.127  0.0  0.0  0.0  0.0
load  9     0.0    -198.585  0.0  0.0  0.0  0.0
load 14     0.0     -68.98   0.0  0.0  0.0  0.0
load 19     0.0     -76.49   0.0  0.0  0.0  0.0
load 24     0.0     -68.98   0.0  0.0  0.0  0.0
}

constraints Plain

numberer Plain

system BandGeneral

test NormDispIncr 1.0e-8  6

algorithm Newton

integrator LoadControl 1

analysis Static

analyze 1

#Reset time to perform pushover analysis

loadConst -time 0.0

# Create horizontal load patterns
# Transverse seismic loads

pattern Plain 4 Linear {
# eleLoad -ele $eleTag1 <$eleTag2 ....> -type -beamUniform $Wy $Wz <$Wx>
eleLoad -ele 1 -type beamUniform 0 10.7 0
}

pattern Plain 5 Linear {
# eleLoad -ele $eleTag1 <$eleTag2 ....> -type -beamUniform $Wy $Wz <$Wx>
eleLoad -ele 2 -type beamUniform 0 10.943 0
}
```

```
pattern Plain 6 Linear {
# eleLoad -ele $eleTag1 <$eleTag2 ....> -type -beamUniform $Wy $Wz <$Wx>
eleLoad -ele 3 -type beamUniform 0 11.208 0
}

pattern Plain 7 Linear {
# eleLoad -ele $eleTag1 <$eleTag2 ....> -type -beamUniform $Wy $Wz <$Wx>
eleLoad -ele 4 -type beamUniform 0 11.351 0
}

pattern Plain 8 Linear {
# eleLoad -ele $eleTag1 <$eleTag2 ....> -type -beamUniform $Wy $Wz <$Wx>
eleLoad -ele 5 -type beamUniform 0 11.352 0
}

pattern Plain 9 Linear {
# eleLoad -ele $eleTag1 <$eleTag2 ....> -type -beamUniform $Wy $Wz <$Wx>
eleLoad -ele 6 -type beamUniform 0 11.21 0
}

pattern Plain 10 Linear {
# eleLoad -ele $eleTag1 <$eleTag2 ....> -type -beamUniform $Wy $Wz <$Wx>
eleLoad -ele 7 -type beamUniform 0 10.946 0
}

pattern Plain 11 Linear {
# eleLoad -ele $eleTag1 <$eleTag2 ....> -type -beamUniform $Wy $Wz <$Wx>
eleLoad -ele 8 -type beamUniform 0 10.703 0
}

# The following eight loading patterns should be activated instead of the previous
eight, when loading in the longitudinal direction


#pattern Plain 12 Linear {
# eleLoad -ele $eleTag1 <$eleTag2 ....> -type -beamUniform $Wy $Wz <$Wx>
#eleLoad -ele 1 -type beamUniform 0 0 11.205
#}

#pattern Plain 13 Linear {
# eleLoad -ele $eleTag1 <$eleTag2 ....> -type -beamUniform $Wy $Wz <$Wx>
#eleLoad -ele 2 -type beamUniform 0 0 11.294
#}

#pattern Plain 14 Linear {
# eleLoad -ele $eleTag1 <$eleTag2 ....> -type -beamUniform $Wy $Wz <$Wx>
#eleLoad -ele 3 -type beamUniform 0 0 11.351
#}

#pattern Plain 15 Linear {
# eleLoad -ele $eleTag1 <$eleTag2 ....> -type -beamUniform $Wy $Wz <$Wx>
#eleLoad -ele 4 -type beamUniform 0 0 11.375
#}

#pattern Plain 16 Linear {
# eleLoad -ele $eleTag1 <$eleTag2 ....> -type -beamUniform $Wy $Wz <$Wx>
#eleLoad -ele 5 -type beamUniform 0 0 11.375
#}

#pattern Plain 17 Linear {
# eleLoad -ele $eleTag1 <$eleTag2 ....> -type -beamUniform $Wy $Wz <$Wx>
#eleLoad -ele 6 -type beamUniform 0 0 11.351
#}
```

```
#pattern Plain 18 Linear {
# eleLoad -ele $eleTag1 <$eleTag2 ....> -type -beamUniform $Wy $Wz <$Wx>
#eleLoad -ele 7 -type beamUniform 0 0 11.294
#}

#pattern Plain 19 Linear {
# eleLoad -ele $eleTag1 <$eleTag2 ....> -type -beamUniform $Wy $Wz <$Wx>
#eleLoad -ele 8 -type beamUniform 0 0 11.205
#}

constraints Plain

numberer RCM

system BandSPD

algorithm Linear

integrator LoadControl 0.01

analysis Static

analyze 100
```

Nonlinear CIP Model Analysis Results

Tables D-11 and D-12 show the displacements and column base reactions for the longitudinal and transverse directions, respectively.

Table D-11. Displacements and Column Base Reactions for Seismic Loads in the Longitudinal Direction

Nodes	Displacement (ft.)
Deck	
1	0.08509
2	0.08626
3	0.08705
4	0.08748
5	0.08753
6	0.08748
7	0.08706
8	0.08626
9	0.08509
Top of the Columns	
12	0.08061
17	0.08061
22	0.08061

Columns	Shear (k)	Axial (k)	Moment (k-ft)
1	-96.663	752.384	1347.070
2	-96.663	752.384	1347.070
3	-96.663	752.384	1347.070

Table D-12. Displacements and Column Base Reactions for Seismic Loads in the Transverse Direction

Nodes	Displacement (ft.)
Deck	
1	0.35992
2	0.36349
3	0.36976
4	0.37430
5	0.37565
6	0.37435
7	0.36984
8	0.36358
9	0.36002
Top of the Columns	
12	0.37534
17	0.37565
22	0.37534

Columns	Shear (k)	Axial (k)	Moment (k-ft)
1	-271.576	753.687	-3623.890
2	-271.585	753.865	-3624.150
3	-271.577	753.672	-3623.890

The drift in the longitudinal and transverse directions for top of the columns are as shown in Table D-13.

Table D-13. Calculated Drift for Top of the Columns

Node	12	17	22
Long. drift (%)	0.3143	0.3143	0.3143
Trans. drift (%)	1.4635	1.4647	1.4635

Nonlinear Model of Structure with Grouted Couplers

The grouted couplers are modeled as separate elements within the columns. They are located at the top and bottom of each column. In addition to the zeroLength elements that model bond slip a second zeroLength element with the same section as the part of the column without couplers was added to the top and bottom of each column to observe the behavior of the materials immediately beyond the coupler region. The zeroLength elements that are located in the same place share the same nodes. The node and element placement can be seen in Figures D-13 and D-14.

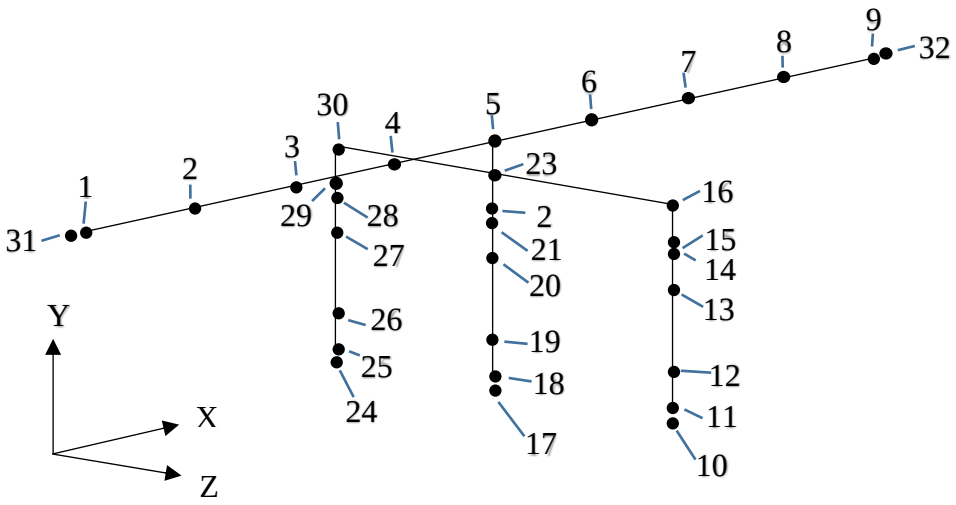

Figure D-13. Nonlinear bridge model with grouted couplers with node numbers

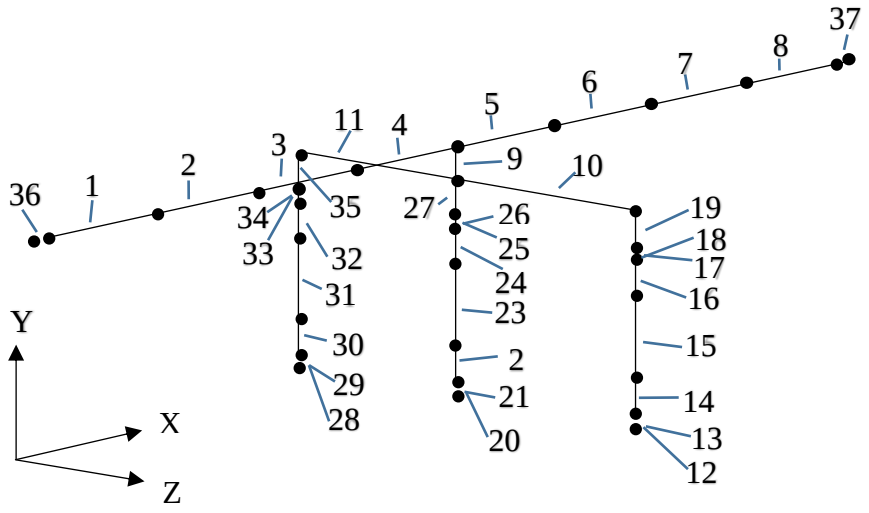

Figure D-14. Nonlinear bridge model with grouted couplers with element number

Material Properties of Grouted Couplers

The material properties of the grouted couplers were obtained from the manufacturer, Splice Sleeve North America (SSNA). The following values apply to the SSNA No. 14 U-X Grouted Coupler which is used for a #14 reinforcing bar.

$A_{coupler}$ = 9.449 in^2	cross-sectional area of coupler
$L_{coupler}$ = 2.034 ft	length of coupler
f_y = 9312.5 ksf	yield stress of the coupler
f_u = 13186.1 ksf	ultimate stress at fracture
E_s = 5707497.6 ksf	modulus of elasticity of coupler
E_{sh} = 378000 ksf	slope of the stress-strain curve at strain hardening
e_{sh} = 0.0019	strain at strain hardening
e_{ult} = 0.0185	ultimate strain

Coupler Section

To model the behavior of the couplers within the columns an area equal to the cross-sectional area of the coupler was left empty where each coupler was located. The couplers were modeled with the same cross-sectional area as the #14 bars but having the material properties listed above. This prevented the material properties of the concrete from affecting the behavior of the couplers. The column cross-section is modeled in OpenSees as seen in Figure D-15.

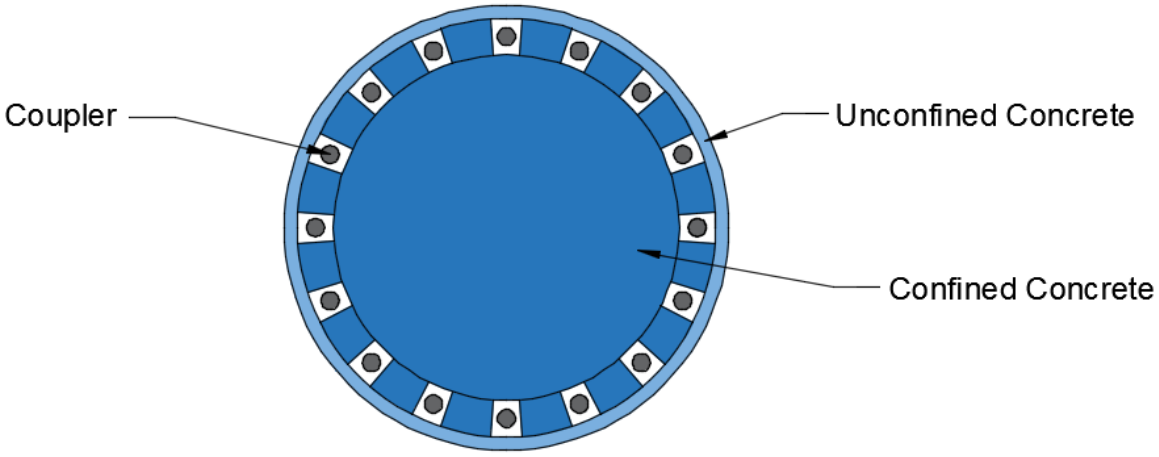

Figure D-15. OpenSees model of column cross-section with couplers

Nonlinear Grouted Coupler OpenSees tlc Script for Seismic Loads is Transverses Direction

```
#Two-span Bridge on US95 at Parma, Idaho, with grouted couplers at the top and bottom
of each column

wipe

#Create model with 3 dimensions and 6 DOF

model BasicBuilder -ndm 3 -ndf 6

#Units are kips and feet

#Create 6 DOF nodes

#Superstructure nodes
#       tag         x             y            z

node     1          0.0         34.459         0.0
node     2         35.275       34.459         0.0
node     3         70.549       34.459         0.0
node     4        105.824       34.459         0.0
node     5        141.009       34.459         0.0
node     6        176.374       34.459         0.0
node     7        211.648       34.459         0.0
node     8        246.914       34.459         0.0
node     9        282.179       34.459         0.0

#Substructure nodes
#       tag         x             y            z

node    10       141.009        0.0          15.322
node    11       141.009        0.0          15.322
node    12       141.009        2.034        15.322
node    13       141.009       23.612        15.322
node    14       141.009       25.646        15.322
node    15       141.009       25.646        15.322
node    16       141.009       28.347        15.322
node    17       141.009        0.0           0.0
node    18       141.009        0.0           0.0
node    19       141.009        2.034         0.0
node    20       141.009       23.612         0.0
node    21       141.009       25.646         0.0
node    22       141.009       25.646         0.0
node    23       141.009       28.347         0.0
node    24       141.009        0.0         -15.322
node    25       141.009        0.0         -15.322
node    26       141.009        2.034       -15.322
node    27       141.009       23.612       -15.322
node    28       141.009       25.646       -15.322
node    29       141.009       25.646       -15.322
node    30       141.009       28.347       -15.322

#Spring support nodes at the abutments

node    31          0.0         34.459         0.0
node    32        282.179       34.459         0.0

#Specify geometric transformation

geomTransf Linear 1  0  0  1
```

```
geomTransf Linear 2 -1  0  0
geomTransf PDelta 3  0  0  1

#Fix column bases and abutments in all DOF's

fix 31 1 1 1 1 1 1
fix 32 1 1 1 1 1 1
fix 10 1 1 1 1 1 1
fix 17 1 1 1 1 1 1
fix 24 1 1 1 1 1 1

#Create uniaxial materials for concrete and steel and zeroLength elements in the
columns

#uniaxialMaterial Concrete01 $matTag $fpc $epsc0 $fpcu $epsU

uniaxialMaterial Concrete01  1  -576.0  -0.002  0  -0.005

#uniaxialMaterial Concrete04 $matTag $fc $ec $ecu $Ec <$ft $et> <$beta>

uniaxialMaterial Concrete04 2  -875.6  -0.0072  -0.019  524736

#uinaxialMaterial ReinforcingSteel $matTag $fy $fu $Es $Esh $esh $eult

uniaxialMaterial ReinforcingSteel  3  9792  13680  4176000  179568  0.0075  0.09

uniaxialMaterial ReinforcingSteel  4  9312.5  13186.1  5707497.6  378000  0.0019
0.0185

#uniaxialMaterial Hysteretic $matTag $s1p $e1p $s2p $e2p $s1n $e1n $s2n $pinchX
$pinchY $damage1 $damage2 <beta>

uniaxialMaterial Hysteretic 5 3583 .0035  4239.0  .03  -3583  -0.0035   -4239.0  -.03
1  1  0  0  0.35

uniaxialMaterial Elastic 6  1e12

#Create fiber sections with Defined Concrete and Rebar

#for CIP column section

section Fiber  1  {
#patch circ $matTag $numSubdivCirc $numSubdivRad $yCenter $zCenter $intRad $extRad
<$startAng endAng>
patch circ 2  44  10  0  0  0  1.573  0  360
patch circ 1 44 2  0  0  1.573 1.75 0  360
#layer circ $matTag $numBar $areaBar $yCenter $zCenter $radius <$startAng $endAng>
layer circ 3  16  0.015625  0  0  1.502 0 360
}

#for grouted coupler section

section Fiber  2  {
#patch circ $matTag $numSubdivCirc $numSubdivRad $yCenter $zCenter $intRad $extRad
<$startAng endAng>
patch circ 2  44  10  0  0  0  1.360  0  360
patch circ 1 44 2  0  0  1.647 1.75 0  360
patch circ 2  44  1  0  0  1.360  1.647 4.353 18.148
patch circ 2  44  1  0  0  1.360  1.647 26.853 40.648
patch circ 2  44  1  0  0  1.360  1.647 49.353 63.148
patch circ 2  44  1  0  0  1.360  1.647 71.853 85.648
patch circ 2  44  1  0  0  1.360  1.647 94.353 108.148
patch circ 2  44  1  0  0  1.360  1.647 116.853 130.648
```

```
patch circ 2  44  1  0  0  1.360  1.647 139.353 153.148
patch circ 2  44  1  0  0  1.360  1.647 161.853 175.648
patch circ 2  44  1  0  0  1.360  1.647 184.353 198.148
patch circ 2  44  1  0  0  1.360  1.647 206.853 220.648
patch circ 2  44  1  0  0  1.360  1.647 229.353 243.148
patch circ 2  44  1  0  0  1.360  1.647 251.853 265.648
patch circ 2  44  1  0  0  1.360  1.647 274.353 288.148
patch circ 2  44  1  0  0  1.360  1.647 296.853 310.648
patch circ 2  44  1  0  0  1.360  1.647 319.353 333.148
patch circ 2  44  1  0  0  1.360  1.647 341.853 355.648
#layer circ $matTag $numBar $areaBar $yCenter $zCenter $radius <$startAng $endAng>
layer circ 4  16  0.015625  0  0  1.502 0 360
}

#Define shear stiffness (GJ) elastic material

set Gc 218640
set Jc  2.95
set GJ [expr $Gc*$Jc]
uniaxialMaterial Elastic 7  $GJ

section Aggregator 3  7 T -section  1

section Aggregator 4  7 T -section  2

#Create deck elements

#element elasticBeamColumn $eleTag $iNode $jNode $A $E $G $J $Iy $Iz $transfTag

element elasticBeamColumn 1  1  2  49.60  765269.3  318862.2  1e10  7493.7  242.06  1
element elasticBeamColumn 2  2  3  49.60  765269.3  318862.2  1e10  7493.7  242.06  1
element elasticBeamColumn 3  3  4  49.60  765269.3  318862.2  1e10  7493.7  242.06  1
element elasticBeamColumn 4  4  5  49.60  765269.3  318862.2  1e10  7493.7  242.06  1
element elasticBeamColumn 5  5  6  49.60  765269.3  318862.2  1e10  7493.7  242.06  1
element elasticBeamColumn 6  6  7  49.60  765269.3  318862.2  1e10  7493.7  242.06  1
element elasticBeamColumn 7  7  8  49.60  765269.3  318862.2  1e10  7493.7  242.06  1
element elasticBeamColumn 8  8  9  49.60  765269.3  318862.2  1e10  7493.7  242.06  1

#Create pier bent elements

#element elasticBeamColumn $eleTag $iNode $jNode $A $E $G $J $Iy $Iz $transfTag

element elasticBeamColumn  9  5 19  196.00   524736  218640  1e10  1e10  1e10  3
element elasticBeamColumn 10 14 19   25.23   524736  218640  1e10  1e10  1e10  2
element elasticBeamColumn 11 19 24  25.23   524736  218640  1e10  1e10  1e10  2

#Create column elements

#element elasticBeamColumn $eleTag $iNode $jNode $A $E $G $J $Iy $Iz $transfTag

#element nonlinearBeamColumn $eleTag $iNode $jNode $numintgrPts $secTag $transfTag

#element zeroLength $eleTag $iNode $jNode -mat $matTag1 $matTag2 ... -dir $dir1 $dir2
...

#element zeroLengthSection $eleTag $iNode $jNode $secTag <-orient $x1 $x2 $x3 $yp1
$yp2 $yp3>

element zeroLength 12 10 11 -mat 6 6 6 5 5 5 -dir 1 2 3 4 5 6
element zeroLengthSection 13 10 11 3 -orient 0 1 0 -1 0 0
element nonlinearBeamColumn 14 11 12 9 4 3
element nonlinearBeamColumn 15 12 13 9 3 3
element nonlinearBeamColumn 16 13 14 9 4 3
```

```
element zeroLength 17 14 15 -mat 6 6 6 5 5 5 -dir 1 2 3 4 5 6
element zeroLengthSection 18 14 15 3 -orient 0 1 0 -1 0 0
element elasticBeamColumn 19 15 16  1e10  524736  218640  1e10  1e10  1e10  3
element zeroLength 20 17 18 -mat 6 6 6 5 5 5 -dir 1 2 3 4 5 6
element zeroLengthSection 21 17 18 3 -orient 0 1 0 -1 0 0
element nonlinearBeamColumn 22 18 19 9 4 3
element nonlinearBeamColumn 23 19 20 9 3 3
element nonlinearBeamColumn 24 20 21 9 4 3
element zeroLength 25 21 22 -mat 6 6 6 5 5 5 -dir 1 2 3 4 5 6
element zeroLengthSection 26 21 22 3 -orient 0 1 0 -1 0 0
element elasticBeamColumn 27 22 23  1e10  5524736  218640  1e10  1e10  1e10  3
element zeroLength 28 24 25 -mat 6 6 6 5 5 5 -dir 1 2 3 4 5 6
element zeroLengthSection 29 24 25 3 -orient 0 1 0 -1 0 0
element nonlinearBeamColumn 30 25 26 9 4 3
element nonlinearBeamColumn 31 26 27 9 3 3
element nonlinearBeamColumn 32 27 28 9 4 3
element zeroLength 33 28 29 -mat 6 6 6 5 5 5 -dir 1 2 3 4 5 6
element zeroLengthSection 34 28 29 3 -orient 0 1 0 -1 0 0
element elasticBeamColumn 35 29 30  1e10  524736  218640  1e10  1e10  1e10  3

#Create uniaxialMaterial for abutment springs

uniaxialMaterial Elastic 8 17.202e3;   # Translational stiffness along X axis of the
abutments, kip/ft
uniaxialMaterial Elastic 9 1e12;   # Translational stiffness along Y axis of the
abutments, kip/ft
uniaxialMaterial Elastic 10 3.2e3;   # Translational stiffness along Z axis of the
abutments, kip/ft
uniaxialMaterial Elastic 11 1e12;   # Rotational stiffness about X axes of the
abutments, kip.ft/radian
uniaxialMaterial Elastic 12 1e12;      # Rotational stiffness about Y axis of the
abutments, kip.ft/radian
uniaxialMaterial Elastic 13 0;      # Rotational stiffness about the Z axis of the
abutment, kip.ft/radian

#Create spring elements using above stiffness values

#element zeroLength $eleTag $iNode $jNode -mat $matTag1 $matTag2 ... -dir $dir1 $dir2
...

element zeroLength 36 31  1 -mat 8 9 10 11 12 13 -dir 1 2 3 4 5 6
element zeroLength 37  9 32 -mat 8 9 10 11 12 13 -dir 1 2 3 4 5 6

#Create recorder files

recorder Node -file Nodes1-9_GCNP_Disp_Long_Parma.out -time -nodeRange 1 9 -dof 1 disp
recorder Node -file Nodes1-9_GCNP_Disp_Trans_Parma.out -time -nodeRange 1 9 -dof 3
disp
recorder Node -file Column_1_Reaction_GCNP_Parma.out -time -node 10 -dof 1 2 3 4 5 6
reaction
recorder Node -file Column_2_Reaction_GCNP_Parma.out -time -node 19 -dof 1 2 3 4 5 6
reaction
recorder Node -file Column_3_Reaction_GCNP_Parma.out -time -node 28 -dof 1 2 3 4 5 6
reaction
recorder Element -file Element_21_Stress-Strain.out -time -ele 21 section fiber -1.502
0.0 stressStrain

#Create vertical load pattern


pattern Plain 1 Constant {
#    tag    FX       FY      FZ   MX   MY   MZ
load  1     0.0    -198.585  0.0  0.0  0.0  0.0
```

```
load  2     0.0    -418.127  0.0  0.0  0.0  0.0
load  3     0.0    -418.127  0.0  0.0  0.0  0.0
load  4     0.0    -418.127  0.0  0.0  0.0  0.0
load  5     0.0    -397.373  0.0  0.0  0.0  0.0
load  6     0.0    -418.127  0.0  0.0  0.0  0.0
load  7     0.0    -418.127  0.0  0.0  0.0  0.0
load  8     0.0    -418.127  0.0  0.0  0.0  0.0
load  9     0.0    -198.585  0.0  0.0  0.0  0.0
load 16     0.0     -68.98   0.0  0.0  0.0  0.0
load 23     0.0     -76.49   0.0  0.0  0.0  0.0
load 30     0.0     -68.98   0.0  0.0  0.0  0.0
}
constraints Plain

numberer RCM

system BandSPD

algorithm Linear

integrator LoadControl 0.1

analysis Static

analyze 10

#Reset time to perform pushover analysis

loadConst -time 0.0

#Create horizontal load patterns
#Transverse seismic loads

pattern Plain 4 Linear {
# eleLoad -ele $eleTag1 <$eleTag2 ....> -type -beamUniform $Wy $Wz <$Wx>
eleLoad -ele 1 -type beamUniform 0 10.7 0
}

pattern Plain 5 Linear {
# eleLoad -ele $eleTag1 <$eleTag2 ....> -type -beamUniform $Wy $Wz <$Wx>
eleLoad -ele 2 -type beamUniform 0 10.943 0
}

pattern Plain 6 Linear {
# eleLoad -ele $eleTag1 <$eleTag2 ....> -type -beamUniform $Wy $Wz <$Wx>
eleLoad -ele 3 -type beamUniform 0 11.208 0
}

pattern Plain 7 Linear {
# eleLoad -ele $eleTag1 <$eleTag2 ....> -type -beamUniform $Wy $Wz <$Wx>
eleLoad -ele 4 -type beamUniform 0 11.351 0
}

pattern Plain 8 Linear {
# eleLoad -ele $eleTag1 <$eleTag2 ....> -type -beamUniform $Wy $Wz <$Wx>
eleLoad -ele 5 -type beamUniform 0 11.352 0
}

pattern Plain 9 Linear {
# eleLoad -ele $eleTag1 <$eleTag2 ....> -type -beamUniform $Wy $Wz <$Wx>
eleLoad -ele 6 -type beamUniform 0 11.21 0
}
```

```
pattern Plain 10 Linear {
# eleLoad -ele $eleTag1 <$eleTag2 ....> -type -beamUniform $Wy $Wz <$Wx>
eleLoad -ele 7 -type beamUniform 0 10.946 0
}

pattern Plain 11 Linear {
# eleLoad -ele $eleTag1 <$eleTag2 ....> -type -beamUniform $Wy $Wz <$Wx>
eleLoad -ele 8 -type beamUniform 0 10.703 0
}

# The following eight loading patterns should be activated instead of the previous
eight, when loading in the longitudinal direction

#pattern Plain 12 Linear {
# eleLoad -ele $eleTag1 <$eleTag2 ....> -type -beamUniform $Wy $Wz <$Wx>
#eleLoad -ele 1 -type beamUniform 0 0 11.205
#}

#pattern Plain 13 Linear {
# eleLoad -ele $eleTag1 <$eleTag2 ....> -type -beamUniform $Wy $Wz <$Wx>
#eleLoad -ele 2 -type beamUniform 0 0 11.294
#}

#pattern Plain 14 Linear {
# eleLoad -ele $eleTag1 <$eleTag2 ....> -type -beamUniform $Wy $Wz <$Wx>
#eleLoad -ele 3 -type beamUniform 0 0 11.351
#}

#pattern Plain 15 Linear {
# eleLoad -ele $eleTag1 <$eleTag2 ....> -type -beamUniform $Wy $Wz <$Wx>
#eleLoad -ele 4 -type beamUniform 0 0 11.375
#}

#pattern Plain 16 Linear {
# eleLoad -ele $eleTag1 <$eleTag2 ....> -type -beamUniform $Wy $Wz <$Wx>
#eleLoad -ele 5 -type beamUniform 0 0 11.375
#}

#pattern Plain 17 Linear {
# eleLoad -ele $eleTag1 <$eleTag2 ....> -type -beamUniform $Wy $Wz <$Wx>
#eleLoad -ele 6 -type beamUniform 0 0 11.351
#}

#pattern Plain 18 Linear {
# eleLoad -ele $eleTag1 <$eleTag2 ....> -type -beamUniform $Wy $Wz <$Wx>
#eleLoad -ele 7 -type beamUniform 0 0 11.294
#}

#pattern Plain 19 Linear {
# eleLoad -ele $eleTag1 <$eleTag2 ....> -type -beamUniform $Wy $Wz <$Wx>
#eleLoad -ele 8 -type beamUniform 0 0 11.205
#}


constraints Plain

numberer RCM

system BandSPD

algorithm Linear

integrator LoadControl 0.01
```

```
analysis Static

analyze 100
```

Results of Nonlinear Model with Grouted Couplers

Tables D-14 and D-15 show the displacements and column base reactions for the longitudinal and transverse directions, respectively.

Table D-14. Displacements and Column Base Reactions for Seismic Loads in the Longitudinal Direction

Nodes	Displacement (ft.)
Deck	
1	0.08498
2	0.08614
3	0.08693
4	0.08736
5	0.08741
6	0.08736
7	0.08693
8	0.08614
9	0.08498
Top of the Columns	
15	0.08039
24	0.08039
33	0.08039

Columns	Shear (k)	Axial (k)	Moment (k-ft)
1	-97.992	752.371	1365.820
2	-97.992	752.371	1365.820
3	-97.992	752.365	1365.830

Table D-15. Displacements and Column Base Reactions for Seismic Loads in the Transverse Direction

Nodes	Displacement (ft.)
Deck	
1	0.35954
2	0.36310
3	0.36936
4	0.37388
5	0.37522
6	0.37392
7	0.36943
8	0.36319
9	0.35964
Top of the Columns	
15	0.37490
24	0.37521
33	0.37490

Columns	Shear (k)	Axial (k)	Moment (k-ft)
1	-272.388	753.540	-3634.250
2	-272.397	753.703	-3634.510
3	-272.388	753.522	-3634.250

The drift in the longitudinal and transverse directions for top of the columns are shown in Table D-16.

Table D-16. Calculated Drift for Top of the Columns

Node	15	24	33
Long. drift (%)	0.3135	0.3135	0.3135
Trans. drift (%)	1.4644	1.4657	1.4644

Dubois Bridge Model Summary

The bridge at Dubois is a two-span bridge with a four column bent. The superstructure is made up of an 8 inch thick deck that rests on 8 steel girders. The substructure is composed of a pier cap, four columns, and their footings, all are cast-in-place (CIP). For the sake of brevity the input files for the Dubois bridge will not be presented in this appendix.

Structure Model

The Superstructure is broken down into eight elements, 29 ft each, attached end to end from south to north. At the midpoint a rigid element, with a large moment of inertia, connects the superstructure to the pier bent. This element starts at the center of gravity of the pier bent, and ends at the center of gravity of the superstructure. The upper portion of each column contains a rigid element that starts at the top of the column and ends at the center of gravity of the pier bent (2.355 ft). Finally, the footings are included in the model as rigid elements that are located at the bottom of the columns. They are modeled using the same properties as the columns, but they are half the depth of the footings in length (2 ft). To model the spring support conditions, extra nodes and ZeroLength elements are assigned to the abutment ends of the superstructure.

Superstructure

- $Overall\ Length$

$L_d = 230\ ft$

- $Compressive\ Strength\ of\ Cast\ in\ Place\ Concrete - Deck\ Slab\ and\ Parapet$

$f'_c = 4.0\ ksi$

- $Modulus\ of\ Elasticity\ of\ Cast\ in\ Place\ Concrete$

$E_c = 3{,}300 \times 0.145^{1.5}\sqrt{f'_c} = 3{,}644\ ksi$

- $Modulus\ of\ Elasticity\ of\ Steel$

$E_s = 29{,}000\ ksi$

- $Modular\ Ratio\ \ of\ Elasticity$

$n = \frac{E_s}{E_c} = \frac{29{,}000\ ksi}{3{,}644\ ksi} = 7.96$

- $Cross\ Sectional\ Area\ of\ Small\ Girder$

$A_g = \left(2 \times (1.25\ in\ \times 18\ in) + (0.625\ in \times 40\ in)\right) = \ 70\ in^2 = 0.48\ ft^2$

- $Cross\ Sectional\ Area\ of\ Big\ Girder$

$A_g = \left(2 \times (1.375\ in\ \times 18\ in) + (0.625\ in \times 58\ in)\right) = \ 85.75\ in^2 = 0.60\ ft^2$

- *Cross Sectional Area of Deck*

$$A_d = \left(\frac{672\ in}{7.96} \times 8\ in\right) = 675.38\ in^2 = 4.69\ ft^2$$

- *Centroid Deck + Small Girdes*

$$\overline{y_1} = \frac{\left(8 \times A_{g_1} \times \overline{y_{g_1}}\right) + (A_d \bar{y}_d)}{8A_{g_1} + A_d} = 35.08\ in$$

- *Centroid Deck + Big Girdes*

$$\overline{y_2} = \frac{\left(8 \times A_{g_2} \times \overline{y_{g_2}}\right) + (A_d \bar{y}_d)}{8A_{g_2} + A_d} = 47.43\ in$$

- *Average Centroid*

$$\bar{y}_{avg} = \frac{35.08\ in + 47.43\ in}{2} = 41.26\ in$$

- *Moment of Inertia About Strong Axis (Deck + Small Girdes)*

$$\bar{I}_{z_1} = \left(\sum \bar{I}_{g_1}\right)_{strong} + \bar{I}_d + 2\left(A_{Flange_1} {d_{Flange_1}}^2\right) + \left(\sum A_{g_1} {d_{1_1}}^2\right) + \left(A_d {d_2}^2\right) = 18.260\ ft^4$$

- *Moment of Inertia About Strong Axis (Deck + Big Girdes)*

$$\bar{I}_{z_2} = \left(\sum \bar{I}_{g_2}\right)_{strong} + \bar{I}_d + 2\left(A_{Flange_2} {d_{Flange_2}}^2\right)\left(\sum A_{g_2} {d_{1_2}}^2\right) + \left(A_d {d_2}^2\right) = 40.322\ ft^4$$

- *Average Moment of Inertia About Strong Axis*

$$\bar{I}_z = \frac{\bar{I}_{z_1} + \bar{I}_{z_2}}{2} = 29.291\ ft^4$$

- *Moment of Inertia About Weak Axis (Deck + Small Girders)*

$$\bar{I}_{y_1} = \left(\sum \bar{I}_{g_1}\right)_{weak} + \frac{\left(\frac{t}{n}\right) b^3}{12} + \left(\sum A_{g_{y1}} {d_{1y_1}}^2\right) + x\left(A_d {d_2}^2\right) = 2{,}226.57\ ft^4$$

- *Moment of Inertia About Weak Axis (Deck + Big Girders)*

$$\bar{I}_{y_2} = \left(\sum \bar{I}_{g_2}\right)_{weak} + \frac{\left(\frac{t}{n}\right) b^3}{12} + \left(\sum A_{g_{y2}} {d_{1y_2}}^2\right) + x\left(A_d {d_2}^2\right) = 2{,}451.71\ ft^4$$

- *Average Moment of Inertia About Weak Axis*

$$\bar{I}_y = \frac{\bar{I}_{y_1} + \bar{I}_{y_2}}{2} = 2{,}339.14\ ft^4$$

- *Steel Shear Modulus of Elasticity*

$$G = \frac{E_s}{2(1+\nu)} = \frac{(29{,}000\ ksi\ \times (144\frac{in^2}{ft^2})}{2\ (1+0.3)} = 1{,}606{,}153.85\ kip/ft^2$$

- *Polar Moment of Inertia*

$J = 1 \times 10^{10}$

Substructure

- *Pier Cap Length*

$L_{pc} = 56\ ft$

- *Pier Cap Height*

$H_{pc} = 4.71\ ft$

- *Pier Cap Cross − Sectional Area in x − y Plane*

$A_{pc_{xy}} = (4.71\ ft\ \times 4\ ft) = 18.84\ ft^2$

- *Column Height*

$H_c = 14.05\ ft$

- *Column Diameter*

$D_c = 3.5\ ft$

- *Column and Footing Cross − Sectional Area*

$$A_c = \frac{\pi d^2}{4} = \frac{\pi(3.5ft)^2}{4} = 9.62\ ft^2$$

- *Gross Moment of Inertia of One Column*

$$I_{cg} = \frac{\pi d^4}{64} = 7.366\ ft^4$$

- *Polar moment of Inertia of One Column*

$$J_g = \frac{\pi d^4}{32} = 14.732\ ft^4$$

Effective Polar Moment of Inertia of One Column

$J_{eff} = 0.2J_g = 0.2(14.732\ ft^4) = 2.946\ ft^4$

Column Reinforcement

The columns are reinforced with 13 No. 11 bars, and a No. 4 spiral with a 3 inch cover as shown in Figure D-16.

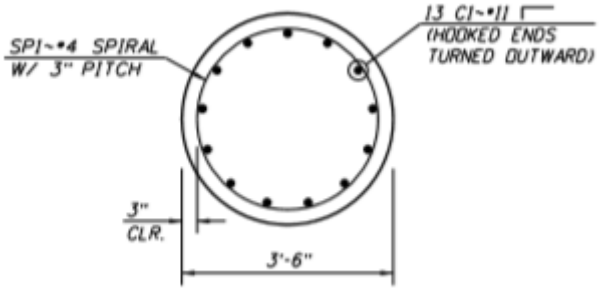

Figure D-16: Column Detail

- $Cross - Sectional\ Area\ of\ No. 11\ bar$

$A_r = 1.56\ in^2 = 0.0108\ ft^2$

- $Total\ Longitudinal\ Steel\ in\ one\ Column\ Cross - Section$

$A_{st} = 13 \times A_r = 20.28\ in^2 = 0.141\ ft^2$

- $Diameter\ of\ No. 11\ Rebar$

$D_r = 1.41\ in$

- $Diameter\ of\ Spiral\ Reinforcing$

$D_s = 0.5\ in$

Linear Elastic Bridge Model

The linear-elastic models of the Dubois bridge with node and element placement are shown in Figures D-17 and D-18, respectively.

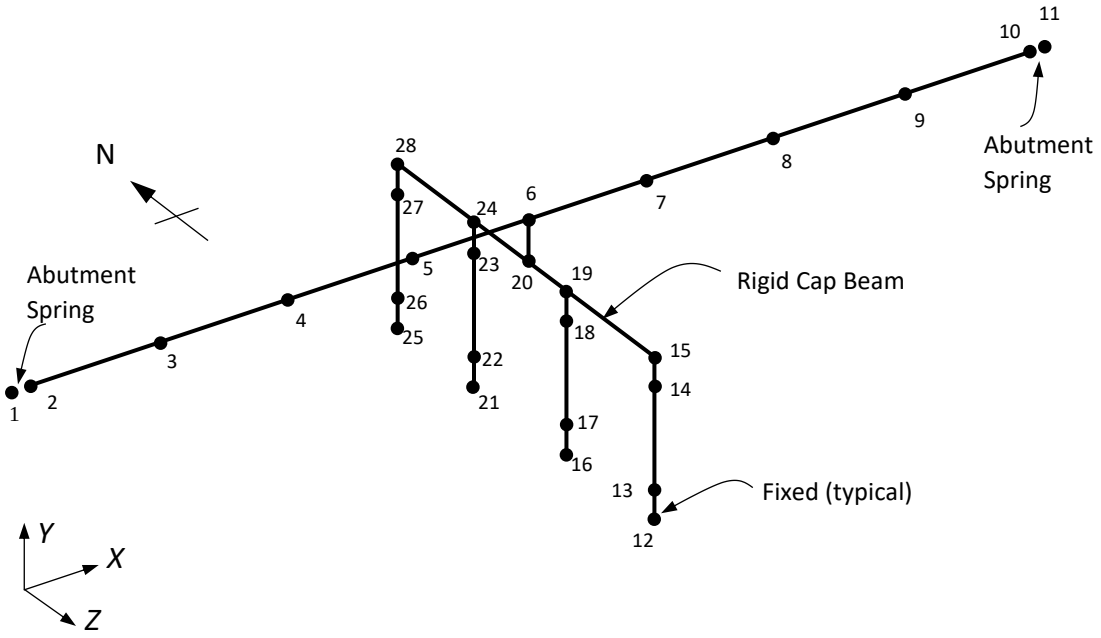

Figure D-17. Linear Elastic Model of the Bridge with Node Numbers

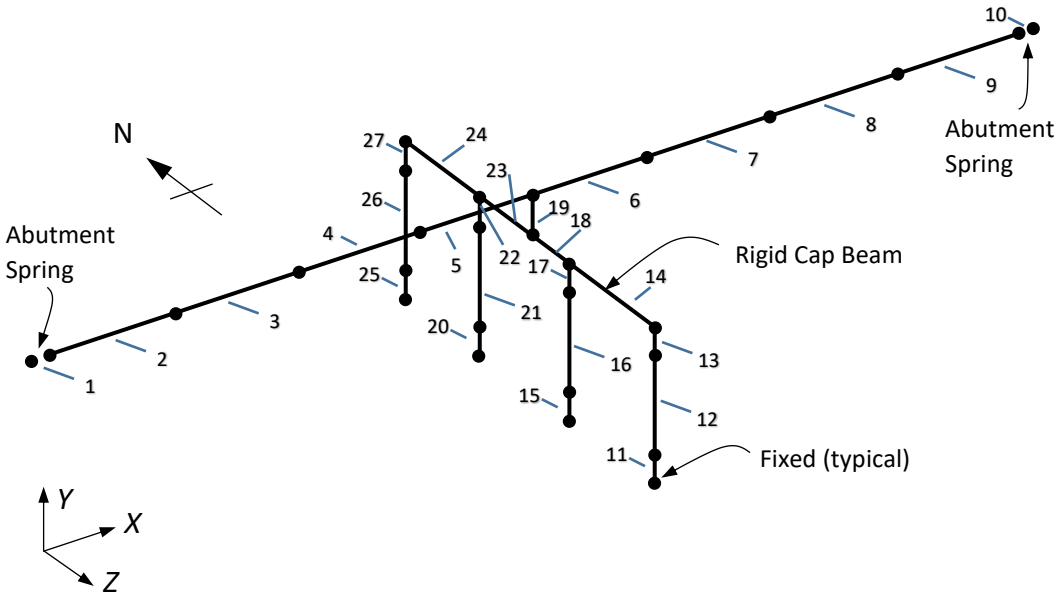

Figure D-18. Linear Elastic Model of the Bridge with Element Numbers

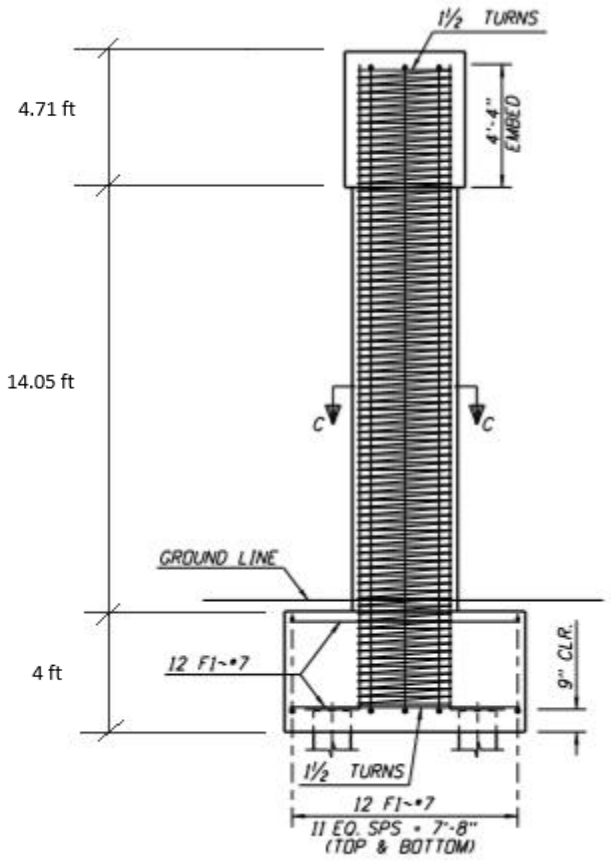

Figure D-19. Side View – Footing, Column, and Pier Cap

Spring Support Conditions

1. Support stiffness: Springs at abutments, fixed column bases
2. Abutment type: Seat type
3. Restraint of superstructure: Abutments with springs in longitudinal and transverse directions, unrestrained rotation about the z axis, and infinite restraint in all other DOF's

Soil Spring Stiffness

Each abutment wall has eight 14X117 H-piles. Each H-pile is oriented with its strong axis parallel to the abutment wall length and its weak axis perpendicular to the abutment wall length. The dimensions of the abutment walls are:

$H_{aw_E} = 8.39\ ft$ $\quad$ *Height of East Abutment Wall*
$H_{aw_W} = 8.38\ ft$ $\quad$ *Height of West Abutment Wall*
$L_{aw} = 56\ ft$ $\quad$ *Length of East and West Abutment Walls*

The soil spring stiffness for the H-piles were derived from the Phase IV Foundation Investigation Report. Figures D-20, D-21, D-22 and D-23 show force vs. deflection graphs up to 11 and 22 ft of depth for one

H-pile in the East and West Abutments for the strong and weak axis. Since spring stiffness equals force divided by deflection ($K = F/d$) the spring stiffness can be estimated by determining the force at 1 in of deflection. About the strong axis the force at 1 in of deflection is:

$$k_{s_E} = 91\frac{kip}{in}$$
$$= 1{,}092\frac{kip}{ft} \qquad Force\ about\ strong\ axis\ (longitudinal)\ at\ 1\ in.defl. - East\ abutment$$
$$k_{s_W} = 116\frac{kip}{in}$$
$$= 1{,}392\frac{kip}{ft} \qquad Force\ about\ strong\ axis\ (longitudinal)\ at\ 1\ in.defl. - West\ abutment$$

And about the weak axis the force at 1 in of deflection is:

$$k_{w_E} = 57\frac{kip}{in} = 684\frac{kip}{ft} \qquad Force\ about\ weak\ axis\ (transverse)\ at\ 1\ in.defl. - East\ abutment$$
$$k_{w_W} = 72\frac{kip}{in} = 864\frac{kip}{ft} \qquad Force\ about\ weak\ axis\ (transverse)\ at\ 1\ in.defl. - West\ abutment$$

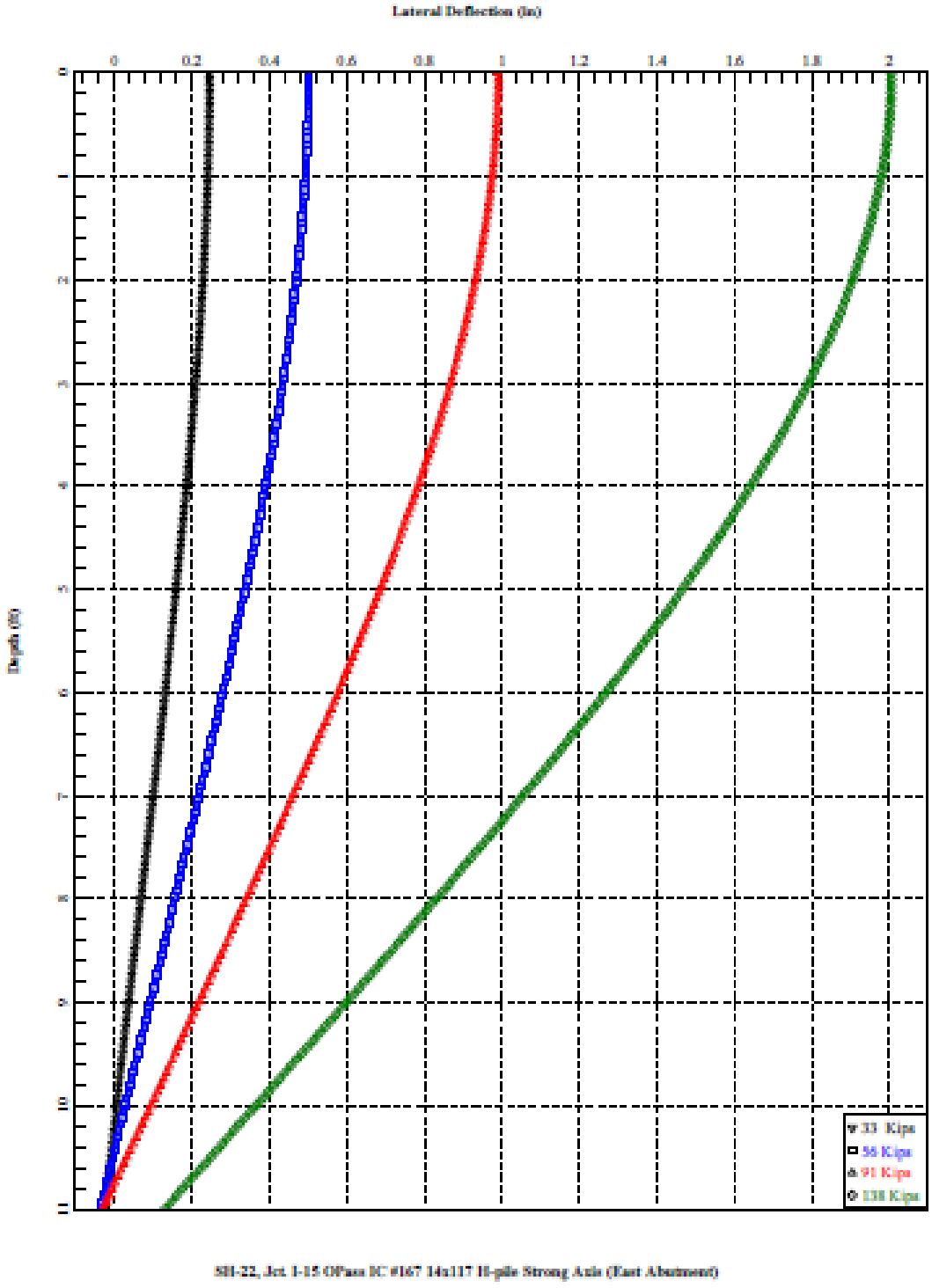

Figure D-20. East Abutment Lateral Deflection vs. Depth of an H-Pie about Strong Axis

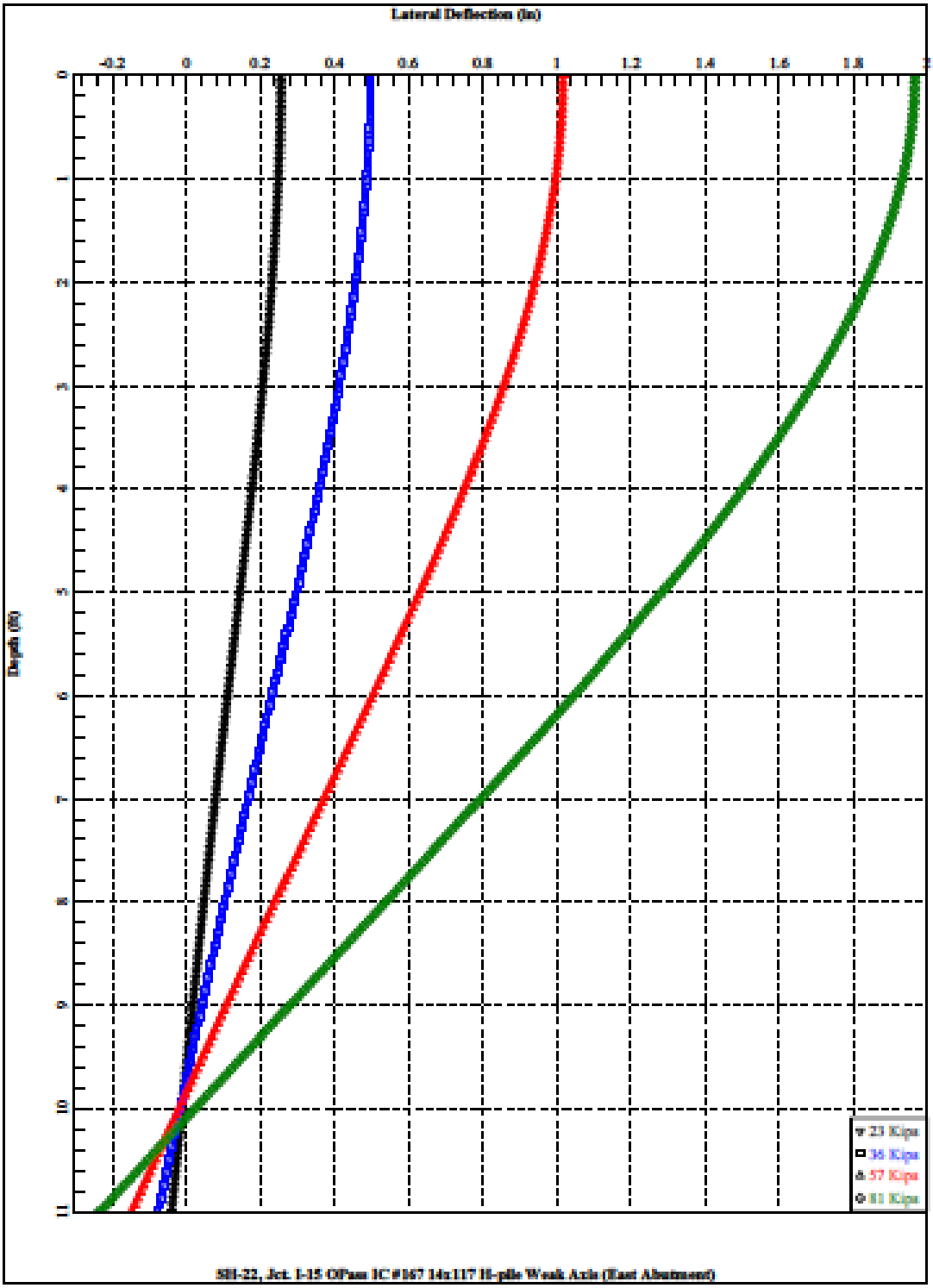

Figure D-21. East Abutment Lateral Deflection vs. Depth of an H-Pie about Weak Axis

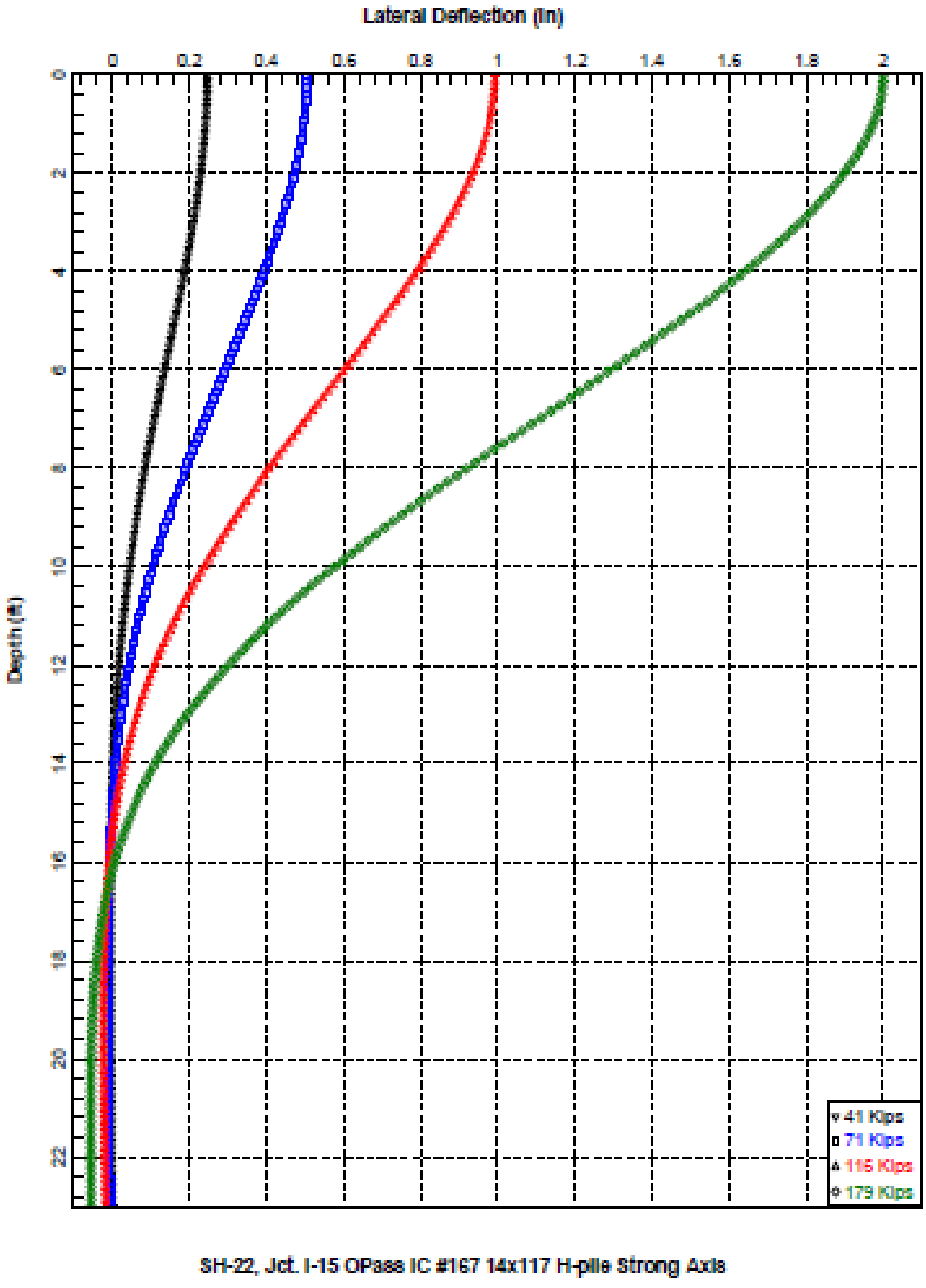

Figure D-22. West Abutment Lateral Deflection vs. Depth of an H-Pie about Strong Axis

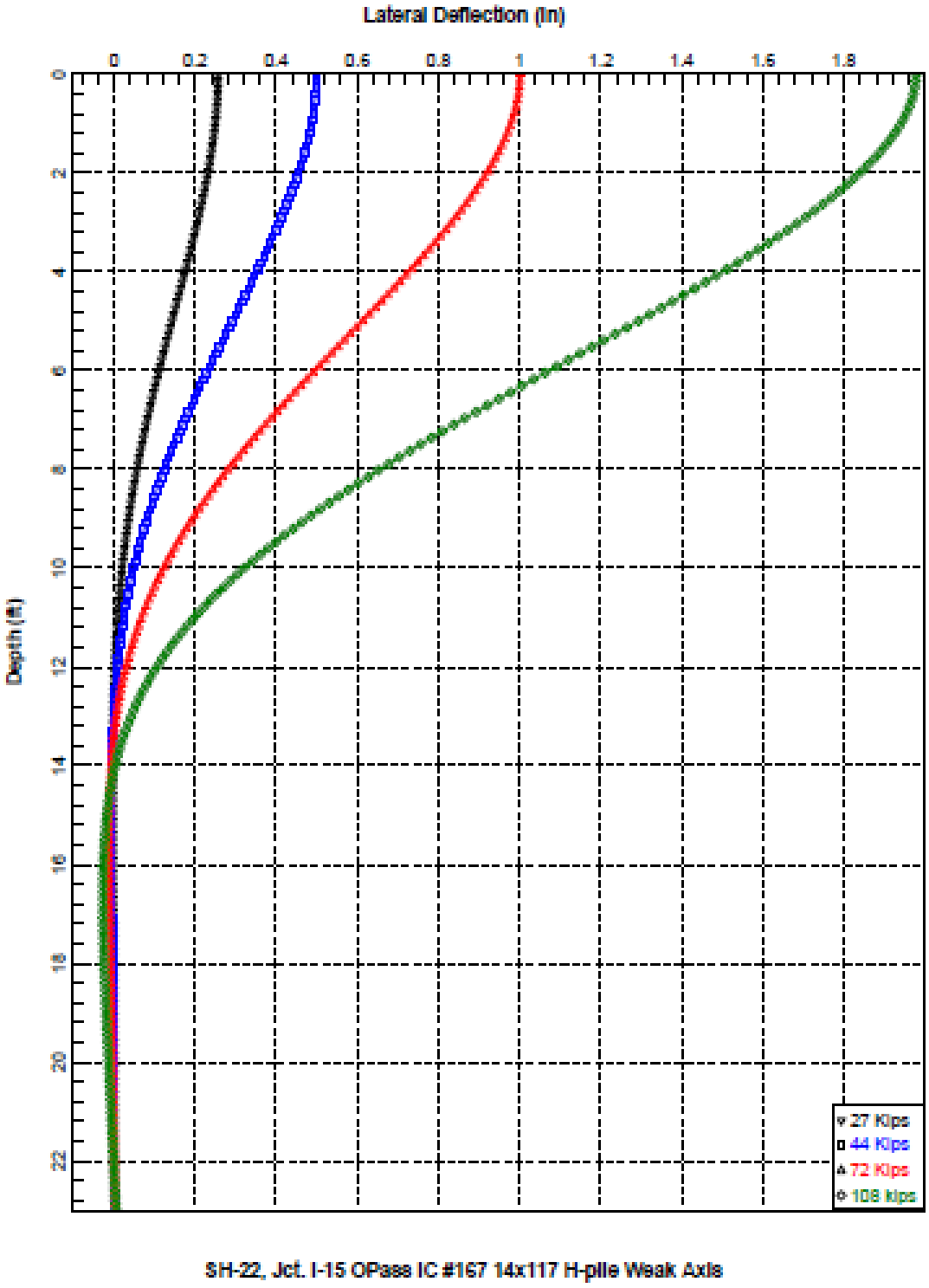

Figure D-23. West Abutment Lateral Deflection vs. Depth of an H-Pie about Weak Axis

The initial value for the soil spring stiffness in the x direction (longitudinal) is calculated by

$$K_{longitudinal} = \frac{nk_{s_E} + nk_{s_W} + \left(\frac{7.7A}{d}\right)}{2} \quad \text{(D-19)}$$

Where,

$K_{longitudinal} = soil\ spring\ stiffness\ in\ x - direction$
$n = number\ of\ H\ piles\ in\ one\ abutment\ wall = 8$
$k_s = East\ or\ West\ soil\ spring\ stiffness\ for\ one\ H - pile\ in\ longitudinal\ direction$
$A_{aw_E} = East\ abutment\ wall\ area = H_{aw_E} \times L_{aw} = 469.84\ ft^2$
$A_{aw_W} = West\ abutment\ wall\ area = H_{aw_W} \times L_{aw} = 469.28\ ft^2$
$d_E = deflection\ needed\ to\ mobilize\ full\ passive\ resistanc - East = 0.02H_{aw_E} = 0.1678\ ft$
$d_W = deflection\ needed\ to\ mobilize\ full\ passive\ resistanc - West = 0.02H_{aw_w} = 0.1676\ ft$

- For the East Abutment, the soil spring stiffness in the strong direction (longitudinal) is:

$$K_{longitudinal_E} = 20{,}716\frac{kip}{ft}$$

- For the West Abutment, the soil spring stiffness in the strong direction (longitudinal) is:

$$K_{longitudinal_W} = 20{,}716\frac{kip}{ft}$$

The initial value for the soil spring stiffness in the z direction (transverse) is calculated by

$$K_{transverse} = nk_w$$

Where,
$K_{transverse} = soil\ spring\ stiffness\ in\ z - direction$
$n = number\ of\ H\ piles\ in\ one\ abutment\ wall = 8$
$k_w = East\ or\ West\ soil\ spring\ stiffness\ for\ one\ H - pile\ in\ transverse\ direction$

If the reactions at the ends of the bridge are greater than the force needed to displace the H-piles times the number of H-piles in a wingwall the excess seismic load will be resisted by the shear capacity of one wingwall, V_c. If the excess seismic force is greater than V_c it can be assumed that the wingwall has broken off and only the H-pile capacity resists the seismic force.

$V_c = shear\ capacity\ of\ one\ wingwall = 0.0316\beta(\sqrt{f'_c})b_v d_v$

Where,
$\beta = 2.0$
$b_{v_E} = height\ of\ East\ wingwall = 99.72\ in$
$b_{v_W} = height\ of\ West\ wingwall = 99.48\ in$
$d_v = thickness\ of\ wingwall\ minus\ distance\ from\ backfill\ face\ to\ main\ fexural\ reinf.$
$= 9.625\ in$

$V_{c_E} = 121.32\ kip$

$$V_{c_W} = 121.03\ kip$$

- For the East Abutment, the soil spring stiffness in the weak direction is:

$$K_{transverse_E} = 8\left(684\frac{kip}{ft}\right) = 5{,}472\frac{kip}{ft}$$

- For the West Abutment, the soil spring stiffness in the weak direction is:

$$K_{transverse_W} = 8\left(864\frac{kip}{ft}\right) = 6{,}912\frac{kip}{ft}$$

A large spring stiffness (1e12) was used for all other DOF's except the rotation about the z axes of the abutments, which were assigned a value of zero.

Weight of Structure

Table D-17. Weight of Structure to Nodes from Deck, Pier Cap, and Top Half of Columns

SECTION	CROSS-SECTIONAL AREA (ft^2)	LENGTH (ft)	WEIGTH OF MATERIAL ($kips/ft^3$)	OVERALL WEIGHT (kips)	WEIGTH PER FOOT (kips/ft)
Wearing Surface					1.568
Deck	37.333	230	0.150	1288.00	5.600
Girders	3.889	230	0.490	438.28	1.906
Parapets	2.389	230	0.150	82.41	0.358
Metal Deck Forms					0.952
Future Utilities					0.050
Intermediate Diaphragms	0.118	49	0.490	28.34	0.123
Exterior Diaphragms	0.181	49	0.490	4.33	0.019
Columns	9.621	14.05	0.150	81.10	11.545
Pier Cap	18.840	56	0.150	158.26	3.230

Table D-18. Weight Assigned to Nodes at Superstructure

SUPERSTRUCTURE	LENGTH (ft)	MATERIALS INVOLVED	WEIGTH TO NODE (kips)
Node 2	14.375	Concrete, steel, wearing surface	152.03
Node 3	28.750	Concrete, steel, wearing surface	304.06
Node 4	28.750	Concrete, steel, wearing surface	304.06
Node 5	28.750	Concrete, steel, wearing surface	304.06
Node 6	28.750	Concrete, steel, wearing surface	304.06
Node 7	28.750	Concrete, steel, wearing surface	304.06
Node 8	28.750	Concrete, steel, wearing surface	304.06
Node 9	28.750	Concrete, steel, wearing surface	304.06
Node 10	14.375	Concrete, steel, wearing surface	152.03

Table D-19. Weight Assigned to Nodes at Substructure

SUBSTRUCTURE	LENGTH (ft)	MATERIALS INVOLVED	WEIGTH TO NODE (kips)
Node 15	11.667	Concrete	47.818
Node 19	16.33	Concrete	62.890
Node 24	16.33	Concrete	62.890
Node 28	11.667	Concrete	47.818

From the above tables, the total weigh of the structure is 2,654 kips giving a distributed load of w(x) = 11.54 kip/ft. The axial force to one interior column is 366.95 kips.

Effective Moment of Inertia of Columns

For the effective moment of inertia, the gross moment of inertia is multiplied by the Elastic Stiffness Ratio ($\frac{I_{eff}}{I_{cg}}$). This is obtained from Figure D-24 with the Axial Load Ratio and the ratio of reinforcing steel to concrete.

$$Axial\ Load\ Ratio = \frac{P}{f'_c \times A_c}$$

Where,

$P = Axial\ load\ to\ column\ from\ self - weight\ of\ bridge = 366.95\ kips$

The axial load on one column is from half the weight of each span divided by four (four columns in total) plus the weight on the node in the pier cap above the column plus half the weight of one column.

$$\frac{P}{f'_c \times A_c} = \frac{(366.948\ kips)}{(4\ ksi\ \times 144\ in^2/ft^2 \times 9.62\ ft^2)} = 0.0662$$

$$\frac{A_{st}}{A_{cg}} = \frac{0.141\ ft^2}{9.62\ ft^2} = 0.0146$$

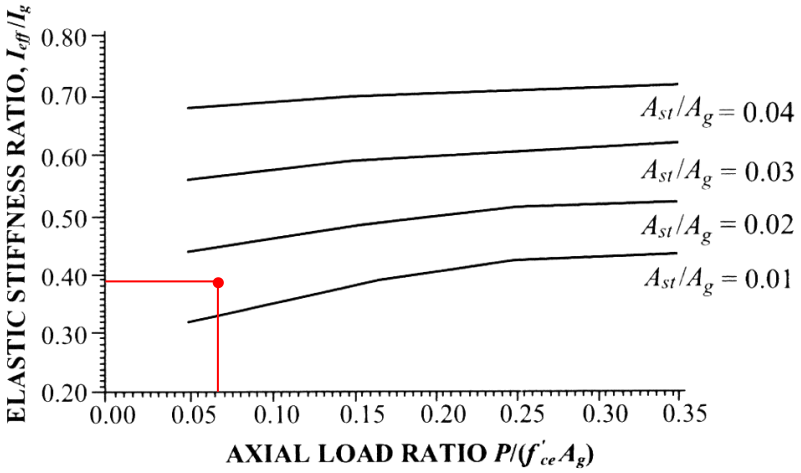

Figure D-24. Elastic Stiffness Ratio (AASHTO *Guide Specifications for LRFD Seismic Bridge Design* (2011), p.5-19)

$$\frac{I_{eff}}{I_{cg}} = 0.39$$

- $Effective\ Moment\ of\ Inertia\ of\ One\ Column$

$$I_{eff} = 0.39 \times I_{cg} = 0.39 \times 7.366\ ft^4 = 2.873\ ft^4$$

Geometric transformation

The geometric transformations used for the Dubois bridge are the same as those used for the Parma bridge.

Seismic Loads

The same USGS seismic design summary report data as given in Figure D-8 is also used for the Dubois bridge. To calculate the seismic loads on the deck of the bridge the displacements at the deck nodes from a uniformly distributed load of 10 kip/ft in the longitudinal and transverse direction are determined and used to calculate the factors α, β, and γ. The factors are used to calculate the loads ($p_e\ (x)$) at the nodes on the deck. The distributed seismic loads on each element is the average of the loads on the nodes. These loads are shown in column 9 of Tables D-20 and D-21.

$$\alpha = \int_0^L v_s(x)\ dx$$
$$\beta = \int_0^L w(x) v_s(x) dx$$
$$\gamma = \int_0^L w(x) v_s\ (x)^2 dx$$

Where,

$v_s(x) = Displacement\ due\ to\ uniformly\ distributed\ load\ of\ 10\frac{kip}{ft}$

$w(x) = Weight\ of\ bridge\ per\ unit\ length = 11.539\ kip/ft$

$dx = Tributary\ length$

$L = Total\ bridge\ length$

$$p_e(x) = \beta C_{sm} w(x) v_s(x)/\gamma$$

Where,

$$C_{sm} = A_s + (S_{DS} - A_s)\left(\frac{T_m}{T_o}\right) \quad for \quad T_m < T_o$$

$$C_{sm} = S_{DS} = 0.907 \quad for \quad T_o < T_m < T_s$$

$$C_{sm} = \frac{S_{D1}}{T_m} \quad for \quad T_m > T_s$$

Where,

$$T_m = 2\pi\sqrt{\frac{\gamma}{P_0 g \alpha}} = 2\pi\sqrt{\frac{5.7}{(\frac{10kip}{ft})(\frac{32.2ft}{s^2})(10.658ft^2)}} = 0.256s \quad for\ longitudinal\ loads$$

$$T_m = 2\pi\sqrt{\frac{\gamma}{P_0 g \alpha}} = 2\pi\sqrt{\frac{14.702}{(\frac{10kip}{ft})(\frac{32.2ft}{s^2})(17.119ft^2)}} = 0.324s \quad for\ transverse\ loads$$

$T_s = \frac{S_{D1}}{S_{DS}} = 0.5358$

$T_0 = 0.2T_s = 0.1072$

$g = 32.2\frac{ft}{s^2}$

$P_0 = 10\frac{kip}{ft}$

Table D-20. Seismic Load Calculations in Longitudinal Direction

Nodes	x (ft)	dx (ft)	vs(x) (ft)	α(x) (ft^2)	β(x) (k-ft)	γ(x) (k-ft^2)	pe(x) (k/ft)	avg. pe (k/ft)
2	0	0	0.0455	0.000	0.000	0.000	10.267	
3	28.75	28.75	0.0461	1.325	15.295	0.705	10.412	10.339
4	57.5	28.75	0.0465	1.337	15.431	0.718	10.504	10.458
5	86.25	28.75	0.0467	1.342	15.490	0.723	10.545	10.524
6	115	28.75	0.0466	1.341	15.474	0.722	10.533	10.539
7	143.75	28.75	0.0467	1.342	15.490	0.723	10.545	10.539
8	172.5	28.75	0.0465	1.337	15.431	0.718	10.504	10.524
9	201.25	28.75	0.0461	1.325	15.295	0.705	10.412	10.458
10	230	28.75	0.0455	1.307	15.082	0.686	10.267	10.339
	Total	230		10.658	122.988	5.700		
						Average	10.443	

Table D-21. Seismic Load Calculations in Transverse Direction

Nodes	x (ft)	dx (ft)	vs(x) (ft)	α(x) (ft^2)	β(x) (k-ft)	γ(x) (k-ft^2)	pe(x) (k/ft)	avg. pe (k/ft)
2	0	0	0.0746	0.000	0.000	0.000	10.484	
3	28.75	28.75	0.0747	2.148	24.784	1.852	10.505	10.494
4	57.5	28.75	0.0747	2.146	24.766	1.849	10.497	10.501
5	86.25	28.75	0.0742	2.133	24.609	1.825	10.430	10.464
6	115	28.75	0.0738	2.122	24.480	1.806	10.376	10.403
7	143.75	28.75	0.0742	2.133	24.609	1.825	10.430	10.403
8	172.5	28.75	0.0747	2.146	24.766	1.849	10.497	10.464
9	201.25	28.75	0.0747	2.148	24.784	1.852	10.505	10.501
10	230	28.75	0.0746	2.143	24.734	1.844	10.484	10.494
	Total	230		17.119	197.532	14.702		
						Average	10.468	

Determination of Final Soil Spring Stiffness

Longitudinal Direction:

The reactions at the abutments, Node 1 and 11 = $R_1 = R_2 = 985.595$ k
The deflections at the abutments, Node 2 and 10 = 0.0475765 ft.
From Figures D-20 and D-22:

F_W = 71 k and F_E = 55 k
The demand is: $R_1 + R_2$ = 985.595 k + 985.595 k = 1971.19 k

From Figure E-1 of Appendix E, F_{bf} = 1017.86 k
The capacity is: $n_1 F_E + n_2 F_w + F_{bf}$ = 8(55 k) + 8(71 k) + 1017.86 k = 2025.86 k

Comparing the demand and capacity,
1971.19 k ≅ 2025.86 k → (2025.86 – 1971.19)/ (2025.86) *100 = 2.7% difference.
Therefore, $K_{Longitudinal\ East} = K_{Longitudinal\ West} = 20{,}716\frac{kip}{ft}$
Transverse Direction:

The reactions (the demand) at the west abutment is: R_{t1} = 551.823 k
Displacement at the west abutment = 0.0798355 ft.
From Figure D-23:
F_W = 69.2 k
The capacity at the west abutment is: $n_1 F_W$ = 8(69.2 k) = 553.6 k

Comparing demand and capacity,
551.823 k ≅ 553.6 k → (553.6-551.823)/ (553.6) *100 = 0.32% difference,
Therefore, no force in the wing wall is needed.
$K_{Transverse\ West}$ = 6912 k/ft. OK

The reactions (the demand) at the east abutment is: R_{t1} = 462.724 k
Displacement at the west abutment = 0.0845621 ft.
From Figure D-21:
F_W = 57 k
The capacity at the east abutment is: $n_1 F_W$ = 8(57 k) = 456 k

Comparing demand and capacity,
462.724 k ≅ 456 k → (462.724 -456)/ (462.724) *100 = 1.45% difference,
Therefore, no force in the wing wall is needed.
$K_{Transverse\ East}$ = 5472 k/ft. OK

Therefore, we get good correlation (within 10%) between abutment acting seismic forces and resulting resistance in both longitudinal and transverse directions. The abutment spring stiffness values remain the same.

$$K_{Longitudinal\ East} = 20{,}716\frac{kip}{ft}$$
$$K_{Longitudinal\ West} = 20{,}716\frac{kip}{ft}$$
$$K_{Transverse\ East} = 5{,}472\frac{kip}{ft}$$
$$K_{Transverse\ West} = 6{,}912\frac{kip}{ft}$$

Linear-elastic Analysis Results

Tables D-22 and D-23 show the displacements and column base reactions for the longitudinal and transverse directions, respectively. The drift in the longitudinal and transverse directions for top of the columns are shown in Table D-24.

Table D-22. Displacements and Column Base Reactions for Seismic Loads in the Longitudinal Direction

Nodes	Displacement (ft.)
Deck	
2	0.04758
3	0.04825
4	0.04868
5	0.04887
6	0.04882
7	0.04887
8	0.04868
9	0.04825
10	0.04758
Top of the Columns	
14	0.03621
18	0.03621
23	0.03621
27	0.03621

Columns	Shear (k)	Axial (k)	Moment (k-ft)
1	-108.94	436.733	1011.02
2	-108.94	436.733	1011.02
3	-108.94	436.733	1011.02
4	-108.94	436.733	1011.02

Table D-23. Displacements and Column Base Reactions for Seismic Loads in the Transverse Direction

Nodes	Displacement (ft.)
Deck	
2	0.07928
3	0.07958
4	0.07991
5	0.08003
6	0.08043
7	0.08177
8	0.08318
9	0.08392
10	0.08404
Columns	
14	0.07929
18	0.07986
23	0.07986
27	0.07929

Columns	Shear (k)	Axial (k)	Moment (k-ft)
1	344.634	436.825	-2781.58
2	347.108	436.764	-2801.56
3	347.109	436.702	-2801.56
4	344.635	436.64	-2781.59

Table D-24. Calculated Drift for Top of the Columns

Node	14	18	23	27
Long. drift (%)	0.2577	0.2577	0.2577	0.2577
Trans. drift (%)	0.5643	0.5684	0.5684	0.5643

Nonlinear CIP Bridge Model

The nonlinear models of the Dubois bridge with node and element placement are shown in Figures D-25 and D-26, respectively.

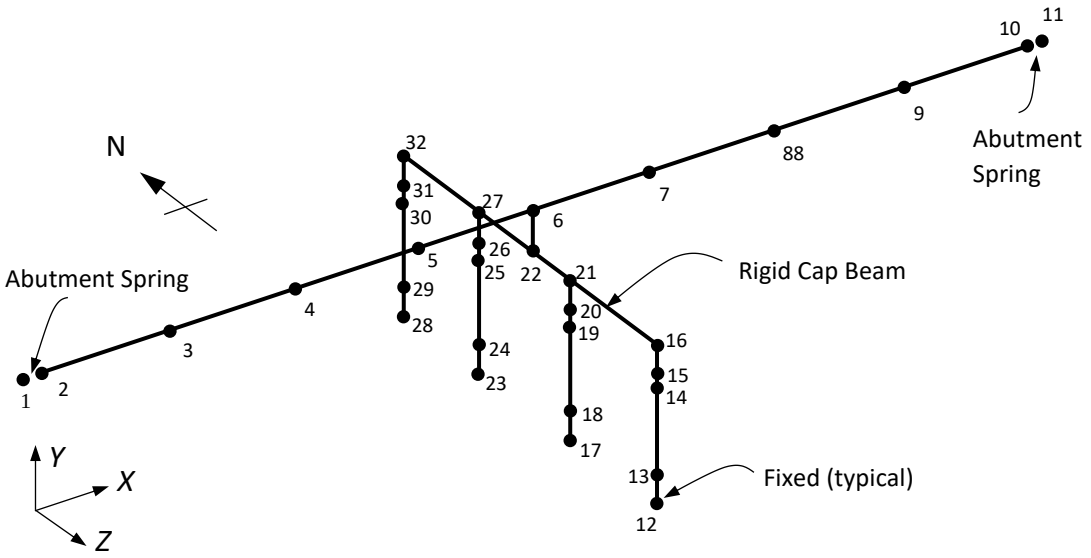

Figure D-25. Nonlinear CIP Model of the Bridge with Node Numbers

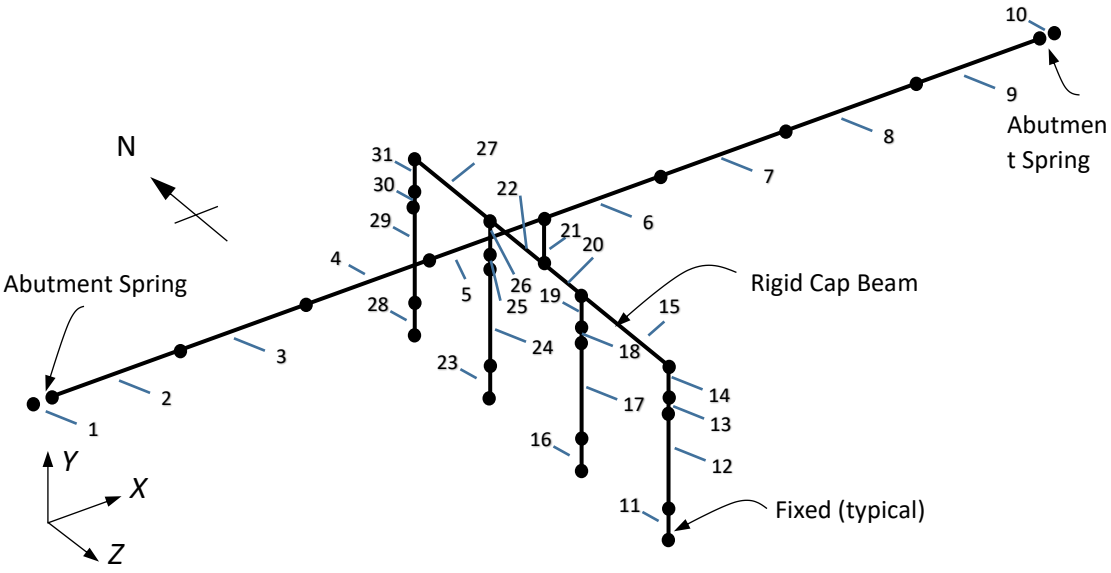

Figure D-26. Nonlinear CIP Model of the Bridge with Element Numbers

Bond-slip Rotation Parameters

The rotation caused by the bond-slip at the base of the column is modeled using a rotational spring with a *Hysteretic* material behavior. The calculation process for obtaining the moment-rotation (M-θ) curve and the moment-curvature input file are presented in Appendix B. Using the approach outlined in Appendix B, Table E-25 shows the moment and rotation values corresponding to the points labeled (M_1^+, θ_1^+) and (M_2^+, θ_2^+) in Figure 3-3 of Chapter 3. The same values were used in both the "push" and "pull" directions.

Table D-25. Ends of the Column Bond-slip Moment-rotation Values for Dubois Bridge

	Moment (kip-ft)	**Rotation (rad)**
Point 1	1,700	0.0020
Point 2	1,947	0.0197

Nonlinear CIP Analysis Results

Tables D-26 and D-27 show the displacements and column base reactions for the longitudinal and transverse directions, respectively. The drift in the longitudinal and transverse directions for top of the columns are shown in Table D-28.

Table D-26. Displacements and Column Base Reactions for Seismic Loads in the Longitudinal Direction

Nodes	Displacement (ft.)
Deck	
2	0.04668
3	0.04734
4	0.04776
5	0.04793
6	0.04787
7	0.04793
8	0.04776
9	0.04734
10	0.04668
Columns	
14	0.03514
19	0.03514
25	0.03514
30	0.03514

Columns	Shear (k)	Axial (k)	Moment (k-ft)
1	-118.191	436.834	991.367
2	-118.191	436.834	991.367
3	-118.191	436.834	991.367
4	-118.191	436.834	991.367

Table D-27. Displacements and Column Base Reactions for Seismic Loads in the Transverse Direction

Nodes	Displacement (ft.)
Deck	
2	0.11219
3	0.11300
4	0.11450
5	0.11585
6	0.11702
7	0.11828
8	0.11906
9	0.11908
10	0.11885
Columns	
14	0.11620
19	0.11661
25	0.11661
30	0.11620

Columns	Shear (k)	Axial (k)	Moment (k-ft)
1	-245.304	437.091	-1748.62
2	-245.346	437.237	-1749.04
3	-245.346	437.228	-1749.06
4	-245.303	437.087	-1748.69

Table D-28. Calculated Drift for Top of the Columns

Node	14	19	25	30
Long. drift (%)	0.2501	0.2501	0.2501	0.2501
Trans. drift (%)	0.8270	0.8300	0.8300	0.8270

Nonlinear Model with Grouted Couplers

The nonlinear models of the Dubois bridge with grouted couplers are shown in Figures D-27 and D-28, respectively.

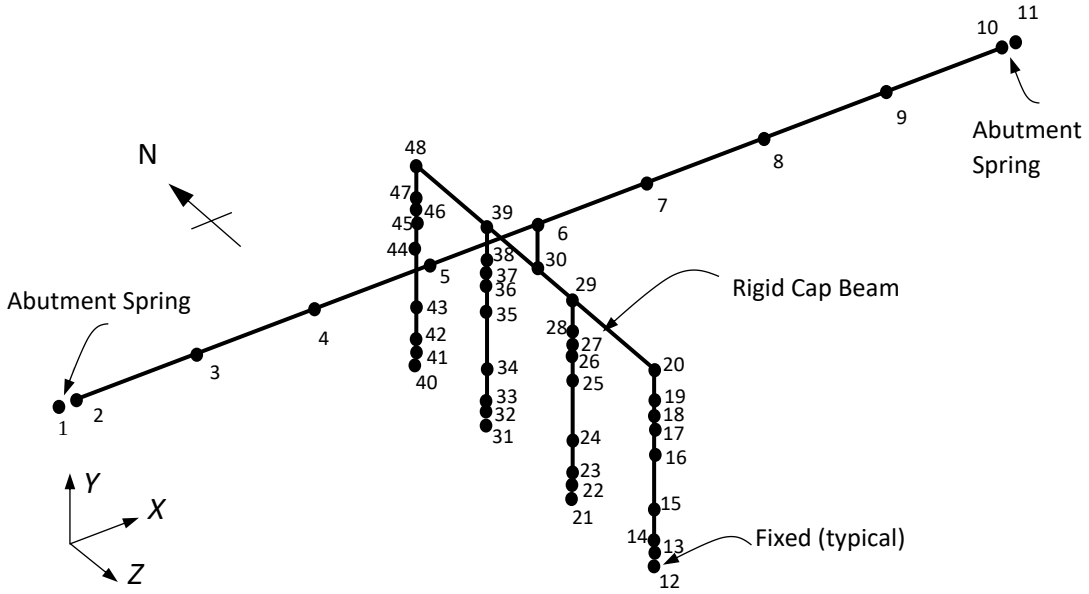

Figure D-27. Nonlinear Model with Grouted Couplers Showing Node Numbers

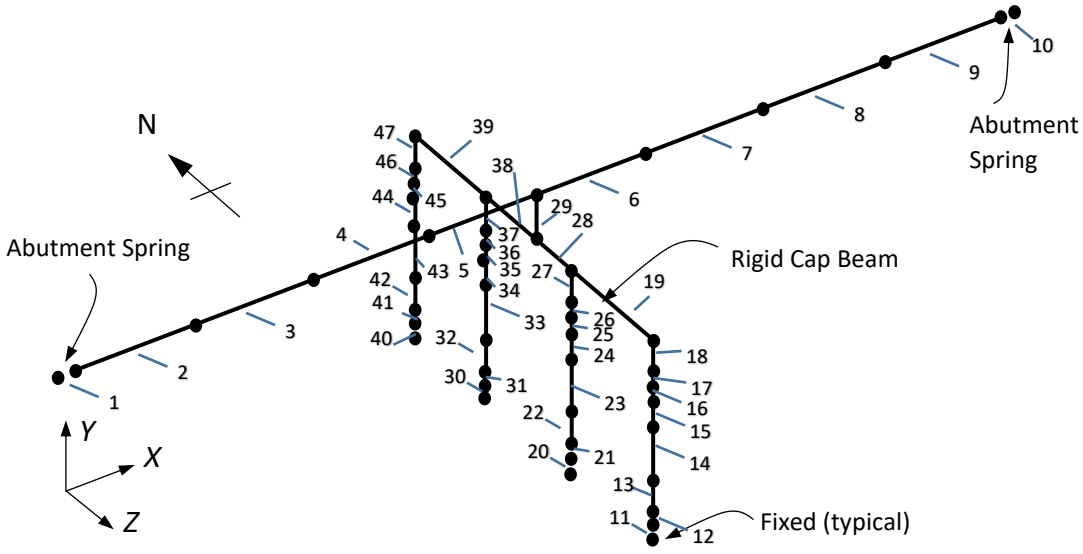

Figure D-28. Nonlinear Model with Grouted Couplers Showing Element Numbers

Results for Nonlinear Model with Grouted Couplers

Tables D-29 and D-30 show the displacements and column base reactions for the longitudinal and transverse directions, respectively. The drift in the longitudinal and transverse directions for top of the columns are shown in Table D-31.

Table D-29. Displacements and Column Base Reactions for Seismic Loads in the Longitudinal Direction

Nodes	Displacement (ft.)
Deck	
2	0.04678
3	0.04744
4	0.04786
5	0.04803
6	0.04797
7	0.04803
8	0.04786
9	0.04744
10	0.04678
Columns	
17	0.03534
26	0.03534
36	0.03534
45	0.03534

Columns	Shear (k)	Axial (k)	Moment (k-ft)
1	-117.191	436.833	981.169
2	-117.191	436.833	981.168
3	-117.191	436.832	981.168
4	-117.191	436.832	981.168

Table D-30. Displacements and Column Base Reactions for Seismic Loads in the Transverse Direction

Nodes	Displacement (ft.)
Deck	
2	0.11227
3	0.11309
4	0.11459
5	0.11595
6	0.11711
7	0.11838
8	0.11916
9	0.11918
10	0.11894
Columns	
17	0.12287
26	0.12328
36	0.12328
45	0.12287

Columns	Shear (k)	Axial (k)	Moment (k-ft)
1	-245.03	437.101	-1746.84
2	-245.073	437.235	-1747.27
3	-245.073	437.235	-1747.29
4	-245.03	437.091	-1746.92

Table D-31. Calculated Drift for Top of the Columns

Node	17	26	36	45
Long. Drift (%)	0.2515	0.2515	0.2515	0.2515
Trans. Drift (%)	0.8745	0.8774	0.8774	0.8745

Three-span Bridge on SH-75 over Salmon River East of Clayton

The bridge over the Salmon River east of Clayton is a 260 foot three-span bridge with two piers located 90 feet and 210 feet from the south end of the bridge. The skew in the bridge was removed to make it easier to model. The overall dimensions of the bridge were maintained and the pier cap and abutment lengths were shortened to match the deck width of 43.542 ft. The superstructure is made up of 8-½" precast deck panels and five 72" prestressed bulb-tee girders. The substructure has a pier cap and a single oval column which rests on a cast-in-place footing in each pier. The pier caps and columns are made of precast concrete.

Spring Support Condition

Support stiffness: Springs at abutments, fixed column bases
Abutment type: Integral
Restraint of superstructure: Abutments with springs in longitudinal and transverse directions, unrestrained rotation about the C. L. abutment.

Soil Spring Stiffness

The south abutment wall has ten 14X117 H-piles. The north abutment wall has eight 14X117 H-piles. Each H-pile is oriented with its strong axis parallel to the abutment wall length and its weak axis perpendicular to the abutment wall length. Both walls have the same dimensions which are:

H_{aw} = 11.375' Height of abutment wall

L_{aw} = 43.542' Length of abutment wall

The soil spring stiffness for the H-piles were derived from the Phase IV Foundation Investigation Report for the Salmon River Bridge. Figures 1 and 2 show force and deflection up to 50 ft of depth for one H-pile. Since spring stiffness equals force divided by deflection ($K = F/d$) the spring stiffness can be estimated by determining the force at 1 in of deflection. About the strong axis the force at 1 in of deflection is 116 kip, and about the weak axis the force at 1 in of deflection is 72 kip.

k_s = 116 kip/in = 1,392 kip/ft.

k_w = 72 kip/in = 864 kip/ft.

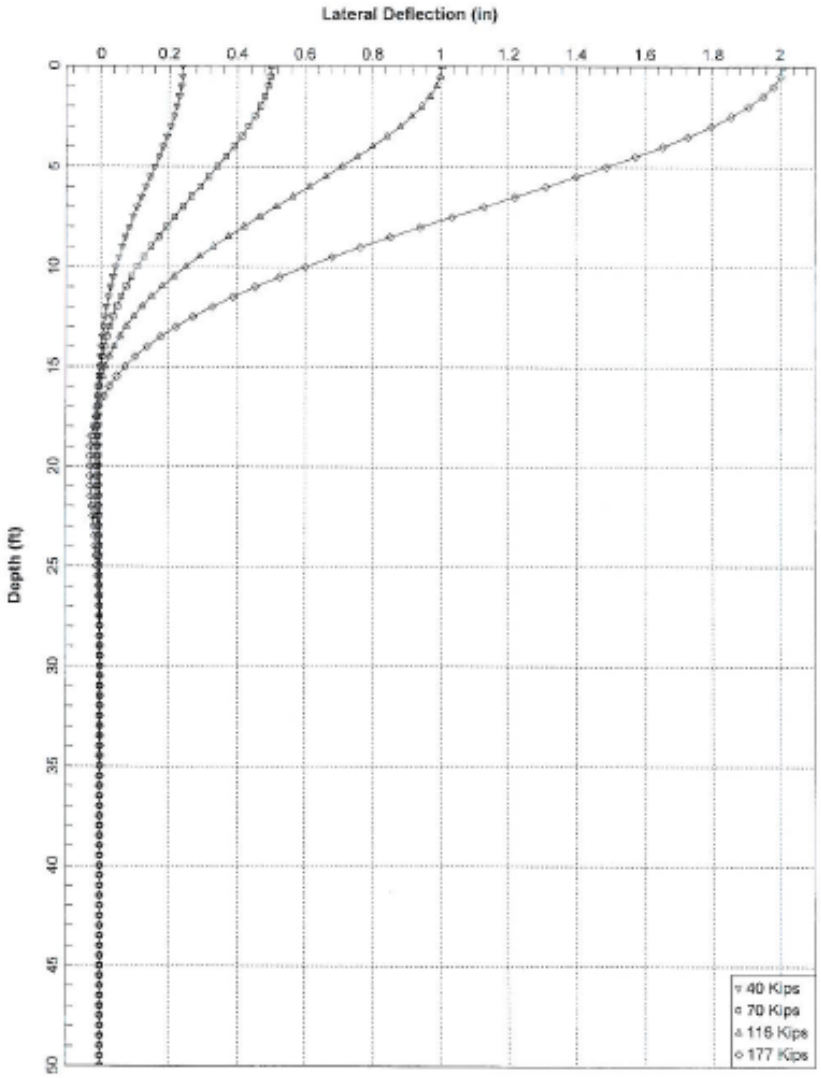

Figure D-29. Lateral Deflection vs. Depth of an H-Pile in the Abutment about the Strong Axis

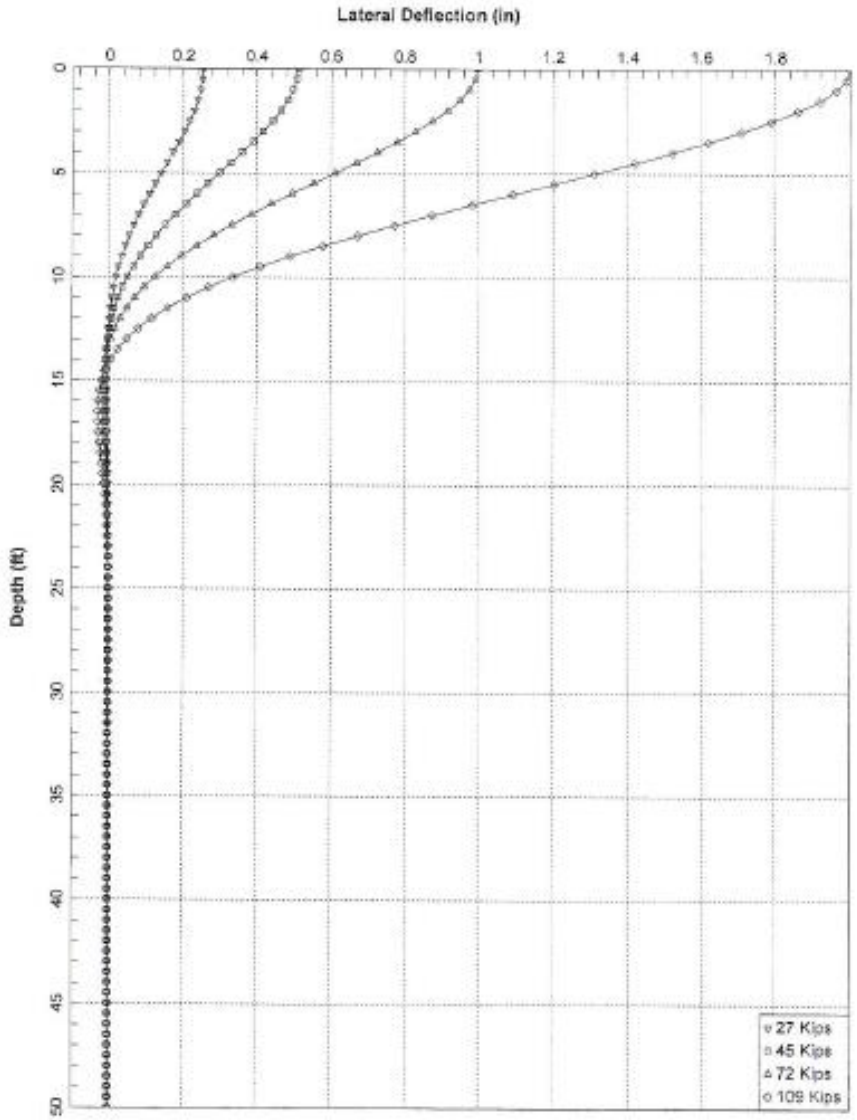

Figure D-30. Lateral Deflection vs. Depth of an H-Pile in the Abutment about the Weak Axis

The initial value due to abutments spring stiffness in the longitudinal direction is calculated by

$$K_l = \frac{n_s k_s + n_n k_s + (7.7 A_{aw}/d)}{2} \quad \text{(D-25)}$$

Where

K_l = the abutments spring stiffness in the longitudinal direction
n_s = the number of H-piles south abutment wall =10
n_n = the number of H-piles north abutment wall = 8
k_s = the initial spring stiffness for one H-pile about the strong axis = 1,392 kip/ft
A_{aw} = the area of the abutment wall = H_{aw} L_{aw} = 495.29 ft^2
d = deflection needed to mobilize full passive resistance = 0.02H_{aw} = 0.23 ft.

Initial value for the soil spring stiffness in the transverse direction at the south abutment is calculated by

$$K_{ts} = n_s k_w \quad \text{(D-26)}$$

Where:
K_{ts} = the initial spring stiffness in the transverse direction at the south abutment

k_w = the initial spring stiffness of one H-pile about the weak axis = 72 kip/in

The shear strength of the wingwall (V_c) can be used to resist the transverse seismic forces if those forces do not exceed the shear strength.

$$V_c = 0.0316\beta\sqrt{f_c'}\,b_v d_v \quad \text{(D-27)}$$

Where:
β = 2
f'_c = compressive strength of concrete of the closure pour = 4.0 ksi
b_v = the height of the wingwall = 128 in
d_v = greater of 0.9d_e or 0.72h = 8.6625 in
h = the depth of the wingwall = 12 in
d_e = the distance to the center of the back reinforcement from the face of the wingwall = 9.625 in

V_c = 140.15 kips

Initial value for the soil spring stiffness in the transverse direction at the north abutment is calculated by

$$K_{tn} = n_n k_w \quad \text{(D-28)}$$

Where:

K_{tn} = the initial spring stiffness in the transverse direction at the north abutment

K_l = 20,818.7 kip/ft	spring stiffness at abutments in the longitudinal direction
K_{ts} = 8,640 kip/ft	spring stiffness at south abutment in transverse direction
K_{tn} = 6,912 kip/ft	spring stiffness at north abutment in transverse direction

A large spring stiffness (1e12) was used for all other DOF's except the rotation about the C. L. abutments, which were assigned a value of zero.

Superstructure

Properties of the superstructure and its elements are as follows

L_d = 260'-0" Overall length of bridge

A_{sup} = 56.9 ft^2 Gross cross-sectional area of superstructure with curb, to be used for weight calculations

f'_{cCIP} = 4.0 ksi Compressive strength of cast-in-place concrete

$f'_{cPrecast}$ = 5.0 ksi Compressive strength of precast concrete

$f'_{cPrestressed}$ = 7.0 ksi Compressive strength of prestressed concrete

$E_{CIP} = 33000*0.145^{1.5}\sqrt{f'_c} = 33000(0.145^{1.5})\sqrt{4.0} = 3{,}644$ ksi

Modulus of elasticity of cast-in-place concrete

$E_{Precast} = 33000*0.145^{1.5}\sqrt{f'_c} = 33000(0.145^{1.5})\sqrt{5.0} = 4{,}074$ ksi

Modulus of elasticity of precast concrete

$E_{Prestressed} = 33000(0.14+0.001f'_c)^{1.5}\sqrt{f'_c} = 33000(0.14+(0.001*7.0))^{1.5}\sqrt{7.0} = 4{,}921$ ksi

Modulus of elasticity of prestressed concrete

To create a transformed moment of inertia for the superstructure the value of I_z and I_y of the deck is divided by the modular ratio *n* before the moment of inertia of the composite section is calculated. The section properties of the curbs are ignored in these calculations.

$n = E_{Prestressed}/E_{Precast} = 4921/4074 = 1.208$

Modular ratio of elasticity

I_{yd} = 4034 ft^4 Transformed moment of inertia of the deck about the y axis

I_{zd} = 1.068 ft^4 Transformed moment of inertia of the deck about the z axis

The distance from the bottom of the superstructure to the centroid of the girder is 34.34 in. The distance from the bottom of the superstructure to the centroid of the deck is 76.25 in. The centroid of the superstructure was calculated to be 55.17 in from the bottom of the superstructure.

The moments of inertia of each section (the girders and the deck) of the superstructure were added to the area of the section which was multiplied by the distance between the centroid of the section and the centroid of the superstructure. These values were totaled to give the transformed moment of inertia for the superstructure. The transformed area of the superstructure was obtained by dividing the gross area of the deck, without the curbs, by the modular ratio, n, and adding it to the areas of the girders.

I_{ysup} = 8383.7 ft^4 Transformed moment of inertia of the superstructure about the y axis

I_{zsup} = 273.3 ft^4 Transformed moment of inertia of the superstructure about the z axis

A_T = 51.38 ft^2 Transformed area of the superstructure

The torsional moment of inertia is calculated by

$$J = \frac{A^4}{40 I_p} \quad \text{(AASHTO LRFD Specifications eq. C 4.6.2.2.1-2)} \qquad \text{(D-29)}$$

Where:

J = Torsional moment of inertia

I_p = Polar moment of inertia = $I_x + I_y$ = 8383.7 ft^4 + 273.3 ft^4 = 8657.0 ft^4

J_{sup} = (51.38 ft^2)^4/40(8657.0 ft^4) = 20.13 ft^4

Where:

ν = Poisson's ratio, typically from 0.15 - 0.2.

$G_{Precast}$ = 4074/2(1+0.2) = 1,697.5 ksi = 244,440 ksf

$G_{prestressed}$ = 4921/2(1+0.2) = 2050.4 ksi =295,260 ksf

Substructure

Properties of the substructure and its elements are as follows

L_p = 43.542 ft Length of pier cap

A_{pxz} = 174.17 ft^2 Cross-sectional area of pier cap in the x-z plane

L_1 = 15.469 ft Southwest column height

L_2 = 15.969 ft Northeast column height

W_c = 3.50 ft Column width

L_c = 9.50 ft Column length

A_{cg} = 30.62 ft^2 Cross-sectional area of one column

I_{cy} = 199.8 ft^4 Gross moment of inertia of one column about the y axis

I_{cz} = 28.80 ft^4 Gross moment of inertia of one column about the z axis

Column Reinforcement

The columns are reinforced with 34 #11 bars within 4 #5 spirals in the main part of the column. The spiral reinforcing has a 4" pitch. At the base of the column there are 34 splice sleeves within 5 sets of 4 #5 hoops as shown in Figure D-31.

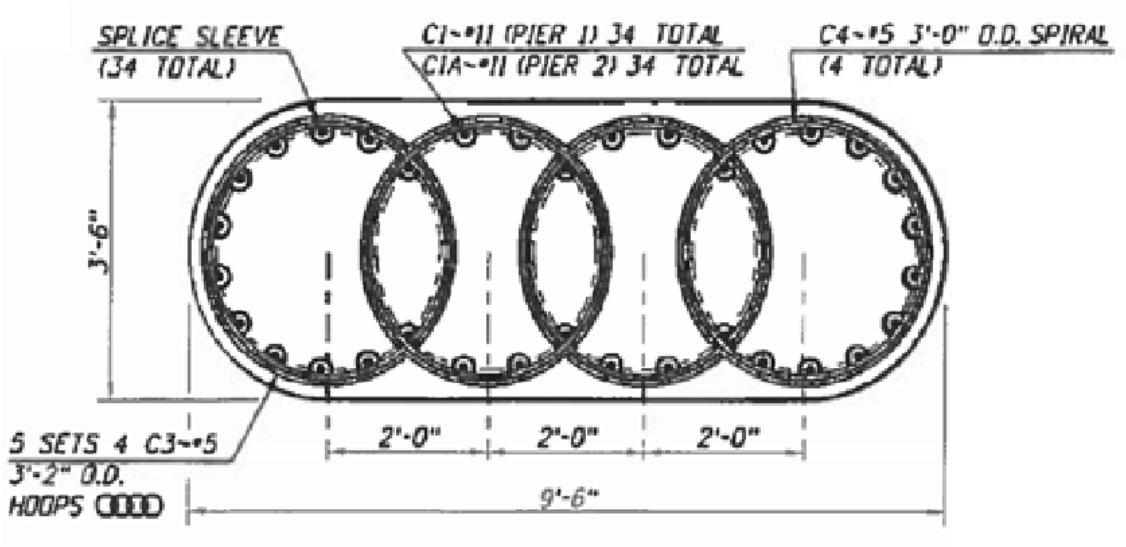

Figure D-31. Reinforced column detail.

A_{r11} = 1.56 in^2 = 0.01083 ft^2 Cross-sectional area of a #11 bar

d_{r11} = 1.410 in = 0.1175 ft Diameter of a #11 reinforcing bar

d_s = 0.625" Diameter of #5 spiral reinforcing

$A_{st11} = 34A_{r11}$ = 0.3683 ft^2 Total longitudinal steel in one column

Effective Moment of Inertia and Torsional Moment of Inertia of the Columns

For the effective moment of inertia the gross moment of inertia is multiplied by the Elastic Stiffness Ratio (I_{eff}/I_{cg}). This is obtained from Figure D-32 with the Axial Load Ratio and the ratio of reinforcing steel to concrete.

$Axial\ Load\ Ratio = P/f'_cA_{cg}$

Where

P = the axial load to the column from the self-weight of the bridge

The axial load on one column is from half the weight of each span that the column supports plus the weight on the node in the pier cap above the column plus half the weight of one column. The dead load to each node is given in Table D-32.

Table D-32. Weight of Structure to nodes from deck, pier cap, and top half of columns

Section	x-sec. Area (ft^2)	Length (ft)	Weight of Concrete ($kips/ft^3$)	Wearing Surface and Utilities/Future Utilities (klf)	Braces (kips)	Weight to Node (kips)
Deck						
Node 101	56.9	15	0.15	2.607	1.4	168.53
Node 102	56.9	30	0.15	2.607	1.4	335.66
Node 103	56.9	30	0.15	2.607	1.4	335.66
Node 104	56.9	30	0.15	2.607	1.4	335.66
Node 105	56.9	30	0.15	2.607	1.4	335.66
Node 106	56.9	30	0.15	2.607	1.4	335.66
Node 107	56.9	30	0.15	2.607	1.4	335.66
Node 108	56.9	27.5	0.15	2.607	1.4	307.81
Node 109	56.9	25	0.15	2.607	1.4	279.95
Node 110	56.9	12.5	0.15	2.607	1.4	140.68
Pier Cap 1						
Node 203	141.03	8	0.15	N/A	N/A	169.24
Pier Cap 2						
Node 303	141.03	8	0.15	N/A	N/A	169.24
Top Half of Columns						
Node 203	30.62	7.73	0.15	N/A	N/A	35.50
Node 303	30.62	7.98	0.15	N/A	N/A	36.65
				Total Weight of Bridge		3321.55
				w(x) (kip/ft)		12.78

Effective moment of inertia for southwest column

P = 1,379.55 kips

f'_c = 720 ksf

A_{cg} = 30.62 ft^2

P/f'_cA_{cg} = 1,379.55 kips/720 ksf * 30.62 ft^2 = 0.063

A_{st}/A_{cg} =0.3683 ft^2/30.62 ft^2 = 0.012

I_{eff}/I_{cg} = 0.36

I_{ceffy} = 0.36 * I_{cy} = 71.93 ft^4 Effective moment of inertia about the y axis

I_{ceffz} = 0.36 * I_{cz} = 10.37 ft^4 Effective moment of inertia about the z axis

Effective moment of inertia for north column

P = 1,157.16 kips

P/f'_cA_{cg} = 1,157.16 kips/720 ksf * 30.62 ft^2 = 0.052

I_{eff}/I_{cg} = 0.35

I_{ceffy} = 0.35 * I_{cy} = 69.93 ft^4 Effective moment of inertia about the y axis

I_{ceffz} = 0.35 * I_{cz} = 10.08 ft^4 Effective moment of inertia about the z axis

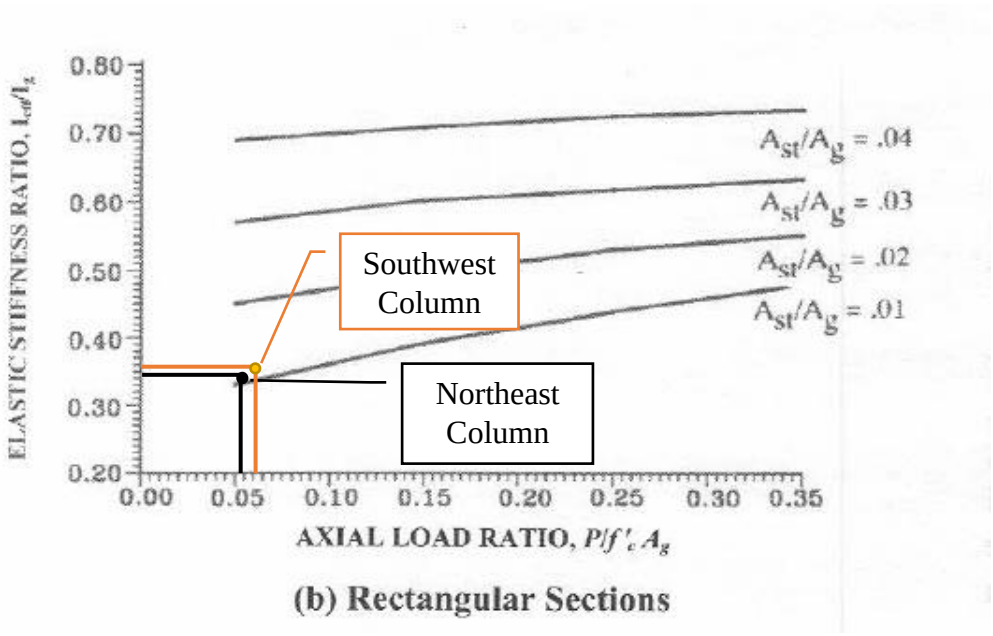

Figure D-32. Elastic Stiffness Ratio (AASHTO 2015)

$$J_{gross} = \beta ab^3 \quad \text{(D-30)}$$

Where:

β = 0.249

a = 8.75 ft

b = 3.5 ft

J_{gross} = 93.4 ft^2 Gross torsional moment of inertia

$J_{eff} = 0.2J_{gross} = 18.68\ ft^4$ Effective torsional moment of inertia

Linear Elastic Model of the Structure

The bridge has three spans of different lengths. The first span, beginning at the centerline of the south abutment and ending at the centerline of the south pier, is 90 ft and is divided into three elements that are 30 ft long. The second span, beginning at the centerline of the south pier and ending at the centerline of the north pier, is 120 ft and has four elements that are 30 ft long. The third span, beginning at the centerline of the north pier and ending at the centerline of the north abutment, is 50 ft and has two elements that are 25 ft long.

The piers consist of a single column that is precast with a column cap at the top and a cast-in-place footing that is 5 ft deep. There is a rigid element that joins the superstructure with the column caps that starts at the centroid of the superstructure and ends at the top of the column cap (4.60 ft). There is one element that is representative of the column cap which begins at the top of the column cap and ends at the top of the column (8.042 ft). The length of the south column is 15.47 ft and the length of the north column is 15.97 ft. The element at the base of the column is representative of the footing and begins at the base of the column and ends at the midpoint of the footing (2.5 ft). The footing element is modeled with the same properties as the column. To model the spring support condition an extra node and zeroLength element is assigned to the abutment ends of the superstructure

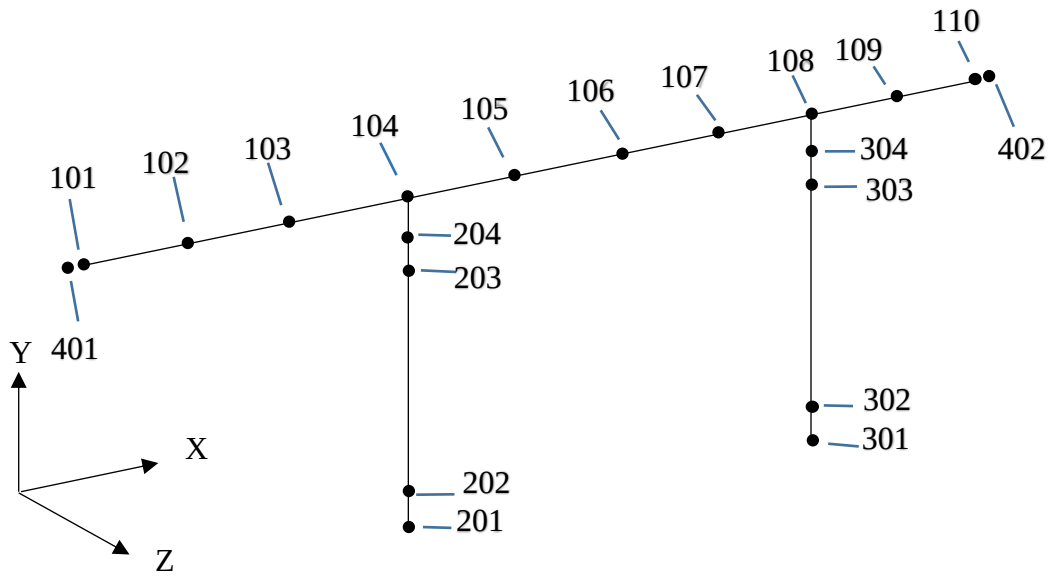

Figure D-33. Linear elastic bridge model with node numbers

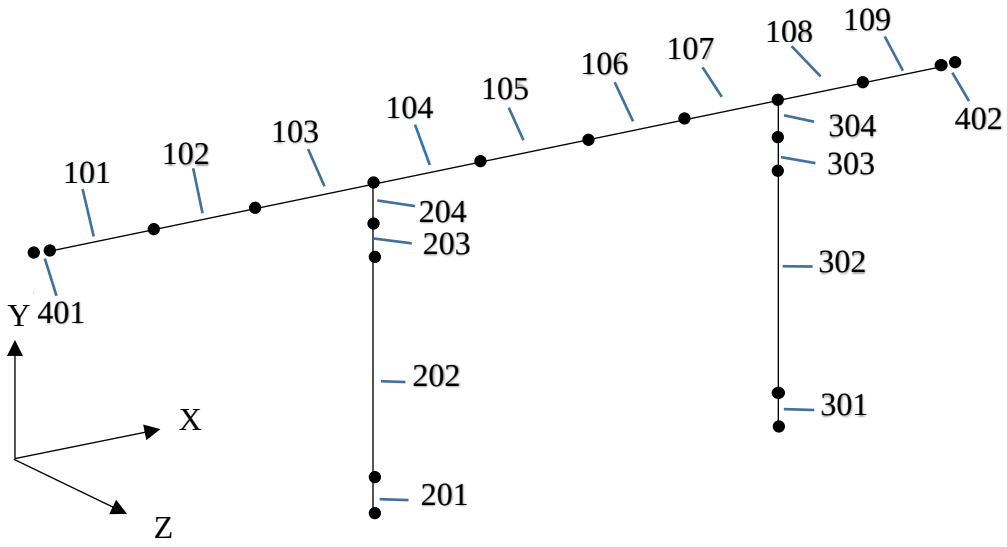

Figure D-34. Linear elastic bridge model with element numbers

Geometric transformation

The geometric transformations used for the Salmon River bridge are the same as those used for the Parma bridge.

Calculation of Seismic Loads

The same USGS seismic design summary report data as given in Figure E-8 is also used for the Salmon River bridge. To calculate the seismic loads on the deck of the bridge the displacements at the deck nodes from a uniformly distributed load of 10 kip/ft in the longitudinal and transverse direction are determined and used to calculate the factors α, β, and γ. The factors are used to calculate the loads (*pe (x)*) at the nodes on the deck. The distributed seismic loads on each element is the average of the loads on the nodes. These loads are shown in column 9 of Tables D-33 and D-34.

$$\alpha = \int_0^L v_s(x)\, dx \quad \text{(E-31)}$$

$$\beta = \int_0^L w(x) v_s(x) dx \quad \text{(E-32)}$$

$$\gamma = \int_0^L w(x) v_s\,(x)^2 dx \quad \text{(E-33)}$$

Where

$v_x\,(x)$ = Displacement due to a uniformly distributed load of 10 kip/ft.
$w(x)$ = Weight of the bridge per unit length = 12.70 kip/ft
dx = Tributary length

L = Total length of bridge

$p_e(x) = \beta C_{sm} w(x) * v_s(x) / \gamma$

Where

$C_{sm} = S_{DS} = 0.907$ for $T_o < T_m < T_s$ and

Where

$T_m = 2\pi\sqrt{\gamma / P_0 g \alpha} = 0.260$s for longitudinal loads

$T_m = 2\pi\sqrt{\gamma / P_o g \alpha} = 0.411$s for transverse loads

$T_s = S_{D1}/S_{DS} = 0.5358$

$T_o = 0.2T_s = 0.1072$

$g = 32.2$ ft/s^2

$P_o = 10$ kip/ft

Table D-33. Calculation of Seismic Loads in the Longitudinal Direction

Nodes	x (ft)	dx (ft)	vs(x) (ft)	α(x) (ft^2)	β(x) (k-ft)	γ(x) (k-ft^2)	pe(x) (k/ft)	ave. (k/ft)
101	0.00	0.00	0.0426	0.000	0.000	0.000	11.420	
102	30.00	30.00	0.0432	1.288	16.359	0.702	11.582	11.501
103	60.00	30.00	0.0436	1.303	16.544	0.718	11.679	11.631
104	90.00	30.00	0.0437	1.310	16.634	0.726	11.709	11.694
105	120.00	30.00	0.0439	1.314	16.683	0.730	11.748	11.729
106	150.00	30.00	0.0438	1.314	16.690	0.731	11.720	11.734
107	180.00	30.00	0.0434	1.307	16.604	0.724	11.626	11.673
108	210.00	30.00	0.0428	1.293	16.423	0.708	11.466	11.546
109	235.00	25.00	0.0425	1.066	13.537	0.577	11.374	11.420
110	260.00	25.00	0.0420	1.055	13.401	0.566	11.237	11.305
	Totals	260.00		11.250	142.874	6.183		

Table D-34. Calculation of Seismic Loads in the Transverse Direction

Nodes	x (ft)	dx (ft)	vs(x) (ft)	α(x) (ft^2)	β(x) (k-ft)	γ(x) (k-ft^2)	pe(x) (k/ft)	ave. (k/ft)
101	0	0	-0.101	0.000	0.000	0.000	10.824	
102	30.00	30.00	-0.103	-3.063	-38.898	3.971	11.026	10.925
103	60.00	30.00	-0.107	-3.146	-39.958	4.191	11.420	11.223
104	90.00	30.00	-0.110	-3.255	-41.334	4.484	11.799	11.609
105	120.00	30.00	-0.113	-3.345	-42.478	4.736	12.062	11.931
106	150.00	30.00	-0.113	-3.384	-42.974	4.847	12.078	12.070
107	180.00	30.00	-0.110	-3.350	-42.543	4.750	11.820	11.949
108	210.00	30.00	-0.107	-3.256	-41.348	4.487	11.407	11.613
109	235.00	25.00	-0.104	-2.630	-33.399	3.513	11.107	11.257
110	260.00	25.00	-0.103	-2.579	-32.759	3.380	10.975	11.041
	Totals	260.00		-25.428	-322.933	34.981		

Determination of Final Soil Spring Stiffness

The final estimations of the bridge transverse and longitudinal abutment stiffness values are accomplished with an iterative process. In the longitudinal direction the backfill behind the abutment wall as well as the embedded piles resist the seismic forces at the ends of the deck. The following procedure is used to achieve a correlation between these.

8. Determine the displacements and reactions at the end nodes of the deck.
9. Add the reactions from both abutments
10. Determine the force that each pile resists based on the displacements and multiply it by the total number of piles from both abutments
11. Determine the wall demand by subtracting the pile resistance from the total reaction
12. Compare the displacement at the end nodes to $0.02H_{aw}$
    a. If it is greater – the wall capacity is $7.7A_{aw}$
    b. If it is smaller – the wall capacity is calculated by a linear interpolation

    $$F = \Delta\left(\frac{7.7A_{aw}}{d}\right)$$

        i. F = the wall capacity
        ii. Δ = the displacement of the end node
13. Compare the wall demand to the wall capacity
    a. If it is greater – increase abutment stiffness
    b. If it is smaller – decrease abutment stiffness
14. Repeat process until the combined wall capacity and pile resistance is within 10% of the value of the reactions.

Table D-35. Results of Longitudinal Soil Spring Estimations

Longitudinal Displacements (ft)					
Iteration	node 1	node 10	Total Reaction (Kip)	K_l (kip/ft)	Correlation (%)
1	0.0495	0.0488	2046.88	20,819	12.38
2	0.0452	0.0445	2123.6	23672	0.17

The transverse abutment stiffness values depend on the resistance of the piles in each abutment wall and the shear strength of the wingwall. Since the initial stiffness is determined as the pile resistance in each abutment the shear resistance is only considered if the seismic demand exceeds the pile resistance. The procedure for determining the transverse resistance is as follows.

6. Determine the displacements and reactions at the end nodes, nodes 401 and 402, of the deck
7. Based on the displacements determine the force that one pile resists
8. Multiply the force that one pile resists by the number of piles in each abutment
9. Compare the force that the piles from each abutment resists plus the shear strength to the reaction of the corresponding node
    a. If it is greater – the wingwall can be assumed to have broken off and only the piles are resisting the seismic forces, increase abutment stiffness
    b. If it is smaller – decrease abutment stiffness
10. Repeat procedure until the pile resistance is within 10% of the abutment reaction

Table D-36. Results of Transverse Soil Spring Estimations

Transverse Displacements (ft)			Reactions (kip)				Correlation (%)	
Iteration	node 1	node 10	node 401	node 402	K_{ts} (kip/ft)	K_{tn} (kip/ft)	node 1	node 10
1	0.1162	0.118	-1004.0	-818.4	8640	6912	15.41	16.25
2	0.1185	0.120	-995.0	-808.9	8400	6720	14.37	14.9
3	0.1311	0.131	-943.7	-756.4	7200	5760	0.4	0.58

As a check, the final abutment stiffness values were used in the OpenSees program with the uniformly distributed load used for calculating the seismic loads to see how the new stiffness values would affect the calculation of the seismic loads. The results are shown in Tables D-37 and D-38. The difference in the transverse values was no more than 1.7% and the difference in the longitudinal values was no more than 0.27%.

Table D-37. Comparison of Updated and Original Longitudinal Design Loads

Updated Design Load (k/ft)	Original Design Load (k/ft)
11.477	11.501
11.627	11.631
11.705	11.694
11.746	11.729
11.752	11.734
11.686	11.673
11.547	11.546
11.407	11.42
11.275	11.305

Table D-38. Comparison of Updated and Original Transverse Design Loads

Updated Design Load (k/ft)	Original Design Load (k/ft)
11.111	10.925
11.344	11.223
11.642	11.609
11.886	11.931
11.981	12.07
11.856	11.949
11.553	11.613
11.240	11.257
11.055	11.041

Displacement Results and Column Drift of Linear elastic model

Column drift is defined as the displacement at the top of a column under a lateral load divided by the column height. The resulting longitudinal and transverse displacements at all of the superstructure nodes and at the top of the columns with the revised abutment stiffness values are shown in Tables D-39 and D-34.

Table D-39. Longitudinal Displacement of Column and Superstructure Nodes

node	101	102	103	104	105	106	107	108	109	110	203	303
displacement (ft)	0.045	0.046	0.046	0.047	0.047	0.047	0.046	0.046	0.045	0.044	0.036	0.046

Table D-40. Transverse Displacement of Column and Superstructure Nodes

node	101	102	103	104	105	106	107	108	109	110	203	303
displacement (ft)	0.131	0.133	0.137	0.141	0.143	0.143	0.140	0.136	0.133	0.131	0.063	0.062

The column height of the southwest column is 15.469 ft and the column height of the northeast column is 15.969 ft. The distance from the top of the column to the centroid of the superstructure is 12.642 ft. This added to the column height gives the height of the bridge at that column. The height of the bridge at the southwest column, node 104, is 28.11 ft and at the northeast column, node 108, 28.61 ft. The drift in the longitudinal and transvers directions at nodes 104, 108, 203, and 303 are shown in Table D-41.

Table D-41. Calculated Drift for Selected Nodes

node	104	108	203	303
long. drift (%)	0.1657	0.1592	0.235	0.2909
trans. drift (%)	0.5004	0.4748	0.4074	0.388

Table D-42. Reactions for the Base of the Columns for Longitudinal Loading

Column	Shear (k)	Axial (k)	Moment (k-ft)
SW	-362.50	1488.59	3555.73
NE	-527.31	1280.06	4873.76

Table D-43. Reactions for the Base of the Columns for Transverse Loading

Column	Shear (k)	Axial (k)	Moment (k-ft)
SW	-678.55	1526.14	-20560.3
NE	-618.41	1291.87	-18729.6

Nonlinear Cast-in-place (CIP) Model of the Structure

The non-linear model of the bridge superstructure is the same as that of the linear elastic model. The columns are modeled with a nonlinearBeamColumn and a fiber section which describes the dimensions and properties of the reinforcing steel in the column. Additionally a zeroLength element is placed at the top and bottom of the columns to model bond-slip at the column-footing and column-bent interfaces and the footing is removed from the model.

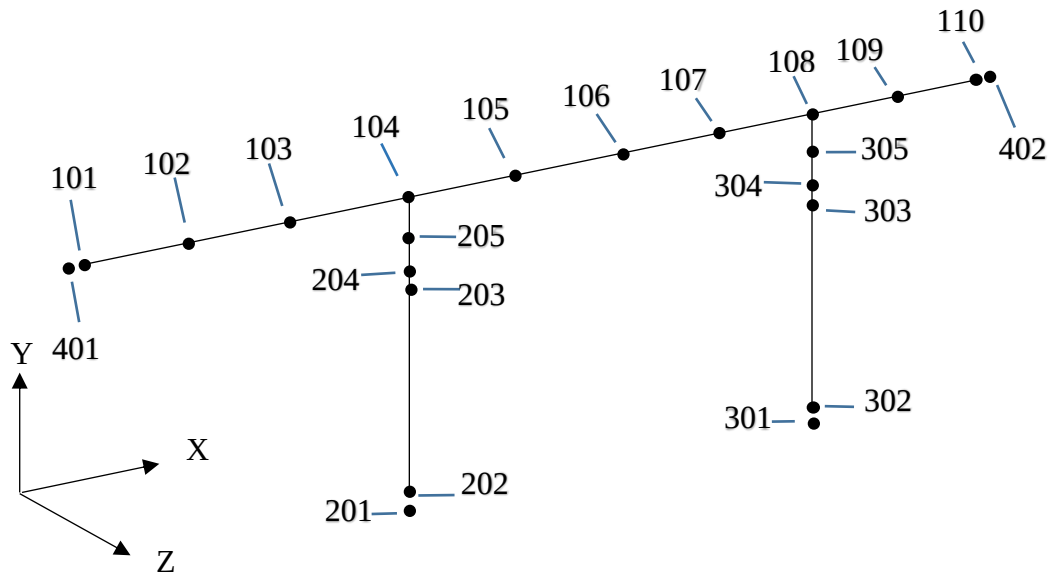

Figure D-35. Nonlinear cast-in-place bridge model with node numbers

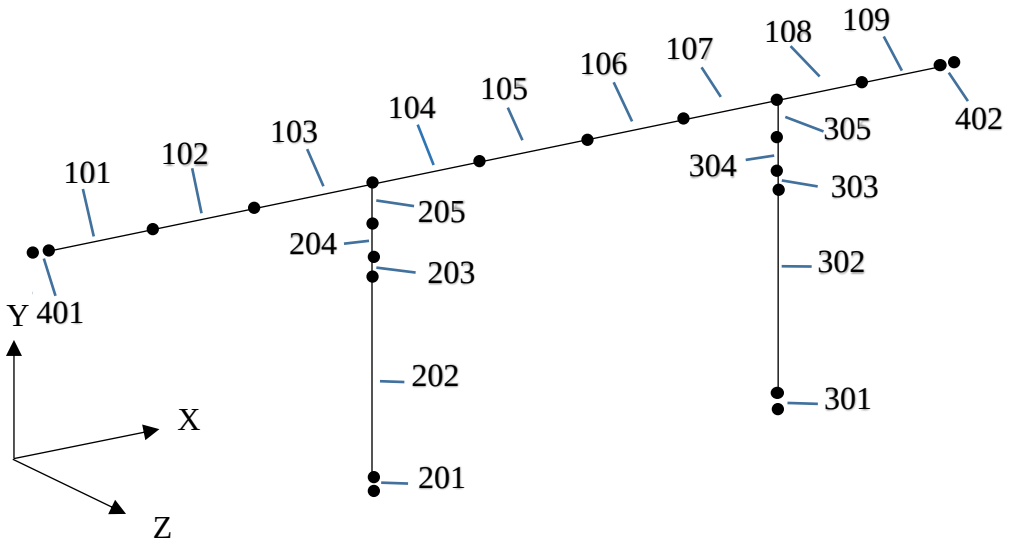

Figure D-36. Nonlinear cast-in-place bridge model with element numbers

Material Properties

Unconfined Concrete

As previously determined the modulus of elasticity, *E*, and the modulus of rigidity, *G*, for precast concrete are:

$E_{Precast}$ = 4,074 ksi = 586,656 ksf Modulus of elasticity of precast concrete

$G_{Precast}$ = 1,697.5 ksi = 244,440 ksf Modulus of rigidity of precast concrete

Peak strain for the 5000 psi concrete is 0.002 and ultimate strain is 0.005.

Reinforcing Steel

The grade of the steel is specified in the plans. For the Salmon River Bridge the steel is Grade 60. The following properties are found in Table 8.4.2-1 in the AASHTO Guide Specifications for LRFD Seismic Bridge Design, 2011, Sec. 8-4.

f_y = 68 ksi = 9,792 ksf

f_u = 95 ksi = 13,680 ksf

The strain for a #11 bar at strain hardening is

e_{sh} = 0.0115

The ultimate strain is

e_u = 0.09

The modulus of elasticity for steel is

E = 29,000 ksi = 4,176,000 ksf

The slope of the line at strain hardening is

E_{sh} = 1247 ksi = 179,568 ksf

Confined Concrete Strength Using Theoretical Stress-Strain Model Developed by Mander et al.

AASHTO Guide Specifications for LRFD Seismic Bridge Design, 2011, Sec. 8.4.4, Concrete Modeling, specifies that confined concrete should be modeled based on Mander's stress-stain model. It also indicates that with equation (8.4.4-1) the compressive strength of confined concrete could be estimated by $f'_{ce} \geq 1.3 f'_c$.

From Mander, et al. (1988a) the compressive strength of confined concrete in a circular column was determined by equation 29:

$$f'_{cc} = f'_{co}\left(-1.254 + 2.254\sqrt{1 + \frac{7.94 f'_l}{f'_{co}}} - 2\frac{f'_l}{f'_{co}}\right) \qquad \text{(D-34)}$$

Where:

f'_{cc} = the confined compressive strength of concrete,

f'_{co}=the unconfined compressive strength of concrete = 5.0 ksi, and

f'_l= the lateral pressure from the transverse reinforcement and is given by equation 19.

$$f'_l = \frac{1}{2} k_e \rho_s f_{yh} \qquad \text{(D-35)}$$

Where:

k_e= The Confinement Effectiveness Coefficient given by equation 15,

ρ_s=The ratio of the volume of transverse confining steel to the volume of the confined concrete core, defined by equation 17, and

f_{yh}= The yield strength of the horizontal reinforcing = 68 ksi.

The Confinement Effectiveness Coefficient for circular spirals is:

$$k_e = \frac{1-\frac{s'}{2d_s}}{1-\rho_{cc}} \quad \text{(D-36)}$$

Where:

s'= The clear vertical spacing between spirals = 3.375 in,

d_s=The diameter of spirals between bar centers = 35.375 in, and

ρ_{cc} =The ratio of the area of the longitudinal steel to the area of the confined concrete.

The ratio of the volume of transverse confining steel to the volume of confined concrete core can be determined by:

$$\rho_s = \frac{4A_{sp}}{d_s s} \quad \text{(D-37)}$$

Where:

A_{sp}=The area of the transverse reinforcing bar = 0.3068 in^2 and

s=The center to center spacing between spirals, or pitch = 4 in.

The ratio of the area of the longitudinal steel to the area of the confined concrete (ρ_{cc}) can be given by:

$$\rho_{cc} = \frac{A_{st}}{A_c} \quad \text{(D-38)}$$

Where:

A_{st}= The area of longitudinal steel = 21.84 in^2 and

A_c= Area of the core of the section enclosed by the center lines of the perimeter

spiral = 982.84 in^2.

In summary:

ρ_s = 0.0087

ρ_{cc} = 0.0222

k_e = 0.9739

f'_l = 0.2787 ksi

f'_{cc} = 6.709 ksi = 966.08 ksf

The strain at maximum strength can be calculated by equation 5:

$$\varepsilon_{cc} = \varepsilon_{co}\left[1 + 5\left(\frac{f'_{cc}}{f'_{co}} - 1\right)\right] \quad \text{(D-39)}$$

Where:

ε_{co} = The strain at maximum strength of unconfined concrete = 0.002.

ε_{cc} = 0.00542

From Paulay and Priestley (1992) the ultimate strain ε_{cu} is defined as the strain at the first fracture of the transverse reinforcement. The following equation can be used to calculate ε_{cu}.

$$\varepsilon_{cu} = 0.004 + \frac{1.4\rho_s f_{yh}\varepsilon_{sm}}{f'_{cc}}$$

Where:

ε_{sm} = The strain of the transverse reinforcement at peak stress = 0.09

ε_{cu} = 0.01475

Modeling Column Reinforcement

The nonlinear model of the Salmon River Bridge requires a section be included in the model of the nonLinearBeamColumn. The section consists of patch commands for the outer unconfined concrete, two circular and two rectangular, and the inner confined concrete, two circular and one rectangular, with fiber commands for each of the 34 steel reinforcement bars. An illustration of the section for the OpenSees file can be seen in Figure D-37.

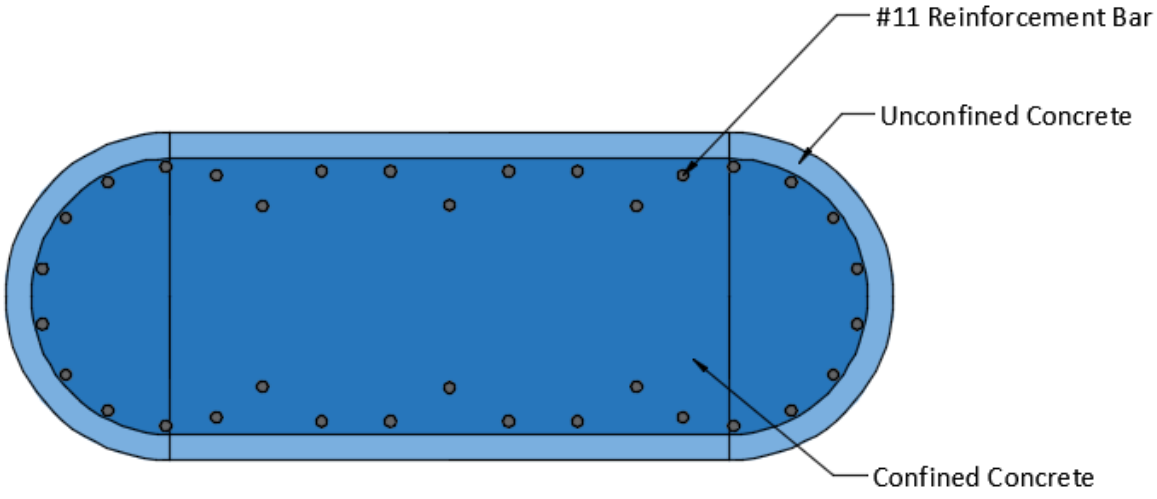

Figure D-37. Cross-section of a Column with Reinforcing

To check the validity of the section for the OpenSees model separate files for a column of confined concrete, a column of steel, and a column of the reinforcing bars only was created. The displacements from each of the columns was compared to hand calculations.

Column Deflection Check with Longitudinal Reinforcing

Hand Calculations

Deflection is calculated by:

$$\Delta = \frac{FL^3}{3EI} \qquad \text{(D-40)}$$

Where:

Δ = deflection in ft

F = force applied to column

L = height of column = 10 ft

E = modulus of elasticity of the material

I = moment of inertia, for the column, $I_z = 28.8\ ft^4$ $I_y = 199.8\ ft^4$

All confined concrete column deflection

E = 586656 ksf

In the Z direction

$\Delta = 1kip\ (10ft)^3/3\ (586656\ ksf)\ (199.8\ ft^4) = 2.84*10^{-6}\ ft$

In the X direction

$\Delta = 1kip\ (10ft)^3/3\ (586656\ ksf)\ (28.8\ ft^4) = 1.97*10^{-5}\ ft$

All steel column deflection

E = 4176000 ksf

In the Z direction

$\Delta = 1kip\ (10ft)^3/3\ (4176000\ ksf)\ (199.8\ ft^4) = 4.0*10^{-7}\ ft$

In the X direction

$\Delta = 1kip\ (10ft)^3/3\ (4176000\ ksf)\ (28.8\ ft^4) = 2.77*10^{-6}\ ft$

Rebar only deflection

$I_z = 0.47082\ ft^4$ $I_y = 3.0854\ ft^4$

In the Z direction

$\Delta = 1kip\ (10ft)^3/3\ (4176000\ ksf)\ (3.0854\ ft^4) = 2.587*10^{-5}\ ft$

In the X direction

$\Delta = 1kip\ (10ft)^3/3\ (4176000\ ksf)\ (0.47082\ ft^4) = 1.695*10^{-4}\ ft$

OpenSees Results for Deflection Check

All confined concrete deflections

In the Z direction

$\Delta = 2.845*10^{-6}\ ft$

In the X direction

$\Delta = 1.983*10^{-5}\ ft$

All steel deflections

In the Z direction

$\Delta = 3.982*10^{-7}\ ft$

In the X direction

$\Delta = 2.777*10^{-6}\ ft$

Rebar only deflection

In the Z direction

$\Delta = 2.578*10^{-5}\ ft$

In the X direction

$\Delta = 1.690*10^{-4}\ ft$

OpenSees tcl Script for Column Deflection Check - All Confined Concrete with Loading in the X Direction

```
#Clear cached data existing in the program

wipe

#Create model with 3 dimensions and 6 degrees of freedom

model BasicBuilder -ndm 3 -ndf 6

#Create Nodes

#     tag   x     y     z
node   1    0.0   0.0   0.0
node   2    0.0   10.0   0.0

#Specify geometric transformation

geomTransf Linear 1  0  0  1

#Fix node 1

fix   1   1   1   1   1   1   1

#Create uniaxial materials for Concrete and Steel

#uniaxialMaterial Concrete01 $matTag $fpc $epsc0 $fpcu $epsU

uniaxialMaterial Concrete01  1  -720.0  -0.002  0  -0.005

#uniaxialMaterial Concrete04 $matTag $fc $ec $ecu $Ec <$ft $et> <$beta>

uniaxialMaterial Concrete04  2  -966.08  -0.005418  -0.01475  586656

#uinaxialMaterial ReinforcingSteel $matTag $fy $fu $Es $Esh $esh $eult

uniaxialMaterial ReinforcingSteel  3  9792  13680  4176000  179568  0.0115  0.09

#Create fiber section with defined concrete and rebar


section Fiber 1  {
#patch circ $matTag $numSubdivCirc $numSubdivRad $yCenter $zCenter $intRad $extRad
<$startAng $endAng>
#patch rect $matTag $numSubdivY $numSubdivZ $yI $zI $yJ $zJ
patch circ  2  44  2   0  3  1.474  1.75   0  180
patch circ  2  44  2   0 -3  1.474  1.75  180 360
patch rect  2  2  44  -1.75  -3  -1.474  3
patch rect  2  2  44   1.474 -3  1.75  3
patch circ  2  44 10  0 -3  0  1.474  180 360
patch circ  2  44 10  0  3  0  1.474  0  180
patch rect  2  20  44  -1.474 -3  1.474  3
#fiber   0.964  2.0    0.01083  3
```

```
#fiber   1.294  2.495  0.01083  3
#fiber   1.386  3.083  0.01083  3
#fiber   1.224  3.656  0.01083  3
#fiber   0.838  4.108  0.01083  3
#fiber   0.297  4.357  0.01083  3
#fiber  -0.964  2.0    0.01083  3
#fiber  -1.294  2.495  0.01083  3
#fiber  -1.386  3.083  0.01083  3
#fiber  -1.224  3.656  0.01083  3
#fiber  -0.838  4.108  0.01083  3
#fiber  -0.297  4.357  0.01083  3
#fiber   0.964 -2.0    0.01083  3
#fiber   1.294 -2.495  0.01083  3
#fiber   1.386 -3.083  0.01083  3
#fiber   1.224 -3.656  0.01083  3
#fiber   0.838 -4.108  0.01083  3
#fiber   0.297 -4.357  0.01083  3
#fiber  -0.964 -2.0    0.01083  3
#fiber  -1.294 -2.495  0.01083  3
#fiber  -1.386 -3.083  0.01083  3
#fiber  -1.224 -3.656  0.01083  3
#fiber  -0.838 -4.108  0.01083  3
#fiber  -0.297 -4.357  0.01083  3
#fiber   1.339  1.368  0.01083  3
#fiber   1.339  0.632  0.01083  3
#fiber   0.977  0.0    0.01083  3
#fiber   1.339 -0.632  0.01083  3
#fiber   1.339 -1.368  0.01083  3
#fiber  -1.339  1.368  0.01083  3
#fiber  -1.339  0.632  0.01083  3
#fiber  -0.977  0.0    0.01083  3
#fiber  -1.339 -0.632  0.01083  3
#fiber  -1.339 -1.368  0.01083  3
}

#setup time series

timeSeries Linear 1

#Create elastic beam column element

element nonlinearBeamColumn  1  1  2  9  1  1

#create recorder files

recorder Node  -file columndispcheckconfinedconcrete_x_dir.out -node 2 -dof 1 disp
recorder Node  -file columndispcheckconfinedconcrete_z_dir.out -node 2 -dof 3 disp

#set loading pattern for vertical loading

pattern Plain 1 1 {
load 2 0 -100 0 0 0 0
}

integrator LoadControl 1
system BandGeneral
test NormDispIncr 1.0e-8  6
numberer Plain
```

```
constraints Plain
algorithm Newton
analysis Static
analyze 1

#Reset time to perform pushover analysis

loadConst -time 0.0

#set loading pattern for horizontal loading

pattern Plain 2 1 {
load 2 1 0 0 0 0 0
}

#pattern Plain 3 1 {
#load 2 0 0 1 0 0 0
#}

integrator LoadControl 1
system BandGeneral
test NormDispIncr 1.0e-8  6
numberer Plain
constraints Plain
algorithm Newton
analysis Static
analyze 1
```

For the rebar only model an axial load in tension of 100 kip was applied to the column to effectively break the surrounding concrete so that the displacement of the column reflects the displacement of the rebar only.

Modeling Bond-slip

To model the bond-slip of the reinforcing steel at the interfaces between the footing and column and the column cap and the column a zeroLength element with hysteretic material properties is used. The uniaxialMaterial Hysteretic command in OpenSees requires values from a moment-curvature analysis of the cross-section of the column. A zeroLength element with the same cross-section as that of the reinforced column was created in a separate tcl file to analyze the material's behavior. An axial load equal to the axial load seen by the columns and a moment of 1 kip-ft was applied to the element. The stresses and strains in the reinforcing steel on the tension and compression side of the section as well as the concrete at the same location were recorded. The reaction at the fixed node was also recorded.

Because of the oblong shape of the column cross-section the stresses and strains in the reinforcement and the moment reaction differ depending on the direction of the load. To model the bond-slip for a load in the longitudinal direction the section must be oriented so that the long side of the section is parallel to the z-axis. Similarly, to model the bond-slip for a load in the transverse direction the section must be oriented so that the short side is parallel to the z-axis.

The two columns also had different axial loads, however, this did not produce different results when the load was changed in the tcl file.

The slip can be calculated using equations from Section 8.2.3.1 in the Haber report.

$$\delta_{slip} = \begin{cases} \frac{\varepsilon_s L_1}{2} & if \ \ \varepsilon_s \leq \varepsilon_y \\ \frac{\varepsilon_y L_1}{2} + \frac{(\varepsilon_s + \varepsilon_y) L_2}{2} & if \ \ \varepsilon_s > \varepsilon_y \end{cases} \quad \text{(D-41)}$$

Where:

ε_s = strain in the reinforcing steel on the tension side of the column

ε_y = yield strain of the reinforcing steel

L_1 and L_2 can be determined by

$$L_1 = \frac{f_s d_b}{4u} \quad \text{(D-42)}$$

$$L_2 = \frac{(f_s - f_y) d_b}{4u} \quad \text{(D-43)}$$

Where:

f_s = stress in the reinforcing steel on the tension side of the column

f_y = maximum stress of the reinforcing steel

d_b = diameter of one reinforcing bar

u can be calculated by

$$u = \frac{9.5\sqrt{f'_c}}{d_b} \leq 800 \ psi \quad \text{(D-44)}$$

Where:

f'_c = the compressive strength of concrete

Once the slip is found the rotation of the column that corresponds to each moment is calculated by

$$\theta_{slip} = tan^{-1}\left(\frac{\delta_{slip}}{c - d}\right) \quad \text{(D-45)}$$

Where:

c = neutral axis location determined from moment-curvature analysis

d = column diameter

A graph of the moment vs. rotation with an idealized bilinear curve for the Salmon River Bridge for both loading directions is shown in Figures D-38 and D-39.

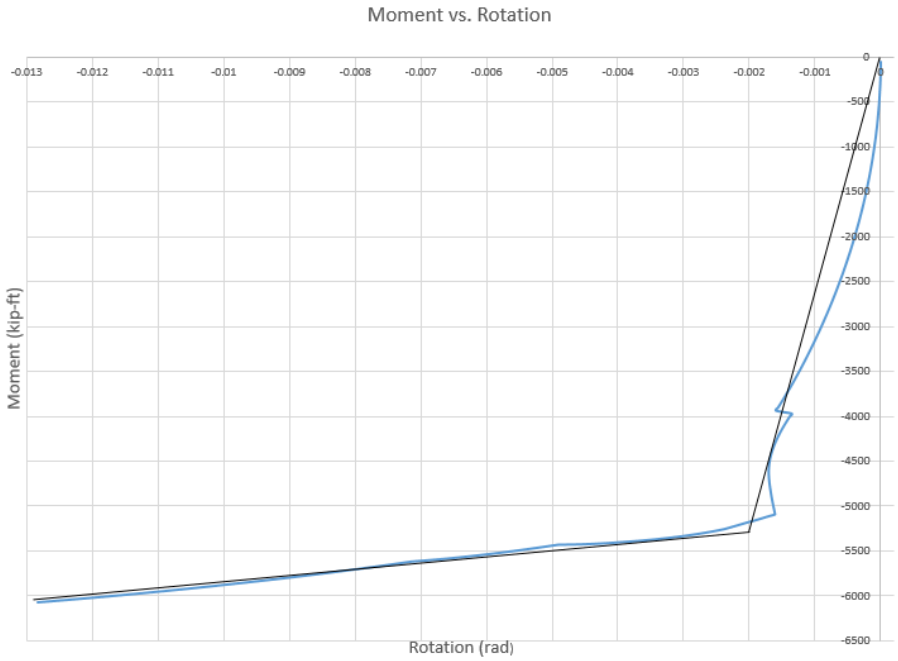

Figure D-38. Moment vs. Rotation for Longitudinal Loading

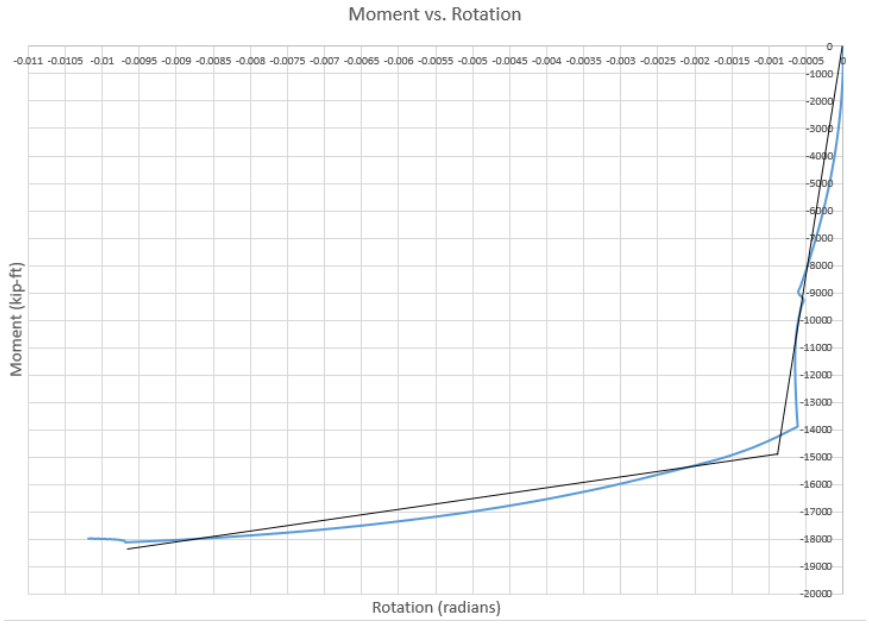

Figure D-39. Moment vs. Rotation for Transverse Loading

The uniaxialMaterial Hysteretic command in OpenSees requires the stress and strain at the first point of inflection and the ultimate stress and strain on the bilinear approximation of the moment-rotation curve. These values are

$s1p_l$ = 5300 k.ft	Moment at the first point of the envelope in the positive direction for longitudinal loading
$e1p_l$ = 0.002	Angle at the first point of the envelope in the positive direction for longitudinal loading
$s2p_l$ = 6050 k.ft	Moment at the second point of the envelope in the positive direction for longitudinal loading
$e2p_l$ = 0.0128	Angle at the second point of the envelope in the positive direction for longitudinal loading
$s1p_t$ = 14800 k.ft	Moment at the first point of the envelope in the positive direction for transverse loading
$e1p_t$ = 0.00067	Angle at the first point of the envelope in the positive direction for transverse loading
$s2p_t$ = 18300 k.ft	Moment at the second point of the envelope in the positive direction for transverse loading
$e2p_t$ = 0.0097	Angle at the second point of the envelope in the positive direction for transverse loading

Because of the symmetry of the column the moments and rotations in the negative direction are the same as those in the positive direction.

Displacement Results and Column Drift of Nonlinear CIP model

The resulting longitudinal and transverse displacements at all of the superstructure nodes and at the top of the columns are shown in Tables D-44 and D-45.

Table D-44. Longitudinal Displacement of Column and Superstructure Nodes

node	101	102	103	104	105	106	107	108	109	110	203	303
displacement (ft)	0.045	0.046	0.046	0.047	0.047	0.0467	0.046	0.0457	0.045	0.0446	0.036	0.047

Table D-45. Transverse Displacement of Column and Superstructure Nodes

node	101	102	103	104	105	106	107	108	`109	110	203	303
displacement (ft)	0.145	0.148	0.1524	0.157	0.160	0.160	0.157	0.152	0.148	0.147	0.072	0.070

From previous sections the column height of the southwest column is 15.469 ft and the column height of the northeast column is 15.969 ft. The height of the bridge at the southwest column, node 104, is 28.11 ft and at the northeast column, node 108, 28.61 ft. The drift in the longitudinal and transvers directions at nodes 104, 108, 203, and 303 are shown in Table D-46.

Table D-46. Calculated Drift for Selected Nodes

node	104	108	203	303
long. drift (%)	0.1658	0.1596	0.2353	0.2948
trans dirft (%)	0.5581	0.5313	0.4686	0.4391

Table D-47. Reactions at the Base of the Columns for Longitudinal Loading

Column	Shear (k)	Axial (k)	Moment (k-ft.)
SW	-432.7	1,485.3	3,691
NE	-556.2	1,298.2	4,455

Table D-48. Reactions at the Base of the Columns for Transverse Loading

Column	Shear (k)	Axial (k)	Moment (k-ft.)
SW	-552.9	1,522.0	-1,5312
NE	-549.6	1,310.5	-1,5144

Nonlinear Model of Structure with Grouted Couplers

The grouted couplers are modeled as separate elements within the columns. They are located at the top and bottom of each column. In addition to the zeroLength elements that model bond slip small (0.001 ft in length) nonlinearBeamColumn elements with the same cross-section as the part of the column without couplers was added to the top and bottom of each column to observe the behavior of the materials immediately beyond the coupler region. The node and element placement can be seen in Figures D-40 and D-41.

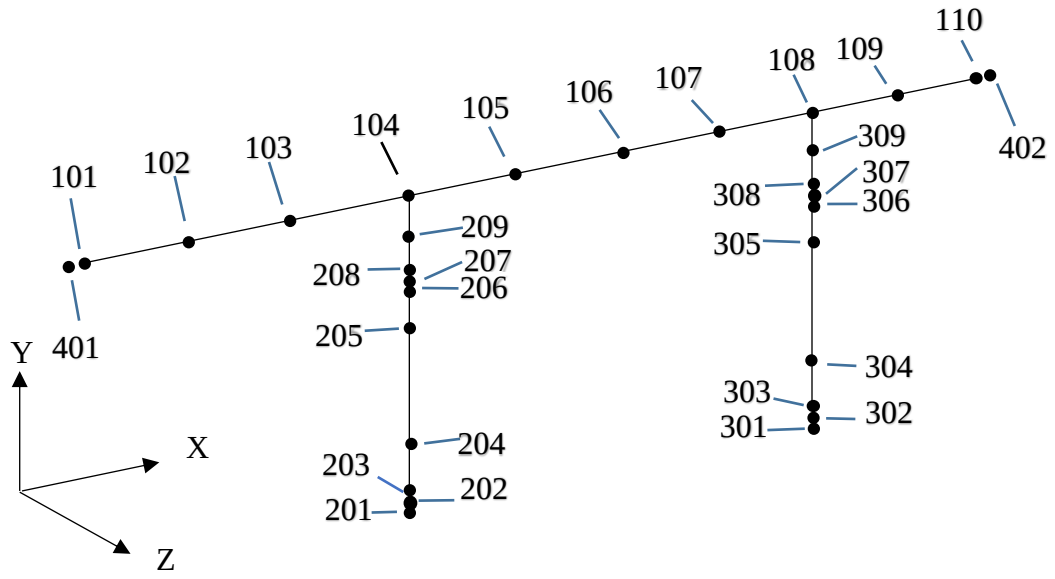

Figure D-40. Nonlinear bridge model with grouted couplers with node numbers

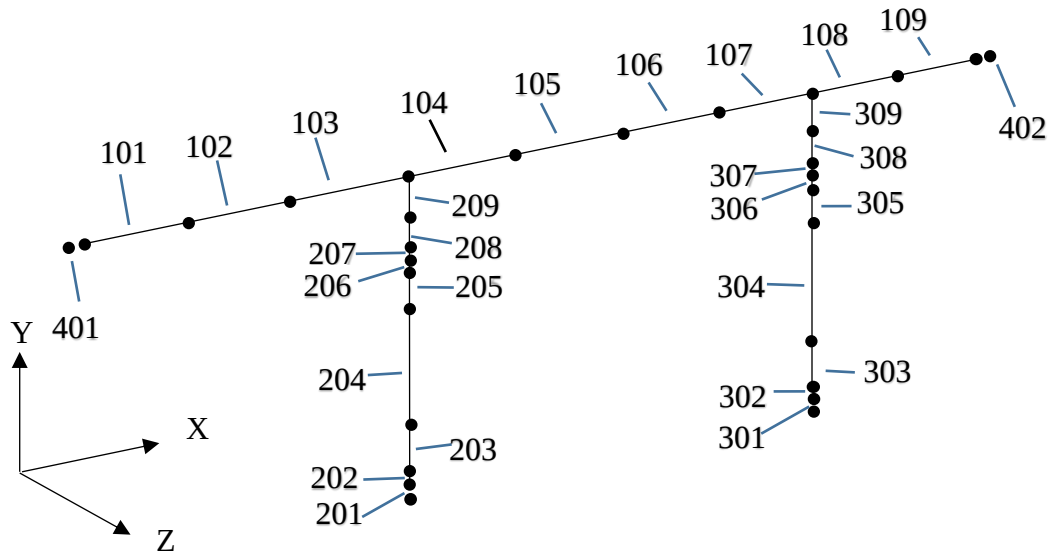

Figure D-41. Nonlinear bridge model with grouted couplers with element numbers

Material Properties of Grouted Couplers

The material properties of the grouted couplers were obtained from the manufacturer, Splice Sleeve North America (SSNA). The following values apply to the SSNA No. SNX11 Grouted Coupler which is used for a #11 reinforcing bar.

$A_{coupler}$ = 7.3118 in^2	cross-sectional area of coupler
$L_{coupler}$ = 1.624 ft	length of coupler
f_y = 9685 ksf	yield stress of the coupler
f_u = 13188 ksf	ultimate stress at fracture
E_s = 3992874 ksf	modulus of elasticity of coupler
E_{sh} = 317216 ksf	slope of the stress-strain curve at strain hardening
e_{sh} = 0.00307	strain at strain hardening
e_{ult} = 0.0165	ultimate strain

Coupler Section

To model the behavior of the couplers within the columns an area equal to the cross-sectional area of the coupler was left empty where each coupler was located. This prevented the material properties of the concrete from affecting the behavior of the couplers. The locations of the circular and rectangular patches are shown in Figure D-42.

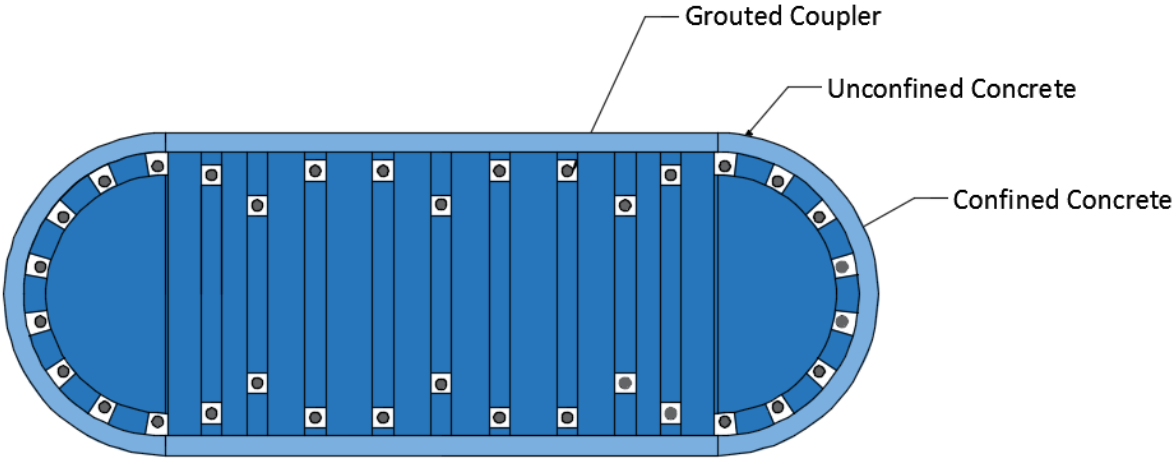

Figure D-42. OpenSees model of column cross-section with couplers

Deflection Check of Column with Grouted Couplers

A check of the column cross-section with the spaces for the grouted couplers was made with a separate tcl file. Again a 10 ft column was loaded laterally with 1 kip and the results were compared to hand calculations. The entire length of the column has the same cross-section as the concrete in the section with the grouted couplers and only confined concrete was used in this comparison.

Hand Calculations

Deflection is calculated by:

$$\Delta = \frac{FL^3}{3EI} \tag{D-46}$$

Where:

Δ = deflection in ft

F = force applied to column

L = height of column = 10 ft

E = modulus of elasticity of the material

I = moment of inertia, for the column, $I_z = 26.59\ ft^4$ $I_y = 185.367\ ft^4$

All confined concrete column deflection

E = 586656 ksf

In the Z direction

$\Delta = 1kip\ (10ft)^3/3\ (586656\ ksf)\ (185.367\ ft^4) = 3.065*10^{-6}\ ft$

In the X direction

$\Delta = 1kip\ (10ft)^3/3\ (586656\ ksf)\ (26.59\ ft^4) = 2.137*10^{-5}\ ft$

OpenSees Results for Deflection Check

All confined concrete deflections

In the Z direction

$\Delta = 3.048*10^{-6}\ ft$

In the X direction

$\Delta = 2.069*10^{-5}\ ft$

OpenSees tcl Script for Column with Grouted Couplers Deflection Check

Loading in the Z Direction

```
#Clear cached data existing in the program

wipe

#Create model with 3 dimensions and 6 degrees of freedom

model BasicBuilder -ndm 3 -ndf 6

#Create Nodes

#     tag   x     y     z
node   1    0.0   0.0   0.0
node   2    0.0   10.0   0.0
```

```
#Specify geometric transformation

geomTransf Linear 1  0  0  1

#Fix node 1

fix   1   1   1   1   1   1   1

#Create uniaxial materials for Concrete and Steel


#uniaxialMaterial Concrete01 $matTag $fpc $epsc0 $fpcu $epsU

uniaxialMaterial Concrete01  1  -720.0  -0.002  0  -0.005

#uniaxialMaterial Concrete04 $matTag $fc $ec $ecu $Ec <$ft $et> <$beta>

uniaxialMaterial Concrete04  2  -966.08  -0.005418  -0.01475  586656

#uinaxialMaterial ReinforcingSteel $matTag $fy $fu $Es $Esh $esh $eult

uniaxialMaterial ReinforcingSteel  3  9792  13680  4176000  179568  0.0115  0.09

uniaxialMaterial ReinforcingSteel  4  9685  13188  3992874  317216  0.00307  0.0165

#Create fiber section with defined concrete and rebar

section Fiber 1  {
#patch circ $matTag $numSubdivCirc $numSubdivRad $yCenter $zCenter $intRad $extRad
<$startAng $endAng>
#patch rect $matTag $numSubdivY $numSubdivZ $yI $zI $yJ $zJ
#cover concrete at the ends
patch circ  2  44  2   0  3  1.516  1.75    0  180
patch circ  2  44  2   0 -3  1.516  1.75  180  360
#concrete between couplers on ends
patch circ  2   4  2   0  3  1.294  1.516   8.076  23.508
patch circ  2   4  2   0  3  1.294  1.516  32.812  48.244
patch circ  2   4  2   0  3  1.294  1.516  57.548  72.98
patch circ  2   4  2   0  3  1.294  1.516  82.284  97.716
patch circ  2   4  2   0  3  1.294  1.516 107.02  122.452
patch circ  2   4  2   0  3  1.294  1.516 131.756 147.188
patch circ  2   4  2   0  3  1.294  1.516 156.492 171.924
patch circ  2   4  2   0 -3  1.294  1.516 188.076 203.508
patch circ  2   4  2   0 -3  1.294  1.516 212.812 228.244
patch circ  2   4  2   0 -3  1.294  1.516 237.548 252.98
patch circ  2   4  2   0 -3  1.294  1.516 262.284 277.716
patch circ  2   4  2   0 -3  1.294  1.516 287.02  302.452
patch circ  2   4  2   0 -3  1.294  1.516 311.756 327.188
patch circ  2   4  2   0 -3  1.294  1.516 336.492 351.924
#cover concrete on the sides
patch rect  2   2  44   -1.75  -3  -1.516  3
patch rect  2   2  44    1.516 -3   1.75   3
#confined concrete at the ends
patch circ  2  44  6  0  3  0  1.294    0  180
patch circ  2  44  6  0 -3  0  1.294  180  360
#confined concrete between couplers in center of column
patch rect  2  16  1  -1.294  2.97   1.294  3.0
patch rect  2  20  2  -1.516  2.608  1.516  2.97
```

```
patch rect  2   1  2  -1.516  2.382 -1.407  2.608
patch rect  2  14  2  -1.181  2.382  1.181  2.608
patch rect  2   1  2   1.407  2.382  1.516  2.608
patch rect  2  20  2  -1.516  2.113  1.516  2.382
patch rect  2   2  2  -1.516  1.887 -1.077  2.113
patch rect  2  12  2  -0.851  1.887  0.851  2.113
patch rect  2   2  2   1.077  1.887  1.531  2.113
patch rect  2  20  2  -1.516  1.481  1.516  1.887
patch rect  2   1  2  -1.516  1.255 -1.362  1.481
patch rect  2  14  2  -1.226  1.255  1.226  1.481
patch rect  2   1  2   1.452  1.255  1.516  1.481
patch rect  2  20  2  -1.516  0.745  1.516  1.255
patch rect  2   1  2  -1.516  0.519 -1.425  0.745
patch rect  2  14  2  -1.226  0.519  1.226  0.745
patch rect  2   1  2   1.452  0.519  1.516  0.745
patch rect  2  20  2  -1.516  0.113  1.516  0.519

patch rect  2   2  2  -1.516 -0.113 -1.077  0.113
patch rect  2  12  2  -0.851 -0.113  0.851  0.113
patch rect  2   2  2   1.077 -0.113  1.516  0.113

patch rect  2  16  1  -1.294 -3.0    1.294 -2.97
patch rect  2  20  2  -1.516 -2.97   1.516 -2.608
patch rect  2   1  2  -1.516 -2.608 -1.407 -2.382
patch rect  2  14  2  -1.181 -2.608  1.181 -2.382
patch rect  2   1  2   1.407 -2.608  1.516 -2.382
patch rect  2  20  2  -1.516 -2.382  1.516 -2.113
patch rect  2   2  2  -1.516 -2.113 -1.077 -1.887
patch rect  2  12  2  -0.851 -2.113  0.851 -1.887
patch rect  2   2  2  -1.077 -2.113  1.516 -1.887
patch rect  2  20  2  -1.516 -1.887  1.516 -1.481
patch rect  2   1  2  -1.516 -1.481 -1.407 -1.255
patch rect  2  14  2   1.255 -1.226  1.481  1.226
patch rect  2   1  2   1.452 -1.481  1.516 -1.255
patch rect  2  20  2  -1.516 -1.255  1.516 -0.745
patch rect  2   1  2  -1.516 -0.745 -1.407 -0.519
patch rect  2  14  2  -1.226 -0.745  1.226 -0.519
patch rect  2   1  2   1.452 -0.745  1.516 -0.519
patch rect  2  20  2  -1.516 -0.519  1.516 -0.113

#fiber $yLoc  $zLoc  $A  $matTag
#couplers
#fiber   0.964  2.0    0.01083  4
#fiber   1.294  2.495  0.01083  4
#fiber   1.386  3.083  0.01083  4
#fiber   1.224  3.656  0.01083  4
#fiber   0.838  4.108  0.01083  4
#fiber   0.297  4.357  0.01083  4
#fiber  -0.964  2.0    0.01083  4
#fiber  -1.294  2.495  0.01083  4
#fiber  -1.386  3.083  0.01083  4
#fiber  -1.224  3.656  0.01083  4
#fiber  -0.838  4.108  0.01083  4
#fiber  -0.297  4.357  0.01083  4
#fiber   0.964 -2.0    0.01083  4
#fiber   1.294 -2.495  0.01083  4
#fiber   1.386 -3.083  0.01083  4
#fiber   1.224 -3.656  0.01083  4
```

```
#fiber   0.838 -4.108  0.01083  4
#fiber   0.297 -4.357  0.01083  4
#fiber  -0.964 -2.0    0.01083  4
#fiber  -1.294 -2.495  0.01083  4
#fiber  -1.386 -3.083  0.01083  4
#fiber  -1.224 -3.656  0.01083  4
#fiber  -0.838 -4.108  0.01083  4
#fiber  -0.297 -4.357  0.01083  4
#fiber   1.339  1.368  0.01083  4
#fiber   1.339  0.632  0.01083  4
#fiber   0.977  0.0    0.01083  4
#fiber   1.339 -0.632  0.01083  4
#fiber   1.339 -1.368  0.01083  4
#fiber  -1.339  1.368  0.01083  4
#fiber  -1.339  0.632  0.01083  4
#fiber  -0.977  0.0    0.01083  4
#fiber  -1.339 -0.632  0.01083  4
#fiber  -1.339 -1.368  0.01083  4
}

#setup time series

timeSeries Linear 1

#Create elastic beam column element

element nonlinearBeamColumn  1  1  2  9  1  1

#create recorder files

recorder Node  -file GCNPcolumndispcheckconfinedconcrete_x_dir.out -node 2 -dof 1 disp
recorder Node  -file GCNPcolumndispcheckconfinedconcrete_z_dir.out -node 2 -dof 3 disp

#set loading pattern for vertical loading

pattern Plain 1 1 {
load 2 0 -100 0 0 0 0
}

integrator LoadControl 1
system BandGeneral
test NormDispIncr 1.0e-8  6
numberer Plain
constraints Plain
algorithm Newton
analysis Static
analyze 1

#Reset time to perform pushover analysis

loadConst -time 0.0

#set loading pattern for horizontal loading

#pattern Plain 2 1 {
#load 2 1 0 0 0 0 0
#}
```

```
pattern Plain 3 1 {
load 2 0 0 1 0 0 0
}

integrator LoadControl 1
system BandGeneral
test NormDispIncr 1.0e-8  6
numberer Plain
constraints Plain
algorithm Newton
analysis Static
analyze 1
```

Displacement Results and Column Drift of Nonlinear Model with Grouted Couplers

The resulting longitudinal and transverse displacements at all of the superstructure nodes and at the top of the columns are shown in Tables D-49 and D-50.

Table D-49. Longitudinal Displacement of Column and Superstructure Nodes

node	101	102	103	104	105	106	107	108	109	110	207	307
displacement (ft)	0.045	0.046	0.047	0.047	0.047	0.047	0.046	0.046	0.045	0.045	0.037	0.047

Table D-50. Transverse Displacement of Column and Superstructure Nodes

node	101	102	103	104	105	106	107	108	109	110	207	307
displacement (ft)	0.145	0.148	0.152	0.157	0.160	0.1601	0.157	0.152	0.149	0.1471	0.072	0.070

From previous sections the column height of the southwest column is 15.469 ft and the column height of the northeast column is 15.969 ft. The height of the bridge at the southwest column, node 104, is 28.11 ft and at the northeast column, node 108, 28.61 ft. The drift in the longitudinal and transvers directions at nodes 104, 108, 205, and 305 are shown in Table D-51.

Table D-51. Calculated Drift for Selected Nodes

node	104	108	207	307
long. drift (%)	0.1662	0.16	0.236	0.2959
trans. drift (%)	0.5585	0.5317	0.468	0.4389

Tables D-52 and D-53 show the reactions at the base of the columns for longitudinal and transverse loading, respectively.

Table D-52. Reactions at the Base of the Columns for Longitudinal Loading

Column	Shear (k)	Axial (k)	Moment (k-ft.)
SW	-423.5	1,486.5	3,617
NE	-539.8	1,301.2	4,339

Table D-53. Reactions at the Base of the Columns for Transverse Loading

Column	Shear (k)	Axial (k)	Moment (k-ft.)
SW	-551.1	1,522.4	-15,241
NE	-547.8	1,315.4	-15,068

Appendix E - Procedure for Estimating Integral Abutment Stiffness Values

The procedures for estimating bridge transverse and longitudinal abutment stiffness values are presented in this appendix. For simplicity, in the procedures outlined below, it is assumed that both abutments have: (a) the same pile lateral force-displacement behavior, (b) identical wingwalls (if present), and (c) identical abutment wall area. In the bridge under consideration, some of these assumptions may not apply and procedure may have to be slightly revised. For example, in one of the Idaho bridges considered, the abutments of the bridge had different pile force-displacement behavior. Also, the procedures below assume that the strong direction of H-piles is oriented longitudinally, while weak direction is oriented in transverse direction.

Longitudinal Stiffness

This procedure assumes the same value of longitudinal abutment stiffness for both abutments. This longitudinal stiffness is half of the sum of the longitudinal stiffness values from the two sets of abutment piles and the stiffness of one abutment backfill. As shown in Figure E-1, a linear relation is assumed between the abutment backfill reaction and the corresponding displacement from zero displacement to $0.02H_{aw}$ where, H_{aw} = height of abutment wall. The corresponding maximum force to mobilize the full passive backfill resistance of $7.7\ k/ft^2$ is $\left(7.7\frac{k}{ft^2}\right)A_{aw}$. Where, A_{aw} is the area of the abutment wall = $H_{aw}\ L_{aw}$ with L_{aw} being the length of the abutment wall. It is further assumed that the full maximum force remains constant beyond the displacement of $0.02H_{aw}$.

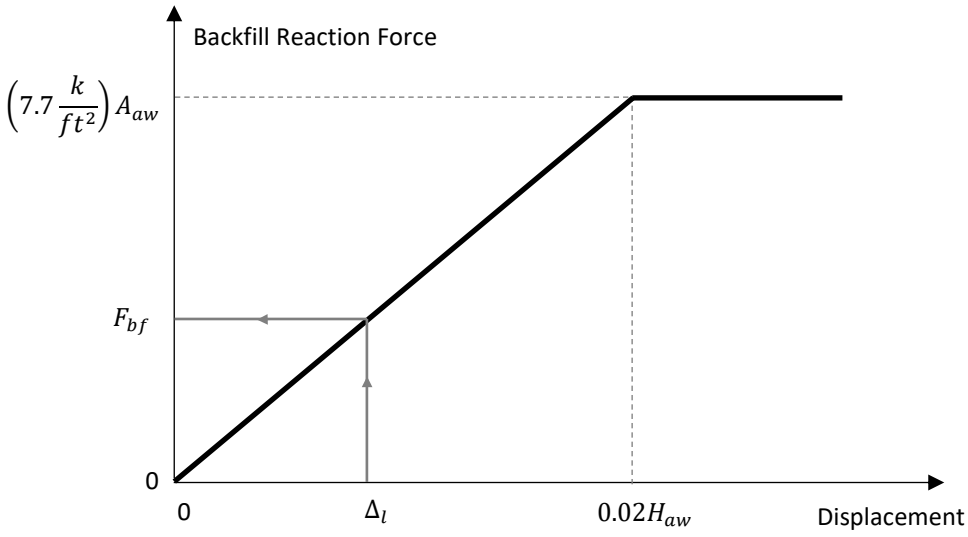

Figure E-1. Abutment Backfill Reaction Force versus Displacement

Figure E-2 shows a typical top of the pile lateral force versus displacement while the pile is bending about the strong axis. In the bridge model, the initial longitudinal pile stiffness is assumed based on $\Delta_o = 1\ in.$ Here, subscript "o" indicates initial estimates. From the pile force versus displacement in the strong direction, the initial force in the strong direction corresponding to displacement of 1 in. is estimated as F_{so}. The initial pile stiffness in the strong direction is $k_{so} = \frac{F_{so}}{\Delta_o}$.

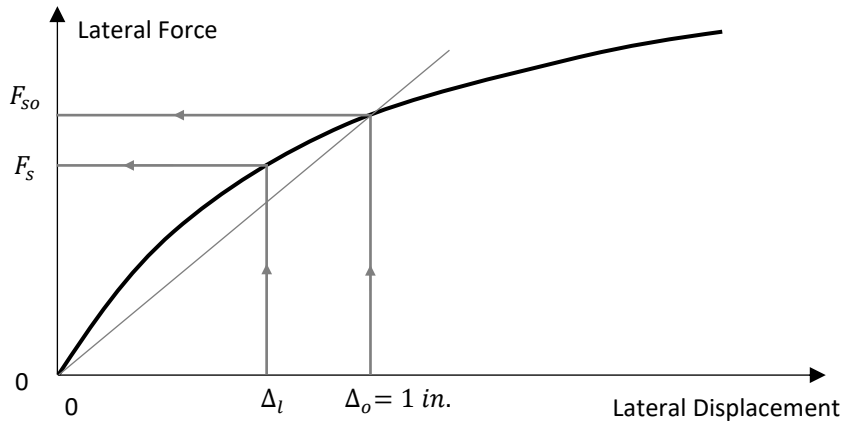

Figure E-2. Top of the Pile Lateral Force versus Displacement, Bending about the Strong Axis (Ebrahimpour, et al. 2016)

The initial abutment longitudinal stiffness K_{lo}, to be used for both abutments, is estimated as:

$$K_{lo} = \frac{(n_1+n_2)k_{so}+\left(\frac{7.7A_{aw}}{d}\right)}{2} \quad \text{(E-1)}$$

Where, n_1 = the number of piles in Abutment 1, n_2 = the number of piles in Abutment 2, k_{so} = the initial pile stiffness in the strong direction, A_{aw} = the area of the abutment wall = $H_{aw}\ L_{aw}$, H_{aw} = height of abutment wall, L_{aw}= length of abutment wall, and $d = 0.02\ H_{aw}$ = deflection needed to mobilize the full passive resistance of $7.7\ k/ft^2$.

After loading the bridge linear-elastic model in the longitudinal direction, the average of the bridge longitudinal abutment displacement, Δ_l, is obtained. The average value of longitudinal displacements is used since in this direction the abutment displacements are very close to one another. In addition, determine the longitudinal seismic forces R_{l1} and R_{l2} for Abutments 1 and 2. Let's assume that Δ_l is less than 1 in. As shown in Figures E-1 and E-2, with the new Δ_l value, an abutment backfill reaction force F_{bf} and a revised pile lateral reaction force, F_s is obtained. Check to see if the equilibrium is reached between the sum of longitudinal seismic forces and abutment backfill resistance, and the lateral pile resistance forces as shown by Equation (E-2):

$$R_{l1} + R_{l2} \stackrel{?}{\cong} (n_1 + n_2)F_s + F_{bf} \quad \text{(E-2)}$$

The symbol $\stackrel{?}{\cong}$ is used to indicate whether the two sides are approximately equal to each other. If Equation (E-2) is not satisfied, change the value of longitudinal abutment stiffness and find the revised average value of longitudinal displacements and abutment seismic forces. With the revised average displacement, find the longitudinal abutment backfill resistance force and the lateral pile resistance forces and see if Equation (E-2) is satisfied. This process is repeated a few times until the two sides of Equation (E-2) are within 10%. When evaluating a pier it is recommended to keep the abutment stiffness on the lower side. This would generally result in higher forces and displacements at the pier(s).

Example

Let's assume the initial springs based on 1" displacement result in ¾" displacement and the corresponding force of 600kips at each abutment (1200kips total longitudinal force to be resisted by abutments). Let's also assume we have 10 piles at each abutment and they resist 30kips each at ¾" displacement, so the total pile resistance from both abutments would be 2*10*30=600kips, leaving 1200-600=600kips to be resisted by one abutment backfill. Now we need to check how much backfill resistance we get from ¾" displacement, assuming linear relation from 0" (0kips) to d=0.02H" ($7.7A_{aw}$). (Any displacement higher than 0.02H" will result in a constant backfill resistance of $7.7A_{aw}$). If ¾" displacement results in backfill resistance considerably higher than 600kips, we might increase abutment stiffness, which would give us higher acting seismic force, but smaller displacements. On the other hand, if ¾" results in backfill resistance quite lower than 600kips, we may need to soften the abutment springs in order to reduce the acting force, but increase the displacement and associated resistance from piles and backfill. We repeat the process until we get good correlation (within 10%) between abutment acting seismic forces and resulting resistance from piles and backfill based on acting displacement.

Transverse Stiffness

In this procedure abutment forces and displacements are evaluated individually. The wing shear capacity can only be considered effective if it is larger than the difference between acting seismic forces and the piles reaction under given displacement. If otherwise, it is assumed that the wingwall has failed and it does not contribute to the transverse stiffness or resistance. The shear force V_c is calculated using Equation (E-3):

$$V_c = 0.0316\beta\sqrt{f_c'}b_v d_v \quad \text{(E-3)}$$

Where, β = 2, f_c'= compressive strength of the concrete, ksi, b_v = the height of the wingwall at the interface of wing and abutment, $d_v = \max\left[d_e - \frac{a}{2}, 0.9d_e, 0.72h\right]$, d_e = the effective depth = distance to the center of the back reinforcement from the face of the wingwall = $h - cover -$

$bar\ diameter/2$, $a = \frac{A_s f_y}{0.85 f_c' b_v}$ = depth of the equivalent compression block; A_s = area of the flexural reinforcement on the backfill side; $f_y = 60\ ksi$ = yield strength of the flexural reinforcement, and h = the depth of the wingwall (typically 12 in.).

Figure E-3 shows a typical top of pile lateral force versus displacement while the pile is bending about the weak axis. Note that here the force values are shown smaller compared to Figure E-2 (i.e., less force required for a given displacement in the weak direction compared to the strong direction).

In the bridge model, the initial transverse pile stiffness is assumed based on $\Delta_o = 1\ in.$ Here, again the subscript "o" indicates initial estimates. From the pile force versus displacement in the weak direction (Figure E-3), the initial force in the weak direction corresponding to displacement of 1 in. is estimated as F_{wo}. The initial pile stiffness in the weak direction is $k_{wo} = \frac{F_{wo}}{\Delta_o}$.

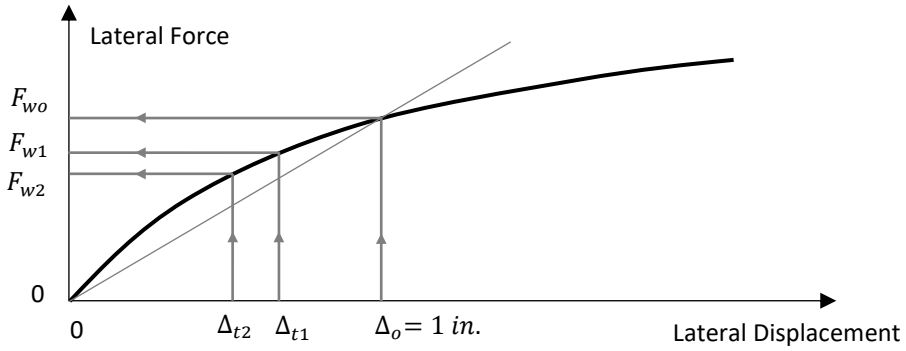

Figure E-3. Top of the Pile Lateral Force versus Displacement, Bending about the Weak Axis (Ebrahimpour, et al. 2016)

For one of the two abutments, let's say Abutment 1, the initial value for the transverse stiffness is estimated using Equation (E-4). Here, initially the contribution of the wing is not included.

$$K_{t1,o} = n_1 k_{wo} \tag{E-4}$$

Where, n_1 = the number of piles in Abutment 1, and k_{wo} = the initial pile stiffness in the weak direction.

Repeat the same process for Abutment 2 to obtain initial value for its transverse stiffness, $K_{t2,o}$:

$$K_{t2,o} = n_2 k_{wo} \tag{E-5}$$

Where, n_2 = the number of piles in Abutment 2.

With the above initial estimates for the abutment transverse stiffness values, load the bridge linear-elastic model in the transverse direction. Determine the transverse displacements and the corresponding seismic forces for Abutments 1 and 2. Note, here unlike the longitudinal direction, the abutment displacements may be significantly different and the use of average value may not be suitable. Let's call the transverse displacements Δ_{t1} and Δ_{t2} and call the transverse forces R_{t1} and R_{t2}. Let's also assume that the displacements are both less than 1 in. with the corresponding top of the pile reactions in the weak direction as F_{w1} and F_{w2} as shown in Figure E-3. Now, examine to see if the force equilibrium is maintained as shown by Equations (E-6) and (E-7).

$$R_{t1} \stackrel{?}{\cong} n_1 F_{w1} + F_{wing} \tag{E-6}$$

$$R_{t2} \stackrel{?}{\cong} n_2 F_{w2} + F_{wing} \tag{E-7}$$

Where, F_{wing} is the shear force demand on a single wing with a value $F_{wing} \leq V_c$.

If the left hand sides of Equations (E-6) and (E-7) are larger than the right hand side, reduce the transverse spring stiffness values $K_{t1}$and K_{t2}. This will result in larger transverse displacements and thus lead to larger values for F_{w1} and F_{w2} (see Figure E-3). This process is repeated a few times until the two sides of Equations (E-6) and (E-7) are within 10%. Again, it is recommended to keep the abutment stiffness values on the lower side. This would generally result in higher forces and displacements at the pier(s). The numerical example below assumes a symmetrical bridge with the same number of piles in each abutment (i.e., $n_1 = n_2$).

Example

Let's assume that initial abutment springs based on 1" displacement result in ½" movement with 400kips of acting seismic force at each abutment. Assuming that ½" top of pile movement results in 20kips resistance, we would get 10*20=200kips of pile resistance at each abutment, leaving 400-200=200kips to be resisted by one wing. If one wing can resist only 100kips, we might try to reduce abutment springs as to reduce the acting seismic force, but increase displacement, which in turn will increase pile reactions and reduce demand on the wing. Assume that softer springs would result in the movement of ¾" and the acting force of 350kips per abutment. Now the resistance from piles may be increased to let's say 10*30kips/pile=300kips leaving 350-300=50kips to be resisted by a wing, which is ok, since the wing resistance is 100kips. If on other hand we conclude that acting seismic force is higher than combined resistance of piles and one wing (despite the softening of abutment springs) we may assume the wing will be sheared off and we may have to adjust the abutment springs based on piles alone, until we get good convergence again between acting force and pile resistance under given displacement.

Appendix F - Grouted Coupler Detailed Information

Introduction

This appendix provides background information for the use of grouted couplers. It also provides figures and tables giving grouted coupler dimensions and mechanical properties.

Key Items Found in the Literature or by Contacting the Manufacturers

- The total length of mechanical bar splice shall not exceed $15d_b$, where d_b is the longitudinal bar diameter. This requirement is to minimize the adverse effect of coupler length on the rotational capacity of a ductile member (Tazarv and Saiidi 2015).
- A spliced bar shall fracture outside coupler region regardless of the loading type. Coupler region is defined as the length of coupler plus $1.0d_b$from each face of the coupler (Tazarv and Saiidi 2015).
- Strain capacity of the spliced bar outside coupler region should exceed 12% for No. 10 and smaller bars, and should exceed 9% for No. 11 bars and larger (AASHTO 2015).
- Mechanical couplers in areas away from plastic hinge zones must develop 125% of the specified yield strength of the connected reinforcing. Mechanical couplers in areas adjacent to or in plastic hinge zones must develop 150% of the specified yield strength of the connected reinforcing (UDOT 2015).
- Clear cover:
  - Generally, the clear cover is more than the cast-in-place sections (Tazarv and Saiidi 2015).
  - Adjust the cover to the reinforcing and spiral or ties to accommodate the larger grouted splice coupler section (UDOT 2015).
  - Question posed to SSNA, Inc.: "*What suggestions do you have regarding minimum cover for the couplers?*" Answer: "*I believe just same as the minimum concrete cover for the reinforcements based upon ACI 318*."
  - Precast concrete (manufactured under plant control conditions), concrete exposed to earth or weather, members other than wall panels, No. 14 and No. 18 bars, prestressing tendons larger than 1-1/2 in. diameter, use 2 in. cover. No. 6 through No. 11 bars, prestressing tendons larger than 5/8 in. diameter through 1-1/2 in. diameter, use 1.5" cover. (ACI 318, Section 7.7.3). (ACI 318 2014)
  - Cover for pretensioned prestressing strand, anchorage hardware, and mechanical connections for reinforcing bars or post-tensioned prestressing strands shall be the same as for reinforcing steel. According to AASTHO LRFD Bridge Specs. Table 5.12.3-1, for unprotected main reinforcing steel for exterior other than direct exposure to salt water, cast against earth, coastal, exposure to deicing salts, deck

surfaces subjected to tire studs or chain wear, use 2.0 in. cover (AASHTO LRFD Bridge Design Specification, 2014, Section 5.12.3). (AASHTO 2014)

- Coating:
  - Question posed to SSNA, Inc.: "*What suggestions do you have regarding coating requirements for the couplers, the longitudinal reinforcing bars being connected, and the hoops/ties?*" Answer: "*Since the sleeves are encased in concrete, just black sleeves are good for most occasions, but for DOT projects, quite often epoxy coated and galvanized sleeves are used for corrosion protection*."
- Minimum gap between the couplers:
  - Minimum and maximum clear distances between mechanical couplers are recommended to be the same as those specified for reinforcing bars (Tazarv and Saiidi 2015).
  - Detail the minimum gap between the grouted couplers to be the greatest of (1) 1 in., (2) 1.33 times the maximum aggregate size of the coarse aggregate, and (3) nominal diameter of the connected reinforcing (UDOT 2015).
  - Minimum spacing of reinforcing bars: For precast concrete manufactured under plant control conditions, the clear distance between parallel bars in a layer shall not be less than: (1) the nominal diameter of the bars, (2) 1.33 times the maximum size of the coarse aggregate, or (3) 1.0 in. (AASHTO LRFD Bridge Design Specification, 2014, Section 5.10.3.1.2). (AASHTO 2014)
  - In spirally reinforced or tied reinforced compression members, clear distance between longitudinal bars shall be not less than $1.5d_b$ nor less than 1-1/2 in. See also Sec. 3.3.2. (ACI 318, Section 7.6.3). Nominal maximum size of coarse aggregate shall be not larger than: (a) 1/5 the narrowest dimension between sides of forms, nor (b) 1/3 the depth of slabs, nor (c) 3/4 the minimum clear spacing between individual reinforcing bars or wires, bundles of bars, individual tendons, bundled tendons, or ducts. (ACI 318, Section 3.3.2). (ACI 318 2014)
- Grout:
  - Only use the manufacturer's grout (SS Mortar, in the case of NMB grouted couplers; ICC-ES Report ESR-3433, 2016). (SSNA 2016)
  - For grouted couplers, grout shall be provided by the manufacturer (Tazarv and Saiidi 2015).

Grouted Coupler Dimensions

Figure F-1 shows the connector configuration for the NMB Type U-X and A11W splice-sleeves. Figure F-2 shows connector configuration for the NMB SNX11 splice-sleeve. Tables F-1 and F-2 show the dimensions and the required rebar embedment lengths corresponding to Figures F-1 and F-2, respectively.

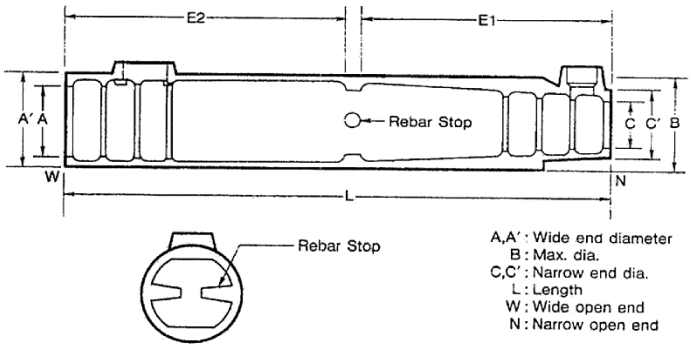

Figure F-1. NMB Type U-X and A11W Splice Sleeves (SSNA 2016)

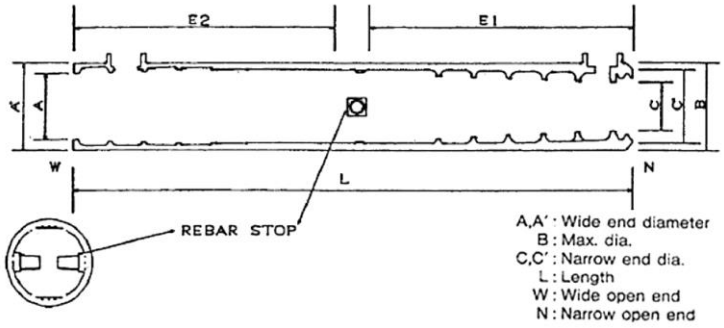

Figure F-2. NMB SNX11 Splice Sleeve (SSNA 2016)

Table F-1. Dimensions of NMB Type U-X and A11W Splice-Sleeves (SSNA 2016)

DIMENSIONS OF NMB U-X SLEEVES											REQUIRED REBAR EMBEDMENT LENGTH			
Sleeve No.	Bar Diameter (in.) [mm]	Bar Size		Sleeve Length (in.) [mm]	Narrow End Diameter (in.) [mm]		Maximum Diameter (B) (in.) [mm]	Wide End Diameter (in.) [mm]			Dowel (E1) (in.) [mm]		Dowel (E2) (in.) [mm]	
		ASTM	JIS		I.D. (C)	O.D. (C')		I.D. (A)	Total Tolerance [1]	O.D (A')	Min.	Max.	Min.	Max.
5U-X	0.625 [16]	#5	D16	9.65 [245]	0.87 [22]	1.50 [38]	1.89 [48.0]	1.26 [32.0]	0.63 [16.0]	1.89 [48.0]	4.13 [105]	4.33 [110]	4.13 [105]	4.92 [125]
6U-X	0.750 [19]	#6	D19	11.22 [285]	1.02 [26]	1.65 [42]	2.05 [52.0]	1.42 [36.0]	0.67 [17.0]	2.05 [52.0]	4.92 [125]	5.12 [130]	4.92 [125]	5.71 [145]
7U-X	0.875 [22]	#7	D22	12.80 [325]	1.14 [29]	1.77 [45]	2.36 [60.0]	1.73 [44.0]	0.86 [21.8]	2.36 [60.0]	5.71 [145]	5.91 [150]	5.71 [145]	6.50 [165]
8U-X	1.000 [25]	#8	D25	14.57 [370]	1.30 [33]	1.93 [49]	2.52 [64.0]	1.89 [48.0]	0.89 [22.6]	2.52 [64.0]	6.50 [165]	6.69 [170]	6.50 [165]	7.48 [190]
9U-X	1.128 [29]	#9	D29	16.34 [415]	1.42 [36]	2.06 [52.4]	2.67 [67.9]	2.01 [51.0]	0.89 [22.6]	2.67 [67.9]	7.40 [188]	7.56 [192]	7.40 [188]	8.35 [212]
10U-X	1.270 [32]	#10	D32	17.91 [455]	1.57 [40]	2.28 [58]	2.87 [73.0]	2.17 [55.0]	0.89 [22.6]	2.87 [73.0]	8.19 [208]	8.35 [212]	8.19 [208]	9.13 [232]
11U-X	1.410 [36]	#11	D36	19.49 [495]	1.73 [44]	2.40 [61]	3.03 [77.0]	2.32 [59.0]	0.91 [23.1]	3.03 [77.0]	8.98 [228]	9.13 [232]	8.98 [228]	9.92 [252]
14U-X	1.693 [43]	#14	D43	24.41 [620]	2.01 [51]	2.80 [71]	3.46 [88.0]	2.60 [66.0]	0.91 [23.1]	3.46 [88.0]	11.42 [290]	11.61 [295]	11.42 [290]	12.40 [315]
A11W	1.410 [36]	#11	D36	19.49 [495]	1.73 [44]	3.31 [84]	3.31 [84.0]	2.60 [66.0]	1.19 [30.2]	3.31 [84.0]	8.86 [225]	9.69 [246]	8.27 [210]	9.50 [241]

[1]Total tolerance is determined by subtracting bar diameter from the wide end inside diameter (A).

Table F-2. Dimensions of NMB SNX11 Splice-Sleeve (SSNA 2016)

DIMENSIONS OF NMB SNX SLEEVE											REQUIRED REBAR EMBEDMENT LENGTH			
Sleeve No.	Bar Diameter (in.) [mm]	Bar Size		Sleeve Length (in.) [mm]	Narrow End Diameter (in.) [mm]		Maximum Diameter (B) (in.) [mm]	Wide End Diameter (in.) [mm]			Dowel (E1) (in.) [mm]		Dowel (E2) (in.) [mm]	
		ASTM	JIS		I.D. (C)	O.D. (C')		I.D. (A)	Total Tolerance[1]	O.D (A')	Min.	Max.	Min.	Max.
SNX11	1.410 [36]	#11	D36	19.09 [485]	1.69 [43]	3.03 [77]	3.03 [77.0]	2.32 [59]	0.91 [23.1]	3.03 [77]	8.86 [225]	9.25 [235]	8.27 [210]	9.45 [240]

[1]Total tolerance is determined by subtracting bar diameter from the wide end inside diameter (A).

Figure F-3 shows the connector configuration for Erico's Lenton Interlok couplers and Table F-3 shows the dimensions and cut length for reinforcing steel.

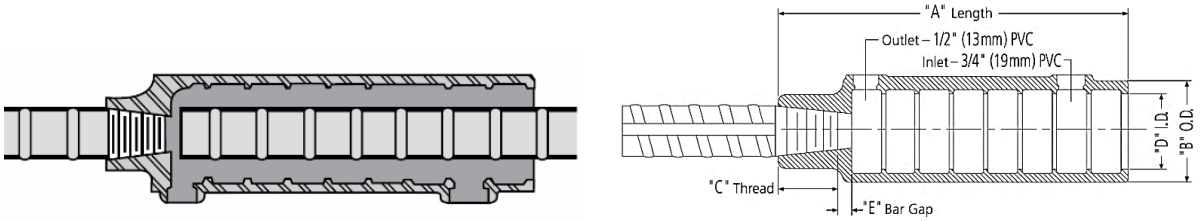

Figure F-3. Erico's Lenton Interlok Rebar Splicing System (Erico 2013)

Table F-3. Coupler Dimensions and Bar Cut Lengths for Lenton Interlok System (Erico 2013)

Rebar Size in-lb	Rebar Size Canadian	Coupler Part No.	"A"	"B"	"C"	"D"	"E" Reference	"X" Max.	"X" Min. Type 1*	"X" Min. Type 2**
#5	15M	LK5	7-13/16"	2-9/16"	7/8"	1-7/8"	13/16"	6-1/8"	5-1/4"	5-1/2"
#6	20M	LK6	7-13/16"	2-9/16"	1-1/8"	1-7/8"	9/16"	6-1/8"	5-1/4"	5-3/8"
#7	---	LK7	7-13/16"	2-9/16"	1-1/4"	1-7/8"	7/16"	6-1/8"	5-1/4"	
#8	25M	LK8	8-5/8"	2-11/16"	1-3/8"	2"	1/4"	7"	6"	
#9	30M	LK9	9-3/4"	2-13/16"	1-1/2"	2-1/8"	1/4"	8"	6-7/8"	
#10	---	LK10	10-13/16"	3"	1-9/16"	2-5/16"	1/4"	9"	7-3/4"	
#11	35M	LK11	11-15/16"	3-1/8"	1-11/16"	2-7/16"	3/8"	9-7/8"	8-1/2"	
#14	45M	LKT14	15-3/16"	3-11/16"	2-1/8"	2-3/4"	5/16"	12-3/4"	11"	
#18	55M	LKT18	20-5/16"	4-1/2"	2-3/4"	3-1/4"	9/16"	17"	14-3/4"	

* "X" Min. Type 1 will develop 125% of the specified yield strength of the rebar in tension and compression (125% f_y).
** "X" Min. Type 2 meets Type 1 and will develop the specified tensile strength of the rebar in tension (f_u).

Table F-4 summarizes the data from Tables F-1 to F-3 and also includes the recommendations by the latest University of Nevada, Reno report. (Tazarv and Saiidi 2015)

Table F-4. Ratio of Sleeve Length to Reinforcing Bar Diameter

(SSNA 2016, Erico 2013, Tazarv and Saiidi 2015)

Bar Size	Bar Diam., in.	Ratio of Sleeve Length to Reinforcing Bar Diameter		
		Splice Sleeve North America, Inc.	Erico's Lenton Interlok	Recommended by UNR Report (Tazarv & Saiidi, 2015)
#4	0.500	--	--	≤ 15
#5	0.625	15.44	12.50	≤ 15
#6	0.750	14.96	10.42	≤ 15
#7	0.875	14.63	8.93	≤ 15
#8	1.000	14.57	8.63	≤ 15
#9	1.128	14.49	8.64	≤ 15
#10	1.270	14.10	8.51	≤ 15
#11	1.410	13.82, 13.82, 13.54 [a]	8.47	≤ 15
#14	1.693	14.42	8.97	≤ 15
#18	2.257	--	9.00	≤ 15

[a] For Sleeve Nos. 11U-X, A11W, and SNX11, respectively.

Using ratio of 15 seems reasonable. As shown in Table F-5, most SSNA couplers meet this requirement. All Erico's Lenton Interlok couplers meet this requirement.

U.S. Code Requirements on Mechanical Bar Couplers

- ACI 318 Type 1 and Type 2 bar couplers:
  - Type 1 couplers are capable of developing 125% of the specified yield of the bar in tension (i.e., $1.25\ f_y$). Type 1 bar couplers are not to be used in the plastic hinge of ductile members of special moment frames neither in longitudinal nor in transverse bars (ACI 318-2014 Section 18.2.7). (ACI 318 2014)
  - Type 2 couplers meet Type 1 requirement and are capable of developing the specified tensile strength of the bar in tension (i.e., $1.0\ f_u$). Type 2 bar couplers are not to be used within one-half of the beam depth in special moment frames but are allowed in any other members at any location (ACI 318-2014 Section 18.2.7 & 25.5.7). (ACI 318 2014)
- Caltrans Seismic Design Criteria (2013), Chapter 8: For ductile members, no splicing is allowed in the plastic hinge region. "Ultimate" splices are permitted outside of the plastic hinge zones of ductile members. "Service" splices are allowed in capacity protected members (i.e., members that are not likely to experience seismic damage). (Caltrans 2015)
  - Service splices must be able to accommodate a minimum strain of 2% in the spliced bar.

  - Ultimate splices must be able to accommodate a minimum strain of 6% in No. 11 and larger bars and 9% in No. 10 and smaller bars.
- AASHTO Full Mechanical Connection (FMC) Requirements (AASHTO LRFD Bridge Design Specifications, Section 5.11.5.2.2): FMC couplers must not be used in the plastic hinge zones of columns in SDC C and D (*AASHTO Guide Specifications for LRFD Seismic Bridge Design*, Section 8.8.3). (AASHTO 2014, AASHTO 2015)
  - The FMC couplers must be able to achieve 1.25 times the specified yield stress (i.e., $1.25\ f_y$) of the coupled bar.
  - The FMC couplers must have a maximum slip of 0.01 in. for No. 3-14 bars and 0.03 in. for No. 18 bar. Slip within the coupler is measured by loading the spliced bar from 3 ksi in tension to 30 ksi in tension and then unloading to 3 ksi in tension. Displacement is measured over the coupler region for the initial and final 3 ksi loading. The difference between these two measurements is the slip.

Tensile Capacities of Splice Sleeve and Lenton Interlok Grouted Couplers

- NMB Splice Sleeve: Splice Sleeve North America, Inc. NMB Splice Sleeve grouted couplers for Grade 60 bar with sizes of No. 6, 8, 11 and 14 met at least 150% of specified bar tensile yield strength. See Table 10 of Laboratory Test Report ER-5645 (Wiss, Jenney, Elstner Associates, Inc. 2013). This table is repeated here as Table F-5 with appropriate values in a red box. Note that the last five rows of Table F-5 are for Grade 100 bar and should not be considered. Assuming a specified 90 ksi ultimate strength for Grade 60 bars, these couplers meet the ACI Type 2 and AASHTO FMC coupler strength requirements (i.e., $1.0\ f_u$ and $1.25\ f_y$, respectively).
- Erico Lenton Interlok: All Lenton Interlok grouted couplers listed in Table F-4 of this document meet ACI Type 1 requirement in tension and compression and the ACI Type 2 requirement in tension. They also meet the AASHTO FMC strength requirement.

Table F-5. Tensile Strength Data for NMB Splice Sleeve Couplers

(Wiss, Janney, Elstner Associates, Inc 2013)

Test I.D. No.	Bar Size	Bar Lot	Bar Area (in^2)	Alignment	Deformation Pattern	Grout Batch	Average Grout Strength	Cyclic Load Levels (Stages 1, 2, 3)				Cycles Applied			Tensile Strength (Stage 4)					Final Result
								P_{min} (kips)	P_{max1} (kips)	P_{max2} (kips)	P_{max3} (kips)	n_1	n_2	n_3	(kips)	(ksi)	($\%f_{y=60}$)	($\%f_{ya}$)	($\%f_{u=90}$)	
4388	6	A	0.44	Misaligned	Diagonal	PII-7	13,023	-13.2	25.1	29.0	33.7	20	4	4	46.1	104.8	175%	166%	116%	Bar break
4389	6	A	0.44	Misaligned	Diagonal	PII-7	13,023	-13.2	25.1	29.0	33.7	20	4	4	46.1	104.8	175%	166%	116%	Bar break
4390	6	A	0.44	Misaligned	Diagonal	PII-7	13,023	-13.2	25.1	29.0	33.7	20	4	4	46.0	104.5	174%	165%	116%	Bar break
4391	6	A	0.44	Misaligned	Diagonal	PII-7	13,023	-13.2	25.1	29.0	33.7	20	4	4	46.0	104.5	174%	165%	116%	Bar break
4392	6	A	0.44	Misaligned	Diagonal	PII-7	13,023	-13.2	25.1	29.0	33.7	20	4	4	46.1	104.8	175%	166%	116%	Bar break
4382	8	C	0.79	Misaligned	Diagonal	PII-7	13,023	-23.7	45.0	59.5	67.0	20	4	4	87.5	110.8	185%	159%	123%	Bar break
4383	8	C	0.79	Misaligned	Diagonal	PII-7	13,023	-23.7	45.0	59.5	67.0	20	4	4	87.7	111.0	185%	159%	123%	Bar break
4384	8	C	0.79	Misaligned	Diagonal	PII-7	13,023	-23.7	45.0	59.5	67.0	20	4	4	87.6	110.9	185%	159%	123%	Bar break
4384	8	C	0.79	Misaligned	Diagonal	PII-7	13,023	-23.7	45.0	59.5	67.0	20	4	4	87.6	110.9	185%	159%	123%	Bar break
4386	8	C	0.79	Misaligned	Diagonal	PII-7	13,023	-23.7	45.0	59.5	67.0	20	4	4	87.6	110.9	185%	159%	123%	Bar break
4396	14	G	2.25	Misaligned	Diamond	PII-10	12,208	-67.5	128.3	143.0	158.0	20	4	4	208.3	92.6	154%	145%	103%	Bar break
4397	14	G	2.25	Misaligned	Diamond	PII-10	12,208	-67.5	128.3	143.0	158.0	20	4	4	208.5	92.7	154%	145%	103%	Bar break
4398	14	G	2.25	Misaligned	Diamond	PII-10	12,208	-67.5	128.3	143.0	158.0	20	4	4	209.3	93.0	155%	146%	103%	Pullout - wide end
4399	14	G	2.25	Misaligned	Diamond	PII-10	12,208	-67.5	128.3	143.0	158.0	20	4	4	207.9	92.4	154%	145%	103%	Pullout - wide end
4400	14	G	2.25	Misaligned	Diamond	PII-10	12,208	-67.5	128.3	143.0	158.0	20	4	4	208.4	92.6	154%	145%	103%	Bar break
4402	SNX11	A	1.56	Misaligned	Bamboo	PII-11	12,213	-46.8	88.9	101.0	109.0	20	4	4	154.4	99.0	165%	152%	110%	Bar break
4403	SNX11	A	1.56	Misaligned	Bamboo	PII-11	12,213	-46.8	88.9	101.0	109.0	20	4	4	154.3	98.9	165%	152%	110%	Bar break
4404	SNX11	A	1.56	Misaligned	Bamboo	PII-11	12,213	-46.8	88.9	101.0	109.0	20	4	4	154.6	99.1	165%	152%	110%	Bar break
4405	SNX11	A	1.56	Misaligned	Bamboo	PII-11	12,213	-46.8	88.9	101.0	109.0	20	4	4	153.8	98.6	164%	152%	110%	Bar break
4406	SNX11	A	1.56	Misaligned	Bamboo	PII-11	12,213	-46.8	88.9	101.0	109.0	20	4	4	154.2	98.8	165%	152%	110%	Bar break
4662	10	D	1.27	Misaligned	Diagonal	PII-21	12,627	-38.1	72.4	80.3	87.9	20	4	4	135.0	106.3	177%	N/A	118%	Coupler
4663	10	D	1.27	Misaligned	Diagonal	PII-21	12,627	-38.1	72.4	80.3	87.9	20	4	4	165.1	130.0	217%	N/A	144%	Pullout - wide end
4664	10	D	1.27	Misaligned	Diagonal	PII-21	12,627	-38.1	72.4	80.3	87.9	20	4	4	118.5	93.3	156%	N/A	104%	Coupler
4665	10	D	1.27	Misaligned	Diagonal	PII-21	12,627	-38.1	72.4	80.3	87.9	20	4	4	170.9	134.6	224%	N/A	150%	Pullout - wide end
4666	10	D	1.27	Misaligned	Diagonal	PII-21	12,627	-38.1	72.4	80.3	87.9	20	4	4	139.7	110.0	183%	N/A	122%	Coupler

Slip Behavior of Splice Sleeve and Lenton Interlok Grouted Couplers

In a study by Jansson (2008), NMB Splice Sleeve and Lenton Interlok couplers for No. 6 and 11 bars passed the AASHTO slip requirements for FMC couplers (see Tables 4.1 and 5.1 of the report by Jansson, 2008). (Jansson 2008) In addition, the NMB Splice Sleeve couplers for No. 8 bar passed the laboratory slip tests conducted by Haber, et al. (2013). (Haber, et al. 2013) Table F-6 summarizes the slip test results of these two studies. Three tests were performed for each type of coupler considered. As noted in Section 4 of this document, the maximum slip in AASHTO's FMC couplers for No. 3 to No. 14 bars is limited to 0.01 in.

Table F-6. Grouted coupler slip test results (Jansson 2008, Haber, et al. 2013)

Coupler for Bar Size	Slip, in.	
	NMB Splice Sleeve	Lenton Interlok
#6	0.008, 0.007, 0.006	0.004, 0.003, 0.005
#8	0.001, 0.000, 0.002	--
#11	0.010, 0.009, 0.009	0.006, 0.006, 0.003